

UNIVERSITY OF BIRMINGHAM

Fungi exploits natural defence to cause neuronal and glial loss in the *Drosophila* brain

By

Deepanshu Singh

A thesis submitted to the University of Birmingham in fulfilment of the degree
DOCTOR OF PHILOSOPHY

School of Biosciences

College of Life and Environmental Sciences

University of Birmingham

March 2023

UNIVERSITY OF
BIRMINGHAM

University of Birmingham Research Archive

e-theses repository

This unpublished thesis/dissertation is copyright of the author and/or third parties. The intellectual property rights of the author or third parties in respect of this work are as defined by The Copyright Designs and Patents Act 1988 or as modified by any successor legislation.

Any use made of information contained in this thesis/dissertation must be in accordance with that legislation and must be properly acknowledged. Further distribution or reproduction in any format is prohibited without the permission of the copyright holder.

Abstract

Parasites have evolved behaviour manipulation strategies to exploit their host for nutrition and reproduction. In *Drosophila*, the fungus *Enthomophthora muscae* affects the nervous system altering behaviour (Carolyn et al., 2018). Furthermore, volatile compounds produced by fungi can cause dopaminergic neuron loss and locomotion deficits, reminiscent of Parkinsonism (Inamdar et al., 2013). In humans, genetics accounts for a small fraction of Parkinson's disease onset and environmental triggers are likely a common cause. How fungi affect the brain and the causal links between cellular phenotypes and behaviour are poorly understood.

Innate immune response is the first line of defence against a pathogenic infection which is mediated by Toll signalling. Tolls are evolutionary conserved and have varied functions from immunity to regulation of cell number plasticity regulated via different pathways. The fungus *Beauveria bassiana* is a known activator of Toll signalling in *Drosophila* and Tolls are present throughout the brain. Thus, the aim of the thesis is to investigate whether *B. bassiana* alters the fruit-fly brain by exploiting Toll signalling.

Here, I provide evidence that upon natural exposure to *B. bassiana,* the spores enter the brain. *B. bassiana* spores could enter into the brain through feeding and damage the blood brain barrier. Exposure causes neuronal and glial loss, loss of the dopaminergic neurons and a decrease in brain size over time. Expression of anti-microbial peptides is upregulated in the brain upon *B. bassiana* exposure, demonstrating activation of Toll signalling. Importantly, expression of the pro-apoptotic Toll signalling adaptors *sarm* and *wek* (Foldi et al., 2017) is also upregulated. These neurodegeneration phenotypes correlate with impaired locomotion and shorter lifespan. Furthermore, upon downregulating the expression of Toll-1, *wek* or *sarm*, *B.bassiana* cannot induce cells and dopaminergic neurons loss in the adult *Drosophila* brain. This indicate the non-canonical Toll signalling Wek and Sarm could have a role in *B.bassiana* induced neuronal and glial cell loss in the adult *Drosophila* brain.

Together these findings reveal that fungi exploited an evolutionary opportunity to bypass defense to their advantage.

For Ma,

~ whose unwavering perseverance taught me to never give up,

Papa,

~ whose steadfast persistence taught me the value of hard work,

Gudda,

~ whose infinite patience taught me the importance of taking things slow,

Akshu,

~ whose boundless love taught me that true joy comes from giving to others

Acknowledgement

I would like to express my sincere gratitude to Prof. Alicia Hidalgo, my guru and supervisor, for providing me with the opportunity to work in her lab. Her exceptional guidance, unwavering support, and profound knowledge have played a crucial role in shaping me into the researcher I am today. Her passion for *Drosophila* has inspired me, and her constructive feedback has helped me grow both personally and professionally. Without her encouragement and inspiration, this project would not have been possible. Thank you and I will always cherish the lessons I have learned from you.

I'm grateful for my family constant support throughout my PhD journey. Their love and encouragement have given me the courage to pursue my dreams and overcome challenges. I cannot thank them enough for their sacrifices and unwavering presence in my life. I would like to thank my girlfriend, Akshata Pradhan, for always believing in me and sticking by my side through thick and thin.

I would like to express my deepest gratitude to Dr. Liz Ballou and Dr. Hung-Ji Tsai for providing me with the opportunity to work with B. bassiana in their lab, and for their valuable suggestions and feedback. I am also grateful to all the members of the HAPI lab and Tsai lab for welcoming me and making my time at IMI a wonderful experience. In addition, I would like to thank our collaborators, Dr. Manuel Forero and Prof. Enrique Quesada, for their support and contribution to this project. Last but not least, I want to thank David Alliband, a previous Master's student in our lab, for his assistance in this research

I would like to thank my lab family, including Marta, Lizzie, Jun, Guiyi, Lola, Naser, and Anna, for making our lab an amazing place to work and for keeping up with me. I also want to express my gratitude to Anand, Karthik, and Laurie for their motivation and friendship. Furthermore, I would like to thank all the PIs and students on the 6th floor for their suggestions, help, support, and friendship. Finally, I am deeply grateful to my funding body, The Darwin Trust, for funding my PhD. Without their support, I would not have had the opportunity to study at UoB and meet the incredible people I have mentioned above.

CONTENTS

Chapter 1: INTRODUCTION

1.1. Behavioural manipulation by parasites 2

1.2. Behaviour manipulating fungi 5

1.2.1 *O. unilateralis:* The fungus that turns ants into zombies 5

1.2.2 *E. muscae*: The parasitic fungus that controls fly behaviour 7

1.2.3 B. bassiana: A generalist fungal pathogen 8

1.3 An evolutionary arms race between *Drosophila* and *B. bassiana* 13

1.4 Toll receptors in *Drosophila* 15

1.4.1. Structure of Toll receptors and their ligands 15

1.4.2 Toll signalling and function in immune system 18

1.4.2.1 Function of Toll receptors in immunity 22

1.4.3 Toll signalling and function in development 23

1.4.3.1 Function of Toll receptors in development 25

1.4.4 Toll signalling and function in the nervous system 26

1.4.4.1 Function of Tolls in the CNS 28

1.5 Mammalian TLRs 32

1.5.1 Evolutionary arm race between TLR and fungi 34

1.5.2 Mammalian TLR signalling 35

1.5.3 Function of TLR in nervous system 36

1.5.4 Function of TLR in learning and memory 37

1.6 The model system: *Drosophila melanogaster* 39

1.6.1 *Drosophila* adult brain structure 40

1.6.2 *Drosophila* dopaminergic system 42

1.7 Exposure to fungal volatiles causes neurodegeneration in the adult brain 43

1.8 AIM 45

Chapter 2: Materials and Methods

2.1 Genetics 46

2.1.1 Fly maintenance 46

2.1.2 Genetics protocol 46

2.2 *B. bassiana* culture and spore collection 46
2.2.1 *B. bassiana* spore collection 46
2.2.2 *B. bassiana* culture 47
2.3 Infection chamber 47
2.4 Longevity assay 48
2.5 Climbing assay 48
2.6 Proboscis extension response 49
2.6.1 Preparing flies for PER assay 50
2.6.2 Transferring flies to the 20µl pipette tip 50
2.6.3 PER assay 50
2.7 Feeding assay 51
2.8 Injecting flies with Dextran red fluorescent dye 52
2.9 Staining spores in the adult brain 53
2.9.1 Staining spores with FM4-64 dye 53
2.9.2 Staining spores with Calcofluor white stain 55
2.10 Quantitative Reverse Transcriptase (qRT)-PCR 56
2.11 Immunohistochemistry 57
2.12 Microscopy and imaging 57
2.13 Quantification of cell number using *Deadeasy* 59
2.14 Data analysis 60

Chapter 3: *B. bassiana* affects *Drosophila* behaviour and enters the brain
3.1 Introduction 63
3.2 Results 66
3.2.1 Exposure to B. bassiana reduces lifespan of the adult flies 66
3.2.2 Exposure to B. bassiana affects the negative geotaxis behaviour of adult flies 67
3.2.3 Toll-1 and Sarm are expressed in the sub-esophageal Ganglion and proboscis 67
3.2.4 Sarm neurons were involved in the proboscis extension response 69
3.2.5 Adult Drosophila flies ingested B. bassiana spores through feeding 69

3.2.6 *B. bassiana* spores damaged the blood brain barrier 70
3.2.7 *B. bassiana* spores entered the brain 71
3.2.8 *B. bassiana* activated immune signalling in the adult brain 73
3.3 Discussion 74

Chapter 4 *B. bassiana* causes neurodegeneration in the adult *Drosophila* brain
4.1 Introduction 78
4.2 Results 80
4.2.1 Exposure to *B. bassiana* decreased the size of the adult brain 80
4.2.2 Exposure to *B. bassiana* decreases glial cells in the brain 81
4.2.3 Exposure to *B. bassiana* decreased the Sarm cells in the central brain 81
4.2.4 Exposure to *B. bassiana* downregulates the TH mRNA in the adult brain 82
4.2.5 Exposure to B. bassiana cause loss of dopaminergic neurons 83
4.3 Discussion 83

Chapter 5 *B. bassiana* causes neurodegeneration via Toll-1 in the adult brain 86
5.1 Introduction 86
5.2 Results
5.2.1 Adult Toll-1 RNAi knockdown rescued the loss of MyD88+ Cells caused by *B. bassiana* infection 88
5.2.2 *B. bassiana* could not induce loss of MyD88+ cells upon Toll-1^{10b} overexpression in the adult brain 89
5.2.3 Toll-1RNAi knockdown rescued the loss of Repo+ glial Cells caused by *B. bassiana* infection 90
5.2.4 Toll-1RNAi knockdown rescued the loss of PPL1 and PPM3 neurons caused by B. bassiana infection 91
5.3 Discussion 92

Chapter 6 Non-canonical Toll signalling in B. bassiana induced neurodegeneration 96
6.1 Introduction 96
6.2 Results 97
6.2.1 *B. bassiana* infection upregulates the expression of *sarm* and *wek* in the adult brain 97
6.2.2 Adult *wek*RNAi knockdown rescued MyD88+ cell loss induced by *B. bassiana* 98
6.2.3 Adult wek-HA overexpression also rescued MyD88+ cell loss induced by *B. bassiana* 99
6.2.4 Adult wekRNAi knockdown rescued the loss of Repo+ glial cells caused by *B. bassiana* infection 100
6.2.5 *wek* overexpression also rescued the loss of Repo+ glial cell number caused by *B. bassiana* infection 100
6.2.6 wekRNAi knockdown did not rescue the loss of dopaminergic neurons caused by *B. bassiana* 101
6.2.7 *B. bassiana* infection induced loss in the dopaminergic neurons in the adult flies overexpressing *wek* 101
6.2.8 Overexpression of wek in the DAN neurons PAM cluster mimics the cell loss induced by *B. bassiana* infection 103
6.2.9 Adult sarmRNAi knockdown rescued the MyD88+ cell loss induced by *B. bassiana* 103
6.2.10 Adult sarmRNAi knockdown rescued Repo+ glial loss induced by *B. bassiana* 104
6.2.11 Adult sarmRNAi knockdown rescued loss of dopaminergic neurons in PPM3 cluster induced by *B. bassiana* 104
6.3 Discussion 105

Chapter 7 Discussion
7.1 Summary of discussion 109
7.2 *B. bassiana* spores enters the adult Drosophila brain 111
7.3 *B. bassiana* cause neurodegeneration in the adult Drosophila

brain 116
7.4 *B. bassiana* causes neurodegeneration via Toll-1 in the adult *Drosophila* brain 118
7.5 Non-canonical Toll signalling in *B. bassiana* induced neurodegeneration 121
7.6 Conclusion and implication 124

Appendix 125-154
References 155-170

LIST OF FIGURES

Figure 1.1: Infection cycle of *Beauveria bassiana*

Figure 1.2: Structure of Toll receptors

Figure 1.3: Structure of Toll ligands

Figure 1.4: Activation of innate immunity by Toll and IMD pathway.

Figure 1.5: Toll signalling in establishing dorsal ventral polarity in *Drosophila* embryo.

Figure 1.6: Toll signalling pathway in CNS.

Figure 1.7: Structure of mammalian TLR receptor.

Figure 1.8: Evolutionary arm race between TLRs and *C. albicans*.

Figure 1.9: UAS-GAL4 system in *Drosophila melanogaster*

Figure 1.10: Schematics of Dopaminergic neurons in adult brain.

Figure 2.1: Genetics protocol for generating Tubgal80^{ts};SarmNP0257Gal4.

Figure 2.2: Genetics protocol for generating Tubgal80^{ts};SarmNP7460Gal4.

Figure 2.3: Cell number is quantified using *Deadeasy*.

Figure 3.1: Exposure to B. bassiana causes reduction in lifespan of adult flies.

Figure 3.2: Exposure to *B. bassiana* affected the negative geotaxis behaviour.

Figure 3.3: Toll-1 and Sarm are expressed in sub-esophageal ganglion and proboscis.

Figure 3.4: Sarm neurons are involved in the proboscis extension response.

Figure 3.5: Adult flies like to eat *B. bassiana* spores.

Figure 3.6: *B. bassiana* spores breaks the blood brain barrier.

Figure 3.7: Staining *B. bassiana* spores with FM4-64 in the brain.

Figure 3.8: Calcofluor white stained *B. bassiana* spores in the brain.

Figure 3.9: GFP transformed *B. bassiana* spores entered the brain.

Figure 3.10: *B. bassiana* infection activated the immune response in the adult brain

.
Figure 4.1: Exposure to *B. bassiana* decreased size of the adult brain

Figure 4.2: Exposure to *B. bassiana* decreased glial cells in the adult brain.

Figure 4.3: Exposure to *B. bassiana* decreased the Sarm+ neurons in the central brain.

Figure 4.4: Exposure to *B. bassiana* decreased TH mRNA levels in the dissected adult brain.

Figure 4.5: Exposure to *B. bassiana* caused dopaminergic neurons loss in PAM cluster.

Figure 4.6: Exposure to *B. bassiana* caused loss of neurons in the dopaminergic clusters.

Figure 5.1: Adult *Toll-1*RNAi$^{KK/100078}$ knockdown rescued the loss of MyD88+ cells caused by *B. bassiana* infection.

Figure 5.2: Adult Toll-1RNAi^{JF10491} knockdown rescued the loss of MyD88+ cells caused by *B. bassiana* infection.

Figure 5.3: Constitutively activated UASToll-1^{10b} did not induce MyD88+ cell loss in the adult brain.

Figure 5.4: Constitutively activated *Toll-1^{10b}* overexpression increased brain size upon *B. bassiana* infection

Figure 5.5: Adult *Toll-1*RNAi$^{KK/100078}$ knockdown rescued the loss of Repo+ cells caused by *B. bassiana* infection.

Figure 5.6: Toll-1 receptor is expressed in the dopaminergic neurons.

Figure 5.7: Adult *Toll-1*RNAi$^{KK/100078}$ knockdown rescued the loss of dopaminergic neurons in PPM3 cluster caused by *B. bassiana* infection.

Figure 5.8: Adult *Toll-1*RNAi$^{KK/100078}$ knockdown rescued the loss of dopaminergic neurons in different cluster caused by *B. bassiana* infection.

Figure 6.1: *B. bassiana* infection increased the expression of Wek mRNA and Sarm mRNA in dissected adult brain

Figure 6.2: Adult *wek*RNAi^{TRIPMHC046534} knockdown rescued MyD88+ cell loss induced by *B. bassiana.*

Figure 6.3: Adult *wek*-HA overexpression also rescued MyD88+ cell loss induced by *B. bassiana.*

Figure 6.4: Adult *wek*RNAi^{TRIPMHC046534} knockdown rescued the loss of Repo+ glial caused by *B. bassiana* infection.

Figure 6.5: *wek* overexpression also rescued the loss of glial cell number caused by *B. bassiana* infection

Figure 6.6: wekRNAi knockdown did not rescue the loss of dopaminergic neurons in PPM3 cluster caused by *B. bassiana*.

Figure 6.7: wekRNAi knockdown did not rescue the loss of dopaminergic neurons in different cluster caused by *B. bassiana.*

Figure 6.8: *B. bassiana* infection induced loss of dopaminergic neurons in PPM3 cluster in the adult flies overexpressing *wek*-HA.

Figure 6.9: *B. bassiana* infection induced loss of dopaminergic neurons in PAL, PPL1 and PPL2 clusters upon adult *wek*-HA overexpression.

Figure 6.10: Overexpression of *wek in* dopaminergic neurons of PAM cluster mimics the cell loss caused by *B. bassiana* infection.

Figure 6.11 Adult *sarm*RNAi^{JF01681} knockdown rescued loss of MyD88+ cells caused by *B. bassiana* infection.

Figure 6.12 Adult *sarm*RNAi^{JF01681} knockdown rescued loss of Repo+ glial cells caused by *B. bassiana* infection.

Figure 6.13 Adult *sarm*RNAi^{JF01681} knockdown rescued loss of dopaminergic neurons in PPM3 cluster caused by *B. bassiana* infection.

Figure 7.1 *B. bassiana* cannot induce neurodegeneration without Wek.

Figure 7.2 Wek causes both cell proliferation and cell death.

Figure 7.3 B. bassiana induces neurodegeneration through Sarm.

Figure 7.4 Evolutionary arms race between *Drosophila* and *B. bassiana* for Toll Signalling.

List of tables **Page No.**

Table 2.1 Stock list 50

Table 2.2 List of primers 51

Table 2.3 – 2.6 PCR reactions 56 - 58

Table 2.7 List of antibodies 58

Table 5.1 Summary of findings 86

Table 6.1 Summary of Wek data 97

Table 6.2 Summary of Sarm data 98

List of abbreviations

BDNF:	Brain derived neurotrophic factor
CRC:	Cystine-rich cluster
DAG:	Diacylglycerol
DAMPs:	Damage Associated Molecular Patterns
Dif:	Dorsal-related immune factor
DANs:	Dopaminergic neurons
ELAV	Embryonic lethal abnormal vision
Eve:	Even skipped
FM4-64	*N*-(3-Triethylammoniumpropyl)-4-(6-(4-(Diethylamino) Phenyl) Hexatrienyl) Pyridinium Dibromide
FRS2:	Factor Receptor Substrate 2
GAPDH	Glyceraldehyde 3-phosphate dehydrogenase
GAB1:	GRB-associated binder
GMC	Ganglion Mother Cells
GNBP3	Gram negative bacteria binding 3
Grass:	Gram-positive-specific serine protease
GRB2:	Growth Factor Receptor Bound Protein 2
HPLC	High performance liquid chromatography
Ins(1, 4, 5)P3:	inositol-1,4,5-trisphosphate
IRS1:	Insulin Receptor Substrate 1
IRS2:	Insulin Receptor Substrate 2

KC:	Kenyon cells
LC-MS:	Liquid Chromatography- Mass Spectrometry
LPS:	Lipopolysaccharide
MARCM:	Mosaic Analysis with a Repressible Cell Marker
MB:	Mushroom Body
MiMIC:	*Minos* mediated integration cassette
MMPs:	Matrix metalloprotease
MyD88:	Myeloid differentiation primary response 88
NB:	Neuroblast
NF-kB:	nuclear factor kappa-light-chain-enhancer of activated B cells
NGF:	Nerve growth factor
NT:	Neurotrophins
PAL:	Protocereberal anterior lateral
PAM:	Protocereberal Anterior Medial
PPL1:	Protocereberal posterior lateral 1
PPL2:	Protocereberal posterior lateral 2
PPM3:	Protocerebral posterior media 3
PH3:	Phosphor-Histone-H3
PRR:	Pattern Recognition Receptor
Rbf:	Retinoblastoma-family protein
REPO	Reverse polarity
SPE:	Spz processing enzyme
SOG:	Sub-esophageal ganglion
Spz:	Spätzle
T1:	Thoracis 1
TH	Tyrosine hydroxylase

TLR:	Toll-like receptor
Trk:	Tropomycin receptor kinase
Wek:	Weckle
Yki	Yorkie

Chapter 1

Introduction

Parasites infect and cause mortality in their hosts for nutrition, enhance their transmission, and reproduction. Over time, parasites have evolved “extended phenotypes” as a means to enhance their transmission and survival (Dawkins, 1982). An extended phenotype is characterized by a gene that generates a phenotype which extends beyond the individual’s body and increases the transmission of the gene to subsequent generations (Lefevre et al., 2009, Thomas et al., 2005). This suggest that alteration of the host’s behaviour by a parasite is an extended phenotype as it facilitates parasite transmission. However, the host-pathogen relationship is complex, and what appears to be a host manipulation could be a host compensatory response to eliminate the parasite from its system (Lefevre et al., 2009). Behavioural changes could also be a host adaption to reduce the infection (Moore and Gotelli, 1990, Poulin, 1995). For instance, increased grooming has been observed in adult *Drosophila* flies infected with entomopathogenic fungi (Yanagawa et al., 2018). Therefore, determining the adaptive nature of behavioural changes induced by a parasite is crucial.

To understand the manipulation of host behaviour by parasites, Poulin proposed the concept of "true adaptive invasion" in the context of transmission (Poulin, 1995). To meet the criteria for adaptive invasion, the phenotypic trait induced by a parasite should be a complex trait that eases parasite transmission and is favoured by natural selection (Poulin, 2010, Poulin, 1995). Additionally, the trait should have a purposive design, meaning the onset of the behavioural changes should coincide with the developmental phase of the parasite. Furthermore, the phenotypic trait is more likely

to be an adaptation if it has arisen independently in several lineages of host and parasite. Finally, the trait should favour the fitness of the parasite.

Parasites can achieve true adaptive manipulation of behaviour through either direct or indirect mechanisms (Thomas et al., 2005, Poulin and Thomas, 1999). The parasite could directly affect the host nervous system or muscle by producing a neuroactive compound that alters the host behaviour. For example the trematode parasite *Schistosoma mansoni* secretes opioid peptides in its host, which may have a role in immune evasion (Kavaliers et al., 1999). Alternatively, parasites can use an indirect mechanism by affecting the host biochemical pathway. For instance, several viruses alter the production of dopamine and serotonin in their host that make them more aggressive, such as Herpes simplex virus (Lycke and Roos, 1974). This suggest that the parasites have evolved different strategies that alter the behaviour of their host.

This thesis examines the evolutionary arms race hypothesis between hosts and parasites, which suggests that hosts and parasites have co-evolved over time. Parasites have developed strategies to modify host behaviour to enhance their transmission and reproduction, while hosts have evolved strategies to evade parasites and strengthen their immune systems. As a result, an ongoing evolutionary arm race exists between host and parasites

1.1 Behavioural manipulation by parasites

The phenomenon of host manipulation by parasites has been extensively documented across a diverse range of parasites, spanning major phyla of living organisms including bacteria, fungi, and viruses (Poulin and Thomas, 1999, Moore, 2002, Thomas et al.,

2005). These studies have highlighted the wide range of phenotypic traits that parasites can exploit for their benefit (Thomas et al., 2005, Poulin, 2010).

Reports have demonstrated that an acanthocephalan worm, *Polymorphus minutus* parasites on shrimp *Gammarus lacustaris* by altering their colouration and behaviour that make them more susceptible to predation by ducks. (Hindsbo, 1972, HOLMES, 1972). The infected shrimps appeared blue in colour rather than red, and spectrophotometric analysis revealed a decrease in carotenoids in the haemolymph of the infected blue shrimps compared to non-infected brown shrimps (Hindsbo, 1972). Hindsbo observed the behaviour of infected and non-infected shrimps in an aquarium with light exposed top and dark bottom and found that infected blue shrimp resided more towards the light exposed top and showed positive phototropism, while non-infected brown shrimps resided at the bottom. When a duck was introduced to the aquarium, the light exposed infected shrimps were preyed upon more than non-infected shrimps, providing the first evidence of host manipulation by a parasite.

A field study has demonstrated that a nematode parasite, *Myrmeconema neotropicum*, induces changes in its ant host *Cephalotes atratus*, including the turning of the abdomen to cherry red and the driving of the ant to perch with its abdomen raised, making them more vulnerable to bird predation (Yanoviak et al., 2008). Dissection of infected ant's abdomen revealed the presence of *M.neotropicum* eggs (Poinar and Yanoviak, 2008). Spectrophotometer analysis did not detect red pigment in the abdomen of the infected ant, rather, the density of pigments in the abdomen was affected, causing it to appear translucent amber in combination with the yellow-white nematode egg, creating the appearance of red (Yanoviak et al., 2008). Analysis of

cuticle thickness from the electron microscopy scans revealed that infected ants had thinner cuticle compared to non-infected ants (Verble et al., 2012) . Infected ants also exhibited more frequent gaster flagging, walking with their abdomen upright. However, there is a lack of evidence on whether the infected ants are more prone to predation by frugivorous birds (Yanoviak et al., 2008). When preyed upon by birds, the parasite completes its life cycle in the bird's gut. In both cases, pathogens exploit their intermediate hosts for nutrition and further induce behavioural changes to increase their predation rate to complete their life cycle.

Toxoplasma gondii is a protozoan parasite that increases the predation risk of rat by their feline predator, the cat. Behavioural experiments have demonstrated that when rats were orally infected with 20 cyst of *T.gondii*, 25% of infected rat did not show avoidance to the cat scented area (Berdoy et al., 2000). Furthermore, infected rats behaved similarly to non-infected rats with respect to areas containing their own smell, neutral smell, and rabbit odour (Berdoy et al., 2000). This suggest that the potentially fatal attraction is not caused by the impairment of olfactory system, rather It might be altering specific olfactory receptors responsible to detect cat odour.

T. gondii reproduces sexually in the intestine of cats and oocysts are excreted in their faeces. When a rat ingests these oocysts, *T. gondii* is transmitted to the rat (Vyas and Sapolsky, 2010). The parasite then alters the behaviour of the rat by abolishing the innate fear that the rodents have for the odour of cats. This leads to an increase in the predation risk of the infected rodent by the cat, thereby completing the parasite's life cycle (Vyas and Sapolsky, 2010). However, the underlying mechanism is still unknown.

Together, these reports describe the physiological changes induced by pathogens to exploit their host, but the underlying molecular mechanism by which parasites alter behaviour is not known.

1.2 Behaviour manipulating fungi

Fungal parasites that exploit insects for nutrition and transmission are known as entomopathogenic fungi. These parasites reduce the reproductive success of their hosts, thereby affecting their survival (Samson et al., 1988, Evans, 1988). They are distributed among all groups, from Phycomycetes to Ascomycetes and Basidiomycetes (Ferron, 1978). Since they are pathogenic to insects but not humans, they are used as a biological control agent in the regulation of pest insects, for example, *Ophiocordyceps unilateralis*, *Entomophthora muscae* and *Beauveria bassiana* (McCoy, 1990, Samson et al., 2013).

1.2.1 *O. unilateralis*: The fungus that turns ants into zombies

Ophiocordyceps unilateralis is a fungus that alters the behaviour of carpenter ants, specifically Camponotous Leonardi (Evans, 1982). Worker ants infected with the fungus walk abnormally and bite into the abaxial leaf vein, also known as the "death grip," which affixes the ant and is followed by the growth of fungal stalks bearing conidia from the ant's head (Evans, 1982, Andersen et al., Hughes et al., 2011). The molecular mechanism by which *O. unilateralis* manipulates ants behaviour is not known. However, data from several reports could indicate potential genes that *O. unilateralis* could exploit to kill its ant host.

RNAseq data from two transcriptomic analysis studies has revealed the downregulation of core clock genes, *takeout* (tk) and circadian locomotor output cycle *kaput* (clk), in the manipulated ants as compared to non-manipulated ants (De Bekker et al., 2015, Will et al., 2020). This suggest that *O. unilateralis* affects the circadian rhythm of ants. Studies have shown that *takeout* (tk) encodes a protein that interact with juvenile hormone, which is speculated to be involved in foraging and feeding behaviour of ants (Sarov-Blat et al., 2000, Meunier et al., 2007). This suggests that *takeout* may be a potential gene that *O. unilateralis* could exploit to alter the foraging behaviour of ants. However, the precise role of *tk* in ant locomotion, its expression within the ant central nervous system, and its involvement in olfactory receptors have not been fully explored and require further investigation.

Apart from the clock genes, immune related genes like *peptidoglycan recognition receptor protein*, *cytochrome P450 6k1* (signalling), *prophenoloxidase*, and some *AMPs* were downregulated in the head of the manipulated ants as compared to non-manipulated ants (De Bekker et al., 2015). However, the compounds produced by *O. unilateralis* to downregulate immune response in ants are not known. Interestingly, tyrosinase, which is involved in dopamine synthesis was upregulated in the manipulated ants (De Bekker et al., 2015). This suggest that fungal manipulation might feel rewarding for the ants.

To summarise, RNA sequencing analysis has identified various genes that *O. unilateralis* can exploit to manipulate ants. However, the mechanisms underlying this process have yet to be determined. Thus, genetic analysis is necessary to examine the molecular pathway responsible for fungal-induced behavioural manipulation.

1.2.2 *E. muscae*: The parasitic fungus that controls fly behaviour

Enthomophthora muscae affects the locomotion of its host by inducing abnormal climbing behaviour, a phenomenon known as “summit disease”(Evans, 1982, Keller, 1987). The compounds or metabolite that cause summit disease in the fungi host are mostly unknown. In late phase of *E. muscae* infection, adult Drosophila climb upwards and extends their proboscis, which sticks to the stalk, thus affixing the fly. The fly then raises its wings to ease the spore dispersal from its abdomen (Elya et al., 2018).

(Elya et al., 2018) have demonstrated that after 48 hours following *E. muscae* infection in adult Drosophila, safranin-0-fast green stained spores were present in the adult brain and ventral nerve cord (VNC). This suggest that spores enter the brain upon infection. This was further confirmed via in situ hybridization FISH with a fluorescent probe targeting abundant repeat 18mer mRNA in *E. muscae*. Fluorescent tagged *E. muscae* spores were found inside the adult brain and VNC. Furthermore, RNAseq gene expression data revealed that 48 hours post-infection, immune Toll signalling was upregulated along with *wek* mRNA, which is a downstream adaptor of the Toll receptor. Genes involved in sensory pathways were also upregulated. It would be interesting to determine whether the Toll pathway is upregulated in order to combat the infection and eliminate the fungus, or whether it is part of the mechanism that manipulates behaviour. However, the underlying mechanism exploited by *E. muscae* to affect host behaviour and immune system is not known.

Electron microscopy scan of the protoplast (single cell structure without cell wall) stained with lead citrate upon *Eyrnia neoaphidis* infection in adult pea aphids has

revealed that entomopathogenic fungi can also exist as protoplasm inside their host (Butt et al., 1981). There may be a possibility that in the early phase of infection, entomopathogenic fungi can remain as protoplast in the host haemolymph to evade the host immune system. However, the cell wall is required to produce infective conidia and hyphae (Butt et al., 1996). Whether *E. muscae* exist as protoplast in its host haemolymph to evade immune response needs further investigation.

In summary, the above reports demonstrate that the model organism *Drosophila* can also serve as a useful tool for investigating behavioural manipulation by fungi. Spores have been detected in the brains of adult *Drosophila*, suggesting that fungi can directly impact the brain. However, the pathway by which the spores reach the brain remains unclear. Notably, RNAseq data suggests that Toll signalling and its adaptor *wek* could be involved in the fungal manipulation of the fly brain. So, in my thesis, I asked whether activation of Toll signalling via *wek* could be a mechanism by which fungi manipulate their host.

1.2.3 *B. bassiana*: a generalist fungal pathogen

B. bassiana is a pathogenic fungus which causes muscardine disease in a wide range of insects, including termites, thrips, whiteflies, aphids and various beetles. It is known to infect more than 700 species of arthropods (Inglis et al., 2001). First discovered by Agostino Bassi in the 19th century, *B. bassiana* has since been used as a pest control agent (Wang et al., 2021). *B. bassiana* is readily cultivable and can easily be isolated from their ecology (Ortiz-Urquiza and Keyhani, 2016a). *B. bassiana* provides a tractable system that can be used to study the evolutionary relationship between the

fungal pathogen and their host (Boomsma et al., 2014, Ortiz-Urquiza and Keyhani, 2016b).

The genome of the *B. bassiana* has been completely sequenced, making it one of the most extensively studied entomopathogenic fungi (Xiao et al., 2012). Over the past five years, a number of genomic studies have been conducted on *B. bassiana*, including telomere fingerprinting, DNA karyotyping, mitochondrial DNA sequencing, and identification of transposable elements (Maurer et al., 1997, Bai et al., 2022, Viaud et al., 1996). DNA Karyotyping of 9 isolates of *B. bassiana* using contour- clamped homogenous electric field (CHEF) estimated the genome size of *B. bassiana* to range from 34.3 to 44.1 MB (Viaud et al., 1996). Additionally, the mitogenome of eight strains of *Beauveria* have been annotated and analysed using illumina DNA and mRNA sequencing (Bai et al., 2022). The *B. bassiana* genome also contains a transposable element named *hupfer*, which could be used for generating transgenic lines and would help in understanding the genetics of *B. bassiana* (Maurer et al., 1997).

Analysing different *B. bassiana* mutants has revealed the function of several genes involved in survival, reproduction and infection processes in *B. bassiana.* For instance, a mutation in the CYP52X1 gene in *B. bassiana* causes a reduction in virulence and impaired germination on insect cuticle, indicating that the CYP5261 gene is responsible for cuticular targeting of *B. bassiana* (Zhang et al., 2012). The SOD1 and SOD2 gene function in mediating survival of *B. bassiana* in stress condition, as mutation in these genes increase colony sensitivity to superoxides, colony sensitivity to high osmotic (NaCl) stress and conidial sensitivity towards UV (Li et al., 2015, Xie et al., 2012, Xie et al., 2010). This suggest that SOD1 and SOD2 might help *B.*

bassiana to survive within host haemolymph. *B. bassiana* has also been used to study the host defence system and has illuminated many aspects of innate immunity with direct relevance to human immunology.

The genomic analysis of *B. bassiana* has revealed that its genome encoded 8 genes similar to bacterium *Bacillus thuringiensis* endotoxin (Bt-CRY), indicating that *B. bassiana* has higher oral toxicity (Xiao et al., 2012). *B. bassiana* is one of the few fungus whose genome contain 3 genes that encodes for bacterial zeta toxin like protein (Xiao et al., 2012). This enables *B. bassiana* to control cell death by using a bacterial toxin-antitoxin-like system, which helps the fungus to sense and adapt to different environmental niches. With the availability of genetic and physiological studies, *B. bassiana* could serve as a valuable model organism to study host-pathogen interactions.

B. bassiana produces different type of mono-nucleated cells including aerial conidia, blastospores, and submerged conidia which upon gemination produce hyphal filaments and mycelium (Boucias et al., 1988, Holder and Keyhani, 2005). Single cell blastopores and submerged conidia are hydrophilic in nature, whereas the cell surface of aerial conidia is hydrophobic (Holder et al., 2007). The surface properties of these mono-nucleated cells, along with array of depolymerases and secondary metabolites produced by the fungi, form the basis of the host pathogen interaction (Holder et al., 2007).

All stages of *B. bassiana* are infectious, including aerial conidia, blastopore and submerged conidia stages (Figure 1.1). The hydrophobic spores or aerial conidia

known as primary conidia, attach to the surface of host cuticle to initiate the infection (Figure 1.1 a) (Boucias, Pendland et al. 1991). In many insects, the probability of infection is high at the less sclerotized cuticle of the mouth and anus, but the infection can occur anywhere on the host cuticle (Ortiz-Urquiza, 2016). The outermost layer of the spores contains hydrophobins that mediate the hydrophobic interaction and adhesion between the spores and host cuticle. The outer layer of *B. bassiana* spores consist of two hydrophobins proteins, Hyd1 and Hyd2 (Cho et al 2007; Kirkland and Keyhani 2011, Zhang et al 2011b). Hyd1 is predominant in the surface of aerial and submerged conidia and at the base of germinating conidia, while Hyd2 is only localized in the surface of aerial conidia and at the base of the germinating conidia. Whether additional factors and cues are used by the fungus to initiate infection is largely unknown.

After adhesion and germination of spores on the host cuticle, the next step is the penetration of the insect cuticle (Figure 1.1 b). *B. bassiana* secretes a number of chitinases and proteases that breakdown and penetrate the host cuticle. Genomic data has revealed that *B. bassiana* produces 20 chitinases, 23 trypsins, and 43 subtilisins, and more virulent strains can be constructed by overexpressing trypsins and chitinases (Fan et al., 2007, Zhang et al., 2008, Fang et al., 2009). The host cuticle has two layers: the outhermost waxy lipid rich layer, followed by protein chitinaceous part of the cuticle (Ortis-urquiza 2006). Growth of spores on the waxy lipid layer leads to the induction of lipid assimilatory pathway, along with the production of set of P450 monooxygenases and other enzymes that are involved in the oxidation of fatty acid (Pedrini et al., 2010). These cytochrome P450 enzymes leads to the epicuticle degradation and penetration of the host cuticle.

Figure 1.1 Infection cycle of *Beauveria bassiana*

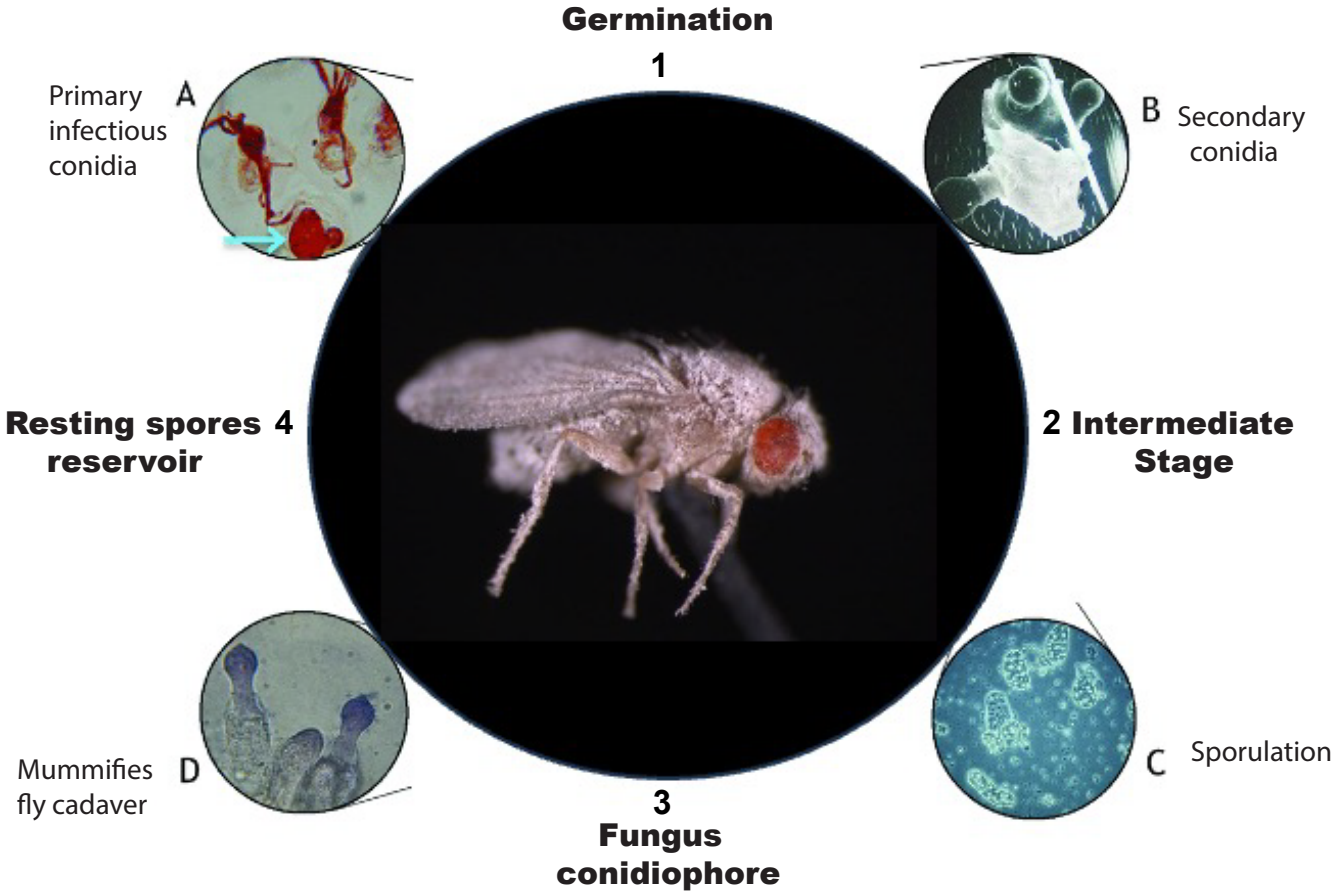


Figure 1.1 Infection cycle of *B. bassiana*

1) Primary infectious conidia (a) adhere to the cuticle of the adult drosophila at various sites on the head, thorax and abdomen, and then germinate into hyphae and secondary conidia (b). 2) Intermediate stage is marked by the degradation of the cuticle by the hyphae via constant secretion of chitinases and proteases to penetrate host's body and sporulate (c) in the haemocoel and body cavity. 3) The final stage involves the production of primary spores bearing fungus conidiophore on the cadaver of the host (d). 4) Fly cadaver covered with *B. bassiana* spores act as resting spores reservoir. This figure is redrawn from Gryganskyi et al., 2017, the centre photograph of fly covered in *B. bassiana* is from Taylor & Kimbrell., 2007.

After penetrating the cuticle, the hyphal bodies grow and proliferate in the hemocoel of their host and evade the host immune system (Figure 1.1 c) (Lewis et al., 2009). Death of the host occur upon the hyphae proliferation in the hemocoel (Figure 1.1 d). Conidial spores can also germinate within the hemocoel upon phagocytosis by the host, however, the signal cascade that leads to the growth of hyphae from the spore is largely unknown.

The final stage of the fungal infection involves the production of the spores bearing conidia on the cadaver of the host (Figure 1.1). This appears as a white fluffy growth, representing the *B. bassiana* infection, and is known as muscardine disease. In summary, significant research has been done in genetic characterization of *B. bassiana* in the past 5 years, leading to the development of a robust protocol for genetic manipulation. Combined with the availability of the fungal genome, has led to the discoveries of many fungal genes involved in the stress response, virulence and fungal development.

B. bassiana also exists as an endophytic insect pathogenic fungus (EIPF) and shares a symbiotic relationship with plants. Studies have identified two fungal species localized on various parts of *Phasiolus vulgaris* (haricot beans) (Branine et al., 2019, Behie et al., 2015). The detection of translational elongation factor 1-alpha (EF-1α) using restriction fragment length polymorphism revealed the presence of *M. robertsii* while *B. bassiana* was observed on the leaves of *P. vulgaris* (Behie et al., 2015). This suggests that both *B. bassiana* and *M. robertsii*, the two entomopathogenic fungi, are localized in haricot beans. Further analysis showed that *B. bassiana* isolates were

predominantly found in the roots (70 percent), followed by the hypocotyl (20 percent), and the leaves (10 percent), while *M. robertsii* was solely detected in the roots (100 percent) and absent in the leaves (Behie et al., 2015). This indicates that while *M. robertsii* is primarily restricted to the root and to some extent the stem, *B. bassiana* colonizes the root, stem, and leaves. In an experiment using radioactive isotopes (^{15}N and ^{13}C) in endophytic *M. robertsii*, it has been demonstrated that the fungus transfers nitrogen from insects to the roots of its plant partner, *P. vulgaris*, in exchange for carbon from the plant (Behie et al., 2012, Barelli et al., 2017). This experiment provided evidence of a symbiotic relationship between entomopathogenic fungi and their plant partners. In this mutualistic relationship, *M. robertsii* provides nutrients from insects to nourish the roots of *P. vulgaris*, while *B. bassiana* offers protection to the plant's aerial parts from invading insects in exchange for carbon.

1.3 An evolutionary arms race between *Drosophila* and *B. bassiana*

The innate immune response is the first line of defence against a pathogenic infection and is mediated by Toll receptor signalling in *Drosophila.* The fungus *Beauveria bassiana* is a known activator of Toll signalling (Gottar et al., 2006, Lemaitre et al., 1997). In *Drosophila*, there are nine Toll receptor paralogues (Toll-1-Toll-9) (Imler and Hoffmann, 2001). Work from our lab has shown that Tolls are present throughout the brain (Li et al., 2020). Tolls also have functions independently of immunity, such as regulation of cell number plasticity, engaging multiple signalling pathways that can promote either cell survival, cell death or cell proliferation (Foldi et al., 2017, McIlroy et al., 2013, Li et al., 2020). Thus, conceivably this could be the context of an evolutionary arms race, whereby the host produces an immune response against the fungus, but the fungus exploits immune Toll signaling to induce host cell death.

Tolls and Toll like proteins are widespread throughout plants, animals and insects (Leulier and Lemaitre, 2008, Luo and Zheng, 2000b). There are ten Tolls in humans and a single gene in *C. elegans* (Tauszig et al., 2000). The LRR component of extracellular domain and the intracellular TIR domain has an ancient evolutionary origin and are identified across plants, most metazoans and in some bacteria and viruses (Leulier and Lemaitre, 2008). Phylogenetics analysis suggest that insects Toll and mammalian TLR's evolved independently from a shared common ancestor (Luo and Zheng, 2000b). Furthermore, genes involved in NF-kB pathway have evolved an immune function in different ways (Friedman and Hughes, 2002).

Genomic analysis in Cnidaria has identified some proteins containing complement C3 and membrane attack complex/perforin domain (MAC/PF) similar to the vertebrate IL1R's but have different TIR domains (Miller et al., 2007). TLR genes are identified in the basal cnidarians sea anemone but are absent in hydra (Putnum et al.). Two Rel-homology-domain (RHD) proteins NF-kB-like protein (Nv-NF-kB) and NFAT-like protein (Nv-NFAT) are present in the genome of the sea anemone (Sullivan et al., 2007). Apart from that the sea anemone genome contain several upstream and downstream signalling protein like Toll, Traf, Myd88 and NF-kB co-activator proteins bcl3 suggesting that these proteins are ancient evolutionary proteins (Sullivan et al., 2007). To conclude, the evolutionary emergence of Toll and Toll-like receptor (TLR) genes can be traced back to an ancient common ancestor of all animal phyla around 700 million years ago.

To summarize, Tolls and TLRs are evolutionarily conserved and play crucial roles in the immune response. It is possible that pathogens and hosts have coevolved, with the host developing Toll-based innate immunity to destroy fungi and the fungi developing mechanisms to exploit Tolls/TLRs to enhance their virulence and kill their hosts.

1.4 Toll receptors in *Drosophila*

1.4.1 Structure of Toll receptor and their ligands

Toll (Toll-1) was first discovered in the *Drosophila* embryo as a gene that controls the dorsal-ventral patterning during early embryogenesis (Anderson and Nüsslein-Volhard, 1986). There are 9 different paralogue of Toll receptor genes in the *Drosophila* genome (Toll-1-Toll-9) and only Toll-1 has a clear immune function (Figure 1.2) (Tauszig et al., 2000, Lemaitre et al., 1996). Tolls are the type-1 transmembrane protein with an extracellular N-terminal and intracellular C-terminal (Imler and Zheng, 2004, Gay and Gangloff, 2007, Leulier and Lemaitre, 2008). The extracellular N-terminal of Toll receptors is a ligand binding domain that contains several leucine rich repeats (LRR's) clusters flanked by cystine rich clusters (Figure 1.2) (Gay and Gangloff, 2007, Leulier and Lemaitre, 2008). The intracellular C-terminal is comprised of an evolutionary conserved Toll/interleukin-1 receptor (TIR) domain (Leulier and Lemaitre, 2008). The TIR domain binds with downstream adaptor to activate signalling events (Gay and Gangloff, 2007). The Toll receptors in Drosophila, with the exception of Toll-9 have similar structure, with a similar intracellular TIR domain and an extracellular LRR repeats (Imler and Zheng, 2004). Toll-9 is the closest to the mammalian Toll-like Receptor (TLR) subfamily.

Figure 1.2: Structure of Toll receptors

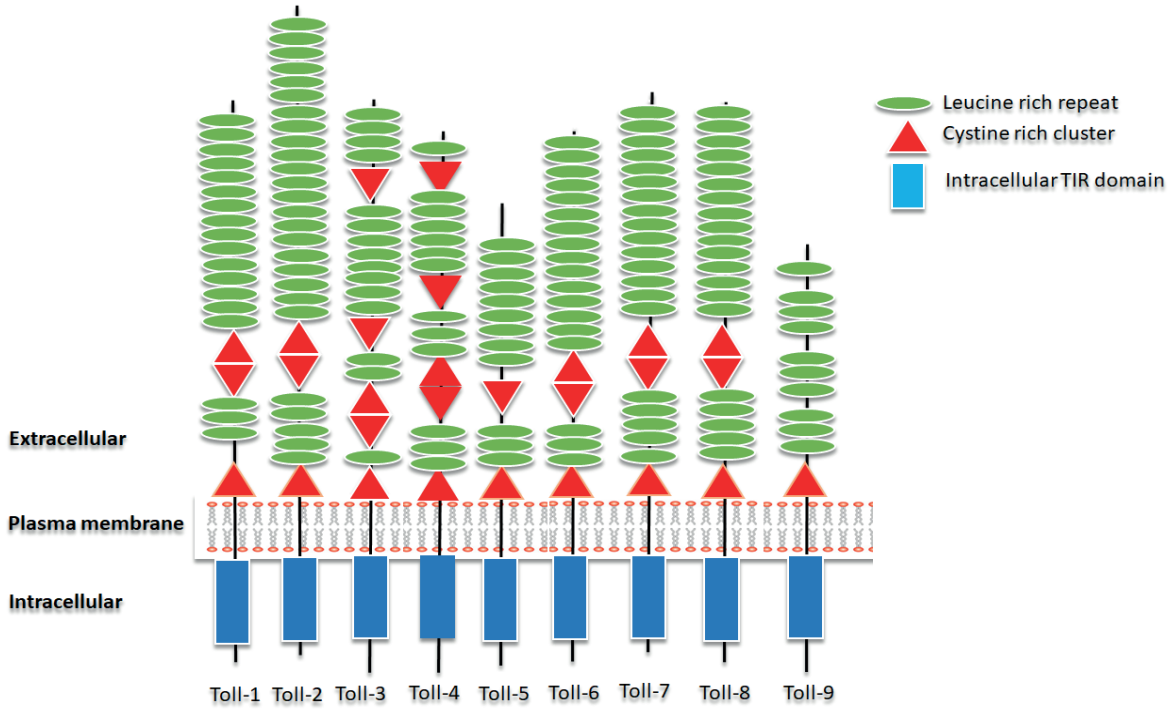


Figure 1.2: Structure of Toll receptors
Toll receptors are composed of an evolutionary conserved TIR domain (blue rectangle) in the intracellular domain. The ectodomain is composed of cystine rich clusters (red triangle) and leucine rich repeats (green oval). The figure is redrawn from (Tauszig et al., 2000, Leulier and Lemaitre, 2008)

The cytokine Spätzle Spz belongs to the cystine-knot family growth factor, act as a ligand for *Drosophila* toll receptor and function in dorsoventral patterning of embryo and innate immunity (Morisato and Anderson, 1994, Lemaitre et al., 1996, Weber et al., 2003, Mizuguchi et al., 1998). The pro-protein of Spz, is made up of a pro-domain (25 kDa) and a C-terminal cystine knot structure (C-106) (14 kDa) (Figure 1.3 A) which is synthesized and released by the cell in an inactive, dimeric form (DeLotto and DeLotto, 1998). The expression of active Easter and Spz on SDS-page gel resulted in a 12kDa carboxyterminal fragment, which was detected by immunoblotting using an anti-Spz carboxyterminal antibody, suggesting that Spz is cleaved by active Easter (DeLotto and DeLotto, 1998). Spz cleavage by Easter activates embryonic dorsal-ventral patterning (Rose et al., 2003, Chasan et al., 1992), while Spz Processing Enzyme, SPE-mediated Spz cleavage activates immune signalling (Jang et al., 2006). Band shift analysis using native-PAGE demonstrated that cystine knot structure (C-106) of Spz binds to the Toll receptor (Weber et al., 2007).

The crystal structure showed that the way Spz binds to Toll resembles mammalian nerve growth factor (NGF) (Figure 1.3 C) and P75 receptor binding (Lewis et al., 2013). Protein based structural analysis of 6 paralogues of Spz (Spz1-Spz6) identified spz5 as closely related to mammalian neurotrophins, hence renamed as DNT2 (Figure 1.3 B) (Zhu et al., 2008). Moreover, DNA sequence analysis using PSI-BLAST and TBLASTN with FUGUE revealed the Drosophila Neurotrophin1 gene (DNT1) (Figure 1.3 B) from the Drosophila genome as a homologue of vertebrate neurotrophins (Zhu et al., 2008). Together these data demonstrated that Spz family belongs to the neurotrophin family.

Figure 1.3: Structure of Toll ligands

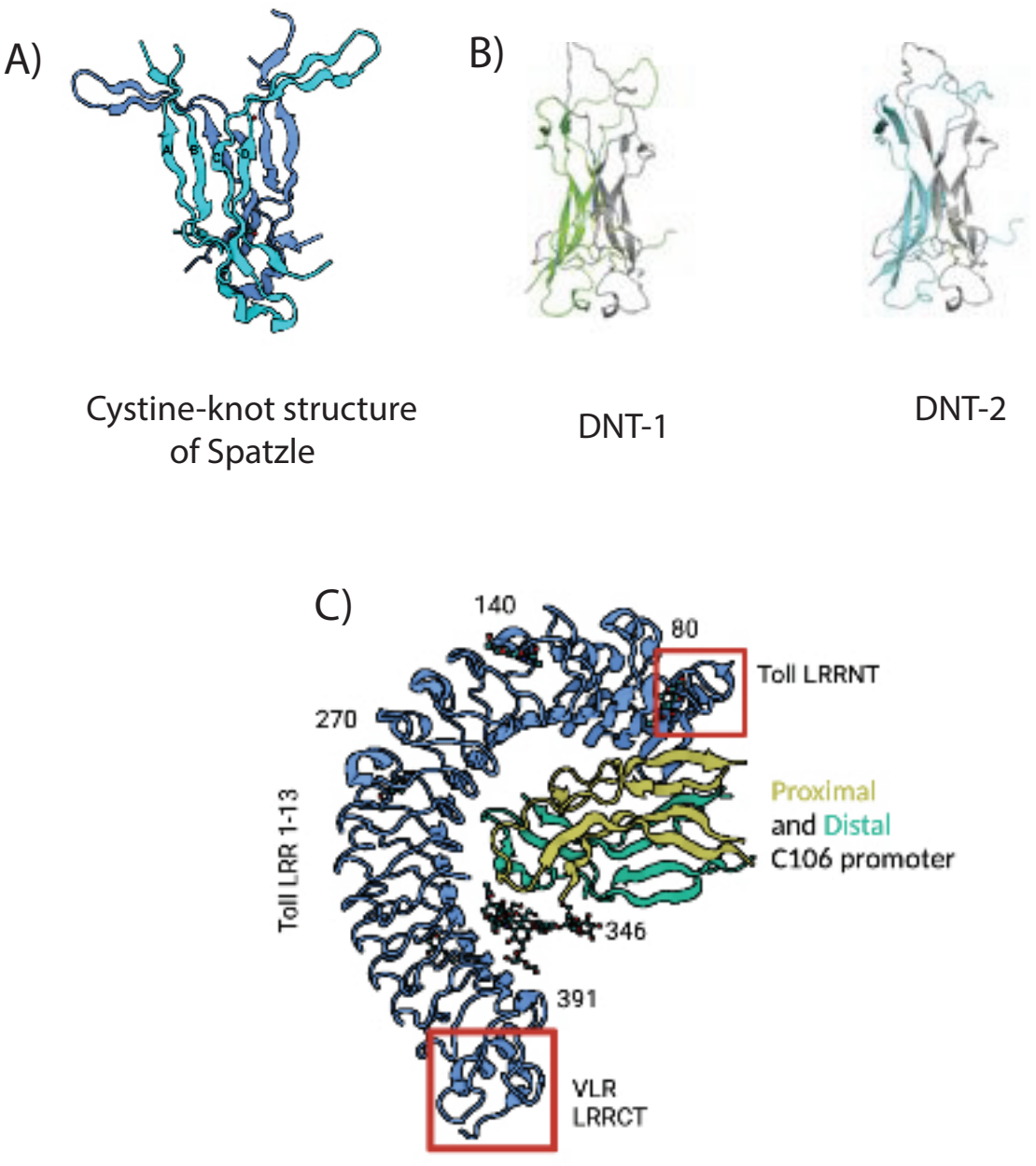


Figure 1.3: Structure of Toll ligand
A) The illustration of Spz C106 is depicted as a schematic, showcasing four-stranded antiparallel β-sheets labeled A to D as described in Lewis et al., 2013, B) Strucure of DNT-1 and DNT-2 as described in Foldi et al., 2017 C) The overall structure of Toll–Spz C106 as described in Lewis et al.,2013 involve glycan structures attached to Asn residues at positions 80, 140, 270, 346, and 391, with the first N-acetylglucosamine residue playing a crucial role in this interaction.

In the three tier mechanism paper by (Foldi et al., 2017), it was first demonstrated that the receptor binding interface of *Spz* is different and not evolutionarily conserved in DNT1 and DNT2. The pro-domains of Spz, DNT-1, and DNT-2 exhibit differences, with DNT-1 having a pro-domain twice as long as that of DNT-2. Furthermore, Spz pro-domain lacked furin sites whereas multiple highly conserved sites were identified in DNT1 and DNT2. Additionally, western blots upon overexpressing full length DNT1 and DNT2 tagged with anti-GFP in the retina revealed that DNT1 predominantly found in its pro-form and DNT2 in its mature form. This suggest that Spz, DNT1, and DNT2 are distinct neurotrophins with differing processing mechanisms.

The DNT's and *Spz* are also expressed and functions in the larval CNS (Sutcliffe et al., 2013, Ulian-Benitez et al., 2017). DNTs interact with Kek and Toll receptors to regulate structural plasticity and affect neuromuscular junction in the larvae (Ulian-Benitez et al., 2017). In adult flies, overexpression of pro DNT1,2 in the retina increased the number of pJNK+ cells compared to the control, indicating that Pro-DNTs are apoptotic (Foldi et al., 2017). Pro-DNTs could be cleaved intracellularly and secreted as mature DNT's. Furthermore, stimulation of Toll-6 and Toll-7 transfected S2 cells with purified mature DNT2-CK resulted in the induction of *Dorsal* or *Dif* phosphorylation, suggesting that mature DNT2-CK activates NF-kB signalling (Foldi et al., 2017). In-vivo, overexpression of mature DNT1-CK and DNT-2-CK in retina revealed that DNT1 and DNT2 activate the pro-survival signalling pathways NF-κB and ERK through Toll-6 and Toll-7, while pro-DNT1 activates the proapoptotic JNK pathway (Foldi et al., 2017). This implies that pro-DNTs promote apoptosis, while mature DNTs promote cell survival.

In summary, Spz, DNT-1, and DNT-2 are ligands that bind to Toll receptors, activating the Toll signalling pathway. Once activated, this pathway performs varied functions, including establishing dorsal-ventral polarity in embryos, activating the innate immune response, and regulating cell death and survival in the CNS. Since different ligands can activate Toll signalling, entomopathogenic fungi may secrete compounds analogous to Toll ligands that can activate the Toll pathway to increase cell death and kill the host.

1.4.2 Toll signalling and function in the immune system

Toll receptor signalling also activates an immune response via Dif in the *Drosophila* (Lemaitre et al., 1996). Toll is a central receptor which regulates several aspects of *Drosophila* immune responses, such as the melanisation cascade, resistance to bacteria, and blood cell activation (Brennan and Anderson, 2004). Genetic analysis of *Toll* and *imd* mutants suggested the involvement of two signalling pathways in activating the immune response in *Drosophila* against bacteria and fungi (Figure 1.4) (Lemaitre et al., 1995).

The first pathway activates Toll signalling in response to gram positive bacteria and fungi. Pattern recognition receptors (PRRs) recognize conserved molecular epitopes or pattern associated molecular patterns (PAMPs) such as B-glucan and peptidoglycan present on the surface of the pathogens (Hultmark, 2003). Gram-positive bacteria are recognised by members of the PGRP family receptors, namely PGRP-SA (Figure 1.4) and PGRP-SD (Michel et al., 2001, Bischoff et al., 2004). GNBP3 is recognized for its role in detecting fungi, and studies have revealed that overexpressing GNBP3 alone can activate Toll signalling in the absence of fungal

Figure 1.4 : Activation of innate immunity by Toll and IMD pathway

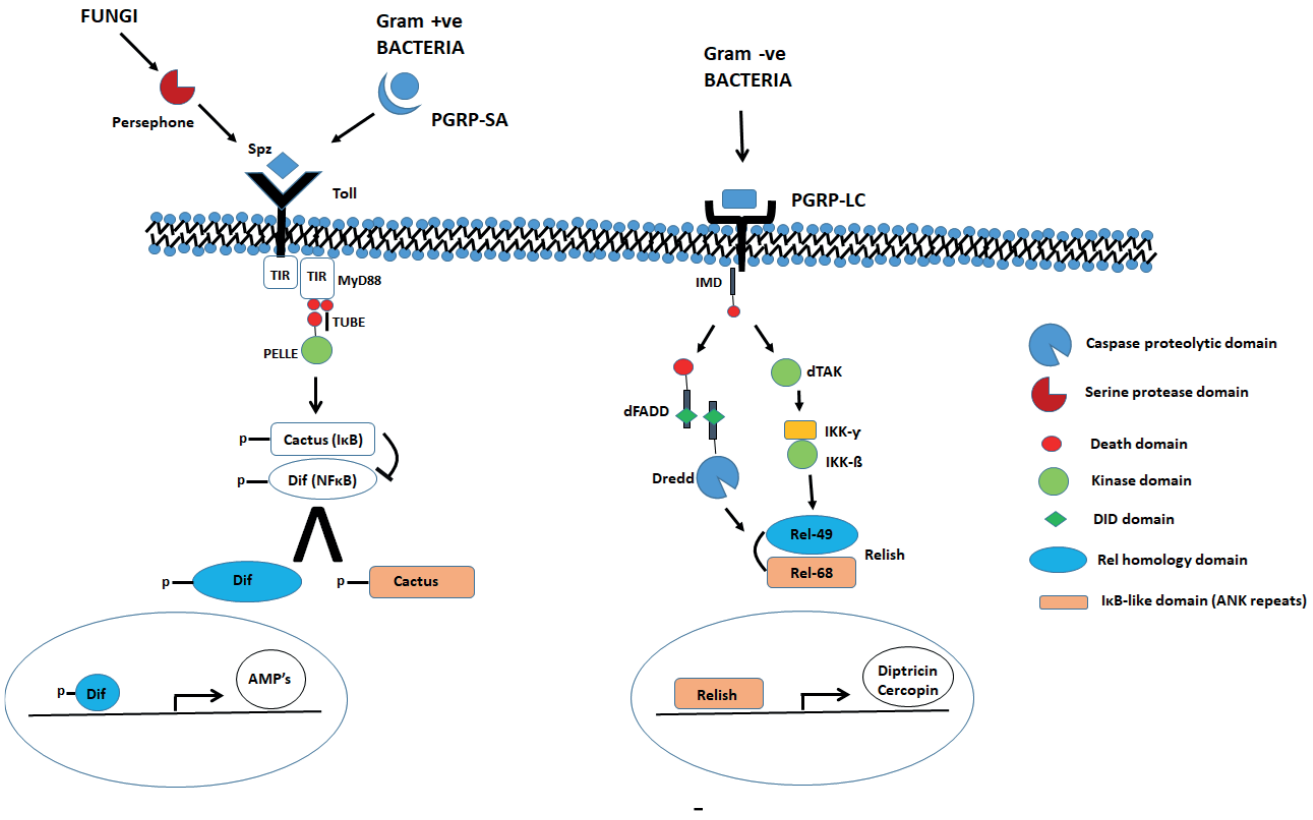


Figure 1.4: Activation of innate immunity by Toll and IMD pathway
The figure illustrates that the Toll-1 signalling pathway activates the innate immunity via MyD88-NF-κB. However, in response to the gram-negative bacteria the innate immunity is activated via the IMD pathway. This figure is adapted from Hultmark et al., 2003 and Brennan et al., 2004

infection (Gottar et al., 2006). This fundamental sensing mechanism is ancient, as homologs of GNBP3 were also found in lepidopteran and hymenopteran insects, both of which share a common ancestor with *D. melanogaster* from 420 million years ago (Ochiai and Ashida, 2000). *Drosophila* can also sense fungi independent of GNBP3 receptors, indicating towards the existence of a secondary sensing system (Ferrandon et al., 2007, Gottar et al., 2006, Ligoxygakis et al., 2002).

A previous report has demonstrated an upregulation of *drosomycin* upon natural infection by *B. bassiana* in GNBP3 null mutants and *spz* mutants, suggesting that flies can sense *B. bassiana* in a GNBP3 independent manner (Gottar et al., 2006). Presephone (psh) is a serine protease encoding a clip pro-domain, which activates immune toll signalling only in response to *B. bassiana*, as *psh* mutants showed resistance to bacterial infection but increased susceptibility to natural infection by *B. bassiana* (Ligoxygakis et al., 2002). Loss of function GNBP3 and *persephone* (*psh)* double mutant flies resulted in early mortality upon infection compared to single mutant flies, indicating that GNBP3 and psh function in two distinct pathways that work together upstream of Toll to detect fungal infections (Gottar et al., 2006).

B. bassiana spores secrete PR1 protease, which degrades the fly cuticle (Clarkson and Charnley, 1996). PR1 mutants failed to induce *drosomycin* in adult flies, while overexpression of PR1 induced *drosomycin* expression in the absence of immune challenge (Gottar et al., 2006). Moreover, co-expression of PR1 and Psh upregulated *drosomycin* in the absence of immune challenge, suggesting that PR1 can activate *psh* directly which further activates Toll signalling (Gottar et al., 2006, Ligoxygakis et al., 2002).

In summary, PR1 is a virulence factor that directly triggers the activation of Persephone, a haemolymph zymogen presents in adult flies. Once activated, Persephone matures into an active protease, which in turn activates Spätzle, a ligand for the Toll receptor, leading to the activation of the Toll signalling pathway.

Fungi recognition by the PRRs initiates proteolytic cleavage of Spätzle by the Spatzle Processing Enzyme (SPE), activating toll signalling (Figure 1.4) (Weber et al., 2003, Hu et al., 2004, Jang et al., 2006). These events activate a cytoplasmic cascade involving Myd88, Pelle and Tube*,* resulting in the phosphorylation and degradation of Cactus, permitting nuclear translocation of NF-kB factor Dif (Brennan and Anderson, 2004, Lemaitre et al., 1996, Ip et al., 1993, Wu et al., 2015). This initiates expression of several antimicrobial peptides (AMP's) that protect *Drosophila* from fungal and bacterial infections.(Brennan and Anderson, 2004).

A Second pathway activates IMD signalling in response to gram negative bacteria (Figure 1.4) (Lemaitre et al., 1995). NF-kB Relish plays a crucial role in the regulation of humoral immunity as it undergoes proteolytic cleavage within seconds of infection, resulting in the formation of two distinct parts (Stöven et al., 2000). The first part is an N-terminal, Rel homology DNA binding domain that translocates to the nucleus and activates AMPs, and the second part is a C-terminal IkB like protein that remains in cytoplasm (Stöven et al., 2000). This signal dependent cleavage of Relish is mediated by the *Drosophila* IkB kinase complex consisting of IKK(beta) and IKK(gamma) (Silverman et al., 2000). Analysis of the null mutants of human MAP kinase homolog in flies, dTAK1, has revealed that dTAK1 null mutant flies fail to induce an immune

response after bacterial infection (Vidal et al., 2001). This indicated that proteolytic cleavage of Relish can also be mediated via a different protein, dTAK1. Genetic analysis has further demonstrated that dTAK1 is upstream of the IKK complex and downstream of IMD protein (Leulier et al., 2002, Vidal et al., 2001). Finally, IMD protein have death domain similar to mammalian RIP (receptor interacting protein) and overexpression of the IMD protein causes apoptosis that can be blocked by a kinase inhibitor (Georgel et al., 2001).

Antimicrobial peptides belong to a class of small, positively charged peptides that exert their antimicrobial effects by targeting the negatively charged membranes of microbial cells (Lai and Gallo, 2009, Brogden, 2005). When the immune system is activated due to a pathogenic challenge, the expression of several AMPs is initiated. These AMPs integrate into the negatively charged microbial membrane, leading to its destabilization and subsequent cell death of pathogenic microbes (Joo et al., 2016). There are several specialized AMPs that detect and combat both fungal and bacterial pathogens. For instance, Drosomycin and Metchnikowin are peptides secreted in response to fungal pathogens (Fehlbaum et al., 1994, Levashina et al., 1995) while Drosocin, Attacin, and Diptericin respond to bacterial pathogens (Kragol et al., 2001, Åsling et al., 1995, Cudic et al., 1999, Hedengren et al., 2000, Bulet et al., 1996). Other AMPs, such as Cercopins and Defensins, display both antifungal and antimicrobial properties (Hultmark et al., 1980, Ekengren and Hultmark, 1999, Cociancich et al., 1993, Tzou et al., 2002). While many of these genes are highly induced in the fat body in response to systemic infection, others are expressed in various other tissues, such as the trachea, gut, ganglia, or reproductive tracts (Ferrandon et al., 1998, Tzou et al., 2000). Recently, a new class of antimicrobial peptides, known as Bomanins, has been

discovered. Bomanins are composed of a 16-residue domain and are regulated by the Toll pathway (Clemmons et al., 2015). Bioinformatics analysis has identified a family of 12 genes associated with Bomanins, and deleting 10 out of these 12 genes leads to a decrease in fly survival similar to the Toll pathway signaling (Clemmons et al., 2015). These findings underscore the diverse expression patterns of antimicrobial peptides, highlighting their versatility and significance in the immune defense system against various pathogens.

1.4.2.1 Function of Toll receptors in immunity

There are some reports that suggest that Toll-5 may possess an immune function. Chimeric construct of Toll-5 activated the promoter of drosomycin in S2 cells (Tauszig et al., 2000). While drosomycin was activated, none of the gene promoters for antibacterial peptides could be activated by the Toll-5 chimera construct in the transfection assay (Tauszig et al., 2000). However, previous report has shown that drosomycin can also be activated independently of Toll signalling (Ferrandon et al., 1998, Gottar et al., 2006). Therefore, it is not clear whether Toll-5 can also activate the innate immune response.

Structural analysis has revealed that Toll-9 is the only *Drosophila* Toll receptor that exhibits structural similarity with mammalian TLRs (Bilak et al., 2003, Imler and Zheng, 2004). Toll-9 activates the drosomycin promoter upon microbial challenge similar to Toll-1 gain of function mutants, indicating that Toll-9 might function in immunity (Ooi et al., 2002). Later, a study reported that the anti-microbial peptides diptericin and drosomycin are upregulated in Toll-9 loss-of-function null mutant adult flies after gram-

negative bacteria ingestion (Narbonne-Reveau et al., 2011). This suggested that Toll-9 is not required to mount an anti-bacterial response.

In summary, only Toll-1 plays a role in immunity, while the majority of *Drosophila* Toll receptors are not involved in immune function.

1.4.3 Toll signalling in development

Several Toll receptors in *Drosophila* are expressed in high levels during critical developmental stages of embryogenesis and metamorphosis suggesting their roles in development (Tauszig et al., 2000).

The Drosophila Toll-Dorsal pathway is best characterised for establishing the *dorsal-ventral* patterning of the embryo (Figure 1.5) (Anderson and Nüsslein-Volhard, 1986). Analysis of gain and loss of function mutations of the *Toll* receptor has revealed that the Toll protein is distributed uniformly around the circumference of the dorsal-ventral region of the embryo and act as a receptor of Spätzle (Spz), which is secreted in the perivitelline space of the embryo (Stathopoulos and Levine, 2002, Schneider et al., 1991). The Spz gets cleaved by Easter and binds to Toll receptor to activate Toll signalling, thus triggering a cytoplasmic signalling pathway involving Tube, Pelle and Cactus, which control the expression of NF-kB transcription factor Dorsal (Morisato and Anderson, 1994, Weber et al., 2003, Belvin and Anderson, 1996b). These specific components of Toll-Dorsal pathway were identified by analysing the phenotypes caused by mutations in the *Drosophila* embryo, as maternal effect mutation in *tube*,

Figure 1.5: Toll signalling in establishing dorsal-ventral patterning in *Drosophila* embryo

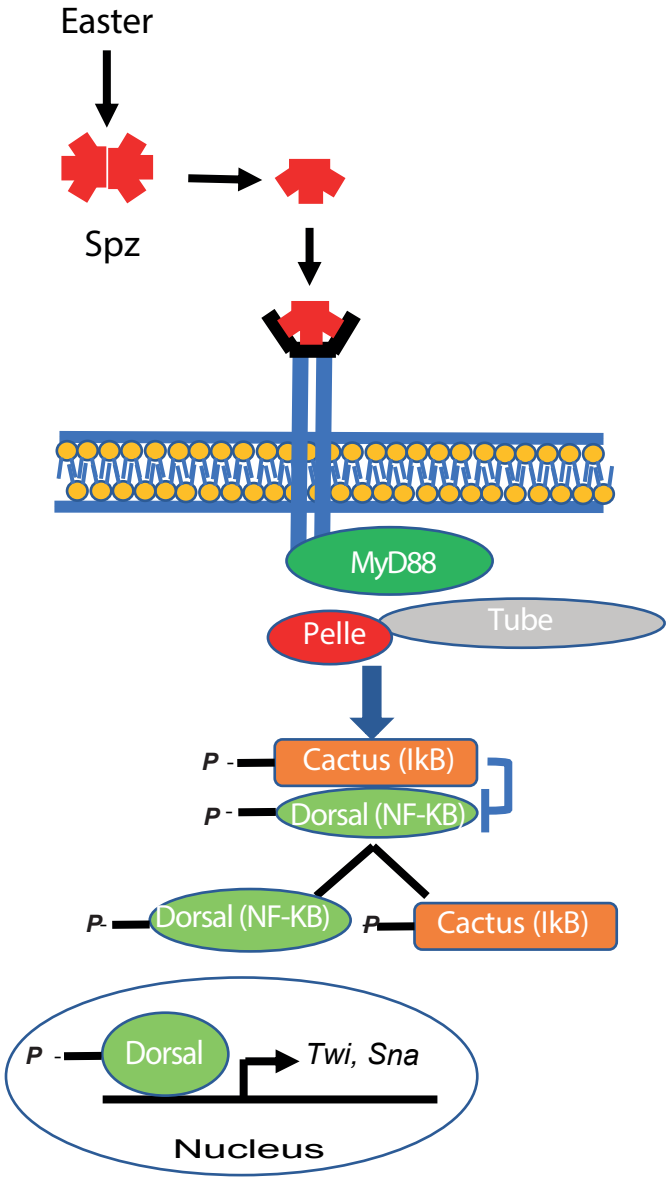


Figure 1.5: Toll signalling in establishing Dorsal ventral patterning in *Drosophila* embryo

In the Spatzle-Toll pathway, Spz is cleaved by a serine protease, Easter, after which the cleaved Spz binds to the Toll receptor and activates it. The cytoplasmic signalling then triggers the degradation of Cactus and nuclear localization of Dorsal. Dorsal initiates the expression of *twist* and *snail*, which are crucial for establishing dorsal-ventral patterning in Drosophila embryo.

pelle, Toll, spz and dorsal caused dorsalization of the embryo (Hecht and Anderson, 1993).

In the resting state, prior to Toll receptor activation by Spz, the IkB family protein Cactus is bond to the NFkB family protein Dorsal in the cytoplasm (Belvin and Anderson, 1996b). Toll activation leads to the degradation of the Cactus/Dorsal complex in the Cytoplasm (Hecht and Anderson, 1993, Belvin and Anderson, 1996b, Moussian and Roth, 2005).

Myeloid Differentiation factor 88 (MyD88) is a downstream adaptor protein that binds to the TIR domain of activated Toll and recruits Tube and Pelle to plasma membrane (Medzhitov et al., 1998). *tube* and *pelle* are two maternally transcribed genes that act between the Toll and Dorsal/Cactus complex (Hecht and Anderson, 1993, Belvin and Anderson, 1996b). *tube* and *pelle* interact with each other to form a complex which activates *pelle* (Belvin and Anderson, 1996b, Xiao et al., 2012). Activated Pelle act as a protein kinase which phosphorylates and degrade Cactus, leading to the release of the transcription factor Dorsal*,* which translocate to the nucleus and regulates the expression of different genes responsible for dorsal-ventral axis formation in embryo (Moussian and Roth, 2005).

Nuclear Dorsal drives the expression of *twist (twi)* and *snail (sna)* which shapes the ventral midline and CNS (Stathopoulos and Levine, 2002). *Twist* and *Snail* drive the formation of mesoderm, mesectoderm and neuroectoderm. Mesoderm forms muscle, mesectoderm forms ventral midline and neuroectoderm forms the CNS (Stathopoulos and Levine, 2002). Hence, through these pathways Toll signalling mediates the

formation of the nerve cord at the ventral midline and heart at the dorsal midline of the embryo.

1.4.3.1 Function of Toll receptors in development

The Toll-Dorsal pathway have other functions as well. Null mutations in *Toll*, *tube*, *pelle* and *cactus* decreased the homozygotes survival to adult stages and result in shorter pupae (Letsou et al., 1991, Belvin and Anderson, 1996a). This indicates that *Toll*, *tube*, *pelle* and *cactus* also regulate body shape. Invitro analysis has shown that heat shock induced expression of Toll in S2 cells causes cellular aggregation (Keith and Gay, 1990). Immunostaining of S2 cells with anti-Toll antibody upon heat shock induced expression of Toll has indicated the expression of Toll at the plasma membrane at cell-cell interaction (Keith and Gay, 1990). These findings suggest that Toll protein may also have role in cell adhesion.

In situ hybridization detected Toll-2 mRNA transcripts in the epithelium of ovarian follicle cells undergoing posterior and centripetal migration (Kleve et al., 2006). Loss of function mutant clones showed delayed migration of ovarian follicle cells, suggesting that Toll-2 facilitates cell migration (Kleve et al., 2006). Studies have speculated that Toll-1 might also function as cell adhesion protein (Wang et al., 2005a, Rose et al., 1997, Halfon et al., 1995). In addition, in situ hybridization revealed the expression of Toll-1 transcript in cardioblast surface and in the secondary phase of heart formation (Wang et al., 2005a). Toll-1 deficient mutant embryo showed defects in dorsal vessel structure (Wang et al., 2005a). These reports indicate that Toll-1 might mediate cell-cell interaction between muscle and motor neurons and in heart

development. However, these studies did not show whether these functions are due to direct interaction between Tolls.

Fluorescent in situ hybridization has demonstrated the expression of Toll-2, Toll-6 and Toll-8 in the overlapping transverse stripes along anterior posterior axis (Paré et al., 2014). Loss-of-function mutations of Toll-2, 6 and 8 *eve* and *runt* mutant embryos revealed defects in cell intercalation, convergent extension, and planar cell polarity (Paré et al., 2014). These finding suggest that eve and runt regulated transcription of Toll-2, 6 and 8 mediates cell-cell interaction to drive convergent extension. To conclude, Tolls could also act as cell adhesion proteins. Toll-1, 2, 6, and 8 can mediate cell-cell interaction, and Toll-2 could facilitate cell migration.

1.4.4 Toll signalling and functions in the nervous system

Work from our lab has demonstrated that Toll receptors interact with neurotrophins that can either promote cell death via Wek-Sarm-JNK pathway and cell survival via MyD88-NFkB pathway in the larva and early pupa CNS (Figure 1.6) (Foldi et al., 2017, McIlroy et al., 2013). Toll-6 and Toll-7 loss-of-function mutants showed an increase in anti-cleaved caspase 3 labelled apoptotic cells in the embryonic VNC, which was rescued by overexpression of Toll-6 and Toll-7, thus confirming that Toll-6 and Toll-7 are required for neuronal survival (McIlroy et al., 2013). In vitro, the addition of DNT2CK shifted the protein mobility of the extracellular domain of Toll-6 and Toll-7, with an appearance of a new band on the top of the native gel compared to controls, indicating the interaction of DNT2 with Toll-6 and Toll-7 (McIlroy et al., 2013). Furthermore, the coimmunoprecipitation assay in S2 cell culture showed the

Figure 1.6 Toll signalling pathway in CNS

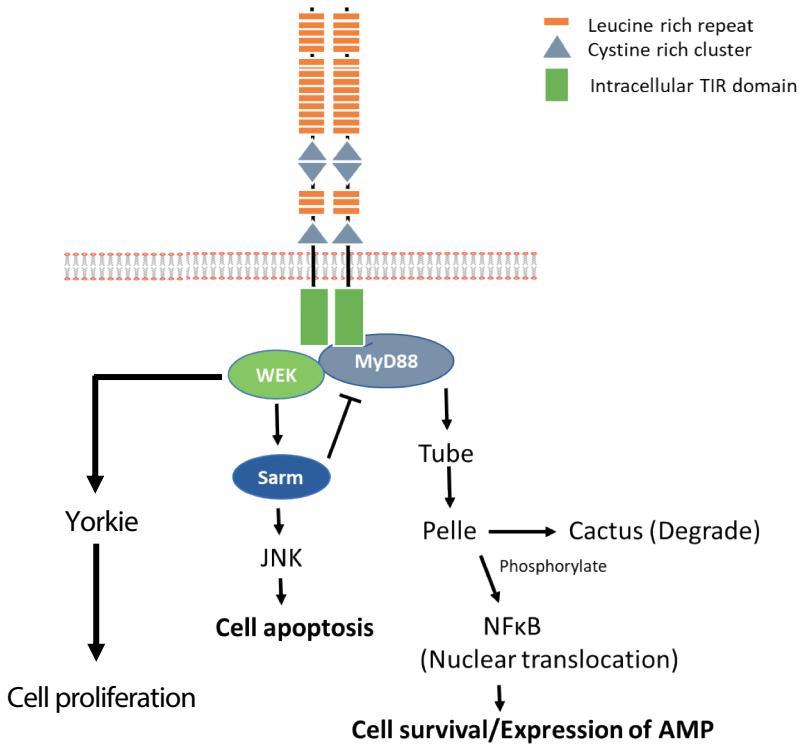


Figure 1.6 Toll signalling pathway in CNS

The figure illustrates the Toll signalling pathway promotes apoptosis via Wek, Sarm, and JNK as well as promotes cell survival via MyD88, NFκB pathway. This figure is adapted from Foldi et al., 2017 and Li et al., 2020

interaction between DNT1 and Toll-7, and between DNT2 and Toll-6 (McIlroy et al., 2013). Additionally, in vivo, transgenic flies overexpressing DNT-1-CK and full length Toll-7 were coimmunoprecipitated together, suggesting that DNT-1 binds with Toll-7 (McIlroy et al., 2013). Together, these findings suggest that DNT-1 function as a ligand for Toll-7 and DNT-2 is a ligand for Toll-6 and Toll-7.

The coimmunoprecipitation data from in vitro experiments showed that MyD88 co-purified with Toll-6 and Toll-7, indicating that MyD88 is downstream of Toll-6 and Toll-7 (Foldi et al., 2017). Additionally, MyD88 protein was found in the embryonic CNS neuropile. When Toll-6 and MyD88 are overexpressed in the *Drosophila* larvae, the number of Toll 6 neurons (marked by Eve) increased, which suggests that Toll-6 could physically bind with MyD88 and promotes cell survival (Foldi et al., 2017). These findings imply that both Toll-6 and Toll-7 can interact with MyD88 both in vitro and in vivo. Interestingly, upon neuronal overexpression of MyD88, Toll-6 and Toll-7 induced apoptosis in pupae. Moreover, Toll-6 induced apoptosis in the MyD88 mutant background. This suggest that Toll-6 could promote apoptosis independently of MyD88 in pupae.

The decreased number of Eve+ neurons in the pupal ventral nerve cord (VNC) upon neuronal overexpression of dSarm, both in normal and MyD88 mutant backgrounds, suggests that dSarm induces apoptosis. Moreover, the number of DCP1+ apoptotic cells decreased when JNK was downregulated with JNK-RNAi in neurons overexpressing dSarm. Furthermore, the co-immunoprecipitation assay revealed that dSarm was co-purified with precipitated MyD88. Together, these data demonstrate that dSarm promote apoptosis via JNK pathway by inhibiting MyD88. However, S2

cells that were co-transfected with *Toll6-Flag* or *Toll7-Flag* and *dsarm-HA* revealed that Toll-6 or Toll-7 did not co-precipitate with dSarm, indicating that dSarm does not directly bind to Toll-6 to induce apoptosis.

The co-transfection of S2 cells with Toll6-Flag or dsarm-Flag and wekHA demonstrated that Wek was co-precipitated with Toll-6 or Sarm, suggesting that Wek interacts with both Toll-6 and Sarm. Further, rescue of increased apoptosis resulting from Toll6^{cy} overexpression upon loss of Wek function in pupae indicates that Toll-6 requires Wek to promote apoptosis. *wek* loss of function did not rescue apoptosis induced by dsarm overexpression indicate that dSarm works downstream of Wek. Moreover, rescue of apoptosis induced by Wek overexpression upon *dsarm* knockdown suggests that Wek triggers apoptosis upstream of dSarm. Together this data suggest that Wek is positioned downstream of Toll and upstream of dSarm. In summary, Tolls interact with neurotrophins, leading to apoptosis through the Wek-Sarm-JNK pathway.

To conclude, *Drosophila* Tolls modulate development via MyD88-Dorsal pathway, immunity via MyD88-Dif pathway, and induce apoptosis via Wek-Sarm-JNK pathway. Since they are involved in protecting the flies and regulating cell number, entomopathogenic fungal pathogens could hijack the Toll signalling pathways to cause neurodegeneration in their host.

1.4.4.1 Function of Tolls in the CNS

A genetic mosaic screen revealed Wek as a maternal gene involved in the determination of the dorsoventral axis in the embryo, encoding a zinc finger

transcription factor (Luschnig et al., 2004, Ashburner et al., 1999). This suggests that Wek can localize in nuclei. However, Wek is also found in the plasma membrane of the embryo, as it colocalizes with phosphotyrosine on the membrane (Chen et al., 2006). Moreover, Wek binds to Toll and suggested to be required for membrane localization of dmMyD88 (Chen et al., 2006). Overexpression of *wek* in transfected S2 cells failed to induce *drosomycin*, and downregulation of *wek* in S2 cells using RNAi had a minimal effect on the induction of the *drosomycin* promoter by toll suggesting that it is not essential for MyD88 function (Chen et al., 2006). Furthermore, there was no effect on *drosomycin* mRNA induction when *wek* heterozygote and transheterozygote adult flies were challenged with *Micrococcus luteus* and *B. bassiana* (Chen et al., 2006). Both in vitro and in vivo analysis suggest that Wek does not have an immune function.

Our lab has shown that Toll bound with Wek modulates structural plasticity in adult brain by regulating cell number and brain size (Li et al., 2020). Adult specefic overexpression of Toll-2 using Tubulingal80ts increased Toll-2>histoneYFP+ cells and MyD88+ cells in adult central brain and optic lobes (Li et al., 2020). Moreover, neuronal activation of Toll-2 with TrpA1 increased the Toll-2>HisYFP+ neuron number in the medulla which was rescued by Toll2-RNAi knockdown (Li et al., 2020). These findings suggest that Toll-2 modify cell number and neuronal activity, which in turn may impact brain plasticity in the adult brain (Figure 1.6).

Inducing overexpression of Wek and downregulating MyD88, downstream adaptors of Toll signalling, resulted in an increase in cell number (Li et al., 2020). These results suggest that Wek may not only induce apoptosis, but it may also increase cell number

(Figure 1.6). In addition, the increase in cell number caused by Toll-2 overexpression was rescued by knocking down either Wek or Yki (Li et al., 2020). Overexpression of Toll-2 in MARCM clones showed that Toll-2 gain of function promotes cell proliferation in the adult brain, which was confirmed with cell cycle markers PCNA-GFP and FUCCI (Li et al., 2020). Together this data implies that Toll-2 signalling alters structural plasticity in the adult brain by inducing proliferation via Yki downstream in the adult brain (Figure 1.6).

Toll-2 is expressed throughout pupae and adult brain including subesophageal ganglion (SOG) (Li et al., 2020). Loss of function Toll-2 mutants flies showed impaired climbing behaviour (Li et al., 2020). Walking behaviour analysis using Buridan arena showed that loss of Toll-2 mutant flies walked shorter distance and spent less time walking as compared to controls (Li et al., 2020). This behaviour was also found with adult specific knock-down of Toll-2 in neurons with tubulingal80ts (Li et al., 2020). These findings suggest that Toll-2 modulates locomotion behaviour of the adult flies.

Using Toll specific antibody, Toll was found to be expressed in late embryonic CNS and in somatic musculature, and zygotic loss of function Toll mutants showed defects in motor neuron number and muscle patterning (Halfon et al., 1995). Toll null mutant affected R53 motor neurons growth (Rose et al., 1997). In the *Drosophila* pupal brain, Toll-6 and Toll-7 mediates the targeting of projection neurons dendrites and axon of olfactory neurons (Ward et al., 2015). Toll-7 is mainly responsible for targeting olfactory receptor neuron axons, while Toll-6 targets projection neuron dendrites, and both are involved in synaptic matching (Ward et al., 2015). It is important to note that the events mentioned above do not depend on ligand binding, the cytoplasmic

domains of Toll-6 and Toll-7, or downstream nuclear signalling, suggesting that they rely on cell-to-cell contact. However, the formation of connectivity does not depend on direct contact between Toll-7 and Toll-6, and it is currently unclear how it occurs. It is possible that the cell-to-cell functions of Tolls involve both homophilic and heterophilic contacts, but whether other factors are involved is currently unknown.

Recently it has been showed that expression of *spz* mRNA was upregulated in the sleep deprived flies, moreover spz knockdown in the astrocytes hampered sleep recovery after sleep deprivation (Blum et al., 2021). This indicate that Spz could have a role in the regulation of sleep homeostasis. Additionally, RNAi knockdown of Toll receptor in the R5 neuron delayed the sleep recovery following sleep deprivation (Blum et al., 2021). Together this data suggests that astrocytes specific Spätzle and Toll receptors on R5 neurons could be involved in promoting sleep homeostasis (Blum et al., 2021).

The distribution of Toll-6 along the motor axons of the neuromuscular junction (NMJ) of muscle 6/7 was demonstrated using a membrane GFP reporter, mcD8-GFP (Ulian-Benitez et al., 2017). Loss of Toll-6 resulted in a smaller neuromuscular junction with fewer 1b boutons, shorter HRP-positive axon length, and reduced branching compared to control (Ulian-Benitez et al., 2017). Moreover, Toll-$6^{-/-}$ mutants also showed Brp+ active zones suggesting Toll-6 is required for active zone formation (Ulian-Benitez et al., 2017).

Immunostaining with antibodies specific to Toll-7 and GFP-tagged Toll-6MIMICGFP has revealed the expression of Toll-6 and Toll-7 in the embryonic and larvae VNC and

in locomotor circuit including motor neuron, interneurons and dopaminergic neurons in the brain (McIlroy et al., 2013). Both single and double Toll-6 and Toll-7 mutant larvae showed defect in FasII^{+} neurons targeting and axonal misrouting (McIlroy et al., 2013). Moreover, larvae crawling behaviour analysis revealed that Toll-6 and Toll-7 double mutant larvae crawled more slowly than controls (McIlroy et al., 2013). DNT2$^{-/-}$ mutant also crawled slowly and travelled less distance as compared with the controls (McIlroy et al., 2013). DNT2 is a ligand for Toll-6 (Foldi et al., 2017). Together, these findings demonstrate that Toll-6 and Toll-7 is required in the regulation of locomotion and the targeting of motor neurons. In Summary, these findings suggest that Toll-6 is essential for active zone formation and homeostasis, and thus plays a crucial role in modulating synaptic plasticity.

1.5 Mammalian TLRs

The mammalian homologue of Tolls are the Toll-like receptors (TLRs). Mammalian genomes have 10-13 distinct TLRs that directly recognize pathogens and initiate signalling through NF-kB to activate innate and adaptive immunity (Kumar et al., 2009, Akira et al., 2006, Pasare and Medzhitov, 2005). The presence of a conserved intracellular TIR domain and an ectodomain composed of LRRs and cystine-rich clusters in both *Drosophila* Toll and mammalian TLRs suggests a shared evolutionary origin. (Leulier and Lemaitre, 2008, Kumar et al., 2009). One key difference is in the ectodomain, *Drosophila* Tolls have two or more cystine cluster flanking both C and N terminal of LRR domain, while mammalian TLRs have only one cystine cluster at the C-terminal end of LRR domain (Figure 1.7) (Luo and Zheng, 2000a, Gay and Gangloff, 2007). Another major difference between mammalian TLRs and *Drosophila* Toll is the interaction with their ligands (Yagi et al., 2010). Mammalian TLRs are pathogen

Figure 1.7: Structure of mammalian TLR receptor

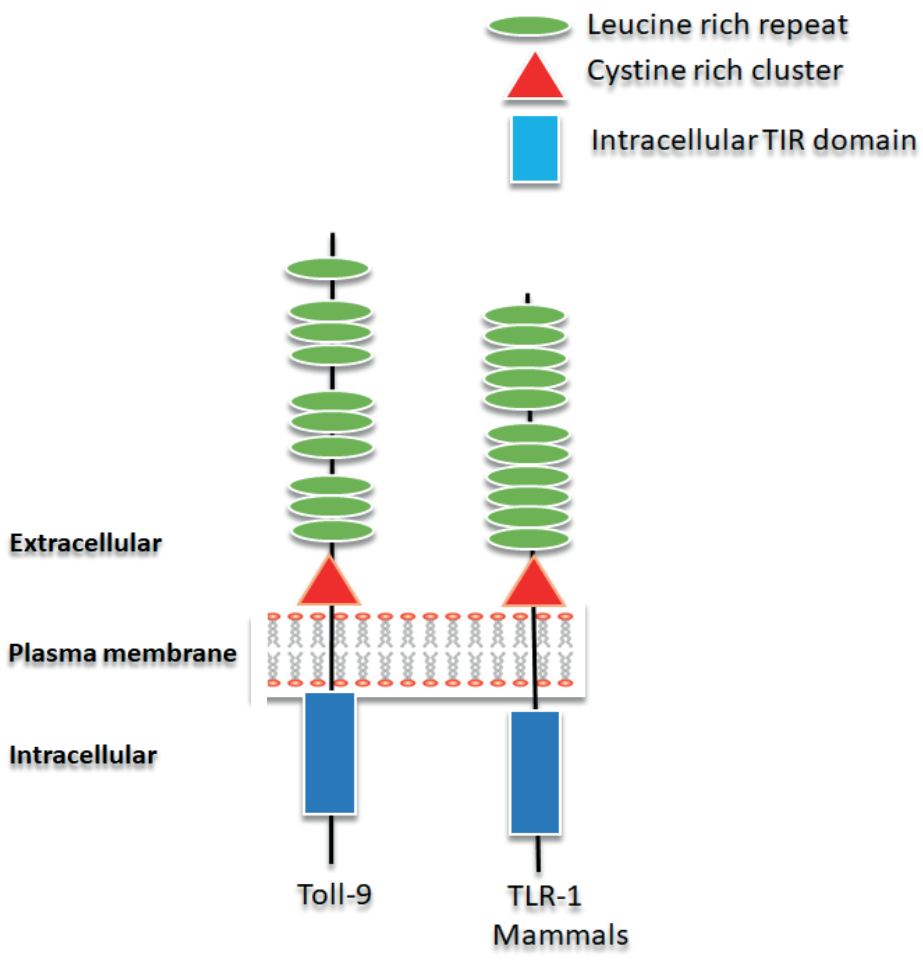


Figure 1.7: Structure of mammalian TLR receptor

The figure illustrates the structural similarity between mammalian TLRs and the Drosophila Toll receptors, only Toll-9 shares similarity with mammalian TLR-1. The figure was redrawn from Tauszig et al., 2000 and Leulier and Lemaitre., 2008

recognition receptors (PRR's) which directly binds to the pattern associated molecular pattern (PAMPs) (Hultmark, 2003), while *Drosophila* Tolls binds to *Spz* ligand instead and initiate a signalling cascade.

Mammalian PRRs can be classified into two divisions: 1) PRR that binds to cell wall of bacteria 2) PRRs that bind to nucleic acid of bacteria or viruses (Kumagai and Akira, 2010). Loss of function mutations in one of TLR genes leads to LPS induced endotoxin shock in mice, this suggest that TLR act as a receptor for LPS (Poltorak et al., 1998). Furthermore, ex-vivo studies and analysis of knockout mice have demonstrated that TLR2 and TLR4 bind to LPS and peptidoglycan present in the outer membrane of bacteria (Means et al., 2000, Takeuchi et al., 1999). TLR-9 deficient mice demonstrated an inhibition in splenocyte proliferation and inflammatory cytokine production from macrophages in response to unmethylated CpG dinucleotides, which is a characteristic of bacterial DNA (Hemmi et al., 2000). This demonstrate that TLR-9 act as a receptor for bacterial DNA. Imidazoquinolinone compounds imiquimod and R-848 are low molecular weight immune activators which have anti-viral and anti-tumour properties. TLR-7 deficient mice responded normally to CpG DNA inducing an immune response but inhibited the splenocyte proliferation and inflammatory cytokine production in response to imiquimod and R848 (Hemmi et al., 2002). This indicate that TLR7 detects antiviral DNA. Together, these findings illustrate that TLR-2 and TLR-4 recognize the surface antigens from bacteria, whereas TLR-7 can detect viral antigens.

Nod-2 belongs to a different class of PRR receptors that regulate host immunity against other microbial pathogens (Shaw et al., 2008). It has been reported that Nod

deficient mice produced less interferons and are unable to clear the *T. gondi* infection from their system (Shaw et al., 2009). This demonstrates that Nod-2 is involved in detecting and mounting an immune response against parasite *T. gondi.* NALP3 is another Nod-2 like receptor recognizes fungal pathogen and upregulates the production of interleukin IL-1β against the fungal pathogen (Gross et al., 2009, Joly et al., 2009, Hise et al., 2009). In addition to recognizing fungal pathogens, NALP-3 inflammasome is also activated by influenza virus and *S. aureus* via an unidentified ligand (Kumagai and Akira, 2010). To summarise, TLRs recognizes wide range of pathogens and activates an immune repone against them in order to protect the host.

1.5.1 Evolutionary arm race between TLR and fungi

The heterodimer of TLR-2/TLR-6 recognizes zymogen which is present in the cell wall of *Saccharomyces cerevisiae* (Underhill et al., 1999, Ozinsky et al., 2000). MyD88 deficient mice lacking the intracellular TIR domain were more susceptible to *Candida albicans* infection, indicating towards the role of TLRs in detecting fungal pathogens (Bellocchio et al., 2004). TLR-2 and TLR-4 detect both *C. albicans* and *S. cerevisiae* (Figure 1.8) (Netea et al., 2002, Bellocchio et al., 2004). The TLR-4 defective mutant mice were more susceptible to *C. albicans* infection and showed a decrease in keratinocyte-derived chemokine (KC) and macrophage inflammatory protein-2 (MIP-2) at the site of infection (Netea et al., 2002). This suggest that TLR-4 provides protection against *C. albicans* by inducing the production of chemokines (Figure 1.8). However, TLR-2 deficient mice were less susceptible to *C. albicans* infection and induced low anti-inflammatory IL-10 and decreased T-regulatory $CD4^{+}$,$CD25^{+}$ cell number at the site of infection (Netea et al., 2004). This suggest that *C. albicans* can engage with TLR-2 to increase the production of anti-inflammatory IL-10 and T-

Figure 1.8: Evolutionary arm race between TLR's and *C. albicans*

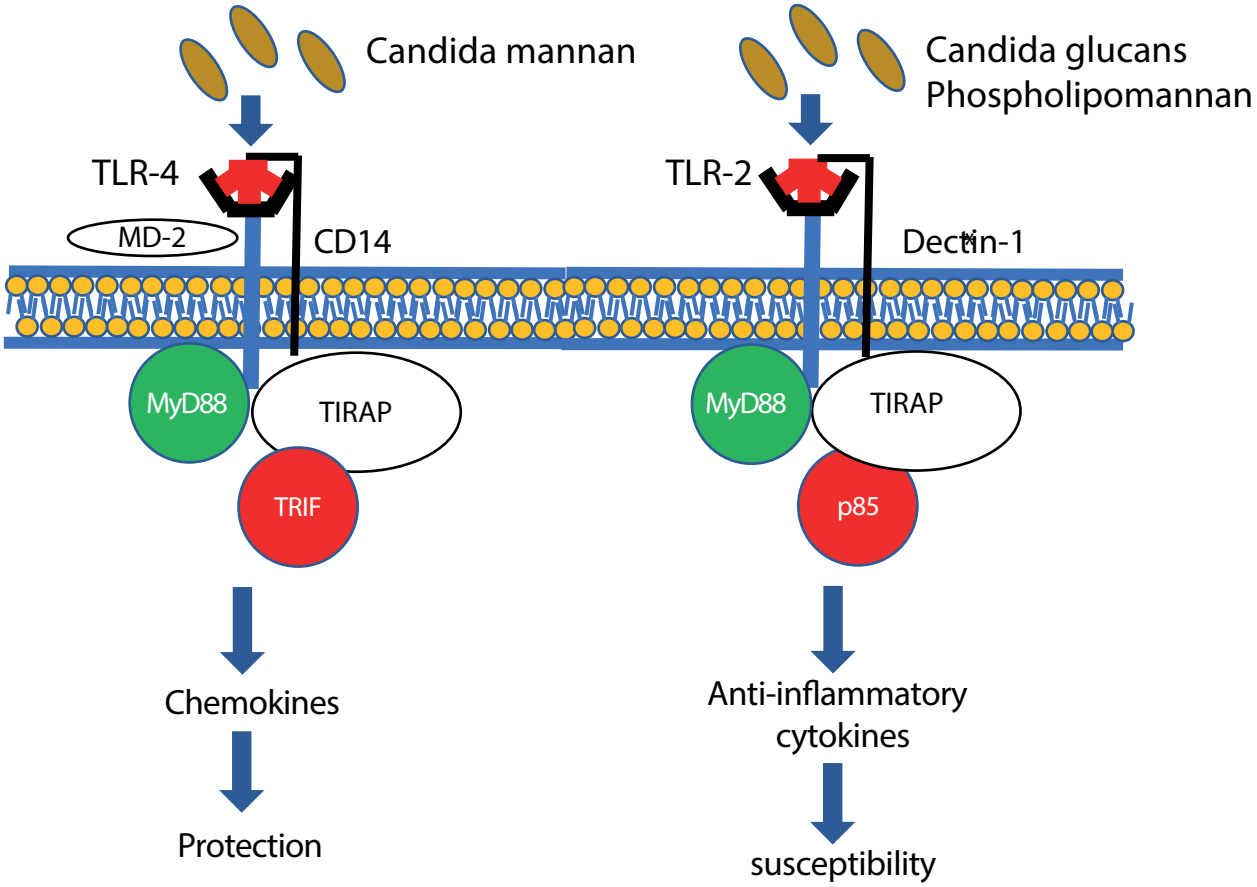


Figure 1.8: Evolutionary arm race between TLR's and *C. albicans*
The figure illustrates an evolutionary race between C. albicans and TLR's. TLR-4 detects C. albicans and triggers the release of chemokines, production of leukocytes, and protection of the host from the infection. On the other hand, C. albicans binds to TLR-2, which leads to increased release of anti-inflammatory cytokines. This process enables C. albicans to evade the host immune response and increase the suceptibility to candida infection. The figure is adapted from Netea et al., 2004.

regulatory cells that makes its mice host more susceptible to *C. albicans* infection (Netea et al., 2007). This is a scenario of an evolutionary arm race between TLR and fungi, where the host tries to protect itself by activating immune response against the *C. albicans* infection by recruiting chemokines. However, *C. albicans* activates TLR to induce anti-inflammatory cytokines to evade host immune defence and increases host susceptibility to infection.

1.5.2 Mammalian TLR signalling

In mammals, there are two distinct signaling pathways that activate TLR signaling: the MyD88-dependent pathway and the TRIF-dependent pathway. TLR-5, TLR-7, TLR-9 and TIR-11 use adaptor MyD88 while TLR-1, TLR-2, TLR-4 and TLR-6 uses adaptor TRIF along with MyD88 in activate downstream signalling cascade (Kumar et al., 2009).

The MyD88-dependent signalling pathway recruits members of the IL-1 receptor-associated kinase (IRAK) family, including IRAK4, IRAK1, and IRAK2, to MyD88 (Kawagoe et al., 2008). IRAK1 and IRAK 2 are orthologues of Drosophila Tube and Pelle (Akira and Takeda, 2004). The activated IRAK family forms a complex with TNF receptor associated factor 6 (TRAF6) and an E3 ubiquitin ligase, which further activates Transforming growth factor Beta activated kinase 1 (TAK1) and TAK1 binding protein (TAB) (Adhikari et al., 2007). This leads to the activation of NF-kB and AP-1 (activator protein-1) transcription factors for inflammatory cytokine genes through canonical IKK complex, MAPK kinase, and JNK pathway (Adhikari et al., 2007).

In the TRIF dependent pathway, NF-kB is activated via TRIF by two different signalling pathway (Imler and Hoffmann, 2003). The interaction between the N-terminal of TRIF and TRAF6 is facilitated by the TRAF6 binding motif, while the C-terminal of TRIF binds to receptor interacting protein-1 (RIP1), with both of these interactions work together to activate NF-kB (Sato et al., 2003, Meylan et al., 2004). TLR3 and TLR 4 activate NF-kB via TRIF dependent pathway and upregulate the expression of inflammatory cytokines (Kumar et al., 2009, Imler and Hoffmann, 2003).

1.5.3 Function of TLR in nervous system

TLRs are widely expressed in the glia, microglia and neurons (Olson and Miller, 2004, Carpentier et al., 2008). When mouse primary microglia are stimulated with several TLR agonists, such as LPS, CPG DNA, and peptidoglycan, the mRNA of innate immune genes is upregulated (Olson and Miller, 2004). This suggests that TLRs mount an immune response in the mouse CNS. After brain injury, Damage Associated Molecular Pattern (DAMPs) activates TLRs, which induce the expression of inflammatory genes to mediate tissue repair (Piccinini and Midwood, 2010). In summary, TLRs have immune function in the CNS from their expression in microglia, upregulating antimicrobial gene expression, clearing pathogen and cell debris. But TLRs also have functions in neurons unrelated to immunity.

TLRs regulate neural proliferation and differentiation. In TLR2 deficient mice, neural progenitor cells (NPC's) only produce astrocytes, whereas TLR2 overexpression results in the production of only neurons (Rolls et al., 2007). By contrast, in TLR4 mutant mice, NPC produce more progeny cell, the majority of which are neurons (Rolls et al., 2007). In Myd88 knockout mice and TLR4, TLR2 double mutant mice, progenitor

cell only produces neuron. This indicates that TLR4 and Myd88 are required for determination of astrocyte fate, while TLR2 is required to determine neuronal fate. Another report has demonstrated that knocking down TLR8 in cortical neurons inhibit neurite growth and causes apoptosis, suggesting TLR8 might be involved in negative regulation of neurite growth and positive regulation of cell survival (Ma et al., 2006b).

1.5.4 Function of TLRs in learning and memory

Several reports have indicated that TLRs affect memory and learning (Okun et al., 2010, Okun et al., 2011, Okun et al., 2012, Madar et al., 2015). TLR2 forms heterodimer with either TLR1 or TLR6, depending upon ligand activating TLR2 (Buwitt-Beckmann et al., 2006). Upon activating TLR2 postnatally with a synthetic lipoprotein isolated from a *Mycoplasma salivarium*, FSL-1, TLR2/6 heterodimerise and improve motor function and fear learning in TLR2 adult mice (Madar et al., 2015). However, postnatal activation of $TLR2^{+/+}$ with Pam3CSK4, TLR2/1 heterodimerise and impaired spatial learning in $TLR2^{+/+}$ adult mice, suggesting TLR2 affect memory and learning in adult mice (Madar et al., 2015).

Performance analysis using a hippocampal dependent cognitive test demonstrated an improvement in spatial memory but reduced fear conditioning in TLR4 deficient mice (Okun et al., 2012). In contrast, when TLR4 was blocked using a pharmacological inhibitor in $TLR4^{+/+}$ adult mice, the spatial memory was not affected (Okun et al., 2012). Therefore, the precise role of TLR4 in memory and learning remains unclear.

The role of TLR3 in hippocampal dependent learning and memory was investigated in adult mice using the Morris water maze (MWM) test (Okun et al., 2010). MWM analysis

revealed that TLR3$^{-/-}$ deficient adult mice showed enhanced working memory compared to wild type adult mice (Okun et al., 2010). When TLR3 was centrally activated using polyinosinic:polycytidylic acid (Poly(I:C)) in adult mice, their performance was impaired compared to peripheral activation of TLR3 using artificial cerebrospinal fluid (aCSF) (Okun et al., 2010). This suggests that central activation of TLR3 may impair working memory. Furthermore, analysis of contextual memory extinction revealed that the memory extinction occurs at a slower rate in TLR3$^{-/-}$ deficient mice compared to wild type adult mice (Okun et al., 2010). Together these finding suggest that TLR3 negatively modulates hippocampal dependent learning and memory.

TLR3$^{-/-}$ deficient adult mice showed an increase in hippocampal CA1 and dentate gyrus (DG) volume as compared to wildtype controls adult mice (Okun et al., 2010). However, hippocampal volume, cortical thickness and number of BrdU+ cells in DG remain unaffected in TLR3 deficient mice as compared to control, indicating that TLR3 is not causing neurogenesis in hippocampus. Furthermore, GluR1 protein which contributes to hippocampus dependant working memory, showed upregulation in hippocampus extracts TLR3 deficient mice but remained unaffected in DG. Therefore, due to lack of evidence, it remains unclear whether TLR3 modulates structural plasticity in the hippocampus.

To conclude, besides their role in identifying pathogens, mammalian TLRs also play a crucial role in regulating cell numbers and cognitive processes such as learning and memory. As TLRs can regulate cell numbers, pathogens may exploit these functions to regulate cell numbers and impact behaviour. Investigating whether pathogens could

use TLRs to their advantage would provide valuable insights into development of new therapeutics against the disease-causing pathogens.

1.6 The model system: *Drosophila melanogaster*

The Fruit fly, Drosophila melanogaster has long been recognised as powerful genetic system and has been used as a model organism for more than 110 years. Due to their small size, simple genetics, rapid life cycle and high similarity to the human genome make them an ideal experimental system for biological research in various fields (Bellen et al., 2010, Lloyd and Taylor, 2010). Drosophila has a sophisticated motor behaviour controlled by a nervous system that show homology to humans (Lloyd and Taylor, 2010). Therefore, Drosophila is used widely to understand the working mechanism of human nervous system. Moreover, complete genome sequencing of Drosophila and human genome has revealed that around 75% of all human disease genes have a fly homologue (Bier, 2005).

These genes can be manipulated by using a wide range of powerful genetic tools developed over last century. One such valuable tool is the P element transposon, which can provide insertion in 40% of the genes (Bellen et al., 2004). Transposons are used to generate transgenic animals and are useful in the UAS/GAL4 system. The UAS/GAL4 system is another tool used for the tissue-specific expression of our protein of interest (Brand and Perrimon, 1993). The UAS-GAL4 system consists of two essential components: a driver line and a responder line (Figure 1.9). The driver line contains the gene encoding Gal4, a transcription factor regulated by a gene-specific promoter. Initially discovered in yeast Saccharomyces cerevisiae as a regulator of genes induced by galactose, Gal4 is composed of 881 amino acids (Laughon and

Figure 1.9: UAS-GAL4 system in *Drosophila melanogaster*

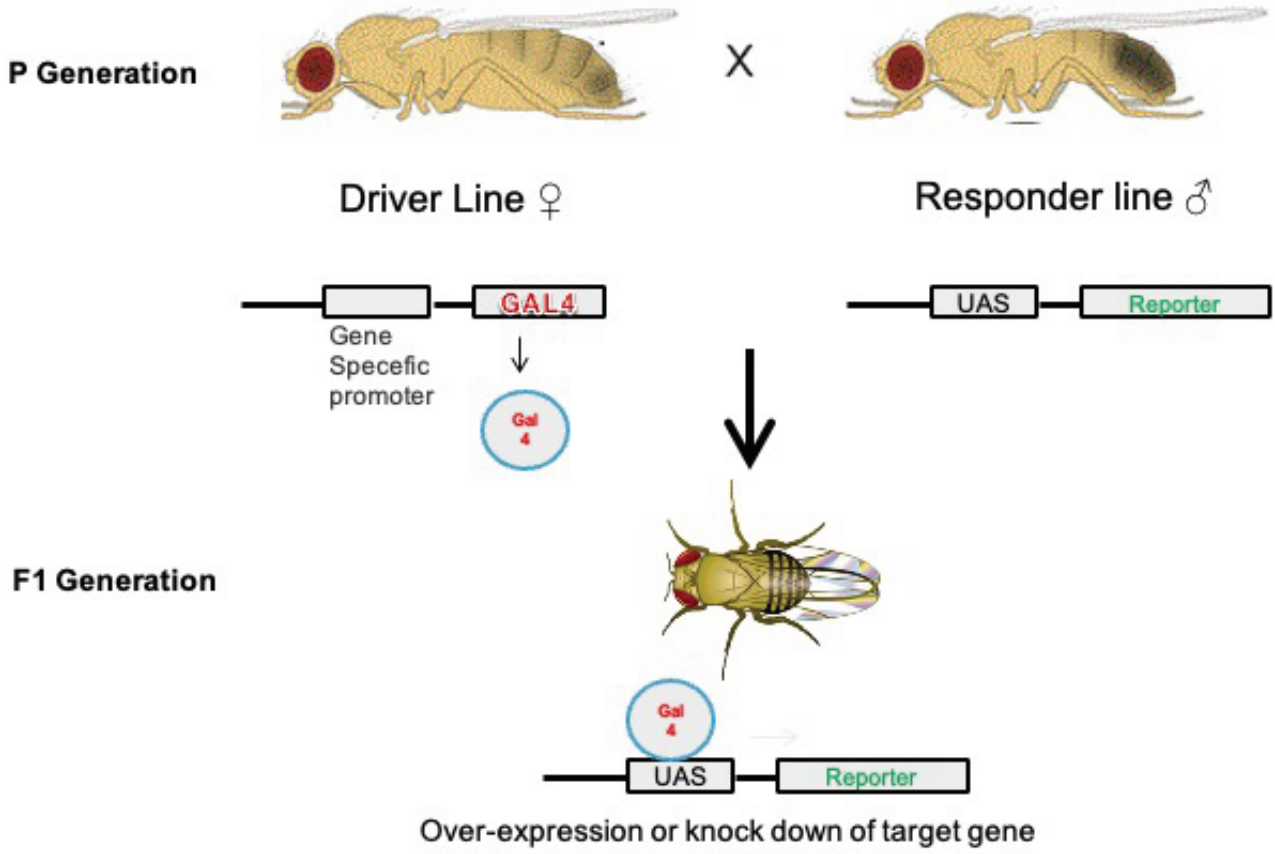


Figure 1.9: UAS-GAL4 system in *Drosophila melanogaster*

The figure provides an overview of the UAS-GAL4 system in Drosophila, a widely utilized genetic tool. This system is composed of two key components: a driver line that expresses GAL4 under the control of a specific gene promoter and a responder line containing a reporter gene (e.g., GFP, YFP), RNAi construct, or gene overexpression downstream of a UAS (Upstream Activating Sequence) element. Upon conducting a cross between flies expressing GAL4 and those containing the UAS-responder construct, GAL4 protein specifically binds to the UAS element, leading to the activation of the downstream reporter gene or the manipulation of the target gene through RNA interference or overexpression.

Gesteland, 1984, Laughon et al., 1984). On the other hand, the responder line contains an upstream activating sequence (UAS) positioned upstream of a reporter, an RNAi knockdown, or an overexpression construct. Transcription of these elements in the responder line requires Gal4 and typically remains inactive in the absence of Gal4. Therefore, to initiate tissue-specific transcription of the reporter, the flies carrying the responder line are crossed with those containing the driver line. Once the resulting progeny is obtained, the reporter, RNAi, or overexpression construct is expressed in a transcriptional pattern that reflects the GAL4 pattern of the corresponding driver. This approach is widely used to precisely control and study gene expression in specific tissues or cells, facilitating investigations into various biological processes and gene functions.

1.6.1 *Drosophila* adult brain structure

Drosophila adult brain is composed of central complex, optic lobes, sub-oesophageal ganglion, mushroom body and antennal lobes. The central complex consists of four substructures protocerebral, bridge, ellipsoid body, fan-shaped body and a pair of noduli. The ellipsoid body is formed by the group of laminated ring neurons which mediated motor control functions and multifaceted sensory integration (Xie et al., 2017). It also mediates navigation and locomotion (Pan et al., 2009). Fan shaped body are required for visual pattern memory and function is processing visual information and sleep (Pan et al., 2009, Xie et al., 2017).

A pair of antennal lobes are situated below the central complex and function in the processing of the olfactory information. The antennal lobes is comprised of highly structures sensory processing network (Silbering et al., 2008). The Sub-oesophageal

ganglion (SOG) is at the ventral side of the optic lobes and consists of the neurons connected to the proboscis and salivary glands. The SOG is known to control proboscis extension and feeding behaviour (Hartenstein et al., 2018).

The SOG is composed of the three fused segmental ganglia that provide neurons to the structure surrounding the proboscis (Hartenstein et al., 2018). The basal part of the SOG is fused with the supraeosophageal ganglion, together they are called subesophageal zone (SEZ) (Ito et al., 2014). On the anterior side SEZ incorporates tritocereberum which is composed of the neuromere innervating the mouth cavity and the gut. The neural circuits present in the tritocerebrum sense food in mouth and generate motor output regulating feeding behaviour (Rajashekhar and Singh, 1994). Labial nerve and the pharyngeal nerves are the two periphery nerves via which the motor and sensory axon connects to the SEZ. The labial nerve carries chemosensory and mechanosensory afferents from maxillary palps and motor neurons in proboscis while pharyngeal nerves receive signals from mouthpart and gut (Rajashekhar and Singh, 1994). There is very little known about the majority of interneurons present in SEZ.

The adult optic lobes are the visual system of the flies and consist of three ganglia medulla, lobulla and lobulla plate (Apitz and Salecker, 2015). The medulla detects colour and is the largest neuropile in the optic lobe (Nériec and Desplan, 2016). Lobulla plate functions in the motion detection whereas lobulla detect orientation and texture (Zhu, 2013).

The mushroom body function in the olfactory memory and learning. It consist of two symmetric neuropil and each neuropil consists of group of cells known as kenyon cells (Heisenberg, 1998). The dendrites of the kanyon cells form a cup shaped calyx with the axons furtur from the neuropils including a a^1, b b^1 and y lobes (Heisenberg 1998). The ab lobes are involved in the long-term memory and y lobe function for the short-term memory (Swinderen 2009).

1.6.2 *Drosophila* dopaminergic system

The *Drosophila* dopaminergic system play important roles in regulating various physiological and behavioural processes such as locomotion, learning, memory, sleep, reward, and motivation (Kasture et al., 2018, Dvořáček and Kodrík, 2021). Dopaminergic system includes several clusters of dopaminergic neurons, namely PAL, PAM, PPL1/2, PPM3, and VUM, located in different region of adult brain (Figure 1.10).

The DAN cluster that projects into the mushroom body lobes are the protocereberal anterior medial (PAM) (Figure 1.10 A) and protocereberal posterior lateral (PPL1) (Figure 1.10 b) (Mao and Davis, 2009, Karthik et al., 2014). Neurons in the PAM cluster functions in reward reinforcement, long term and short-term memory formation, negative geotaxis behaviour and foraging behaviour (Yamagata et al., 2015, Liu et al., 2012, Aso et al., 2012, Sun et al., 2018). PPL1 dopaminergic neurons mediates aversive memory formation and negative reinforcement (Claridge-Chang et al., 2009, Aso et al., 2012).

Figure 1.10: Schematics of dopaminergic neurons in the adult brain

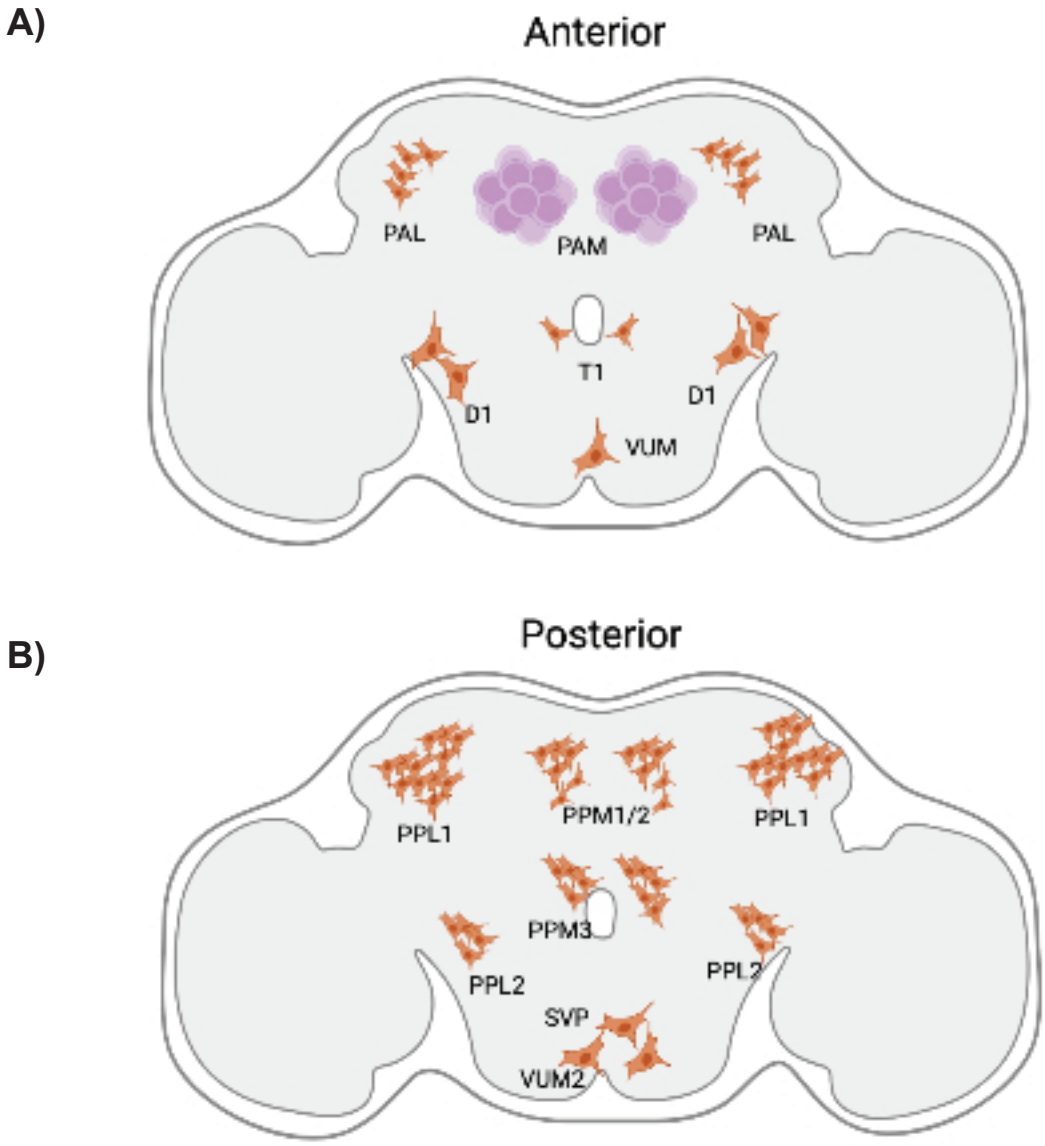


Figure 1.10: Schematics of dopaminergic neurons in the adult brain The figure displays schematics of dopaminergic neurons in the adult brain, illustrating their spatial distribution and organization. **A)** The dopaminergic neurons are categorized into distinct clusters, namely PAL, PAM, T1, D1, and VUM, which are primarily expressed in the anterior part of the brain. **B)** Dopaminergic neurons belonging to the PPL1, PPL2, PPM3, PPM1/2, SVP, and VUM clusters are prominently expressed in the posterior part of the brain.

Dopaminergic neurons in the protocereberal anterior lateral (PAL) cluster are involved in mating drive (Zhang et al., 2016). Activating Protocerebral posterior media (PPM3) cluster neurons and Thoracis 1 (T1) cluster neurons increases aggression in adult flies, suggesting that they might mediate the aggression phenotype (Alekseyenko et al., 2013). Dopaminergic neurons in the VUM cluster are expressed in the SOG and are involved in proboscis extension response (Marella et al., 2012).

In summary, the availability of powerful tools and the simplicity of its genetics make *Drosophila* an excellent model organism to investigate host-pathogen interaction.

1.7 Exposure to fungal volatiles causes neurodegeneration in the adult brain

Poor indoor air quality can lead to flu like symptoms such as dyspnea, watery eyes, itchy skin etc., described by the term sick building syndrome (SBS). Sample analysis from different dampened buildings using HPLC have revealed the presence of several fungal volatiles, such as 2-methyl-1-propanol, 2-methyl-1-butanol, 3-methyl-1-butanol and 1-octen-3-ol (Claeson et al., 2002, Fischer et al., 2008, Matysik et al., 2008). A previous report has demonstrated that upon exposure to fungal volatiles like 1-octen-3-ol, 2-octanone, 2,5DMF and tran-2-octanol decreased life span of adult flies as compared to non-exposed flies (Inamdar et al., 2010). This suggest that fungal VOC's also have a negative effect on the brain.

Inamdar and Bennet showed that adult flies exposed to 1-octen-3-ol died on day 7 as compared to the non-exposed flies (Inamdar et al., 2010). The climbing assay showed that exposed flies took more time to climb 5 cm distance as compared to control non-exposed flies. This indicates that fungal VOCs induce locomotory defects in adult flies.

Furthermore, using a GFP reporter to visualize dopaminergic neurons, they demonstrated that exposure to 1-octen-3-ol caused loss in dopaminergic neurons in PPM1, PPM3, PPL1 and PPL2 clusters. This indicates that exposure to fungal volatiles causes neurotoxicity in dopaminergic neurons.

Additionally, (Inamdar et al., 2013) demonstrated that exposure to 10 ppm concentration of 1-octen-3-ol reduces dopamine uptake in 95% of human embryonic kidney cells expressing human dopamine transporter and human vesicular monoamine transporter (VMAT) orthologue VMAT2. Moreover, Drosophila loss-of-function VMAT mutants exhibited a decrease in longevity and loss of DA-neurons in the adult brain upon exposure to 0.5 ppm 1-octen-3-ol. Overexpression of VMAT using UASdVMAT rescued the reduction in longevity and loss of DA-neurons, indicating that fungal volatiles could affect dopamine uptake and packaging. Later by expressing the human alpha synuclin a report investigated the neural circuit that affect locomotion in *Drosophila* (Riemensperger et al., 2013). Their data unveiled a subset of 15 dopaminergic neurons within the PAM cluster whose progressive dysfunction led to locomotion deficits in adult flies (Riemensperger et al., 2013). Additionally, visualization of these dopamine (DA) neurons' expression pattern using a GFP reporter indicated that they innervate mushroom body (ß) and ß' horizontal lobe. Notably, the locomotion of the flies was severely impaired when these neurons were selectively blocked in the mushroom body (Riemensperger et al., 2013). These observations suggest a significant link between dopaminergic neurons and locomotion. Furthermore, the impact of the fungal pathogen on these dopaminergic neurons could potentially lead to locomotion impairments, reminiscent of Parkinson's disease.

In a broader perspective, these studies aimed to investigate the effect of poor air quality from fungal growth, moldy buildings on human health. However, they only provided evidence for some of the fungal volatiles and not fungal spores which are predominant in poor (moldy and dampened) indoor air (Shi et al., 2014, Provost et al., 2013). Moreover, the mechanism by which the fungal volatiles induced neurodegeneration was not explored. Therefore, further investigation is required to explore the effect of direct exposure to fungal spores on human health. This thesis aims to investigate the impact of direct exposure of fungal spores on the adult *Drosophila* brain.

1.8 AIM

The aim of my thesis was to investigate if *B. bassiana* exploits the Toll signalling to induce neurodegeneration in the adult brain. This was addressed with the following research objective

1. To test whether exposure to *B. bassiana* alters the behaviour of the adult Drosophila flies.
2. To test whether *B. bassiana* can enter the brain and the pathway by which it reaches the brain.
3. To test whether exposure to *B. bassiana* causes neurodegeneration in the brain
4. To test if *B. bassiana* induces neurodegeneration via Toll signalling.
5. To test if *B. bassiana* induces neurodegeneration through Wek and Sarm downstream of the Toll receptor.

Chapter 2

Materials and Methodology

2.1 Genetics

2.1.1 Fly maintenance

The fruit flies were maintained in bottles or vials containing standard cornmeal agar medium. They were cultured at 25°C with a 12-hour light/dark cycle. The stocks were transferred every 5 weeks and kept at 18°C with a 12-hour light/dark cycle. Table 2.1 lists the stocks that were created and utilized for the project.

2.1.2 Genetics protocol

Classical genetics method was used to combine 2nd and 3rd chromosome (Fig 2.1 and 2.2).

2.2 *B. bassiana* culture and spore collection

Beauveria bassiana (80.2 strain) a gift from Jean-Marc. Reichhart and Jean-Luc Imler (University of Strasbourg), GFP transformant of *B. bassiana* (EABb 04/01-Tip GFP5 strain) a gift from our collaborator Prof. Enrique Quesada-Moraga (University of Cordoba) were used in this thesis.

2.2.1 *B. bassiana* spore collection

To isolate *B. bassiana* spores, 10 ml of distilled water was poured on the *B. bassiana* culture in the petri plate and culture was scrapped with a spreader as much as possible without disturbing the agar. The solution was transferred to a 50ml falcon tube using a funnel and centrifuged at 4,000 rpm for 15mins. The supernatant was removed and the pellet was dissolved in the minimum amount of water (2-5ml). This solution was

Figure 2.1 Genetics protocol for generating Tubgal80;SarmNP0257Gal4

Combining 2nd and 3rd chromosome

Stock to make : 1) **Tubgal80ts; SarmNP0257Gal4 / Cyo ; TM6B** 2) **Tubgal80ts; SarmNP7460Gal4 / Cyo ; TM6B**

Required genotypes:

1) IF / Cyo ; MKRS / TM6B

2) yw; + ; SarmNP0257Gal4 / TM6B

3) Tubgal80ts; TM2 / TM6B

G0 Generation : yw; + ; SarmNP0257Gal4 / TM6B X IF / Cyo ; MKRS / TM6B

↓

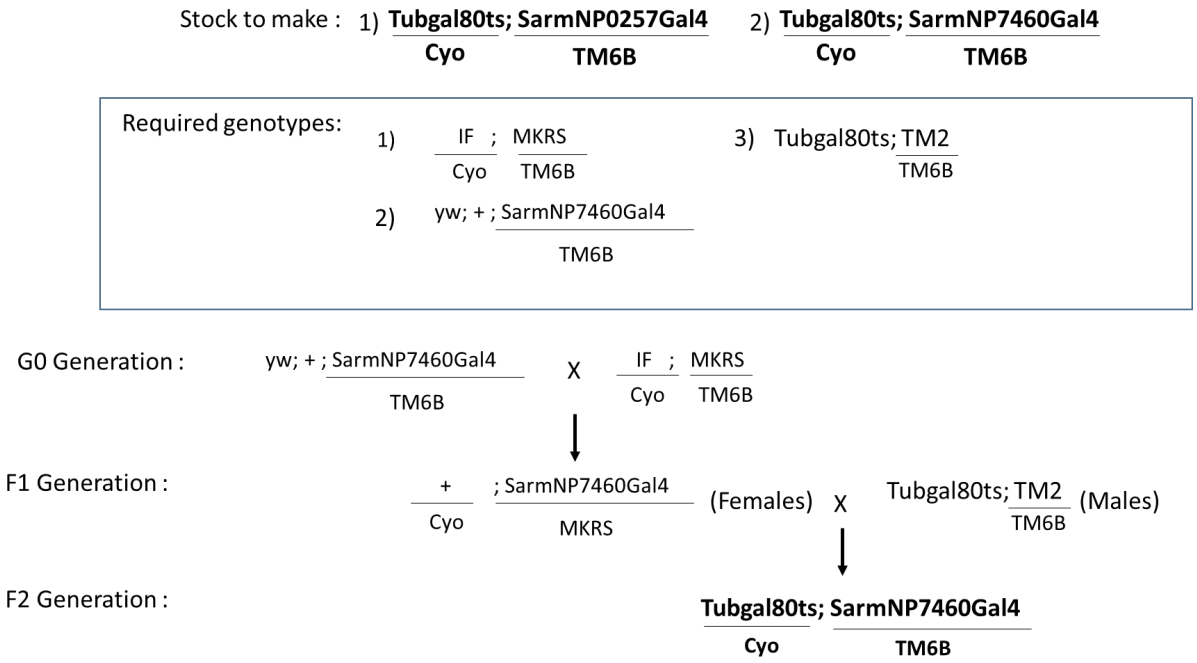
F1 Generation : + / Cyo ; SarmNP0257Gal4 / MKRS (Females) X Tubgal80ts; TM2 / TM6B (Males)

↓

F2 Generation : **Tubgal80ts / Cyo ; SarmNP0257Gal4 / TM6B**

Figure 2.2 Genetics protocol for generating Tubgal80;SarmNP7460Gal4

Combining 2nd and 3rd chromosome



transferred into an Eppendorf tube and centrifuged again for 1-2mins. The supernatant was removed and pellet was dissolved in 1ml distilled water, which was labelled as the principal solution on the Eppendorf. The concentration of the principal solution was calculated by counting spores using a haemocytometer. 10µl of principal solution was diluted in 90µl of water and marked as dilution X10 and spores were counted again by using haemocytometer. The step was repeated until spore conc. of the solution is 3.7 x 10^7 spores/ml. 1ml of the above solution was poured over the SDA media in the glass bottles and then the bottles were transferred to 25°C incubator for 14 days.

2.2.2 *B. bassiana* culture

The plugs were removed from the *Drosophila* glass bottles and autoclaved at 120ºC for 20 mins. To prepare SDA media, 16.25g of 4% SDA was added to 250 ml of distilled water and autoclaved. The hood was then cleaned with 70 % ethanol and the autoclaved glass bottles were placed inside. Next, 10ml of 4% SDA media was transferred into each glass bottle and clean plugs were partially inserted until the media solidified. 1ml of 3.7 x 10^9 spores/ml *B. bassiana* solution was then pipetted and poured into each bottle. The bottles were fully plugged and transferred to 25°C incubator for 14 days.

2.3 Infection chamber

The blade of the packaging knife was heated over a Bunsen burner to cut the 50ml Falcon tube at the 10ml mark and wiped with 70% ethanol. A 12 ml fly food vial was heated in the microwave for 10 sec on a medium setting to melt the fly food. The liquefied fly food was transferred to the nicked falcon tube and kept at 4°C for 10 mins until it solidified. The flies were then transferred to an empty vial and both the flies and

fly food were shifted to the HAPI lab in IMI for infection. The neck of the *B. bassiana* culture bottle was sterilized by exposing it to the Bunsen burner flame. The nicked Falcon tube was wrapped with a double-sided tape and attached to the side of the *B. bassiana* culture bottle with the help of a funnel. The infection chamber was then plugged properly and transferred to the 25°C incubator.

2.4 Longevity assay

Longevity assay was performed as described in (Piper and Partridge, 2016). For the assay, F1 progeny from a cross between wild type Oregon and CantonS flies were raised on standard cornmeal food. Both infected flies and non-infected wild type controls were kept at 25°C incubator. The fly food was replaced every four days in both control and experimental setups, and the number of dead flies and censor events was manually recorded after every transfer. Censor events included the flies that escaped during the fly food transfer and those that got stuck on the food. Dead flies were scored as 1 and the flies that got stuck to the food or escaped were scored as 0. The data was then entered into the GraphPad prism survival test, which used Log rank (Mantel-Cox test) to analyse the data and generate a Kaplan-Meier survival curve. The experiment was conducted with two biological replicates, each consisting of a total of 58 flies.

2.5 Climbing assay

In order to synchronize the age, early emergent flies from the wild type (Oregon x CantonS) crosses were discarded, and the remaining flies were collected the next day. The flies were then transferred to the infection chamber and to bottles containing normal fly food. Climbing assay vials measuring 19cm x 2.85cm were created by joining two clear plastic tubes. To begin the experiment, 10 flies (Cohort-1) were

randomly selected from the infection chamber, and fresh food bottles were transferred to the climbing assay vials. Two additional cohorts were prepared in the same manner. Both the infected and non-infected flies were tested at the same time and on the same day. The infected flies from the infection chamber were flipped 2-3 times to remove excess spores attached to their bodies before being transferred to the climbing assay vials. The vials were then tapped, and the flies were filmed for 10 seconds, followed by a 30-second rest period. This process was repeated 15 times for each cohort. The number of flies that climbed above the 2cm mark was manually observed and counted, after which the performance index was calculated. The experiment was conducted with two biological replicates, with each replicate consisting of three cohorts, each containing 7 to 10 flies.

$$\text{Performance index} = \frac{1/2\ (\text{Total no. of flies} + \text{Flies climbed 2cm} - \text{Flies lower than 2cm})}{\text{Total number of flies}}$$

2.6 Proboscis extension response

2.6.1 Preparing flies for PER assay

The flies were starved for 24 hours before performing the PER assay. One to two-day-old flies fed on regular food were collected and transferred to agar vials, which were then kept in a 25°C incubator for 24 hours. After 24hrs, the flies were transferred to a 20µl pipette tip using a fly aspirator. To prepare the agar vials, 1g of agar was added to 50ml of distilled water and 3ml of agar was then transferred into empty vials. Once the agar had solidified, a filter paper was placed inside each vial. To ensure that the flies remained hydrated, a small amount of water was added to each vial. Once the filter paper was soaked in water, excess water was removed from the vials.

2.6.2 Transferring flies to the 20µl pipette tip

To insert a fly into a 20µl pipette tip, an aspirator was used to position the dorsal thorax (head) of the fly facing towards the tip. The tip was then tapped gently to bring the fly closer. Next, a sharp razor blade was used to mark the portion of the tip between the head and thorax. The tip was inverted and tapped upside down to move the fly slightly away from the tip, and then a horizontal cut was made at the marked area. The fly was then carefully pushed towards the tip with a wick made of Kimtech wipe. Once the fly was in position, the bottom of the tip was sealed using Blu Tack, and the tip was placed on a flat surface.

2.6.3 PER assay

To test whether the immobilized flies in the 20µl tip were fit for the PER assay, they were first given water and 100 mM sucrose solution using tissue paper. Two wicks were prepared for the water and the sucrose solution, and were placed nearby. The 20µl tip with the fly head emerging was fixed on a flat surface and a camera was positioned around it. Next, the haustellum of the fly was gently touched with the water-soaked wick (negative control) and the response was recorded for 60 seconds. Since the flies had been hydrated before the experiment, they should not extend their proboscis when stimulated with water. Any flies that extended their proboscis were discarded. If the fly showed no response to the water, its haustellum was then touched with the sucrose-soaked wick (positive control) and recorded for 60 seconds. Since the flies had been starved before the experiment, they should extend their proboscis when stimulated with sucrose. Any flies that did not show any response to the 100 mM sucrose solution were discarded.

To conduct the experiment, a chamber was first heated to a temperature of 30°C. Flies that exhibited a positive response to sucrose and a negative response to water were transferred to this chamber. After the flies had been inside the chamber for 2-3 minutes, a camera was positioned inside and used to record proboscis extension response for a period of 60 seconds. The experiment was conducted with three replicates, each consisting of 10 flies.

2.7 Feeding assay

To prepare a fly cage, an empty food vial was used, and was cut at 4mm from its base using a heated knife. The base was then sterilized with 70% ethanol. Solutions mixed with 4% brilliant blue dye were transferred to the base and placed in an egg-laying chamber. For the feeding assay, four solutions were prepared, with each egg laying chamber containing only one solution.

1) Negative control 1 = distilled H_2O

2) Negative control 2 = distilled H_2O (950ul) + 50ul 4% brilliant blue dye (95%/5% v/v)

3) Positive control = 100mM Sucrose solution (950ul) + 50ul 4% brilliant blue dye (95%/5% v/v)

4) Test = 7.0025 x 10^7 spores/ml (950ul) + 50ul 4% brilliant blue dye (95%/5% v/v)

For the feeding assay, equal number of wildtype Oregon male and female flies were used (N=10 males, 10 females) and 4 biological replicates were perfromed. The flies were anesthetized on ice and transferred to the 4-feeding assay setup containing the above-mentioned solutions. The set-ups were then placed at 25°C incubator for 24hrs. Next, the flies were collected by anesthetising the flies with CO_2 and transferred to the 1ml Eppendorf tube. The Eppendorf containing flies were dipped in liquid nitrogen for

5 secs, placed in the 50ml Falcon tube, and dropped from a height to separate the flies' heads from their abdomens. The abdomen of the flies was collected using forceps and transferred to an Eppendorf containing 50ul of distilled water. Using a pestle abdomen was homogenised in the Eppendorf and 950ul of dH_2O was added to it. The Eppendorf was then vortexed and centrifuged for 5 mins at 10,000rpm. The supernatant was transferred into the new Eppendorf and kept on ice until analysis.

Next, the homogenised solution was transferred to 1ml cuvette, and the absorbance was recorded using spectrophotometer. Before recording the absorbance of the samples, a blank control containing distilled water was used to optimize the spectrophotometer. The absorbance of the samples was recorded at 630nm and 750nm. The corrected absorbance was calculated by subtracting the mean of 3 readings at 750nm (background) from the mean of 3 readings at 630nm (peak of blue dye).

2.8 Injecting flies with Dextran red fluorescent dye

A manual dye injector was created using a fine needle made from pulled capillary needle attached to a glass Pasteur pipette. To make the fine needle, a capillary tube was inserted into a micropipette puller. The glass pulled capillary needle was then inserted into the glass pasture pipette and sealed with parafilm at the point of insertion. Next, 0.1ul of 25 mg/µl fluorescent Dextran red dye was pipetted onto a piece of parafilm. The dye injector was gently placed onto the dye, which was spread out on the parafilm. The dye diffused into the fine glass pulled capillary needle due to capillary action. The flies were anaesthetised on a CO_2 pad, and the needle was carefully inserted into the thorax beneath the wing. A slight pressure was applied to the rubber

bulb attached to the glass Pasteur pipette. The flies were then transferred to a vial containing fly food and placed in a 25°C incubator for 24hrs to recover. After the 24hrs recovery period, the flies were fixed onto a glass slide using glue, and their retinas were imaged using Leica SP8 confocal fluorescent microscope. 10 flies were used for injection with only one replicate

2.9 Staining spores in the adult brain

2.9.1 Staining spores with FM4-64 dye

The adult Brains were dissected in 20 minutes and fixed in 650ul fixative (650ul 4% paraformaldehyde (PFA) in 1X Phosphate buffer saline (PBS) at room temperature for 20 minutes in a 1.5ml Eppendorf. Subsequently, the brains were washed for 20 mins in 750ul of 0.5% PBT (47.5ml 1xPBS + 2.5ml 10% Triton) for 5 times. Following this, the brains were incubated in FM4-64 dye, 1:200 dilution (1ul FM4-64 dye in 200ul PBS) for 1 hr at room temperature. The brains were washed for 5 times in 0.5% PBT and a final wash in 1XPBS. Finally, the brains were mounted onto slide with DAPI containing Vectashield and kept at 4ºC overnight. The brains were scanned the following day.

Table 2.1 Stock list

S.No	Name	Full genotype	Source
1	Sarm Gal4	yw;P{w+ GawB} Ect4 NP7460/TM6B UAS lacZ	Kyoto #105471
2	Sarm Gal4	yw;P{ GawB} NP0257/TM6, P{UAS-lacZ.UW23-1}	Kyoto #103571
3	MyD88 Gal4 histoneYFP;TubGal80ts	MyD88 Gal4 UAS histone YFP/CyO Gal80;TubGal80ts	Hidalgo lab
4	UAS Flybow 1.1	FB1.1[2609]/Gla Bc (line 4)	Hidalgo lab
5	UAS Wek HA	w;+/(CYO);UAS wek HA [NA12]/TM6B	Hidalgo lab
6	UAS Toll-1 RNAi	Y[1]v[1];UAS Toll-1-RNAi [P.TRiP.JF10491]	Hidalgo lab
7	UAS Toll-1 RNAi	w;UASToll1RNAi(VDRC100078);+	VDRC KK Stocks
8	UAS Histone YFP	w;UAS HistoneYFP;+	Hidalgo lab
9	Spz3 Gal4	w;spz-3 Gal4[Pbac-IT-Gal4-1408G4];+/SM6aTM6B	Bloomington
10	Toll-1 Gal4	w;+/(CYO);Toll-1 Gal4 [CRISPR]/TM6B	Hidalgo lab
11	UAS TrpA1	w;UAS TrpA1 [KattP216]	Flybase 26263
12	UAS Wek RNAi	y sc v; UAS wek RNAi {TRIP MHC 046534} attp40	wek RNAi
13	UAS Sarm RNAi	y v; P{TRIP JF01681}attP2	Hidalgo lab
15	UAS Toll-1 (10b)	w;UAS Toll-1(10bB);+	Hidalgo lab

Table 2.2 List of primers

Primer No.	Original name	Gene	Primer Sequence 5-->3
1	GAPDH Fw qPCR	GAPDH	GTGAAGCTGATCTCTTGGTACGAC
2	GAPDH Rev qPCR	GAPDH	CCGCGCCCTAATCTTTAACTTTTAC
3	Sarm fw qPCR	Sarm	AATTCGGCGGAGATGAAACG
4	Sarm Rev qPCR	Sarm	GGCTTCCTTAATGACGGCTG
5	Wek Fw qPCR	Wek	AGAAGCCCTGTATATGCCCCG
6	Wek Rev qPCR	Wek	TGCTTGTTAAGAATCGCCCGTGT
7	Dros Fwd qPCR	Drosomycin	CCCTCTTCGCTGTCCTGATGC
8	Dros Rev qPCR	Drosomycin	GCACCAGCACTTCAGACTGG
9	Mtk Fwd qPCR	Metchnikowin	TTCTGGCCCTGCTGGGT
11	Mtk Rev qPCR	Metchnikowin	ACCCGGTCTTGGTTGGTTAGG
12	TH Fwd qPCR	TH	CGAGGACGAGATTTTGTTGGC
13	TH Rev qPCR	TH	TTGAGGCGGACCACCAAAG

2.9.2 Staining spores with Calcofluor white stain

The adult brains were dissected, fixed, and first labelled with anti-ELAV. Following this, the brains were incubated in calcofluor white stain (50mg/ml), 1:1000 dilution (1ul calcofluor stain in 1000ul dH_2O) for 1 hr at room temperature. The brains were washed

for 5 times in 0.5% PBT and a final wash in 1XPBS. Finally, the brains were mounted onto slide with Vectashield and kept at 4ºC overnight. The brains were scanned the following day.

2.10 Quantitative Reverse Transcription (qRT)-PCR

20 adult brain were dissected from the wild type Oregon non-infected and infected flies. The dissected adult brains were transferred immediately into the Eppendorf containing TRI reagent (Ambion #AM9738). RNA extraction was carried out according to the TRI reagent protocol using isopropanol. Extracted RNA were treated with DNase to get rid of genomic DNA contamination using DNA-free kit (Ambion #AM1906). 200ng of RNA was reverse transcribed into cDNA by using random primer by following the manuscript of GoScript™ Reverse Transcription System (Promega #A50001) (Table 2.1). A PCR was performed to check the contamination in the RNA and Reverse Transcribed (RT) cDNA (Table 2.2). This is followed by a qRT-PCR. All qRT-PCR experiments were done in triplicate (i.e., 3 well condition). A DNA binding dye SYBR was used to observe the dynamics of the PCR (SensiFast™ SYBR®) and used ABI Prism 7000SDS machine for the qPCR (Table 2.3).

Following qRT-PCR, absolute and relative quantification were performed using the CT value generated by the qPCR machine, as described in (Rao et al., 2013). For the internal control GAPDH (housekeeping\reference gene) was used. For absolute quantification, the expression of the target gene (ΔCT*)* was normalised in infected and non-infected flies by subtracting the CT value of the GAPDH (reference gene) from the CT value of the target gene. For relative quantification, ΔΔCT was calculated by subtracting the ΔCT (Target gene) of the infected flies from the ΔCT (Target gene) of

the non-infected flies. The relative gene expression of the target gene was then calculated in infected and non-infected flies and expressed as fold change ($2^{-\Delta\Delta CT}$). The statistical analysis was conducted on the ΔCT values. 3 biological replicates were used each biological replicate consist of 20 flies.

$$\Delta CT = CT \text{ (a target gene)} - CT \text{ (a reference gene\GAPDH)}$$

$$\Delta\Delta CT = \Delta CT \text{ (non-infected sample)} - \Delta CT \text{ (infected sample)}$$

$$\text{Fold change} = 2^{-\Delta\Delta CT}$$

2.11 Immunohistochemistry

The adult Brains were dissected and fixed in 650ul fixative [4% paraformaldehyde (PFA) in 1X Phosphate buffer saline (PBS)] at room temperature for 20 minutes in a 1.5ml Eppendorf. Subsequently, the brains were washed five times for 20 mins in 750ul of 0.5% PBT (47.5ml 1xPBS + 2.5ml 10% Triton). The adult brains were blocked with 750ul of blocking buffer (Normal Goat Serum (NGS) + 9ml 0.5% PBT) and incubated overnight at 4ºC. After blocking, brains were incubated in primary antibody for 2 days at 4ºC. Upon completion of the incubation the primary antibody was removed and transferred to a new Eppendorf. The brains were washed five times with 0.5% PBT and incubated with 100ul of the secondary antibody overnight at 4ºC. The brains were washed again five times with 0.5% PBT for 20 mins and finally with 1XPBS. They were then mounted on slides and preserved with Vectashield.

2.12 Microscopy and imaging

Samples for SarmNP0257>hisYFP cell counting were imaged using a Zeiss LSM 710 confocal microscope with a 25x oil immersion lens, at a resolution of 1024x1024 pixels.

The zoom was set to 0.6, and scanning was performed at a speed of 7 frames per second (fps), with a line average of 1. For the Z-stack, images were acquired at intervals of 0.96 µm. The resulting images were analyzed using ImageJ software.

Samples for wild type Oregon anti-Repo cell counting were imaged using a Zeiss LSM 710 confocal microscope with a 25x oil immersion lens, at a resolution of 1024x1024 pixels. The Zoom was set to 1 and scanning was performed at a speed of 7 fps, with a line average of 1. For the Z-stack, images were acquired at intervals of 0.96 µm.

Diffusion of Dextran Red dye in the retina of adult flies were imaged using Leica SP8 confocal microscope with a 10X lens, at a resolution of 1024x1024 pixels. The zoom was set to 0.8 and scanning speed was 400Hz.

B. bassiana spores in the adult brain stained with FM4-64 dye, Calcofluor white stain, and transgenic *B. bassiana*-GFP spores were imaged with Leica SP8 confocal microscope with a 20X oil immersion lens, at a resolution of 1024x1024 pixels. The zoom was set to 1 and scanning was performed at a speed of 400 Hz. For the Z-stack, images were acquired at intervals of 0.96 µm. High magnification images of *B. bassiana* spores in adult brain were obtained using the same microscope, with a 63X oil immersion lens and a resolution of 1024x1024 pixels. The zoom was set to 2.0 and scanning was performed at a speed of 400Hz, with a line average of 4. For the Z-stack, images were acquired at intervals of 0.96 µm.

Toll-1>FB1.1, Sarm>FB1.1 adult brains attached with proboscis were imaged using Zeiss LSM Airyscan confocal microscope, with 10X magnification and a resolution of

1024x1024 pixels. The zoom was set to 1.0 and with the speed of 5 fps and a line average of 4. For the Z-stack, images were acquired at intervals of 1 µm.

MyD88>hisYFP samples and MyD88hisYFP anti-REPO samples were imaged using a Leica SP8 confocal microscope with a 20X oil immersion lens, at a resolution of 1024x1024 pixels. The zoom was set to 1 and scanning was performed at a speed of 400 Hz. For the Z-stack, images were acquired at intervals of 0.96 µm.

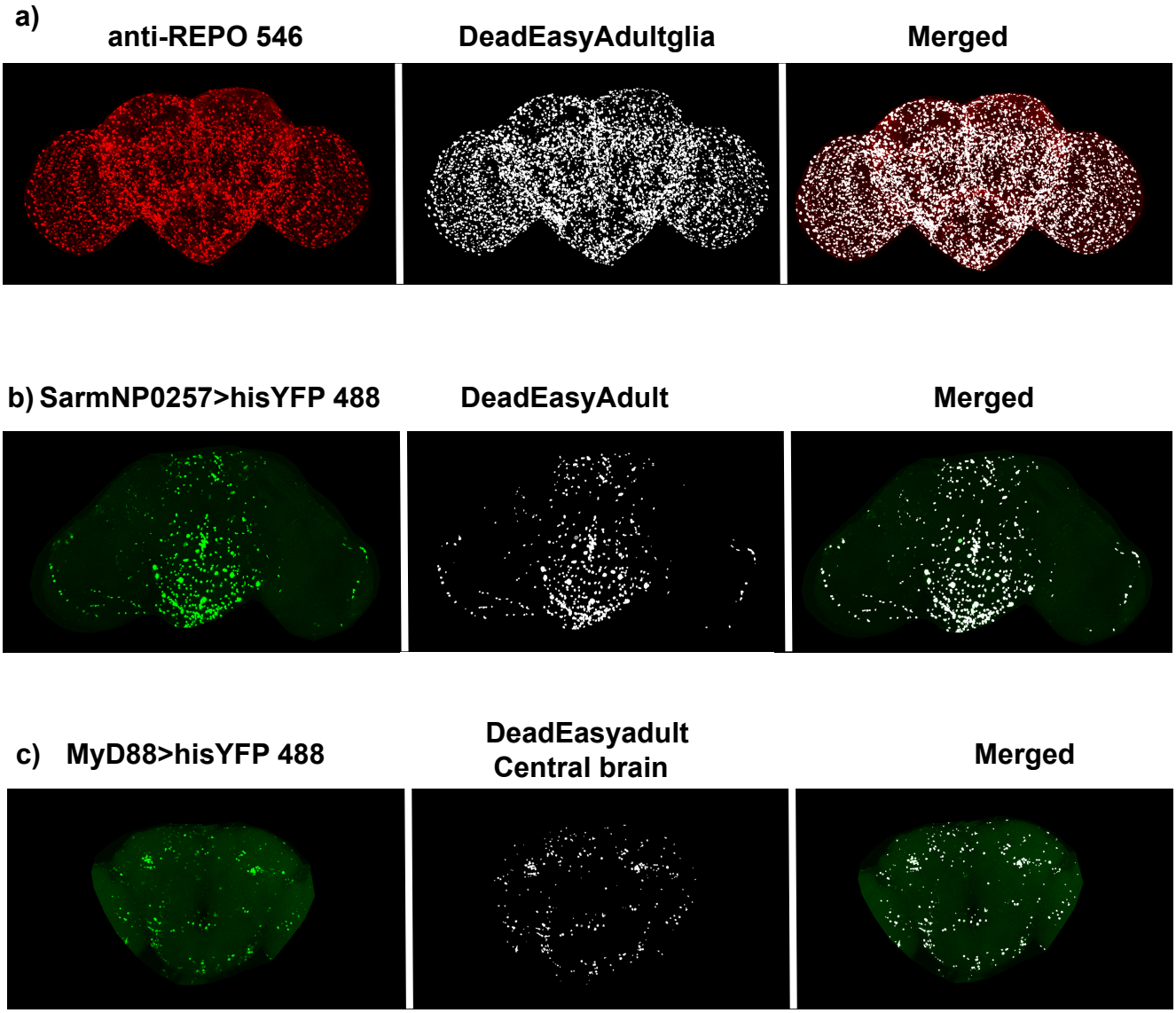
Toll-1>HisYFP, anti-TH+ adult brains were imaged with Leica SP8 confocal microscope with a 20X oil immersion lens, at a resolution of 1024x1024 pixels. The zoom was set to 1.4 and scanning was performed at a speed of 400 Hz. For the Z-stack, images were acquired at intervals of 0.96 µm.

To quantify anti-TH cells in wild type Oregon, adult brains were scanned with Zeiss LSM 710 confocal microscope using a 25x oil immersion lens and a resolution of 1024x1024 pixels. Scanning was performed at a speed of 8 frames per second, with a line average of 1. For the Z-stack, images were acquired at intervals of 0.96 µm. For MyD88>hisYFP anti-TH samples, adult brains were scanned with Leica SP8 confocal microscope with a 20X oil immersion lens, at a resolution of 1024x1024 pixels. The zoom was set to 1.4 and scanning was performed at a speed of 400 Hz. For the Z-stack, images were acquired at intervals of 0.96 µm.

2.13 Quantification of cell number using Deadeasy

The Repo+ cells in the adult brain were counted with an ImageJ plug-in called *Deadeasy* GliaAdult, and the HisYFP+ cells were quantified by *Deadeasyadult* (central

Figure 2.3 Cell number was quantified using DeadEasy



a) Deadeasyadultglia plugin was utilized to count glial cells in the adult brain. The white signal represented the cells recognised and counted by Deadeasy. The merged image showed that Deadeasy could count cell accurately.
b) Sarm+ cells were quantified by DeadeasyAdult plugin
c) MyD88+ cells were quantified in the central brain by Deadeasyadult central brain plugin.

brain) developed by our collaborator and former lab member Dr. Manuel Forero. *Deadeasy* was capable of recognizing cells from 3D stacks and automatically counting them (as illustrated in Figure 2.3).

2.14 Data analysis

Data were collected using *Excel* (Microsoft) and analysed using GraphPad Prism®. Longevity assay data were analysed using Log Rank (Mantel-Cox test) and proboscis extension response data were analysed using Chi-square test. Cell number counting data were numerical and continuous. Datasets with four or more groups were analysed using Two-Way ANOVA followed by Turkey's multiple comparison test. Unpaired t-tests or Mann-Whitney U tests were conducted for sample groups with two data sets that were normally or not normally distributed, respectively

Table 2.3 Components of GoScript™ Reverse Transcription System

Component	Volume
5x Reaction Buffer	4µl
25mM $Mgcl_2$	2µl
Nuclease free water	7µl
PCR nucleotide	1µl
Enzyme (RT)	1µl
Template RNA	200ng/µl
TOTAL	20µl

Table 2.4 Components of GoTaq® Flexi G2 DNA polymerase PCR system

Component	Volume
5xGreen Buffer	5µl
25mM $Mgcl_2$	1.5µl
2mM dNTP	2.5µl
2µm Forward primer	5µl
2µm Reverse primer	5µl
Template DNA	<250ng
Enzyme	0.25µl
dd H_2O	Xµl
TOTAL	25µl

Table 2.4 Components of SensiFast™ SYBR®

Component	Volume
2X Master Mix	5µl
Forward primer	1.5µl
Reverse primer	2.5µl
dd H_2O	5µl
Template (cDNA)	5µl
TOTAL	20µl

Table 2.5 PCR program when using GoScript™ Reverse Transcription System

Temperature	Time
25ºC	5min
42ºC	60min
70ºC	15min
4ºC	Infinite

Table 2.6 PCR program when using GoTaq® Flexi G2 DNA polymerase

Temperature	Time	Cycles
95ºC	2min	1
95ºC	30s	
45ºC - 65ºC	30s	30
72ºC	1min/kb	
72ºC	5min	1
4ºC	Infinite	1

Table 2.7 List of antibodies

Antibody	Donor	Working dilution
Primary antibodies		
Anti-GFP	Rabbit	1:250
Anti-REPO	Mouse	1:20
Anti-ELAV	Rat	1:250
Anti-TH	Rabbit	1:250
Secondary antibodies		
Anti-rabbit-488	Donkey	1:500
Anti-mouse-546	Goat	1:500
Anti-mouse-488	Goat	1:500
Anti-rat-647	Goat	1:500

Chapter 3

B. bassiana affects *Drosophila* behaviour and enters the brain

Abstract

Behaviour altering entomopathogenic fungi manipulates the locomotion and mouthpart of their host. However, specific genes exploited by the entomopathogenic fungi to control mouthpart and locomotion is unknown. Previous studies have demonstrated the *E. muscae* spores in the brain of the adult *Drosophila* flies but the route via which it reaches the brain is still not clear. Whether *B. bassiana* also reach the brain is not known, therefore this chapter aims to resolve if *B. bassiana* spores can also reach brain and the underlying route behind this.

3.1 Introduction

B. bassiana is widely used to infect *Drosophila* for investigating fundamental mechanisms of immunity and host-pathogen interactions (Matskevich et al., 2010, Gottar et al., 2006, Lemaitre et al., 1997, Weber et al., 2003). Fungal infection can be induced in adult *Drosophila* flies by pricking the flies with a spore solution or a solution containing fractionated cell wall and rolling the flies in isolated spores, followed by transferring the flies to 29°C (Gottar et al., 2006, Matskevich et al., 2010, Fehlbaum et al., 1994, Fontaine et al., 2000, Jin et al., 2008, Hanson et al., 2021, Lemaitre et al., 1997, Weber et al., 2003). Pricking the flies causes injury, which can further affect the progression and outcome of the infection. Additionally, the injury site is more susceptible to bacterial infection (Chambers et al., 2014). Furthermore, keeping the flies at 29°C could alter gene expression in the flies (Boothroyd et al., 2007, Etges et al., 2017, Weber et al., 2003). Thus, a new method of exposing the flies to the fungal spores that could mimic a natural way of infection is required.

Entomopathogenic fungi such as *E. muscae* and *O. unilateralis* controls the locomotion and mouthpart of their host (Elya et al., 2018, de Bekker, 2019). However, it is not clear whether *B. bassiana* also affects these behaviour. Climbing assay is a well establish test to evaluate neurodegeneration, as it measures the strong negative geotactic response in adult *Drosophila* which decreases with aging in flies (Ganetzky and Flanagan, 1978, Le Bourg and Lints, 1992, Feany and Bender, 2000). Thus, climbing assay can be used to study the effect of *B. bassiana* on locomotion.

Entomopathogenic fungi could affect the SOG in the adult brain to control proboscis movement but specific genes and the underlying mechanism is unknown. Previous work from our lab has shown that Toll-1 and Sarm are expressed in the SOG of the adult brain (Li et al., 2020), indicating that they could be the potential genes exploited by entomopathogenic fungi to control proboscis. However, there expression pattern in the proboscis and whether they are also involved in the proboscis extension remains to be investigated.

UASFlybow1.1 is an excellent tool to investigate Toll-1 and Sarm expression, as it encodes multiple fluorescent proteins flanked with FRT sites that can be flipped out by heat shocks, making it ideal for studying neuronal morphology. (Hadjieconomou et al., 2011). Nevertheless, UASFlybow1.1 can also function as membrane GFP reporter when maintained at 25°C. To investigate if Toll-1 and Sarm are involved in proboscis extension, Toll-1 and Sarm can be activated using a UASTrpA1. Transient Receptor Potential cation channel A1 (TrpA1) is a receptor that activates at 30°C, leading to an

influx of calcium and sodium which initiates an action potential in the neurons (Sakai et al., 2009). Thus, If Toll-1 and Sarm are expressed in the motor neurons in the proboscis, then by activating them with UASTrpA1 would provoke proboscis extension at 30°C. Therefore, these approaches can provide valuable insights into the function of Toll-1 and Sarm.

The fact that the proboscis traverses through foramen in the brain to reach the gut suggests that esophagus penetrates the brain (McKellar et al., 2020). This indicates that spores may possibly enter the brain via proboscis through feeding and could be tested with a feeding assay. A previous report have showed the presence of The spores of *E. muscae* in adult *Drosophila* brain have been identified through staining the paraffin embedded tissue section with safranin O/ fast green (Elya et al., 2018). Other dyes such as FM4-64 and calcofluor white can also stain fungal spores in the adult brain. FM4-64 is a red fluorescent dye used to stain yeast vacuolar membrane (Roeder and Shaw, 1996). Recently FM4-64 dye has been reported to stain *B. bassiana* spores in-vivo in the haemolymph of tobacco budworm (Lewis et al., 2009), suggesting It's potential use in staining spores in the adult *Drosophila* brain. Calcofluor white is another fluorescent dye which binds to 1-3 beta and 1-4 beta polysaccharides of chitin and cellulose present in fungal cell wall (Hoch et al., 2005). Thus, making it another viable option for visualizing fungal spores in the brain.

In *Drosophila*, GNBP3 recognizes fungal B-1,3 glucans, which activates the immune response via the Toll pathway and upregulates the expression of anti-fungal peptides, such as *drosomycin*, *metchnikowin*, and *baramycin* (Ferrandon et al., 2007, Lemaitre et al., 1997, Hanson et al., 2021). To detect whether exposure to *B. bassiana* induces

immune Toll signaling in the adult brain and whether infection reaches the adult brain, qRT-PCR can be used to detect the expression of mRNA transcripts of the anti-fungal peptides in the brain of adult *Drosophila* flies. This alternative approach is useful for investigating the induction of immune Toll signaling by *B. bassiana* in the adult brain.

Therefore, the chapter aims to investigate if *B. bassiana* spores enters the adult *Drosophila* brain. To test this hypothesis the objectives were:

1. To design an infection set-up that provides the necessary conditions to facilitate natural exposure of adult *Drosophila* flies to *B. bassiana*.
2. To test whether *B. bassiana* affects the locomotion and proboscis extension in adult *Drosophila* flies
3. To explore the expression of Toll-1 and Sarm in proboscis.
4. To investigate if Toll signalling involved in the proboscis extension.
5. To identify the route by which *B. bassiana* spores can reach the brain.
6. To test the effect of B. bassiana exposure on the flies blood brain barrier.
7. To determine if *B. bassiana* spores can enter the brain of adult Drosophila flies.
8. To test if *B. bassiana* activates immune Toll signalling in the adult brain.

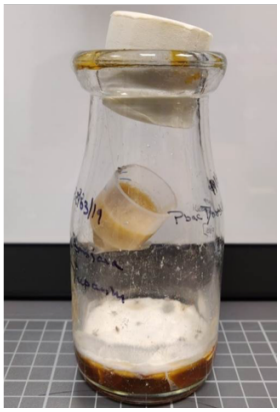
3.2 Results

3.2.1 Exposure to *B. bassiana* reduces lifespan of the adult flies

To mimic natural environmental condition in which flies usually can get infected by fungal spores, an infection chamber was designed (Fig 3.1a). *B. bassiana* was cultured on Sabouraud 4% dextrose agar at the bottom of the bottle. To ensure that the exposed flies were dying due to infection rather than starvation, the fly food was

Figure 3.1 Exposure to *B. bassiana* caused reduction in life span of adult flies

a)



Infection set-up

b)

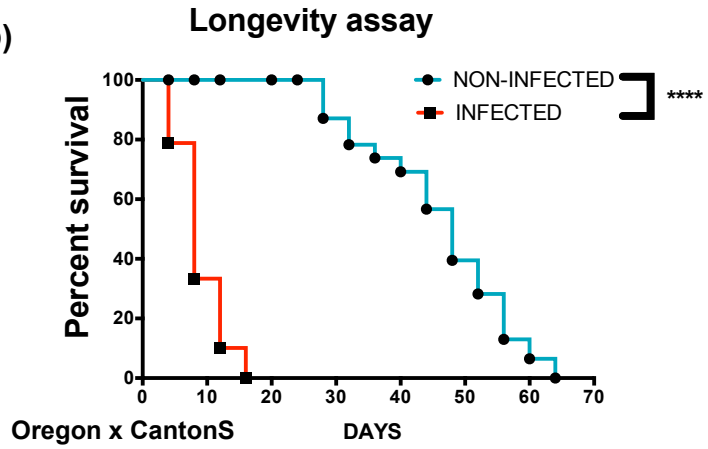


Figure 3.1 Exposure to *B. bassiana* caused reduction in life span of adult flies

a) Infection set-up used to expose the flies. The *B. bassiana* was cultured on the Sabourand 4% agar at the bottom of the bottle. Fly-food is attached on the side in a nicked 50ml falcon tube.

b) Longevity assay representing the percentage of survival of the infected and non-infected flies. The red staircase curve represents the percentage survival of infected flies and the blue staircase curve represents percentage survival the non-infected flies. The dots (circle and square) represent the death/censored observations (Straight line: Fly escaped/stuck to the food, Staircase: death) in a span of 4 days.
Log-rank test, P value = <0.0001. N = 104 (Noninfected flies), 104 (Infected flies)

Genotype: Control = Non-infected Oregon/CantonS
Experiment = Infected Oregon/CantonS

attached to the side of the infection chamber. After transferring the flies to the infection chamber, the set-up was placed at 25°C incubator.

To check the efficiency of the infection chamber, a longevity assay was performed. The experiment was conducted using two biological repeats. Each biological replicate consisted of 58 flies in total. The dead flies were counted on the fungal culture and the flies that escaped during the fly food transfer. The dead flies were scored as 1 and the flies that got stuck to the food or escaped were scored as 0. The flies that were transferred to the infection chamber died on the day 16 compared to the wildtype non-exposed flies which died on day 64 (Fig 3.1b). 20 percent of the flies died on day 4 of the exposure, indicating that *B. bassiana* could initiate the infection within 4 days of exposure. On day 8 more than 50 percent of the flies died in the infection chamber suggesting that the infection becomes severe on day 8. Therefore, to study how *B. bassiana* affects brain and behaviour in the adult flies I chose day 3 and day 7. In summary, the finding indicates that exposing adult flies to *B. bassiana* spores using the infection chamber could result in their death within 20 days of exposure, however three biological replicates would have provided strong evidence.

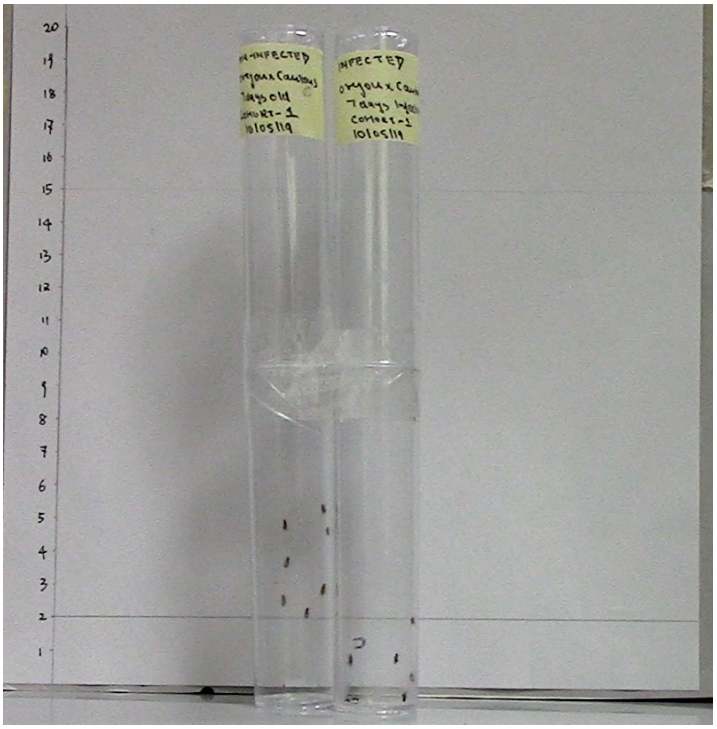
3.2.2 Exposure to *B. bassiana* affects the negative geotaxis behaviour of adult flies

To investigate the effect of the *B. bassiana* infection on the locomotion of the adult flies, climbing assay was performed 3 days and 7 days post exposure. Equal number of male and female flies were used for the experiment. 6 cohorts (Biological replicates) were tested, each cohort consist of 10 flies (See method section). The performance index of 3 days exposed flies did not change compared to 3 days non-exposed flies

Figure 3.2 Exposure to *B. bassiana* affected the negative geotaxis behaviour

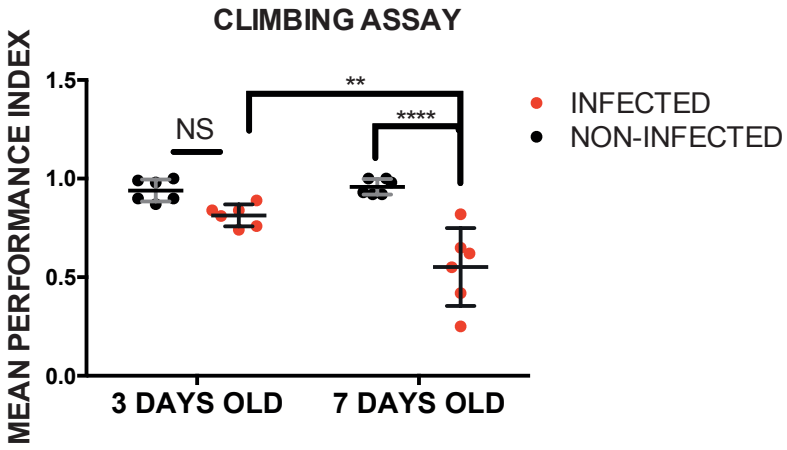
7 days post exposure

a) Climbing assay set-up



Oregon x CantonS

b)



Oregon x CantonS

Figure 3.2 Exposure to *B. bassiana* affected the negative geotaxis behaviour

a) Climbing assay set-up: The left vial consists of the non-infected flies and the right vial consist of the infected vials. Climbing assay for both the non-infected controls and infected flies were done together on the same day and time.
b) Climbing assay representing the mean performance index of the non-infected and infected flies. The non-infected controls are represented by the black dot and the infected flies are represented by the red dot. The error bar shows standard deviation. Each dot represents a one cohort and each cohort consist of 7-10 flies. Two-way ANNOVA followed by Turkey's multiple comparison test (See Appendix 2). N (3 days old) = 60 (non-infected), 60 (Infected). N (7 days old) = 51 (non-infected), 51 (infected). *P value < 0.05, **P value < 0.01, ***P value = 0.001, ****P value < 0.0001

Genotype: Controls = Non-infected Oregon/CantonS

Infected Oregon/CantonS

(Fig 3.2 b), indicating that the infection did not affect the locomotion of the flies 3 days post exposure. However, at 7 days post exposure, the performance index of exposed flies reduced to 0.5 compared to non-exposed controls (Fig 3.2b), indicating that locomotion of the exposed flies was severely affected by the *B. bassiana* spores. Additionally, the performance index of the 7 days exposed flies was lower compared to those exposed for 3 days. This suggests that *B. bassiana* spores could adhere to the fly cuticle and initiate an infection from day 3 to day 7, thereby decreasing the climbing ability of the flies. However, it was unclear whether this effect on locomotion was due to spores or infection reaching the brain.

3.2.3 Toll-1 and Sarm are expressed in the sub-esophageal ganglion and proboscis

Previous work from our lab showed the expression of Toll-1 and Sarm in the sub-esophageal ganglion region of adult brain (li et al). SOG is known to control the proboscis extension. Therefore, to investigate the potential genes exploited by the behaviour altering fungi, we hypothesised that *B. bassiana* might exploit Toll-1 and Sarm to affect the feeding behaviour. To investigate this, we first checked if Toll-1 and Sarm are expressed in the SOG and proboscis by driving the expression of UASFlybow1.1 using Toll-1Gal4, SarmNP7460Gal4 & SarmNP0257Gal4. This showed that Toll-1 and Sarm are expressed in the sub-esophageal ganglion (SOG) (Fig 3.3a).

The adult brain along with proboscis, was dissected. Toll1>FB1.1, $Sarm^{NP7460}$>FB1.1, & $Sarm^{NP0257}$>FB1.1 revealed the expression of Toll-1 and Sarm in the gustatory neurons located in labellum of the proboscis (Fig 3.3b). Additionally, the muscle of the

Figure 3.3 Toll-1 and Sarm are expressed in sub-esophageal ganglion and proboscis

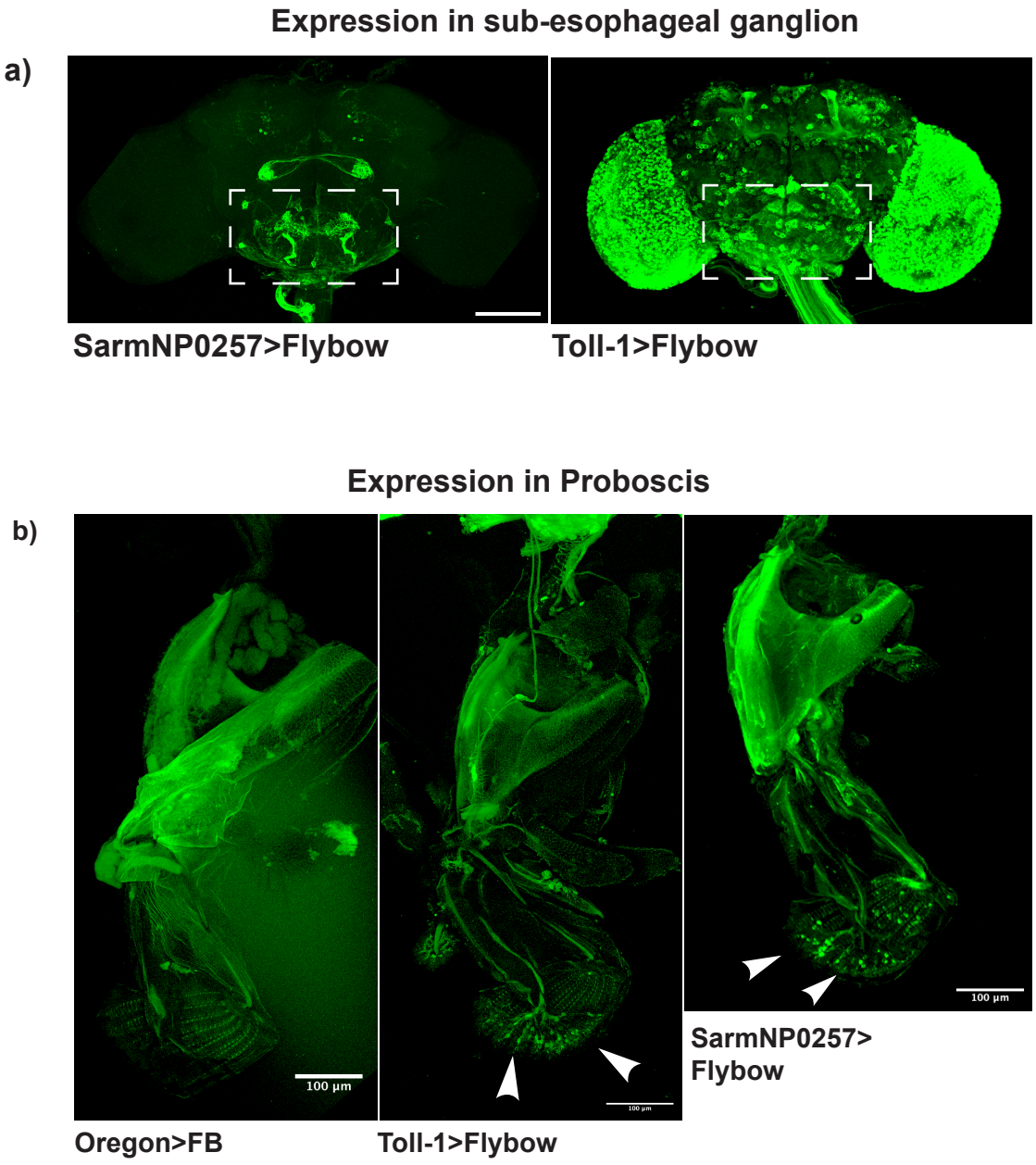


Figure 3.3 Toll-1 and Sarm are expressed in sub-esophageal ganglion and proboscis

a) Z projection showing the expression of Toll-1>Flybow1.1 and SarmNP0257>Flybow1.1 in the subesophageal zone (green) f. White box indicates the subesophageal ganglion (SOG).

Genotype: SarmNP0257Gal4>UASFlybow1.1 & Toll1Gal4>UASFlybow1.1

b) Z projection showing the expression of Toll-1>Flybow1.1, SarmNP0257>Flybow1.1 in the labellum of the proboscis attached to adult brain. White box indicates the proboscis. White arrows indicate the expression of Toll-1 and Sarm in the gustatory neurons of laellum (GFP green).

Toll1>Flybow1.1 N =4 (Proboscis) & N = 6 (Brain), SarmNP0257>Flybow N = 7(proboscis) & N = 3 (Brain)

Genotype: SarmNP0257Gal4>UASFlybow1.1, Toll-1Gal4>UASFlybow1.1

Scale bar: a) 100 um b) 100 um

proboscis emitted signal, which was attributed to autofluorescence, as this signal was also present in the +>FB1.1 control. These findings confirmed that signal emitted by sensory neurons in the proboscis corresponded to expression of Toll-1 and Sarm. Together, these data showed that Toll-1 and Sarm are expressed in the proboscis of adult *Drosophila* flies.

3.2.4 Sarm neurons were involved in proboscis extension response

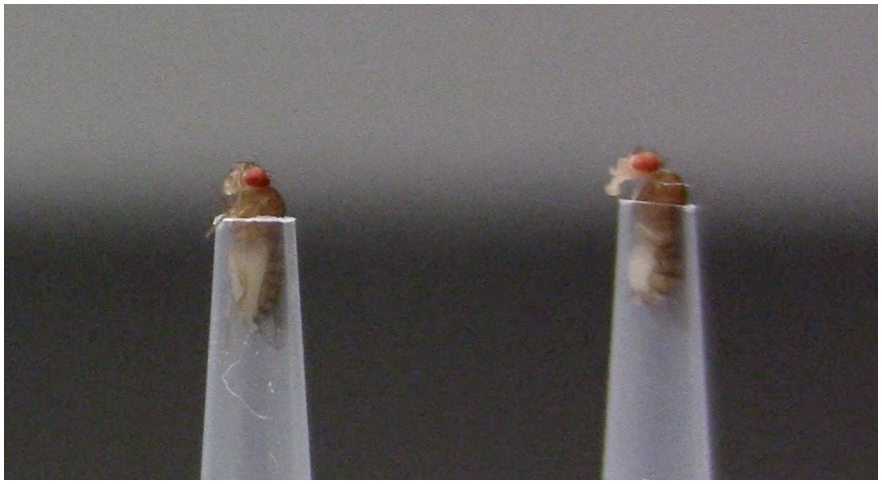
Subsequently, a proboscis extension response (PER) assay was optimized and performed to investigate the role of Toll signalling in the proboscis extension. To activate Sarm neurons, the TrpA1 was used. $Sarm^{NP0257}$Gal4 and $Sarm^{NP7460}$Gal4 were crossed with UASTrpA1. The flies were then transferred to a 20ul pipette tip to immobilize them (Fig 3.4 a). At 30°C TrpA1 receptor channels were activated, leading to an influx of calcium and sodium, causing an action potential in the Sarm neurons. At 30°C, Sarm neurons expressing TrpA1 caused proboscis extension (Fig 3.4a & b). Both $Sarm^{NP0257}$>TrpA1 and $Sarm^{NP7460}$>TrpA1 flies extended their proboscis compared to the +>TrpA1 controls (Fig 3.4b). The data obtained from the PER assay suggested that activation of Sarm neurons in adult flies triggered a proboscis extension response. However, 18 degrees control were missing from the experiment to test if the UASTrPA1 line was not leaky, as it would have an effect on the observed phenotype. Since Sarm is a known adaptor of Toll signalling, these results indicated that Toll-expressing neurons might also be involved in proboscis extension.

3.2.5 Adult *Drosophila* flies ingested *B. bassiana* spores through feeding

Next, to identify the route via which the spores can reach the brain, a feeding assay was designed along with David Alliband (Master's student). The feeding assay set-up

Figure 3.4 Sarm neurons are involved in proboscis extension

a)



Oregon>TrpA1 SarmNP0257>TrpA1 **30°C**

b)

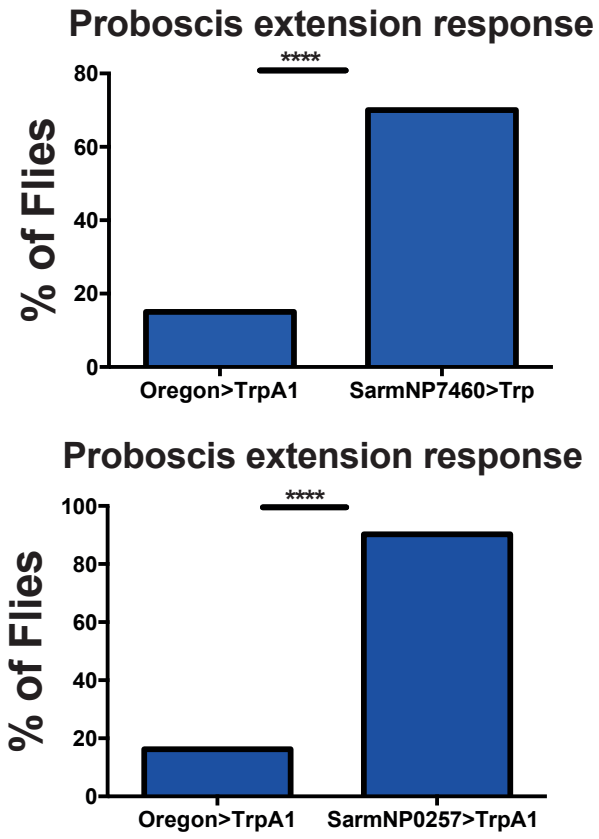


Figure 3.4 Sarm neurons are involved in the proboscis extension response

c) Image showing activated Sarm neurons caused proboscis extension when transferred to 30ºC chamber.

d) Graph representing the percentage of flies extended proboscis upon activating Sarm neurons. Chi-square test, ****<0.0001 (Appendix 3).

SarmNP0257>TrpA1 N = 34, Oregon>TrpA1 N=34

SarmNP7460>TrpA1 N = 40, Oregon>TrpA1 N=40

Genotype:

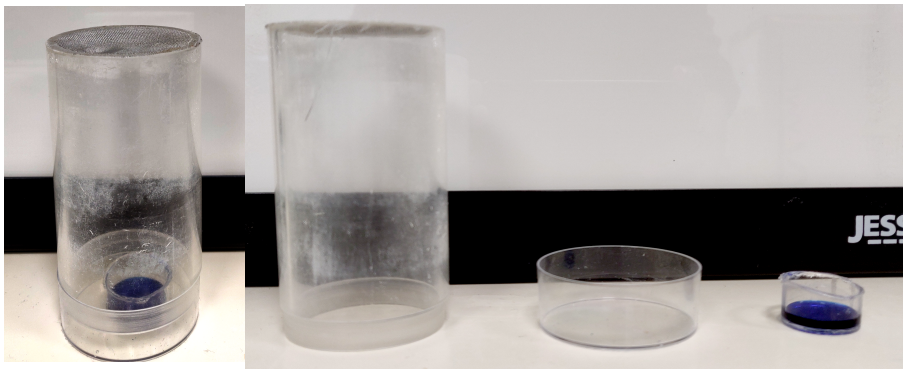
SarmNP7460>TrpA1

SarmNP0257>TrpA1

+>TrpA1

Figure 3.5 Adult flies liked to eat *B. bassiana* spores

a)



Feeding assay set-up

b)

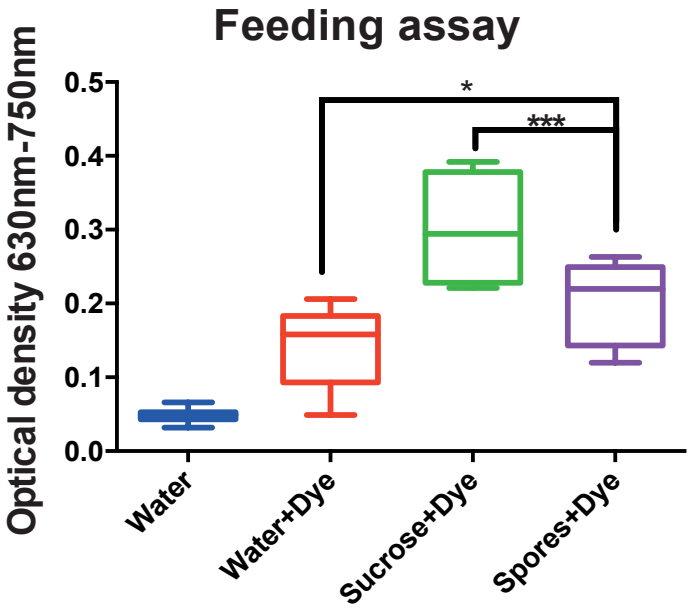


Figure 3.5 Adult flies liked to eat *B. bassiana* spores

a) Feeding assay set-up was made using an egg-laying chamber, a small petri dish and a sliced vial.

b) Box plot representing optical density of water, sucrose and spores mixed with 4% brilliant blue dye in the abdomen of adult flies. Flies preferred to eat spores (purple box plot) compared to water (Red box plot) and spores.

One way ANOVA ****P value <0.0001 (Appendix 4), Turkey's multiple comparison test, * Pvalue < 0.05, **P value < 0.01, ***P value = 0.001, ****P value < 0.0001

Genotype:

Oregon

was made using an egg laying chamber with a base of a 60 mm petri plate (Fig 3.5a). A 25x95mm vial was cut at the bottom and used as a container to provide different solutions mixed with 4% brilliant blue dye (Fig 3.5a). Four setups were used in the experiment: 1) water with 4% brilliant blue dye, 2) 100 mM sucrose solution with 4% brilliant blue dye, 3) 7.0025 x 10^5 spores/ml solution with 4% brilliant blue dye, and 4) water without the dye. Equal number of male and female flies were transferred in an egg-laying chamber for 24 hours, during which they fed on the water, sucrose and spores mixed with dye. The blue colour of the abdomen indicated that the flies have been feeding. Afterward, the abdomen of the flies was homogenized in distilled water, and the optical density was recorded using a spectrophotometer.

The optical density of the dye mixed with 100 mM sucrose ranged between 0.2 and 0.4, which was higher than the OD of the dye mixed with water and spores (Fig 3.5b). This suggested that flies preferred to feed on sucrose compared to water and spores. Interestingly, the OD of the dye mixed with spores was higher than the OD of the dye mixed with water (Fig 3.5b), indicating that flies feed on solutions consisting of spores over water. This finding suggested that feeding could be one of the pathways through which the spores could reach the brain. In conclusion, the feeding assay data suggested that flies could ingest spores via feeding.

3.2.6 *B. bassiana* spores damaged the blood brain barrier

Flies ingested *B. bassiana* spores while feeding, raising the question of whether these spores can penetrate the protective blood-brain barrier and reach the adult *Drosophila* brain. To investigate this question, 0.1ul of 25 mg/ul fluorescent Dextran Red dye was injected into the thorax of adult flies with a manual dye injector made from glass pulled

Figure 3.6 *B. bassiana* spores breaks the blood brain barrier

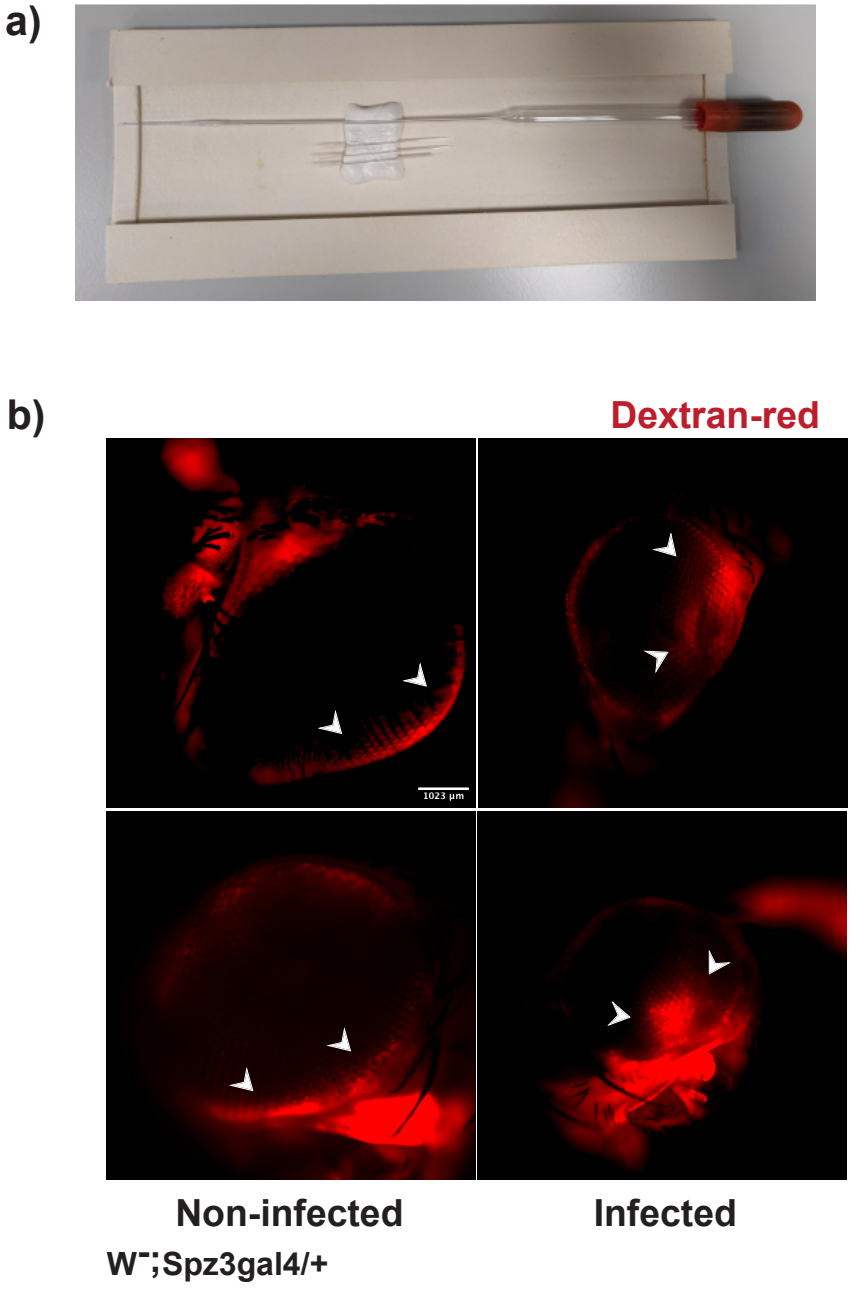


Figure 3.6 *B. bassiana* spores breaks the blood brain barrier

a) Dye injector made with capillary pulled needle attached with a glass Pasteur pipette used to inject fluorescent dextran-red dye into the thorax of adult flies.

b) Image showing accumulation of dextran-red dye in the periphery of the retina in non-infected adult flies. Dye infused inside the retina of infected flies indicating that the broken blood brain barrier had been damaged.

   Genotype: W^{-};Spz3gal4/+

   Scale bar: 1023um

capillary needle attached to a pasture pipette (Fig 3.6a). The flies were then shifted in the fly food vial to recover overnight. Subsequently, the retina of the fly was imaged. In 7 days non exposed control flies, dye accumulated on the periphery of the retina (Fig 3.6b). This meant that the blood brain barrier was intact, preventing the dextran red dye from entering the optic lobe. However, in 7 days exposed flies, the dye diffused into the retina, indicating a leaky blood brain barrier. To conclude, the integrity of the blood brain barrier was compromised after 7 days exposure to *B. bassiana*.

3.2.7 *B. bassiana* spores entered the brain

A damaged blood brain barrier indicated that spore could reach the brain. To investigate this, two fluorescent dyes FM4-64 and calcofluor white stain were used. The adult brain was stained with DAPI, which binds adenine-thymine rich region in DNA and thus labels all nuclei (Fig 3.7a). 3 days post exposure oval spore like structures were found in the optic lobes of the adult brain (Fig 3.7a & b). These oval structures were stained by FM4-64 dye and colocalised with DAPI which confirmed the presence of nuclei in them, thus indicating that they were indeed spores. However, FM4-64 also stained trachea in the brain, suggesting that it lacks specificity and may not be the optimal dye for visualizing spores in the brain. Thus, FM4-64 could not confirm the presence of spores in the adult brain.

As a complementary approach, the spores were stained with calcofluor white after 3 days exposure to *B. bassiana*. To label all neurons in the brain, a pan-neuronal anti-ELAV antibodies was used. Spore like structures were found attached to the optic lobe and in the central brain (Fig 3.8a, b, c). Under high magnification, the spores were found to be clearly attached to the optic lobe and in the central brain (Fig 3.8b, c).

Figure 3.7 Staining *B. bassiana* spores with FM4-64 in the brain

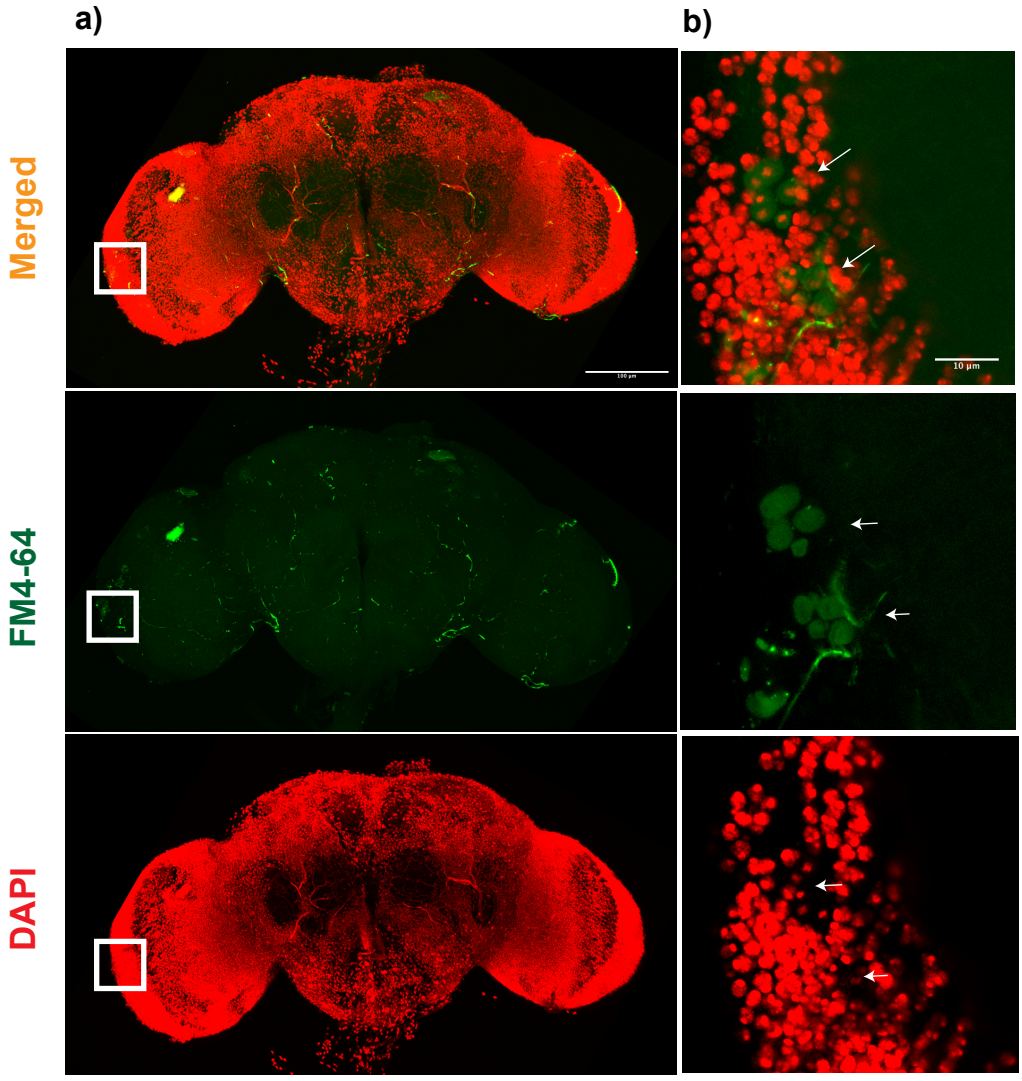


Figure 3.7 Staining *B. bassiana* spores with FM4-64 in the brain

a) Z projection of the adult brain showing the *B. bassiana* spores stained with fluorescent dye FM4-64 (green). Nuclei was labelled by DAPI (red). White arrows indicate spores in optic lobe. Merged

b) High magnification view of detail from (a) within dotted box.

Genotype: Oregon

Scale bar: a) 100 μm, b) 10 μm

Moreover, the spores labelled with calcofluor white did not colocalised with anti-ELAV, thus confirming that round structures stained with calcofluor white attached to the optic lobe were indeed spores (Fig 3.8b, c). However, similar to FM4-64 dye, calcofluor white also stained the trachea in the adult brain. To summarise, spores were detected in the brain with calcofluor white stain but it may not be the most effective method for visualising spores in the brain since it tends to accumulate around the trachea. Due to this limitation Calcofluor white could not confirm whether, *B. bassiana* spores enters the brain.

To further confirm the presence of spores in the adult brain, wild type Oregon flies were exposed to *B. bassiana* strain EABb 04/01-Tip GFP5, which is a *Agrobacterium tumefaciens*-mediated GFP transformant of *B. bassiana*. The expression of GFP was examined in the spores of the EABb strain using a confocal microscope. The outer membrane of spores showed GFP expression and had an oval shape (Fig 3.9a). After exposing flies with GFP transgenic *B. bassiana* for 24hrs, spores were observed inside the optic lobes and central brain (Fig 3.9b, c). The adult brain was stained with DAPI, and the GFP spores colocalised with DAPI, confirming the presence of nuclei in spores (Fig 3.9c). This confirmed the entry of GFP-Transformed *B. bassiana* spores into the brain (Fig 3.9b, c). Additionally, the GFP transgenic strain of *B. bassiana* was more pathogenic than the wild type *B. bassiana* strain as flies died within 48 hours after exposure in the infection chamber.

To conclude, the spores like structure were detected inside the brain with FM4-64 dye and calcofluor white stain but both the dyes lacked specificity. While GFP transformed *B. bassiana*, indicated that the *B. bassiana* spores could enter the brain.

Figure 3.8 Calcoflour white stained *B. bassiana* spores in the brain

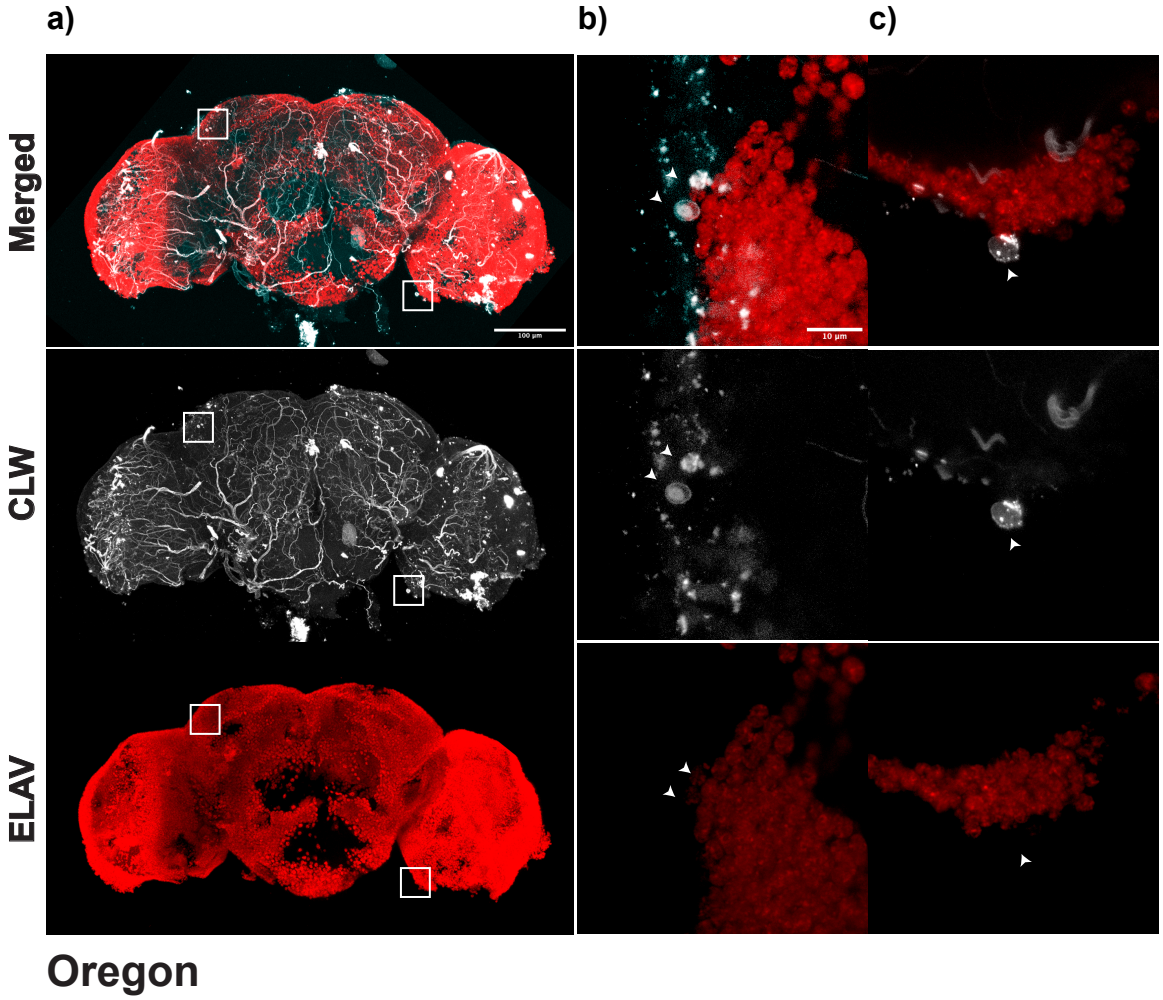


Figure 3.8 Calcofluor white stained *B. bassiana* spores in the brain

a) Z projection of the wild type Oregon adult brain showing B.bassiana spores stained with fluorescent dye calcofluor white. Neurons were l abelled with pan neuronal anti-ELAV. White arrows indicate spores in brain. Spores labelled with calcofluor white did not colocalize with anti-ELAV in neuronal nuclei.

b) Higher magnification detail of data shown in (a) within boxes.

c) Higher magnification detail of data shown in (a) within boxes.

Genotype: Oregon

Scale bar: a) 100 µm, b) 10 µm

Figure 3.9 GFP transformed *B. bassiana* spores entered the brain

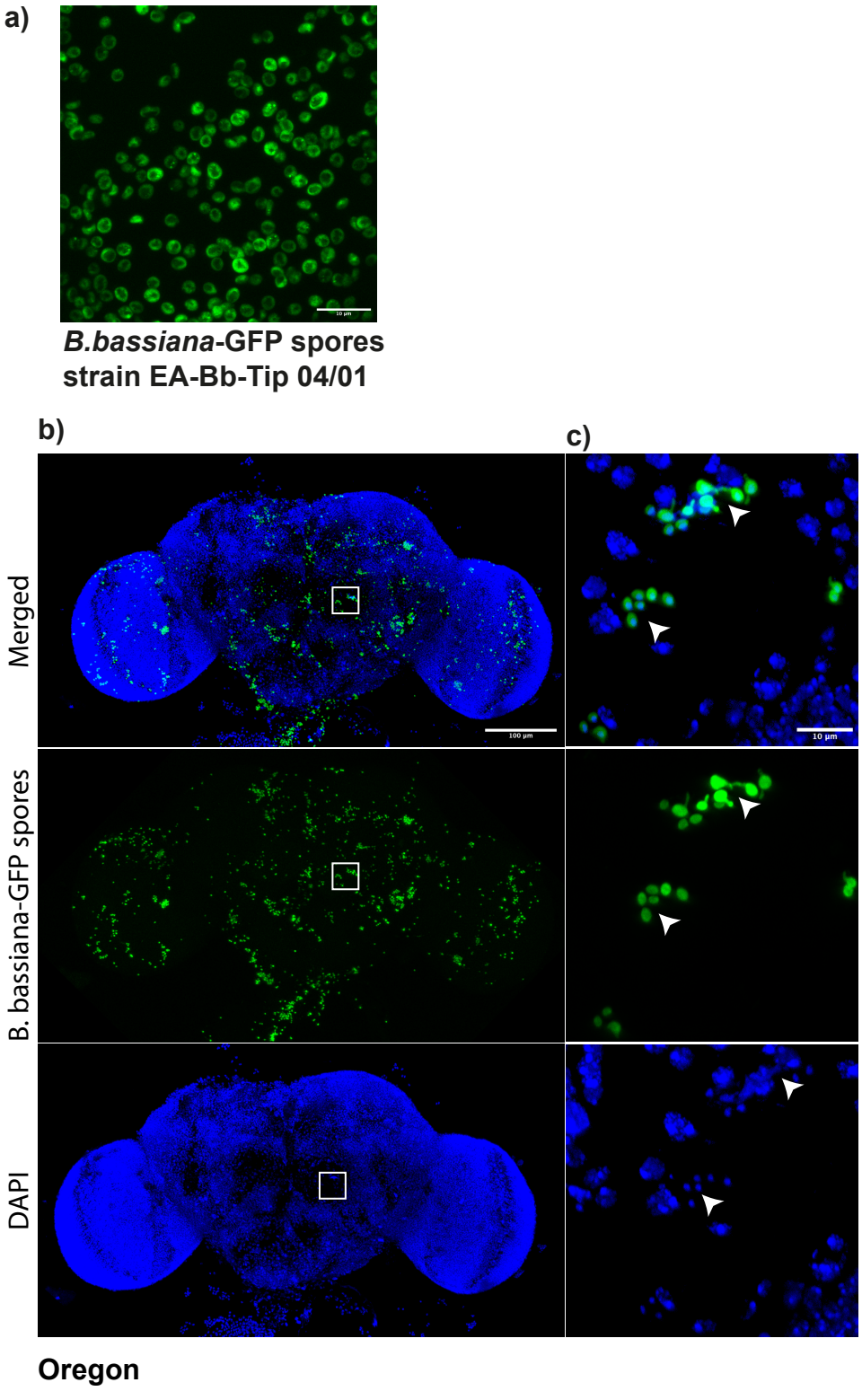


Figure 3.9 GFP transformed *B. bassiana* spores entered the brain

a) Spores of transgenic strain of *B. bassiana*-GFP (EABb 04/01-Tip GFP5).

b) Z projection of wild type Oregon adult brain showing *B. bassiana*-GFP spores entered the brain. Nuclei were labelled with DAPI. White arrows indicate spores in brain. Merged Z projection of the adult brain represent GFP transformed spores colocalised with nucleus labelled with DAPI.

c) High magnification details of data shown in (a) within boxes, demonstrating colocalization between *B. bassiana*-GFP and DAPI.

Genotype: Oregon

Scale bar: a) 10 um, b) 100 um, c) 10 um

3.2.8 *B. bassiana* infection activated immune signalling in the adult brain

GFP tagged-*B. bassiana* spores had indicated their presence inside the brain. Therefore, we hypothesised that if *B. bassiana* has entered the brain, it could potentially induce Toll signalling and upregulate transcription of anti-fungal peptides *drosomycin* (*dros*) and *metchnikowin* (*met*). To investigate this, a qRT-PCR was performed to quantify the expression of *dros* and *met* mRNA in the dissected adult brain after 7 days exposure to *B. bassiana*.

Wild type Oregon flies were used in the experiment and were raised at 25ºC throughout development. Purified RNA was transcribed into cDNA by the reverse transcriptase, which showed an expected band, in contrast to No-RT control, which showed no band (Fig 3.10a). This showed that there was no genomic contamination in the purified RNA. Subsequently, a qRT-PCR was performed using the cDNA as a template, and relative gene expression of *met* and *dros* was calculated using GAPDH as a housekeeping gene, indicated by fold change.

The fold change of the drosomycin in the dissected adult brains of 7 days exposed flies showed a significant increase compared to non-infected controls (Fig 3.10b). This suggested that *dros* was strongly induced in the dissected adult brain after 7 days exposure to *B. bassiana*. However, the fold change of metchnikowin did not show a significant increase in the adult brain of 7 days exposed flies compared to control, indicating that metchnikowin was induced at low levels (Fig 3.10b). In conclusion, these data demonstrate that *B. bassiana* spores induce Toll-1 dependent immune signalling in the brain.

Figure 3.10 *B. bassiana* infection activated the immune response in the adult brain

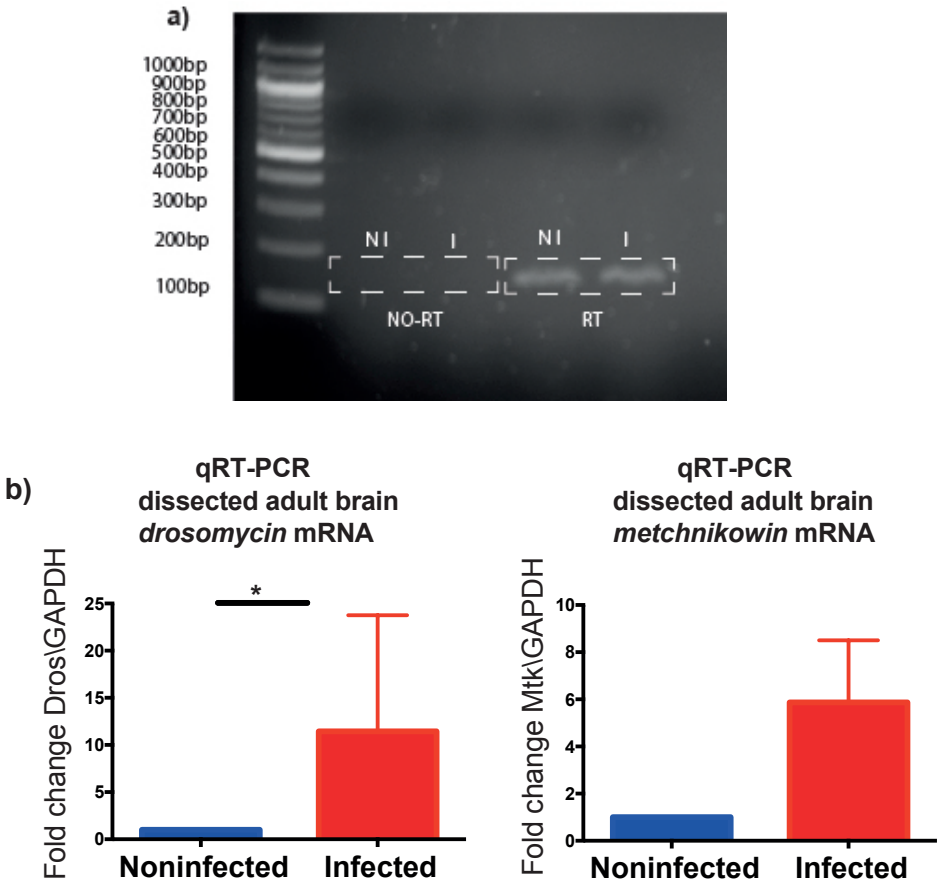


Figure 3.10 *B. bassiana* infection activated the immune response in the adult brain

a) Image of a gel showing the cDNA transcribed from the RNA catalysed by the reverse transcriptase. Transcribed cDNA showed the expected DNA band on the gel. NI = non-infected sample, I = infected sample. RT = cDNA, NoRT = RNA

b) qRT-PCR data representing the fold change in expression of anti-fungal peptides *drosomycin* and *metchnikowin* mRNA in infected flies as compared to non-infected flies upon 7 days exposure to the *B. bassiana*. The expression of *drosomycin* and *metchnikowin* mRNA was normalized by *GAPDH* as a housekeeping control gene. The error bar shows standard deviation.
Unpaired student T-test (Appendix 5), N = 3 biological replicates.
Genotype: Control = Noninfected Oregon
Infected Oregon.

3.3 Discussion

In this chapter, I designed an infection set-up to expose flies to *B. bassiana* spores. The longevity assay showed that exposing the flies to *B. bassiana* affected their lifespan, as exposed flies survived for less than 20 days in the infection chamber. The 7 days exposed flies showed defect in locomotion. Gal4 driving expression of UASFlybow1.1 revealed that Toll-1 and Sarm are expressed in the SOG and gustatory neurons of the labellum in the proboscis. Additionally, activating Sarm neurons with TrpA1 induced proboscis extension. Further, the feeding assay showed that flies ingested spores via feeding, suggesting that spores could reach the brain through proboscis during feeding. The presence of dextran red dye in the retina indicated that ingested spores could potentially damage the blood brain barrier to reach the brain. Staining with FM4-64 and calcofluor white were inconclusive but exposure to GFP transformed indicated that *B. bassiana* spores entered the brain. Additionally, antifungal peptides were upregulated in the brain of 7 days exposed flies further suggested that spores entered the brain and triggered immune Toll signalling.

To infect the flies, I transferred the flies to the infection chamber and the flies were then raised at 25°C incubator. This is in contrast with the conventional methods of infecting the flies. The new infection set-up provides access to the food and a constant exposure to the fungal spores which mimics natural exposure the flies to the spores. A spore concentration of 3.7 x 10^9 spores/ml was used to set-up the *B. bassiana* culture in the infection chamber. However, using the infection chamber, the optimum spore concentration to induce infection in the flies cannot be determined. Since, the infection set-up consist of fly food bottles, it is not an optimum set-up to conduct a large screen for investigating the effect of infection in several mutant lines. To assess

the efficiency of the infection set-up, I conducted a longevity assay, which showed that exposed flies died within 20 days, compared to the non-exposed flies. In the infection chamber, *B. bassiana* flies started to exhibit mortality on day 4, suggesting that *B. bassiana* could induce infection by day 4. More than 50 percent of the flies exhibited mortality on day 8, indicating that the infection had become severe by day 8. This suggested that the infection set-up can effectively induce infection in the flies.

Upon seven days of exposure to *B. bassiana*, a decline in climbing ability was observed in adult flies. This is in contrast with the summit effect induce by the *E. muscae* in the adult flies where the flies climb upwards to reach to a higher ground. This suggest that *B. bassiana* do not exhibit summit effect upon infection rather it decreases the climbing ability. *B. bassiana* also exists as plant endophyte and provide protection to plant from the insects (Branine et al., 2019, Behie et al., 2012, Behie et al., 2015). Thus, in this context the *B. bassiana* could decrease the climbing ability of the flies that could further facilitate more spore adherence and germination on the fly cuticle and eventually kills insect. Further investigation is required to test the effect of *B. bassiana* infection on the locomotion of the flies. This can be achieved by using FlyTracker which is real time motion tracking system and could provide valuable insights into the B. bassiana induced defects in fly locomotion. It is unclear whether infection affects the CNS or motor neurons in the legs to alter locomotion in the adult flies. Unfortunately, I could not further test whether infections affect the motor neurons in the legs.

Expression map of Toll-1 and Sarm revealed the expression of Toll-1 and Sarm in the proboscis and PER assay indicated that they could be involved in the circuit mediating

proboscis extension. Moreover, activating Sarm neurons resulted in proboscis extension. Even though the flies expressing TRPA1 in sarm neurons extended the proboscis, the experiment lacked low-temperature controls. These controls are necessary to verify whether the TRPA1 line I used was not leaky and to provide stronger evidence of whether sarm is involved in the proboscis extension. Since, Toll signalling is present in the proboscis and could potentially play a role in proboscis extension, it's possible that behaviour manipulating fungi like *E. muscae* could exploit it. However, it remains unclear whether *B. bassiana* exploit Toll signalling to affect proboscis extension and need further investigation. It would be worth testing if infected adult flies extend their proboscis by silencing the Toll-1 and Sarm neurons. This could be achieved by driving the expression of tetanus toxin UASTNT using Toll-1Gal4 and SarmGal4 and could further provide evidence if *B. bassiana* exploits the Toll signalling to affect the proboscis extension of the adult flies.

The feeding assay showed that flies ingested spores. This suggests that flies could ingest *B. bassiana* spores that might enter the brain through proboscis during feeding. Notably, Toll-1 is expressed in the gustatory neurons in the proboscis. However, further investigation is needed to determine whether *B. bassiana* exploits Toll in the proboscis. To explore this possibility, it would be interesting to test whether flies demonstrate a preference for feeding on spores when the Toll-1 gustatory neurons are silenced. Such an experiment could provide valuable evidence for the role of Toll-1 in this process.

The *Drosophila* BBB is analogous to the vertebrate BBB as it enwraps the brain and stringently regulates the flow of metabolites (Stork et al., 2008, Mayer et al., 2009, Desalvo et al., 2011). However, *Drosophila* does not have an open circulatory system

and organs usually bathe in the haemolymph (Stork et al., 2008). Thus, the BBB act as a shield and provides protection to the brain. The dextran red dye diffused in the retina of the adult flies which indicated that BBB is damaged upon 7 days exposure to *B. bassiana*. A good approach to strengthen the evidence of blood-brain barrier damage upon infection would be to quantify the concentration of the dye by measuring the fluorescent intensity using imaging software like ImageJ. However, due to lack of evidence it remains unclear whether *B. bassiana* spores are damaging the blood brain barrier. It could also be due to the host response against infection to increase the permeability of BBB for macrophages that could clear the pathogen from the brain (Winkler et al., 2021).

The presence of spores in the adult brain was showed through staining with FM4-64 and Calcofluor white. However, these dyes also labelled the trachea. To address the issue of the dyes staining the trachea, different incubation periods and increased washes with PBT were tried, but the problem persisted. To resolve this, the presence of spores was confirmed through the use of the transgenic *B. bassiana*-GFP strain. In summary, multiple methods were utilized to visualize the spores in the adult brain, all of which confirmed their presence.

The PRR's sense the fungal spores in adult CNS and activate the immune response. However, GNBP3 null mutant flies showed an upregulation of *drosomycin* upon natural infection by *B. bassiana,* suggesting that *B. bassiana* could also activate Toll signalling independently of GNBP3 by producing PR1 virulence factor (Gottar et al., 2006).

It has been demonstrated that neuronal and glial induced upregulation of *drosomycin* and *metchnikowin* leads to an increase in neurodegeneration index in the adult brain (Cao et al., 2013). In addition, IMD-NF-kB dependent AMP expression increases with age and causes neurodegeneration and locomotion defects in the adult flies (Kounatidis et al., 2017). This suggest that activated innate immune system can cause neurodegeneration in the brain. Interestingly, Drosomycin is not effective against *B. bassiana* as flies expressing *drosomycin* could not survive natural *B. bassiana* infection (Tzou et al., 2002). My qRT-PCR data showed an upregulation of *drosomycin* in dissected adult brain upon 7 days exposure to *B. bassiana*. This is consistent with the previous finding which showed that 8 days natural exposure to *B. bassiana* induced strong expression of *drosomycin* in adult flies (Lemaitre et al., 1997). Based on these results it can be hypothesised that *B. bassiana* activates the Toll signalling to upregulate the expression of drosomycin, which can cause neurodegeneration in the brain.

To conclude, the upregulation of *drosomycin* upon 7 days exposure to *B. bassiana* confirms that immune Toll signalling was activated upon infection in the adult brain.

Chapter 4

B. bassiana cause neurodegeneration in the adult *Drosophila* brain

Abstract

Toxic chemicals in the air degrade health and promotes neurodegeneration, but the impact of fungal spores on neurodegeneration lacks evidence. Poor indoor air quality can cause sick building syndrome (SBS) with flu-like symptoms, and analysis of samples from damp buildings revealed various fungal volatiles (Claeson et al., 2002,

Fischer et al., 2008, Matysik et al., 2008). Previous research showed that exposure to fungal volatiles like 1-octen-3-ol, 2-octanone, 2,5DMF, and tran-2-octanol reduced adult flies' lifespan (Inamdar et al., 2010). This chapter aims to provide more evidence on the effect of fungal spores on the brain and explore whether exposure to fungal spores causes neurodegeneration.

4.1 Introduction

The results of my previous chapter have suggested that *B. bassiana* spores could enter the adult brain that might reach brain via proboscis during feeding. However, the effect of *B. bassiana* spores on the adult brain are unknown. Previous studies have shown the effect of fungal volatile organic compound on the dopaminergic system (Inamdar et al., 2013, Inamdar et al., 2010), but effect of fungal volatiles on other areas of the brain has not been explored. As the brain comprises both glial cells and neurons, the effect of fungal infection on both these cell types need to be investigated.

Neurons and glial cells can be labelled with various antibodies that can be further quantified by different methods. For example, pan-glial antibodies, such as anti-REPO binds to the reversed polarity (REPO) a transcription factor specifically expressed in the glial cells and detects these cells in the adult brain (Losada-Perez, 2018). Automated cell counting software, such as *Deadeasy*, can then be used to quantify glial cells (Forero et al., 2010). Similarly, antibodies can be used against tyrosine hydroxylase (TH) to visualize dopaminergic neurons in the adult brain. TH is an enzyme that converts the tyrosine into L-Dopa, which is a precursor substrate in the dopamine production (Daubner et al., 2011). Anti-TH is widely used antibody to study dopaminergic system in the adult drosophila brain. Dead cells can be labelled with an

apoptotic antibody anti-Dcp1 and counted with an automated cell counting software (Forero et al., 2009). Anti-DCP1 binds to Death caspase 1 that cleaves specific protein during apoptosis (Ruiz-Losada et al., 2022). Therefore, the impact of infection on the adult *Drosophila* brain can be studied using above mentioned antibodies.

The expression map from the previous chapter showed that Sarm is expressed in the sog and proboscis and its activation leads to proboscis extension. Thus, making it a potential candidate that *B. bassiana* could exploit to enter the brain. Therefore, the effect of *B. bassiana* exposure on Sarm neurons in the adult brain needs further investigation.

Therefore, the aim of this chapter was to investigate if exposure to *B. bassiana* causes neurodegeneration. To test this hypothesis the objectives were:

1. To test the effect of *B. bassiana* exposure on the adult brain size.
2. To test the effect of *B. bassiana* on glial and Sarm cells in the adult brain.
3. To test the effect of *B. bassiana* on the dopaminergic system in the adult *Drosophila* brain.

4.2 Results

4.2.1 Exposure to *B. bassiana* decreased the size of the adult brain

To investigate the effect *B. bassiana* infection on the brain of adult flies, the size of adult brain was measured 3 days and 7 days post exposure to *B. bassiana*. Wild type Oregon flies were used for this experiment. The anti-Repo antibody was used to visualize the brain (Fig 4.1a & c). After 3 days exposure to *B. bassiana,* the area of the adult brain increased compared to non-infected flies (Fig 4.1b). This suggests that *B. bassiana* infection could potentially have an effect on the brain upon 3 days exposure

Figure 4.1 Exposure to *B.bassiana* infection decreased size of the adult brain

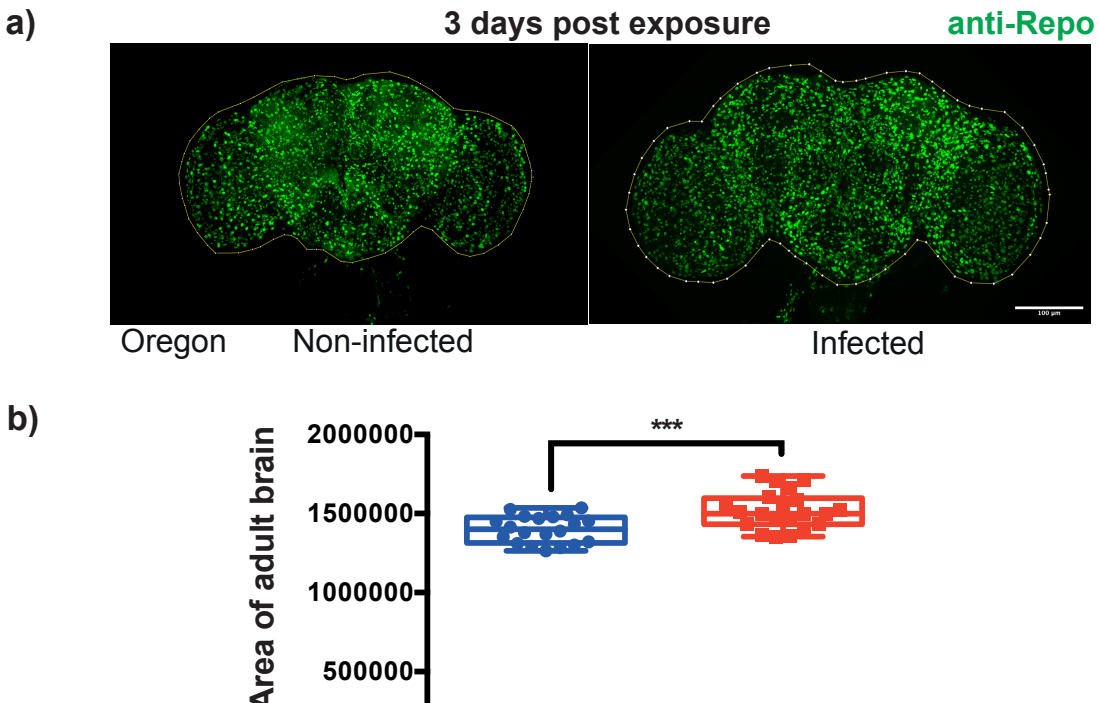


Figure 4.1 Exposure to *B. bassiana* decreased size of the adult brain.

a) Z-projection of the adult brain used to measure the area of the adult brain after 3 days exposure to *B. bassiana*. The brown line around the brain represents the region of interest (ROI) used to measure area via imageJ.
b) Graph representing the area of the adult brain of non-infected and infected after 3 days exposure to *B. bassiana* in the infection chamber. The brain size of non-infected flies is represented by the blue box plot and brain size of the infected flies is represented by a red box plot. Each dot represents a single adult brain. Unpaired student's T-test, p-value = 0.0006, N= 20 (non-infected), 21 (infected)
c) Z-projection of the adult brain showing the area of the adult brain after 7 days exposure to *B. bassiana*. The brown line around the brain represents the region of interest (ROI) that is used to measure the brain size via imageJ.
d) Graph representing the area of the adult brain of non-infected and infected after 7 days exposure to *B. bassiana* in the infection chamber. The brain size of non-infected flies is represented by a blue box plot and brain size of infected flies is represented by a red box plot. Each dot represents a single adult brain. Unpaired student's T-test, p-value = <0.0001, N = 22 (Non-infected), N = 21 (Infected).

Genotype:

Control = Noninfected Oregon

Infected Oregon

to *B. bassiana*. However, after 7 days exposure to *B. bassiana,* the area of the infected adult brain decreased compared to the non-infected adult brain (Fig 4.1c & d). This indicate that the fungal infection could affect the adult brain.

4.2.2 Exposure to *B. bassiana* decreased glial cells in the adult brain

Next, the effect of *B. bassiana* infection on the glia was investigated in the adult brain of Wild type Oregon flies. The glial cells were stained with mouse anti-Repo antibodies. After 3 days exposure to *B. bassiana,* the glial cells remained unchanged in both infected and non-infected adult brain, indicating that the infection did not affect the glia at this stage (Fig 4.2a & b). However, upon 7 days exposure, the number of glial cells decreased in the brain of the infected flies compared to the non-infected flies (Fig 4.2c & d). This reduction in the glial cells upon infection was clearly seen in the scanned images (Fig 4.3c). Cell counting with the *Deadeasy* also showed a decrease in glial cell number in the adult brain, upon 7 days post exposure as compared to non-infected adult brain (Fig 4.4d). This suggested that infection caused reduction in glial cells in the adult brain upon 7 days exposure to the *B. bassiana*.

4.2.3 Exposure to *B. bassiana* decreased the Sarm cells in the central brain

Since exposure to *B. bassiana* caused a decrease in brain size and glial cells, effect of *B. bassiana* on neurons was investigated by counting Sarm+ cells in the central brain. To visualize the expression of Sarm cells in the adult brain, SarmNP0257Gal4 was crossed with UAShistoneYFP (Fig 4.3a & c). HistoneYFP is a fluorescent nuclear reporter which allows identification of cell lineages and easy cell counting (Kurup et al., 2005).

Figure 4.2 Exposure to *B. bassiana* caused loss in the glia of the adult brain

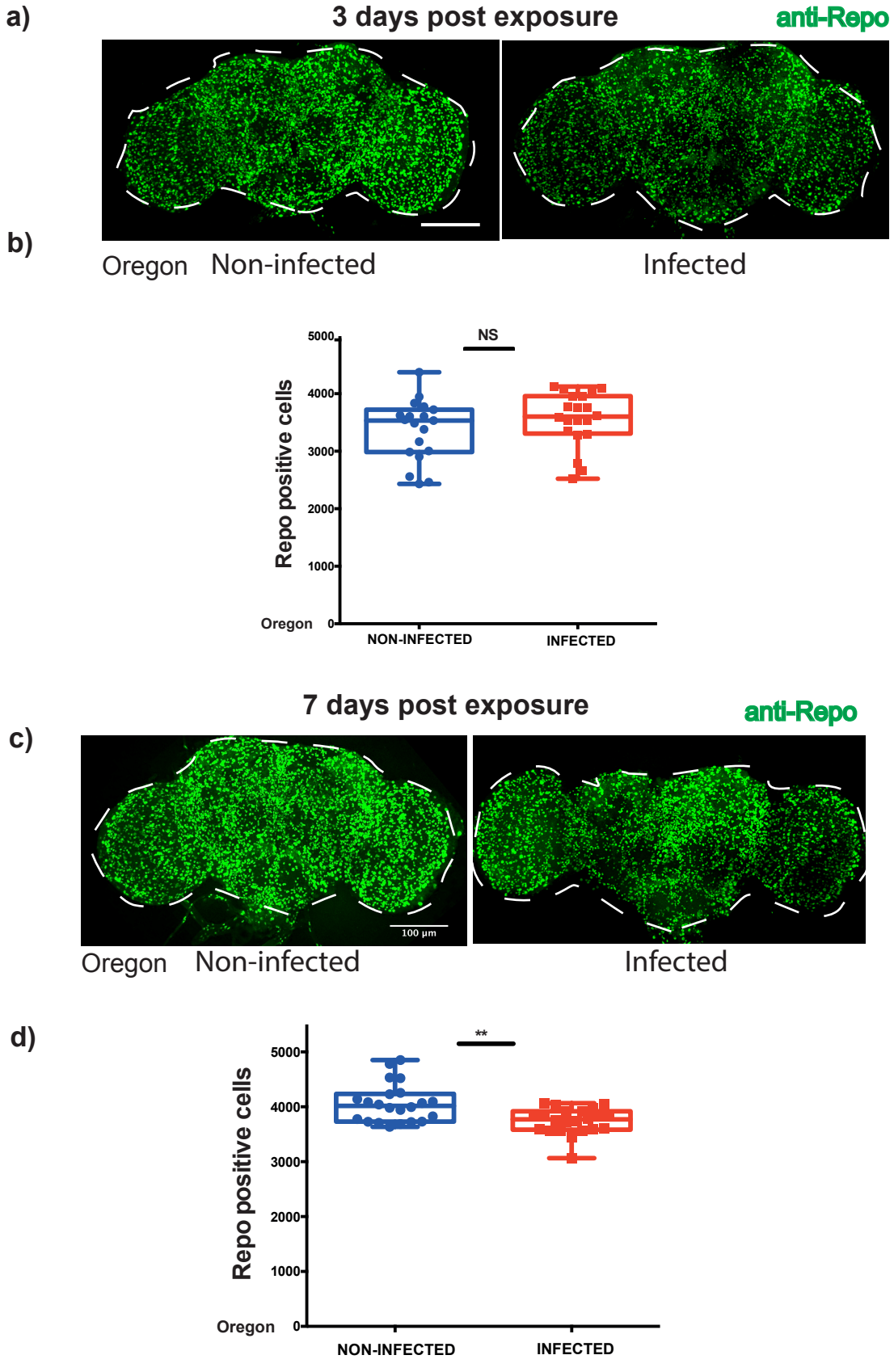


Figure 4.2 Exposure to *B. bassiana* decreased glial cells in the adult brain

a) Z projection of the adult brain showing brain glia cells labelled by anti-Repo in non-infected and infected adult brain after 3 days exposure to *B. bassiana*. Adult brain marked by the dotted white line used as a ROI for cell counting.
b) Graph representing number of glial cells in the adult brain counted by the automated cell counting program *Deadeasy*. The non-infected adult brain is represented by the blue box plot and infected adult brain is represented by the red box plot. Each dot represents a single adult brain. Unpaired T-test. N = 19 (Non-infected), 20 (Infected), NS = not significant
c) Z projection of the adult brain showing the expression of the glial cells labelled by anti-Repo in non-infected and infected adult brain after 7 days exposure to the *B. bassiana*. Adult brain marked by the dotted white line used as a ROI for cell counting.
d) Graph representing number of glial cells in the adult brain by the automated cell counting program *Deadeasy*. The number of glial cells in non-infected adult brain is represented by a blue box plot and glial cells in the infected adult brain is represented by a red box plot. Each dot represents a single adult brain. Unpaired student's t-test, p-value = 0.002. Scale bar = 100μm.

Genotype: Control = Non-infected Oregon

Infected Oregon

Figure 4.3 Exposure to *B.bassiana* decreased Sarm neurons number in the central brain

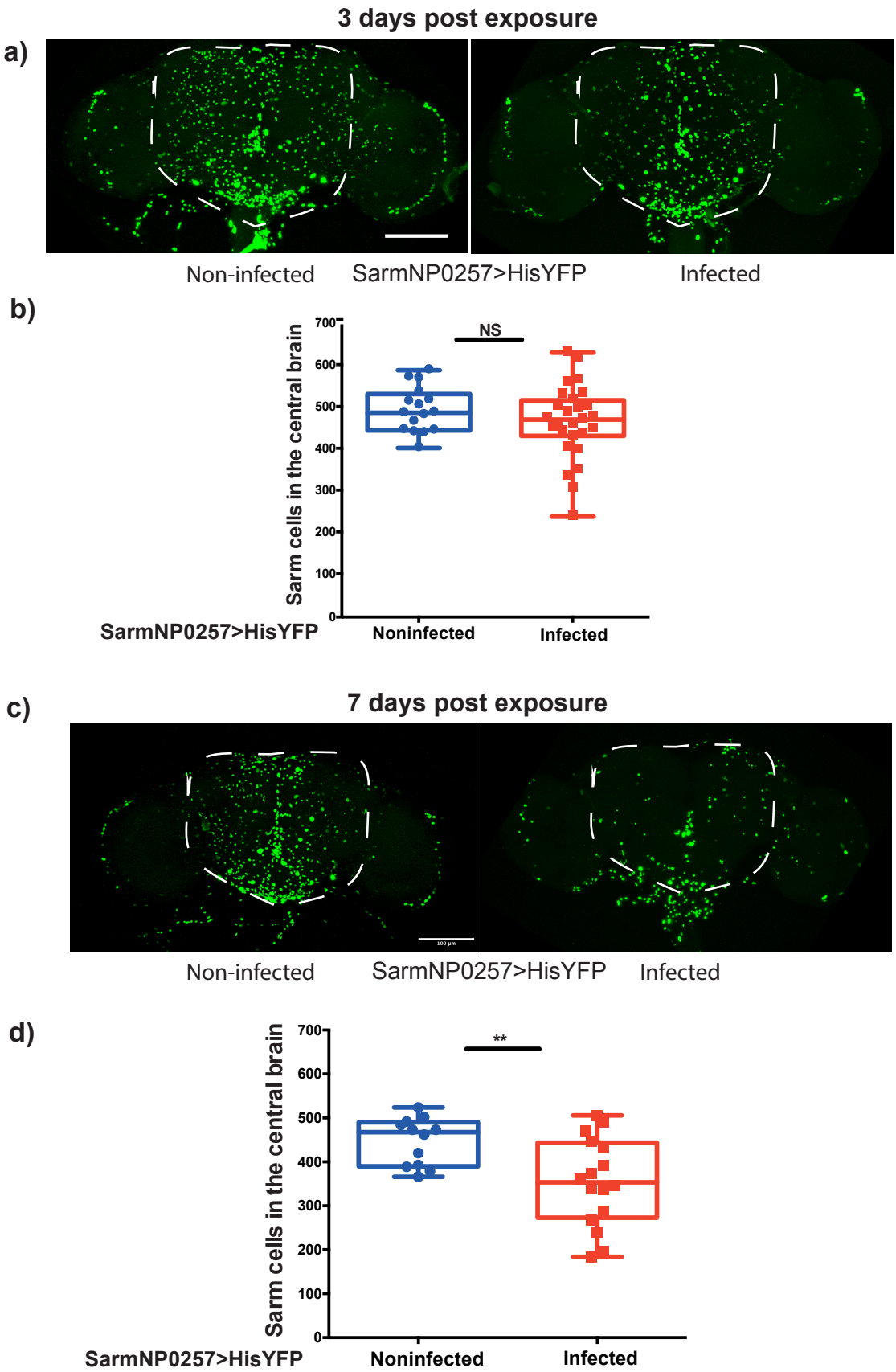


Figure 4.3 Exposure to *B. bassiana* decreased the Sarm+ neurons in the central brain

a) Z projection of the adult brain showing the expression of the Sarm+ cells in non-infected and infected adult brain after 3 days exposure to the *B. bassiana*. Central brain marked by the dotted white line used as a ROI for cell counting.
b) Graph representing number of the Sarm+ cells in the central brain counted by the automated cell counting program Deadeasy. The non-infected adult brain is represented by a blue box plot and infected adult brain is represented by a red box plot. Each dot represents a single adult brain. Unpaired T-test. N = 15 (Non-infected), 27 (Infected)
c) Z projection of the adult brain showing the expression of the Sarm+ cells in non-infected and infected adult brain after 7 days exposure to the *B. bassiana*. Central brain marked by the dotted white line used as a ROI for cell counting.
d) Graph representing number of the Sarm+ cells in the central brain counted by the automated cell counting program *Deadeasy*. The number of Sarm+ cells in non-infected adult brain is represented by the blue box plot and number of Sarm+ cells in the infected adult brain is represented by the red box plot. Each dot represents a single adult brain. Mann-whitney test, p-value = 0.002.
Scale bar = 100μm

Genotype:

Control: Non-infected SarmNP0257 Gal4 UAS Histone YFP

Infected SarmNP0257 Gal4 UAS Histone YFP

In both male and female flies, the number of Sarm+ cells in the central brain remained unchanged after 3 days of exposure to *B. bassiana* when compared to the non-infected controls (Fig 4.3a & b). As there was no difference in the effect of the infection between the sexes, the data for both male and female were pooled (Fig 4.3b). However, 7 days post exposure, the number of the Sarm+ cells in the central brain decreased significantly compared to the non-infected controls (Fig 4.3c). Cell counting with *Deadeasy*, confirmed the decrease in the number of Sarm+ cells in the central brain (Fig 4.3d). These findings suggested that *B. bassiana* infection causes a loss of Sarm+ cells after 7 days exposure to *B. bassiana.*

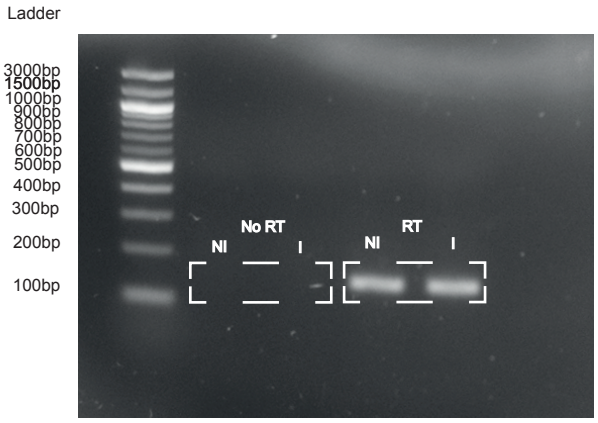
4.2.4 Exposure to *B. bassiana* downregulates TH mRNA expression in the adult brain

Exposure to *B. bassiana* caused a decrease in brain size and loss of both glia and neuron in the adult brain, suggesting that *B. bassiana* is causing neurodegeneration. To investigate this further, a qRT-PCR was performed to quantify the expression of tyrosine hydroxylase in the dissected adult brain, 7 days post exposure.

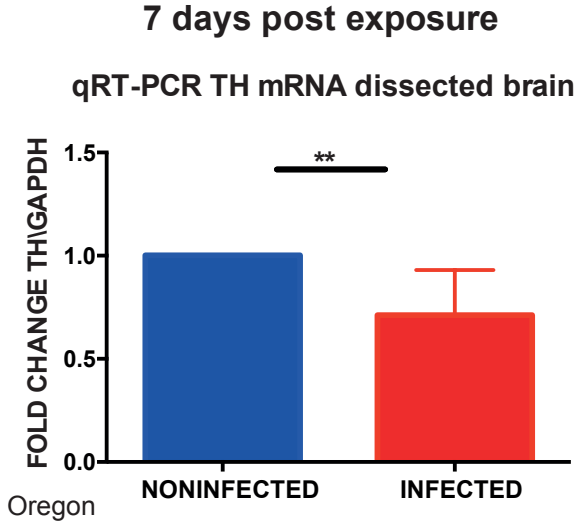
RNA was extracted from dissected adult wildtype Oregon flies and reverse transcribed into cDNA. The expected band was observed, and the No-RT control showed no band, indicating the absence of genomic contamination in the purified RNA (Fig4.4a). Subsequently, a qRT-PCR was performed using the cDNA as a template, and relative gene expression of TH was calculated using GAPDH as a housekeeping gene, indicated by fold change. The expression of TH in the brains of infected flies was downregulated compared to non-infected flies (Fig 4.4b), indicating lower TH levels in adult brain, 7 days post *B. bassiana* exposure. Tyrosine hydroxylase is an enzyme that

Figure 4.4 Exposure to *B. bassiana* decreased TH mRNA levels in the dissected adult brain

a)



b)



Oregon

Figure 4.4 Exposure to *B. bassiana* decreased TH mRNA levels in the dissected adult brain

a) Confirmation of cDNA synthesis by gel electrophoresis. Total RNA was extracted from wild-type Oregon flies and reverse transcribed into cDNA using a GoTaq reverse transcriptase kit. Transcribed cDNA showed the expected band on the gel. NI = non-infected sample, I =infected sample. RT = cDNA, NoRT = RNA

b) qRT-PCR analysis of tyrosine hydroxylase (TH) mRNA expression in dissected adult brain after 7 days exposure to *B. bassiana*. Data are presented as fold change in TH mRNA expression ± standard deviation (SD) relative to noninfected wild type control samples. The expression of the TH mRNA was normalized by GAPDH as a housekeeping gene. Statistical significance was determined using unpaired student t-test on delta-Ct values, P value = 0.0011. N = 3 biological replicates.

Genotype: Control = Noninfected Oregon
Infected Oregon

converts tyrosine to L-Dopa which is a precursor molecule utilized in the dopamine production (insert reference). Therefore, reduction in the levels of the TH mRNA 7 days post exposure indicate that *B. bassiana* might have some role in affecting the production of dopamine in adult brain.

4.2.5 Exposure to *B. bassiana* caused loss of dopaminergic neurons

To determine whether the low TH levels in infected flies corresponded to a decrease in dopaminergic (DAN) neurons cell number, DAN neurons were visualised in vivo in the brain using anti-TH antibodies (Fig 4.5 & Fig 4.6). Schematics of dopaminergic neurons are shown in (Fig 4.5 b). After 7 days exposure to *B. bassiana*, the DAN neurons in the PAM cluster decreased in the infected brain compared to the non-infected brain (Fig 4.5a & c). Additionally, the number of DAN neurons in PPL1, PPL2, PPM1\2 and PPM3 reduced in number upon exposure in the wild type Oregon flies (Fig 4.6a & c). This further confirms that 7 days post exposure the dopamine levels in the brain decrease upon infection. Together, these data suggest that 7 days exposure to *B. bassiana* causes DAN neurons degeneration.

4.3 Discussion

In this chapter, brain size analysis has demonstrated that after 7 days exposure to *B. bassiana,* size of the adult Drosophila decreased compared to non-exposed control flies. Additionally, after 7 days exposure to *B. bassiana*, the number of glial cells and Sarm+ cells in the adult brain decreased. qRT-PCR data showed that TH mRNA was downregulated in the dissected adult brain after 7 days exposure to *B. bassiana*. Moreover, the number of anti-TH labelled dopaminergic neurons in different clusters including PAM, PPL1, PPL2, PPL3 and PPM1/3, decreased in number after 7 days

Figure 4.5 Exposure to *B. bassiana* caused dopaminergic neurons loss in PAM cluster

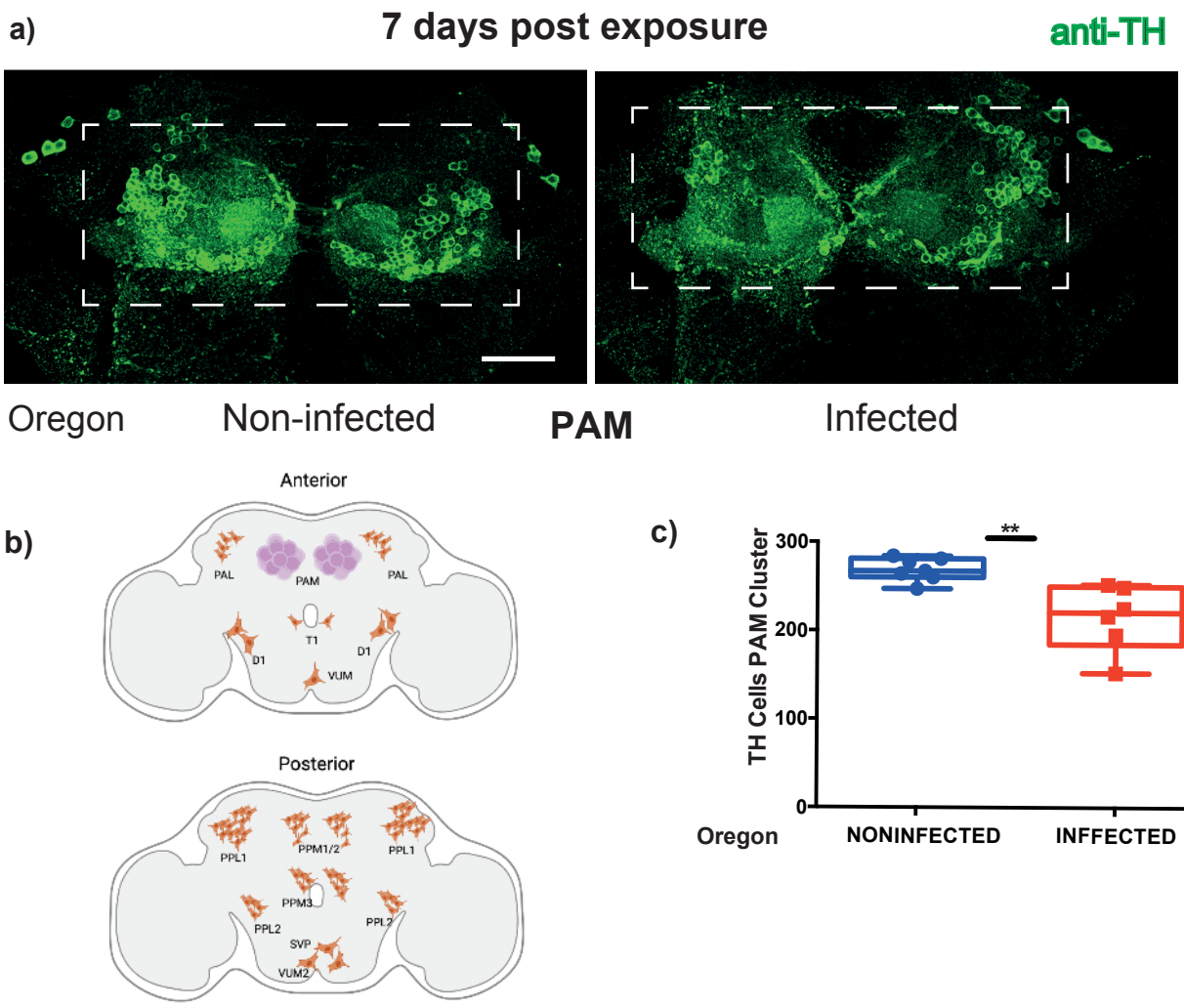


Figure 4.5 Exposure to *B. bassiana* caused dopaminergic neurons loss in PAM cluster

a) Exposure to *B. bassiana* caused loss of dopaminergic neurons within PAM cluster. PAM neurons are labelled by anti-TH in non-infected and infected adult CNS after 7 days exposure to the *B. bassiana*. PAM cluster marked by the dotted white line used as a ROI for the cell counting. Scale bar = 50um.
b) Schematics of dopaminergic neurons in the adult brain
c) Box plot representing the number of the dopaminergic neuron in the PAM cluster of the non-infected and infected flies after 7 days exposure to B.bassiana. Unpaired student t-test, P value = 0.0043. N = 7 (non-infected), 6 (Infected).

Genotype: Control: Non-infected Oregon
Infected Oregon

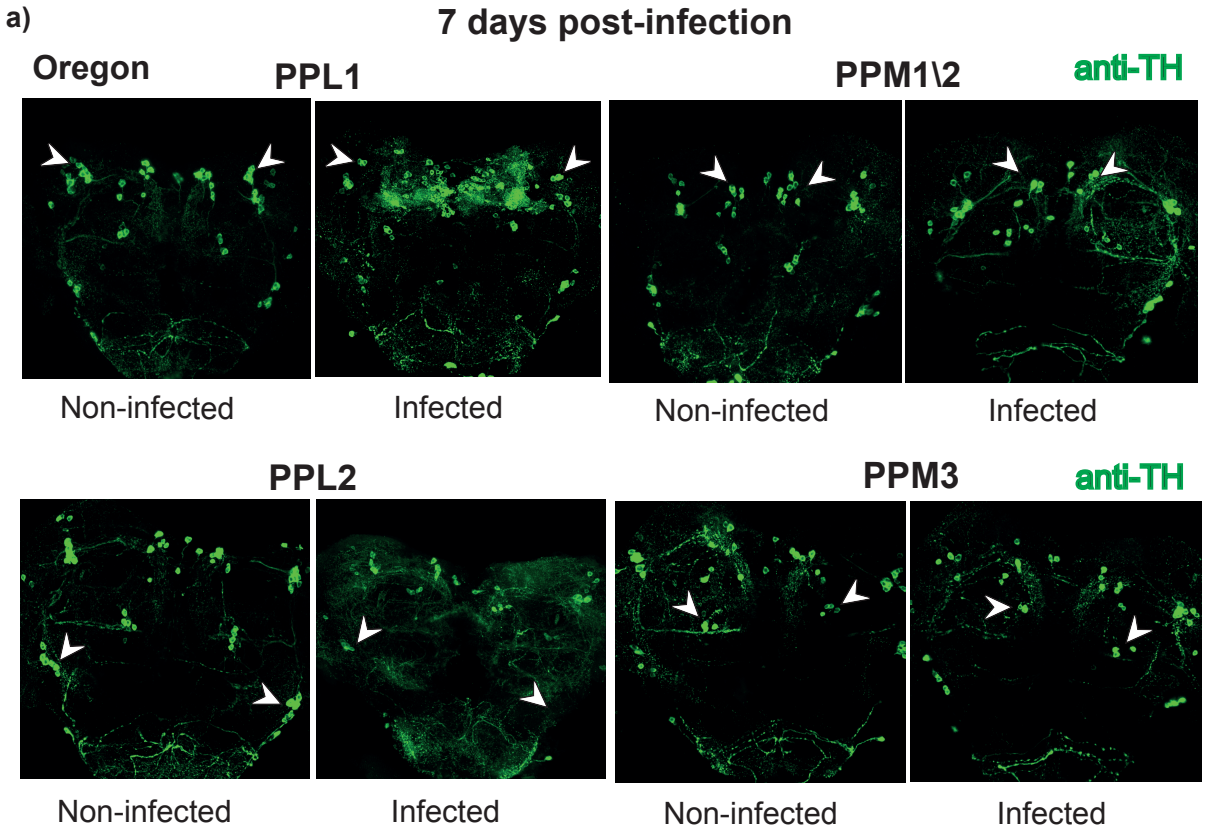
Figure 4.5 Exposure to *B. bassiana* caused dopaminergic neurons loss in PAM cluster

a) Exposure to *B. bassiana* caused loss of dopaminergic neurons within PAM cluster. PAM neurons are labelled by anti-TH in non-infected and infected adult CNS after 7 days exposure to the *B. bassiana*. PAM cluster marked by the dotted white line used as a ROI for the cell counting. Scale bar = 50um.
b) Box plot representing the number of the dopaminergic neuron in the PAM cluster of the non-infected and infected flies after 7 days exposure to *B. bassiana*. Unpaired student t-test, P value = 0.0043. N = 7 (non-infected), 6 (Infected).

Genotype: Control: Non-infected Oregon

Infected Oregon

Figure 4.6 **Exposure to *B. bassiana* caused loss of neurons in the dopaminergic clusters**



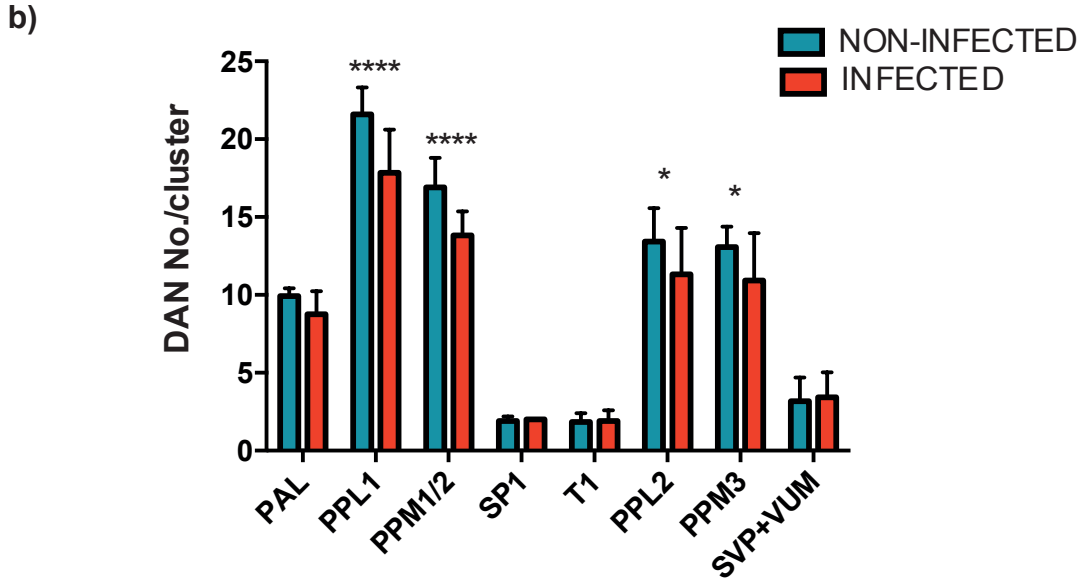


Figure 4.6 Exposure to *B. bassiana* caused loss of neurons in the dopaminergic clusters

a) Dopaminergic neurons in the PPL1, PPM1\2, PPL2 and PPM3 cluster labelled with anti-TH in non-infected and infected brain after 7 days exposure to the *B. bassiana*. PAM cluster marked by the dotted white line used as a ROI for cell counting.
b) Bar graph representing the number of neurons in different dopaminergic clusters of non-infected and infected flies after 7 days exposure to *B. bassiana*. Error bar shows standard deviation. Two-way ANOVA followed by Sidak's multiple comparison test (Appendix 30), P value = **** <0.0001, *<0.018. N = 12 (non-infected), 12 (infected).

Genotype: Control = Non-infected Oregon

Infected Oregon

exposure to *B. bassiana*. Together, these data confirm that 7 days exposure to *B. bassiana* caused neurons and glial loss in the adult brain.

Different approaches were used to investigate the effect of natural exposure of *B. bassiana* on the adult *Drosophila* brain. The brain size analysis showed a decrease in the adult brain size after 7 days exposure to *B. bassiana* which was consistent with the decrease in Sarm+ cells, glial cells, and dopaminergic neurons. These findings suggested that *B. bassiana* affected the neurons and glia in the brain after 7 days of exposure to *B. bassiana*. However, after 3 days of exposure the area of the infected adult brain increased, which contrasted with the Sarm+ cell count and glial cell count data. Neither the Sarm+ cell count nor the glial cell count increased after 3 days of exposure to *B. bassiana*. This suggests that area of the adult brain size may not be an optimum parameter for testing the effect of infection on the brain, as the concentration of the fixative and fixation time could also have an effect on the brain size. Another possibility for the increase in brain size after infection could be an inflammatory response that leads to an influx of macrophages, fluids, and proteins. It has been reported that glia could mount an inflammatory response by recruiting macrophages that cross the blood brain barrier and reach the pupal brain (Winkler et al., 2021). To investigate this possibility, anti-croquemort was used to label macrophages in the brain after infection. However, the brain scans had high background noise, making it difficult to determine whether macrophages entered the brain and caused inflammation. Therefore, further testing of this possibility was not feasible.

To investigate further whether *B. bassiana* caused neurodegeneration in the brain, dead cells were visualized using an anti-apoptotic marker DCP1. Although dead cells

were observed, high background in the scanned images prevented counting the dead cells via Deadeasy plug-in. To overcome this, caspase 3/7 enzyme activity was measured upon infection using the Apo-ONE caspase 3/7 assay kit. However, the protocol could not be optimized for the experiment. Detecting apoptotic cells is challenging since they are swiftly removed via phagocytosis. Thus, effect of *B. bassiana* on the dopaminergic system was investigated as an alternative approach to test if B. bassiana causes neurodegeneration in the adult brain.

Loss of dopaminergic neurons and tyrosine hydroxylase (TH) has been previously reported as an indicator for neurondegeneration in the adult *Drosophila* brain (Inamdar et al., 2013). In this chapter, qRT-PCR data suggest that expression of TH mRNA was downregulated after 7 days of exposure to *B. bassiana* spores in the dissected adult brain. This suggested that the 7 days exposed flies have low dopamine in the brain compared to the non-infected control flies. The anti-TH immunostaining data further indicated towards the reduction in the dopamine levels, as infected flies showed reduction in the neurons of different dopaminergic clusters in the brain. Together these findings suggest that *B. bassiana* might cause neurodegeneration in the adult *Drosophila* brain. Another way to validate the above data and confirm whether *B. bassiana* causes neurodegeneration is by quantifying and visualizing dead cells through the expression of p35 in the nervous system. The number of p35-expressing cells can then be quantified after a 7-day exposure to *B. bassiana*. P35 is known to prevent apoptotic death of infected cells. If B. bassiana is indeed causing neurodegeneration in the brain, the number of P35-expressing cells would be higher compared to non-infected controls. Therefore, quantifying p35 cells in the adult brain

upon infection could provide valuable insights into whether B. bassiana induces neurodegeneration in the adult brain.

Chapter 5

B. bassiana causes neurodegeneration via Toll-1 in the adult *Drosophila* brain

Abstract

The innate immune response, mediated by Toll receptors, serves as the first line of defence. However, Toll receptors have other functions apart from activating immune response. They can bind with different neurotrophins to regulate cell death and survival (Foldi et al., 2017). In mammals, reports indicate that *C. albicans* can engage with TLR-2, leading to increase production of anti-inflammatory IL-10 and T-regulatory cells, making the mice more susceptible to *C. albicans* infection (Netea et al., 2007). Thus, this chapter aims to investigate whether *B. bassiana* could exploit Toll-1 to induce cell death in the adult *Drosophila* brain.

5.1 Introduction

The results of chapter 3 indicated that spores could enter the brain possibly via feeding. Data from chapter 4 have suggested that exposure to *B. bassiana* could potentially cause neurodegeneration in the adult fly brain. Furthermore, the expression of anti-fungal peptide *drosomycin* was upregulated after 7 days exposure to *B. bassiana* in the dissected adult brain, suggesting that Toll signalling is active in the adult brain. Therefore, we hypothesised that *B. bassiana* could exploit Toll signalling to induce neurodegeneration in the adult brain.

In Drosophila, Toll-1 activates the innate immune system, which upregulates anti-fungal peptides via NF-kB pathway to protect the fly from pathogens (Lemaitre et al., 1996, Lemaitre et al., 1997). However, previous work from our lab has shown that Toll signalling can also induce cell death via Wek, Sarm, and JNK pathway (Foldi et al., 2017). Moreover, overexpressing activated Toll-1^{10b} with a pan-neuronal Gal4 driver, *elav*-GAL4, decreased the number of Eve+ neurons in the larval VNC, indicating that Toll-1 is proapoptotic (Foldi et al., 2017). Since Toll signalling protects the fly from the fungal infection and could cause cell death, indicates that entomopathogenic fungal pathogens may have evolved a mechanism to manipulate Toll-1 to induce apoptosis and kill their host.

Therefore, the aim of this chapter is to investigate whether *B. bassiana* causes neurodegeneration in the adult *Drosophila* brain through Toll-1.To test this hypothesis the expression of *Toll-1* was manipulated using RNAi knockdown and overexpression lines, UAS*Toll-1*RNAi^{JF10491} and UAS*Toll-1*^{10b} previously published in (Li et al., 2020, Foldi et al., 2017). Since Toll-1 plays a key role in the development of flies by establishing the dorsal ventral polarity in the embryo (Morisalo and Anderson, 1995), manipulating the expression of *Toll-1* throughout development would be lethal. Therefore, *Toll-1* expression was manipulated only in the adult flies by using Tubulingal80^{ts}. Tubulingal80^{ts} is a temperature sensitive gene that inhibit Gal4 activity at 25ºC, but at 30ºC, the dimer of Tubulingal80^{ts} cannot bind to Gal4, thus enabling gene expression (McClure et al., 2022, Pfeiffer et al., 2010). Both controls and experimental flies were raised at 18ºC throughout development and shifted to 30ºC at eclosion for 48hrs to inhibit TubulinGal80^{ts}, ensuring that *Toll-1* expression is manipulated only in adult flies. The flies were then transferred to an infection chamber

at 25ºC, to maintain consistent infection conditions throughout the project and eliminate the effect of high temperature on gene expression.

5.2 Results

5.2.1 Adult *Toll-1* RNAi knockdown rescued the loss of MyD88+ cells caused by *B. bassiana* infection

Since Toll signalling was upregulated in the dissected adult brain via Toll-1 upon 7 days exposure to *B. bassiana*, I asked whether *B. bassiana* infection could cause cell loss in the absence of Toll-1. To test this, *Toll-1* was downregulated specifically in the adult brain using *Toll-1*RNAi for 48hrs in MyD88 cells, and the flies were infected with *B. bassiana* for 7 days (Fig 5.1 a). Two different *Toll-1*RNAi lines were used (Fig 5.1 and Fig 5.2). To visualize MyD88 cells in the brain, a MyD88 driver MyD88Gal4 was used to express the nuclear reporter UAShistoneYFP abbreviated as MyD88>HisYFP+. MyD88>hisYFP+ cells could be clearly seen in the images (Fig 5.1b, c). After exposing control flies for 7 days with *B. bassiana,* the number of MyD88>hisYFP+ cells decreased in the central brain of infected flies compared to non-infected control flies (Fig 5.1b, d). This indicated that exposure to *B. bassiana* caused MyD88>hisYFP+ cell loss in the adult brain.

By contrast, when *Toll-1* was downregulated in MyD88 cells the number of MyD88>hisYFP+ cells increased in the central brain of non-infected flies (Fig 5.1c, d), suggesting that Toll-1 may have a role in cell number regulation and could be pro-apoptotic. Interestingly, *Toll-1*RNAi$^{KK/100078}$ knockdown rescued the MyD88>hisYFP+ cell loss in the central brain induced by the *B. bassiana* infection (Fig 5.1c, d). Additionally, *Toll-1*RNAi$^{KK/100078}$ infected flies showed an increase in MyD88>hisYFP+

Figure 5.1 Adult Toll-1RNAi$^{KK/100078}$ knockdown rescued the loss of MyD88+ cells caused by *B. bassiana* infection

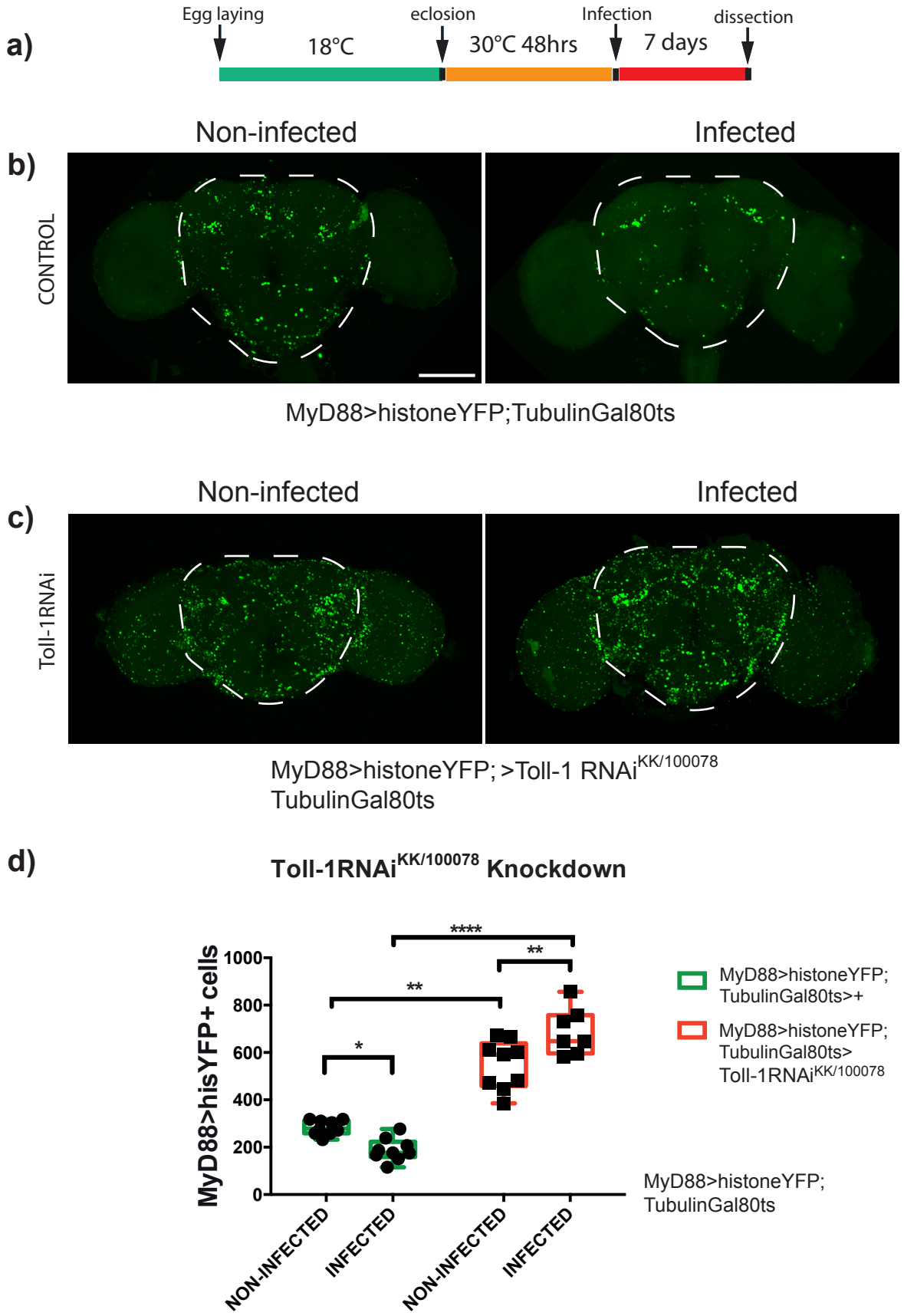


Figure 5.1 Adult *Toll-1*RNAi$^{KK/100078}$ knockdown rescued the loss of MyD88+ cells caused by *B. bassiana* infection.

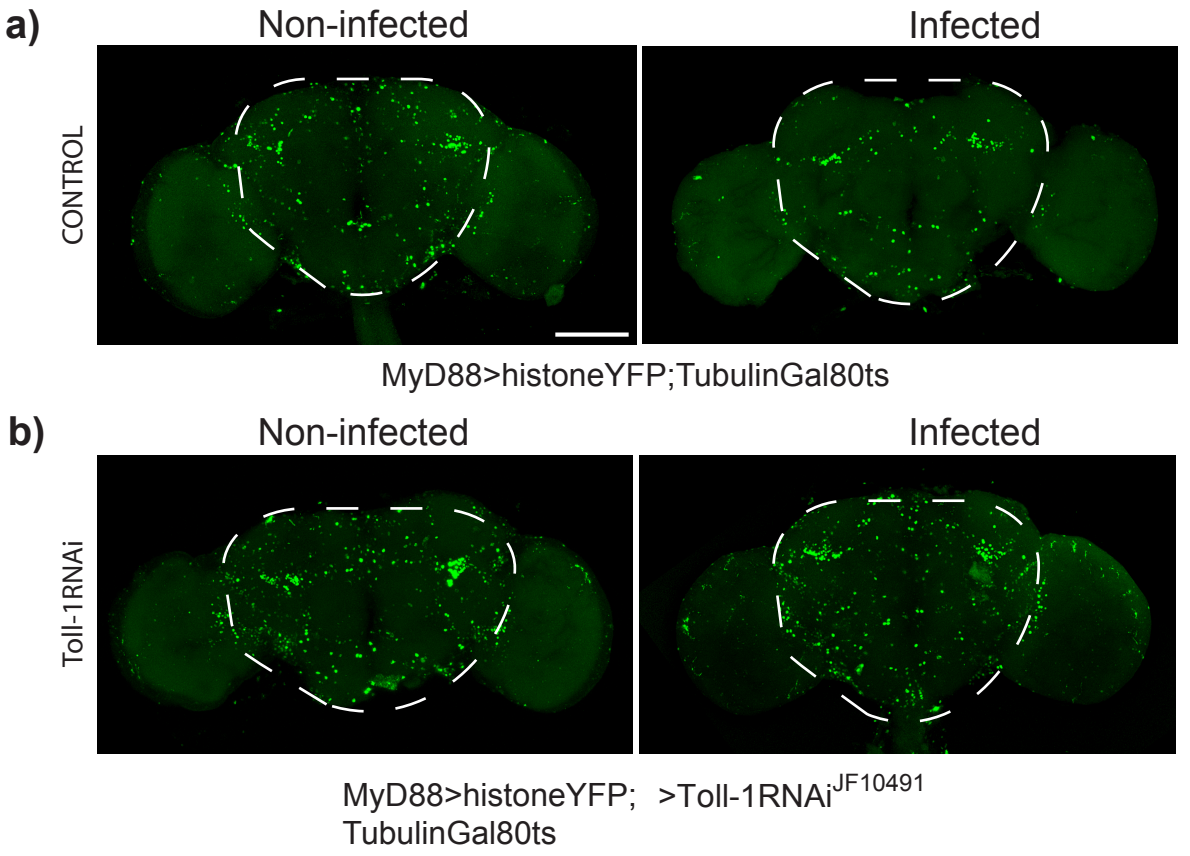
a. Diagram explaining the experimental regime. Flies were raised at 18ºC throughout development until eclosion. Eclosed flies were transferred to a 30ºC chamber for 48hr to deactivate tubulingal80^{ts}. Flies were then transferred to the infection chamber for 7 days and were dissected on 7 days exposure to *B. bassiana*.
b. Z-projection of the adult brain showing expression of MyD88+ cells in central brain of wild-type control non-infected and infected flies upon 7 days exposure to *B. bassiana*.
c. Z-projection of the adult brain showing expression of MyD88+ cells in central brain of *Toll-1*RNAi $^{KK/100078}$ non-infected and infected flies upon 7 days exposure to *B. bassiana*.
d. Box plot representing number of MyD88+ cells in central brain in control flies and in *Toll-1*RNAi $^{KK/100078}$ flies upon 7 days exposure to *B. bassiana*. The number of MyD88+ cells in central brain of non-infected and infected controls are represented by green box plot. The number of MyD88+ cells in central brain of non-infected and infected *Toll-1*RNAi$^{KK/100078}$ flies are represented by red box plot. Two-way ANOVA followed by Turkey's multiple comparison test (Appendix 7): *p value<0.05, **p value < 0.01, ***p value <0.001, ****p value < 0.0001. N = 10 (Noninfected control), 9 (Infected control), 9 (Toll-1RNAi Noninfected), 9 (Toll-1RNAi Infected), Scale bar = 100 um

Genotype

Control:
Non-infected MyD88>HistoneYFP/+;TubulinGal80^{ts} / +
Infected MyD88>HistoneYFP/+;TubulinGal80^{ts} /+

Test:
Non-infected MyD88>HistoneYFP/>Toll-1RNAi$^{KK/100078}$; TubulinGal80^{ts} /+
Infected MyD88>HistoneYFP/>Toll-1RNAi$^{KK/100078}$;TubulinGal80^{ts} /+

Figure 5.2 Adult Toll-1 knockdown with a differnt line Toll-1RNAi^{JF10491} also rescued the loss of MyD88+ cells caused by *B. bassiana* infection



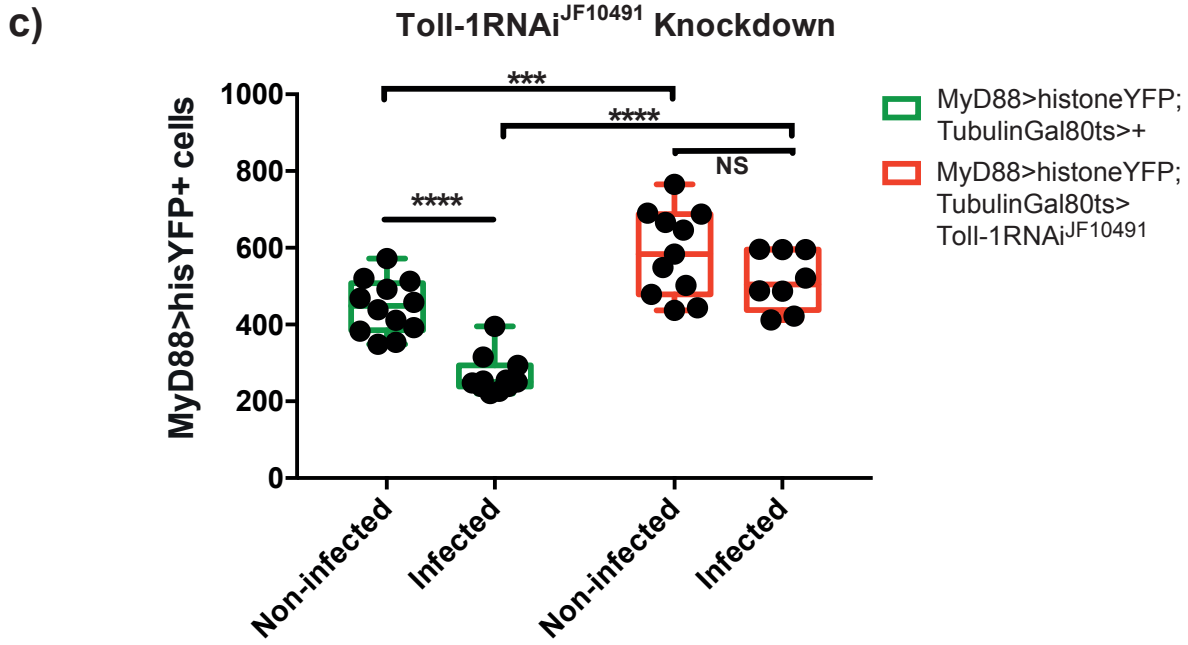


Figure 5.2 Adult Toll-1RNAi^{JF10491} knockdown rescued the loss of MyD88+ cells caused by *B. bassiana* infection.

a) Z-projection of the adult brain showing expression of MyD88+ cells in central brain of wild-type control non-infected and infected flies upon 7 days exposure to *B. bassiana*.
b) Z-projection of the adult brain showing expression of MyD88+ cells in central brain of *Toll-1*RNAi^{JF10491} non-infected and infected flies upon 7 days exposure to *B. bassiana*.
e. Box plot representing number of MyD88+ cells in central brain in control flies and in *Toll-1*RNAi^{JF10491} flies upon 7 days exposure to *B. bassiana*. The number of MyD88+ cells in central brain of non-infected and infected controls are represented by green box plot. The number of MyD88+ cells in central brain of non-infected and infected *Toll-1*RNAi^{JF10491} flies are represented by red box plot. Two-way ANOVA followed by Turkey's multiple comparison test (Appendix 8): *p value<0.05, **p value < 0.01, ***p value <0.001, ****p value < 0.0001. N = 12 (Noninfected control), 11 (Infected control), 11 (Toll-1RNAi Noninfected), 8 (Toll-1RNAi Infected), Scale bar = 100 um

Genotype

Control:
Non-infected MyD88>HistoneYFP/+;TubulinGal80^{ts} /+
Infected MyD88GALUASHistoneYFP/+;TubulinGal80^{ts} /+

Test:
Non-infected MyD88>HistoneYFP/+;TubulinGal80ts/> Toll-1RNAi^{JF10491}
Infected MyD88>HistoneYFP/+;TubulinGal80^{ts} /> Toll-1RNAi^{JF10491}

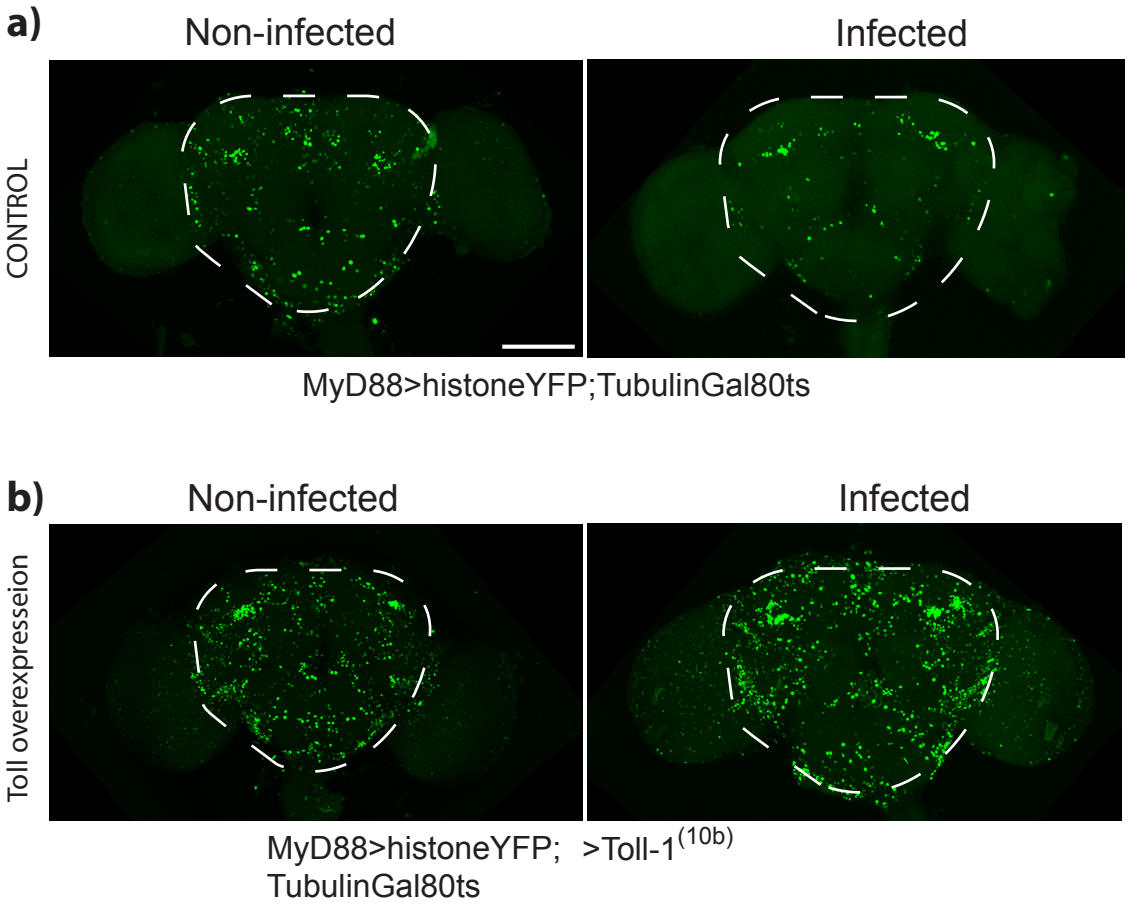
cells compared to the non-infected *Toll-1*RNAi$^{KK/100078}$ flies. Together these data suggest that *B. bassiana* could not induce MyD88>hisYFP+ cell loss without Toll-1.

To further test the above result, *Toll-1* was knocked down in MyD88 cell in the adult brain using a different RNAi line, UAS*Toll-1*RNAi^{JF10491}(Fig 5.2). The number of MyD88>hisYFP cells were decreased in the central brain in infected control flies as compared to the non-infected control flies (Fig 5.2b, d), similar to previous results. knocking down *Toll-1* with UAS*Toll-1*RNAi^{JF10491} in MyD88 cells resulted in an increase in MyD88>hisYFP+ cell number in non-infected *Toll-1*RNAi^{JF10491} flies (Fig 5.2b, c) which again indicated that Toll-1 was pro-apoptotic. Furthermore, infection did not decrease the MyD88>hisYFP+ cell number in the infected flies as compared to the non-infected *Toll-1*RNAi^{JF10491} flies (Fig 5.2b, c). These data showed that *B. bassiana* induced cell loss in the adult brain required Toll-1 signalling.

5.2.2 *B. bassiana* could not induce loss of MyD88+ cells upon *Toll-1^{10b}* overexpression in the adult brain

Next, I asked whether constitutively activated Toll-1 could induce MyD88>hisYFP+ cells apoptosis in the central adult brain. To test this, *Toll-1* was overexpressed in MyD88 cells using a Toll-1 overexpression line UAS*Toll-1^{10b}* (Fig 5.3). Same controls from (Fig 5.1 and Fig 5.2) were used in this test as well. When *Toll-1^{10b}* was overexpressed the number of MyD88>hisYFP+ cells in the central brain of noninfected flies increased as compared to the non-infected control flies (Fig 5.3b, c). This was similar to *Toll-1* knockdown data which showed an increase in MyD88>hisYFP+ cells in *Toll-1*RNAi knockdown noninfected flies (Fig 5.1 & 5.2). This indicated that Toll-1 was not pro-apoptotic and could regulate Myd88 cell number in a different way.

Figure 5.3 Constitutively activated Toll-1$^{(10b)}$ did not induce MyD88+ cell loss in the adult brain



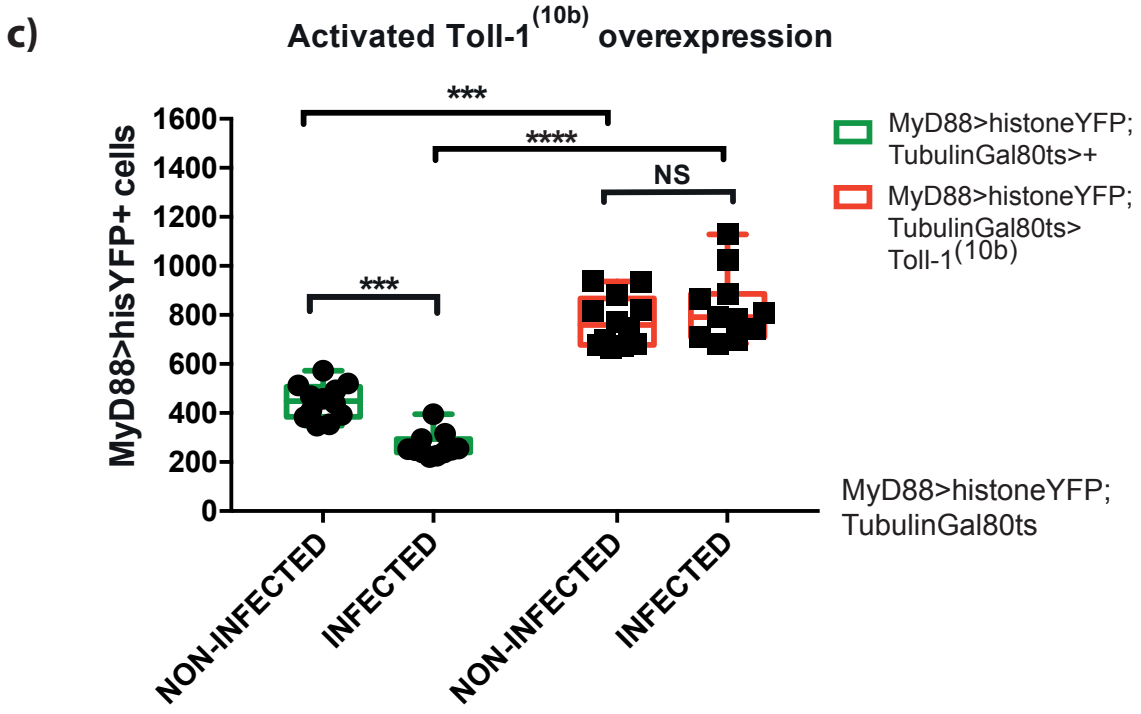


Figure 5.3 Constitutively activated UAS*Toll-1^{10b}* did not induce MyD88+ cell loss in the adult brain.

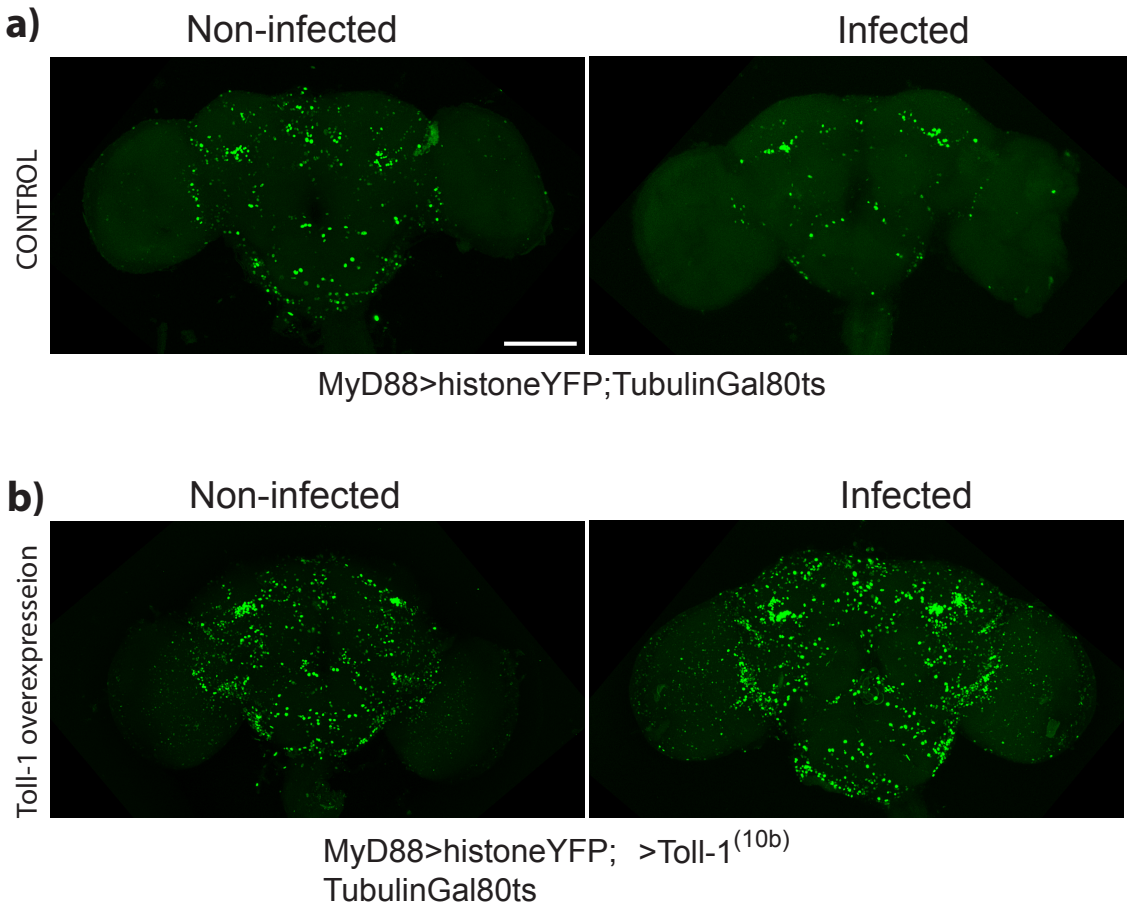
a) Z-projection of the adult brain showing expression of MyD88+ cells in central brain of wild-type control non-infected and infected flies upon 7 days exposure to *B. bassiana*. White line indicates central brain.
b) Z-projection of the adult brain showing expression of MyD88+ cells in central brain of UAS*Toll-1^{10b}* non-infected and infected flies upon 7 days exposure to *B. bassiana*.
c) Box plot representing number of MyD88+ cells in central brain in control flies and in UAS*Toll-1^{10b}* flies upon 7 days exposure to *B. bassiana*. The number of MyD88+ cells in central brain of non-infected and infected controls are represented by green box plot. The number of MyD88+ cells in central brain of non-infected and infected UAS*Toll-1^{10b}* flies are represented by red box plot. Two-way ANOVA followed by Turkey's multiple comparison test (Appendix 9): *p value<0.05, **p value < 0.01, ***p value <0.001, ****p value < 0.0001. N = 12 (Noninfected control), 11 (Infected control), 12 (Toll-1^{10b} noninfected), 12 (Toll-1^{10b} Infected) Scale bar = 100 um.

Genotype

Control:
Non-infected MyD88>HistoneYFP/+;TubulinGal80^{ts} /+
Infected MyD88GALUASHistoneYFP/+;TubulinGal80^{ts} /+

Test:
Non-infected MyD88>HistoneYFP/+;TubulinGal80ts/> Toll-1^{10b}
Infected MyD88>HistoneYFP/+;TubulinGal80^{ts} /> Toll-1^{10b}

Figure 5.4 Constitutively activated Toll-1$^{(10b)}$ could not decrease brain size upon *B. bassiana* infection



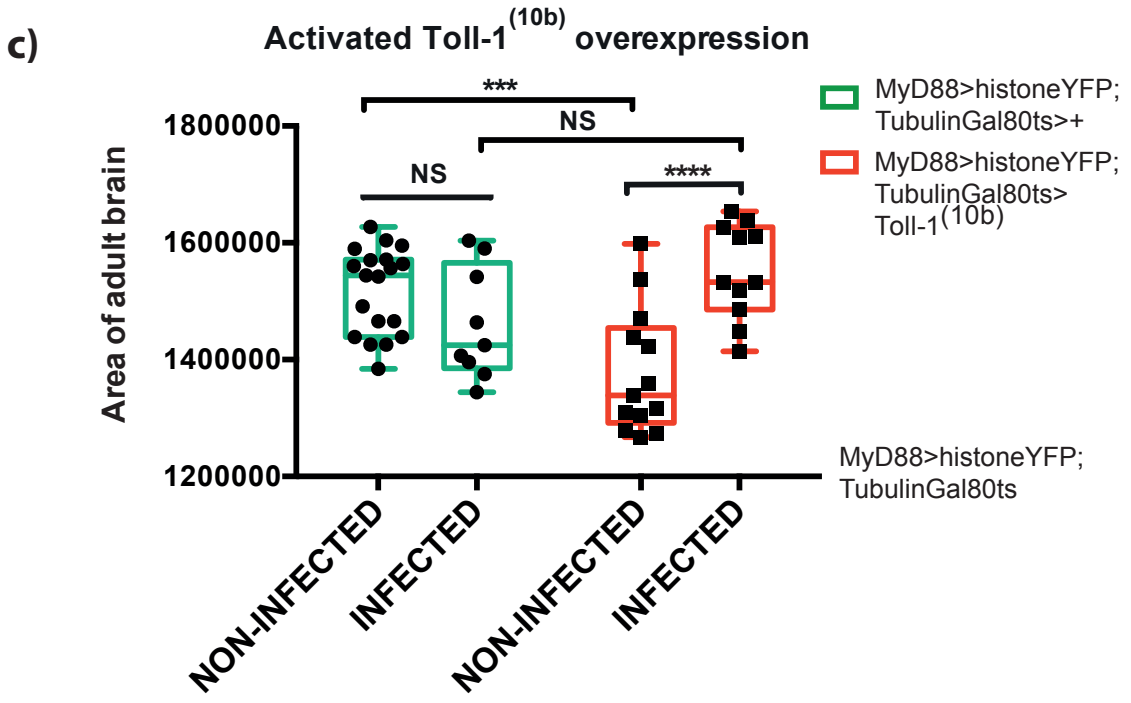


Figure 5.4 Constitutively activated *Toll-1^{10b}* overexpression increased brain size upon *B. bassiana* infection.

a) Z-projection of the adult brain used to measure area of the adult brain of wild-type control non-infected and infected flies upon 7 days exposure to *B. bassiana*.
b) Z-projection of the adult brain used to measure area of the adult brain of *Toll-1^{10b}* overexpression non-infected and infected flies upon 7 days exposure to *B. bassiana*.
c) Box plot representing area of adult brain of control flies and *Toll-1^{10b}* overexpression flies upon 7 days exposure to *B. bassiana*. The area of adult brain of non-infected and infected controls are represented by green box plot. The area of adult brain of non-infected and infected *Toll-1^{10b}* overexpression flies are represented by red box plot. Two-way ANOVA followed by Turkey's multiple comparison test (Appendix 10): *p value<0.05, **p value < 0.01, ***p value <0.001, ****p value < 0.0001. N = 12 (Noninfected control), 11 (Infected control), 13 (Toll-1 10b noninfected), 11 (Toll-10b Infected), Scale bar = 100 um.

Genotype

Control:
Non-infected MyD88>HistoneYFP/+;TubulinGal80^{ts} /+
Infected MyD88GALUASHistoneYFP/+;TubulinGal80^{ts} /+

Test:
Non-infected MyD88>HistoneYFP/+;TubulinGal80ts/> Toll-1^{10b}
Infected MyD88>HistoneYFP/+;TubulinGal80^{ts} /> Toll-1^{10b}

Alternatively, this could also indicate towards the leaky regulation of Toll-1 transcription at 25ºC in infection chamber by tubulingal80^{ts}. Therefore, whether Toll-1 is pro-apoptotic could not be confirmed. Similarly, when *Toll-1^{10b}* overexpressing flies were exposed to *B. bassiana*, the number of MyD88>hisYFP+ cells did not decrease in central brain (Fig 5.3b, c). This could indicate a protective role of Toll-1 against the fungal pathogen.

To use an alternative method to assess the effect of activated *Toll-1^{10b}* overexpression, area of the adult brain was measured (Fig 5.4). When activated *Toll-1^{10b}* was overexpressed the size of the adult brain decreased compared to that of non-infected controls (Fig 5.4b, c), indicating that constitutively activated *Toll-1^{10b}* decrease the size of the adult brain. Surprisingly, the brain size of the activated *Toll-1^{10b}* adult flies increased after 7 days exposure to *B. bassiana* (Fig 5.4b, c). *B. bassiana* infection rescued the size of adult brain induced by the activated *Toll-1^{10b}* overexpression, indicates that *B. bassiana* could affect the brain size through Toll-1.

5.2.3 Toll-1RNAi knockdown rescued the loss of Repo+ glial cells caused by *B. bassiana* infection

To reconcile the discrepancies in the above data and to rule out the potential influence of a leaky promoter, antibody staining was utilized to visualize the cells and determine how *B. bassiana* affect cell number in the adult brain. In chapter 3, It was demonstrated that 7 days exposure to *B. bassiana* decreased Repo+ glial cells in the adult brain. So, to further test if this required Toll signalling, it was investigated if *B. bassiana* could induce glial loss in the adult brain upon *Toll-1* knockdown. *Toll-1* was downregulated using *Toll-1*RNAi$^{KK/100078}$ as described in (Fig 5.1a). Glial cells were labelled with anti-

Figure 5.5 Adult Toll-1RNAi$^{KK/100078}$ knockdown rescued the loss of Repo+ glial cells caused by *B. bassiana* infection

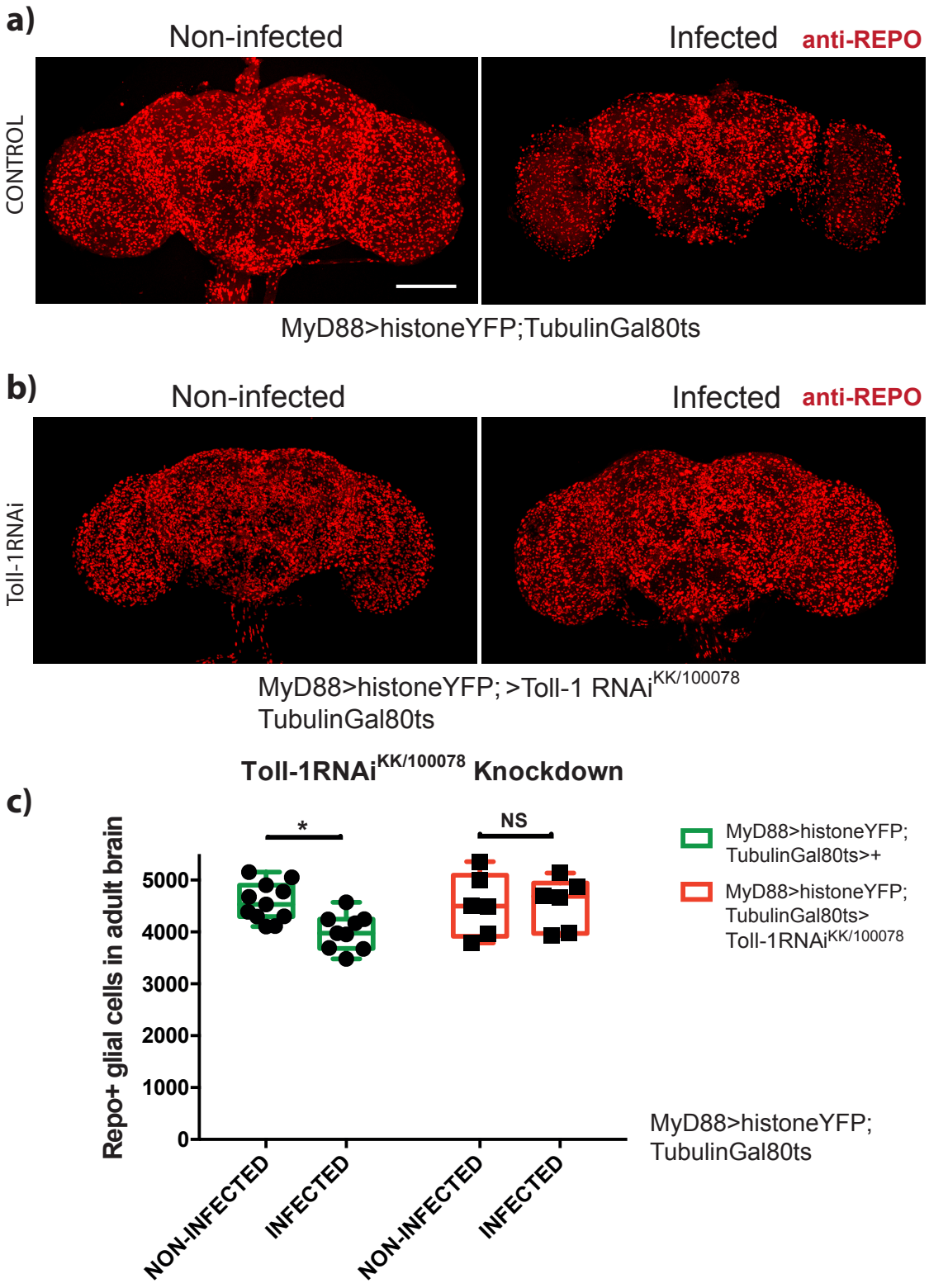


Figure 5.5 Adult *Toll-1*RNAi$^{KK/100078}$ knockdown rescued the loss of Repo+ cells caused by *B. bassiana* infection.

a) Z-projection of the adult brain showing brain glial cells labelled by anti-Repo in wild-type control non-infected and infected flies upon 7 days exposure to *B. bassiana*.
b) Z-projection of the adult brain showing brain glial cells labelled by anti-Repo in Toll-1 knockdown non-infected and infected flies upon 7 days exposure to *B. bassiana*.
c) Box plot representing brain glial cells in control flies and in *Toll-1*RNAi$^{KK/100078}$ flies upon 7 days exposure to *B. bassiana* counted by an automated cell counting program *Deadeasy*. The brain glial cells of non-infected and infected controls are represented by green box plot. The brain glial cells in central brain of non-infected and infected *Toll-1*RNAi$^{KK/100078}$ flies are represented by red box plot. Two-way ANOVA followed by Turkey's multiple comparison test (Appendix 11): *p value<0.05, **p value < 0.01, ***p value <0.001, ****p value < 0.0001. N = 11 (Noninfected control), 8 (Infected control), 6 (Toll-1RNAi Noninfected), 6 (Toll-1RNAi Infected), Scale bar = 100 um.

Genotype

Control:
Non-infected MyD88>HistoneYFP/+;TubulinGal80^{ts} /+
Infected MyD88GALUASHistoneYFP/+;TubulinGal80^{ts} /+

Experiment:
Non-infected MyD88>HistoneYFP/>Toll-1RNAi$^{KK/100078}$; TubulinGal80^{ts} /+
Infected MyD88>HistoneYFP/>Toll-1RNAi$^{KK/100078}$;TubulinGal80^{ts} /+

REPO and counted automatically using *Deadeasy*. Upon exposing the control flies for 7 days with *B. bassiana* the number of glial cells decreased in the central brain of infected flies as compared to non-infected control flies (Fig 5.5a, c).

When *Toll-1* was downregulated in non-infected flies the number of glial cells in the central brain remain unchanged in the central brain compared to the controls (Fig 5.5b, c). This indicated that Toll-1 did not regulate glial cell number in the adult brain. However, adult specific Toll-1RNAi$^{KK/100078}$ knockdown in MyD88 cells rescued the loss of Repo+ glial cells caused by *B. bassiana* infection (Fig 5.5b, c). This data showed that without Toll-1, *B. bassiana* could not induce glial loss in the adult brain.

5.2.4 Toll-1RNAi knockdown rescued the loss of PPL1 and PPM3 dopaminergic neurons caused by *B. bassiana* infection

Data from chapter 4 showed that *B. bassiana* infection induced dopaminergic neurons degeneration. Therefore, it was investigated whether *B. bassiana* could induce loss of dopaminergic neurons without Toll-1. To test this, it was first checked whether Toll-1 is expressed in dopaminergic neurons. This was done by expressing the nuclear histoneYFP reporter in Toll-1 cells using *Toll-1*Gal4 driver followed by immunostaining with anti-TH to label dopaminergic neurons in the adult brain. Toll-1 cells expressing histoneYFP could be clearly seen in the brain images (Fig 5.6a, b). The anti-TH labelled all the dopaminergic neurons of PAL & PAM cluster (Fig 5.6a) and PPL1, PPL2, PPM3, PPM1/2 cluster (Fig 5.6b). From the merged images it was clear that dopaminergic neurons colocalized with Toll-1>hisYFP+ cells (Fig 5.6a, b). These data confirmed that Toll-1 is expressed in dopaminergic neurons.

Figure 5.6 Toll-1 receptor is expressed in the dopaminergic neurons

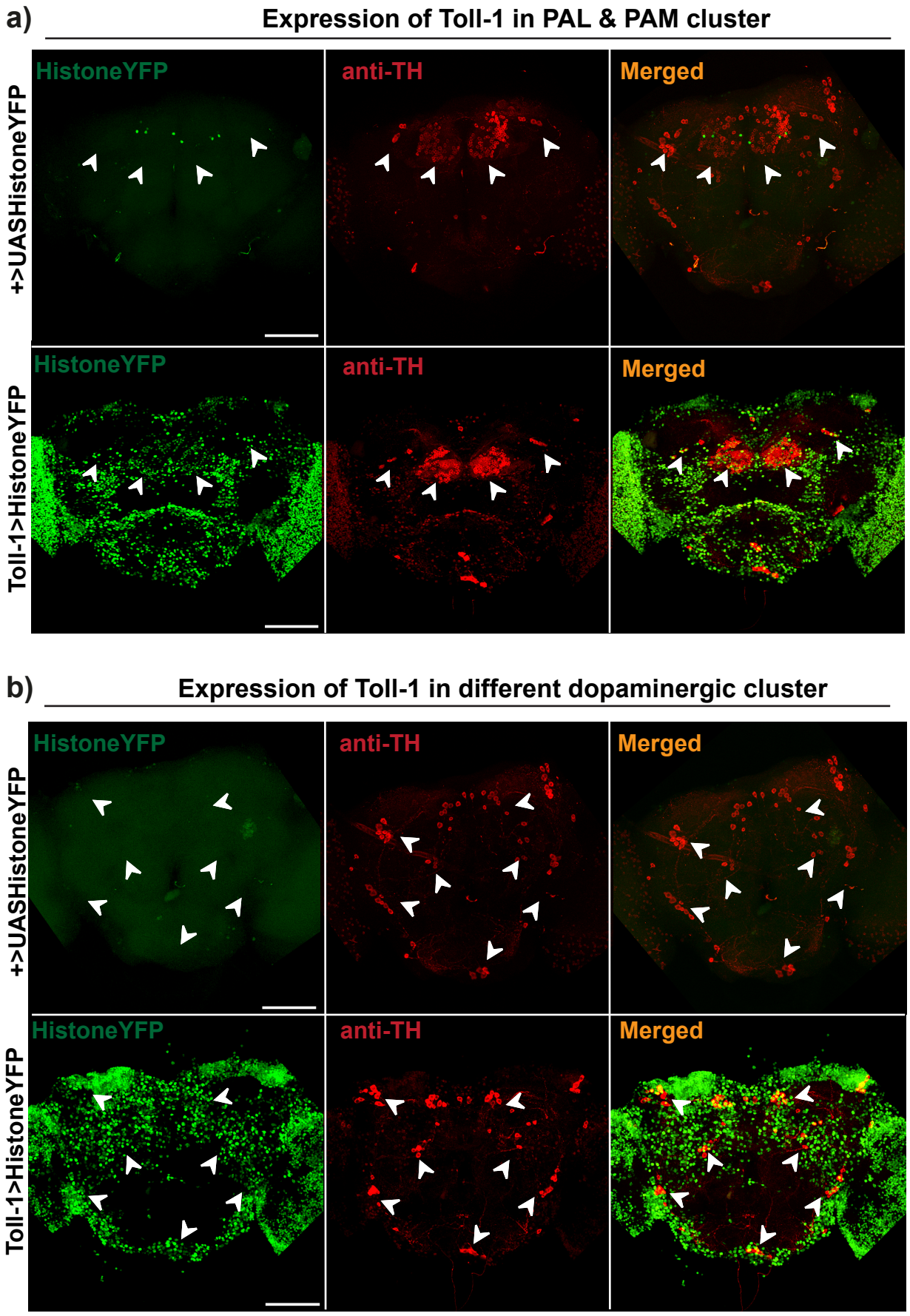


Figure 5.6 Toll-1 receptor is expressed in the dopaminergic neurons

a) Expression of Toll-1 in PAL and PAM cluster. Z projection showing expression of Toll-1 cells using nuclear reporter histoneYFP (Green) in central brain. Dopaminergic neurons of PAL and PAM cluster was labelled by anti-TH (Red). White arrows indicate dopaminergic neurons of PAL and PAM cluster colocalizing with Toll-1 cells. Merged Z projection of central brain (Yellow) showing Toll-1 cells colocalising with anti-TH labelled dopaminergic neurons in PAL and PAM cluster.

b) Expression of Toll-1 in different dopaminergic cluster. Z projection showing expression of Toll-1 cells using nuclear reporter histoneYFP (Green) in central brain. Neurons in different dopaminergic cluster was labelled by anti-TH (Red). White arrows indicate neurons of different dopaminergic cluster colocalizing with Toll-1 cells. Merged Z projection of central brain (Yellow) showing Toll-1 cells colocalising with anti-TH labelled neurons in different dopaminergic cluster. Scale bar: 80um

   N = 5 (control), 5 (Experiment)

Genotype

Control: + > HistoneYFP
Experiment: Toll-1 > HistoneYFP

Figure 5.7 Adult Toll-1RNAi$^{KK/100078}$ knockdown rescued the loss of dopaminergic PPM3 neurons caused by *B. bassiana* infection

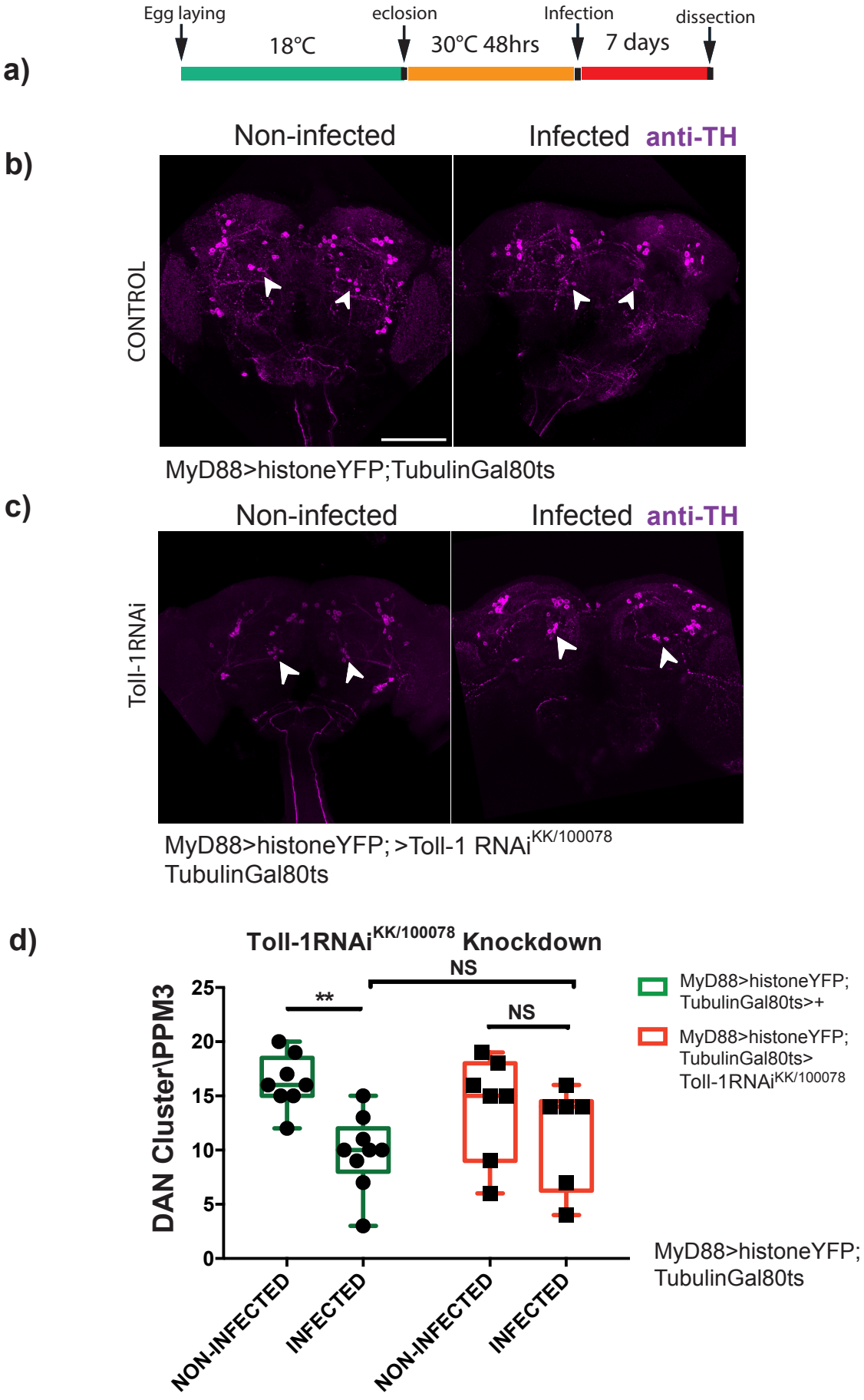


Figure 5.7 Adult *Toll-1*RNAi$^{KK/100078}$ knockdown rescued the loss of dopaminergic neurons in PPM3 cluster caused by *B. bassiana* infection

a) Diagram explaining the experimental regime.
b) Z-projection of the adult brain showing dopaminergic neurons of PPM3 cluster in central brain of wild-type control non-infected and infected flies upon 7 days exposure to *B. bassiana* labelled by anti-TH. White arrows indicate the dopaminergic neurons in PPM3 cluster.
c) Z-projection of the adult brain showing dopaminergic neurons of PPM3 cluster in central brain of *Toll-1*RNAi$^{KK/100078}$ non-infected and infected flies upon 7 days exposure to *B. bassiana* labelled by anti-TH. White arrows indicate the dopaminergic neurons in PPM3 cluster.
d) Box plot representing number of dopaminergic neurons in PPM3 cluster in control flies and in *Toll-1*RNAi$^{KK/100078}$ flies upon 7 days exposure to *B. bassiana*. The number of neurons in PPM3 cluster of non-infected and infected controls are represented by green box plot. The number of neurons in PPM3 cluster of non-infected and infected *Toll-1*RNAi$^{KK/100078}$ flies are represented by red box plot. Two-way ANOVA followed by Turkey's multiple comparison test: **p value<0.05, **p value < 0.01, ***p value <0.001, ****p value < 0.0001 (Appendix 12). N = 8 (Noninfected control), 9 (Infected control), 7 (*Toll-1*RNAi$^{KK/100078}$ Noninfected), 6 (*Toll-1*RNAi$^{KK/100078}$ Infected), Scale bar = 80um

Control:
Non-infected MyD88>HistoneYFP/+;TubulinGal80^{ts} > +
Infected MyD88>HistoneYFP/+;TubulinGal80^{ts} > +
Experiment:
Non-infected MyD88>HistoneYFP/> Toll1RNAi$^{KK/100078}$;TubulinGal80^{ts} > +
Infected MyD88>HistoneYFP/> Toll-1RNAi$^{KK/100078}$;TubulinGal80^{ts} > +

Figure 5.8 Adult Toll-1RNAi$^{KK/100078}$ knockdown rescued the loss of dopaminergic PPL1 neurons caused by *B.bassiana* infection

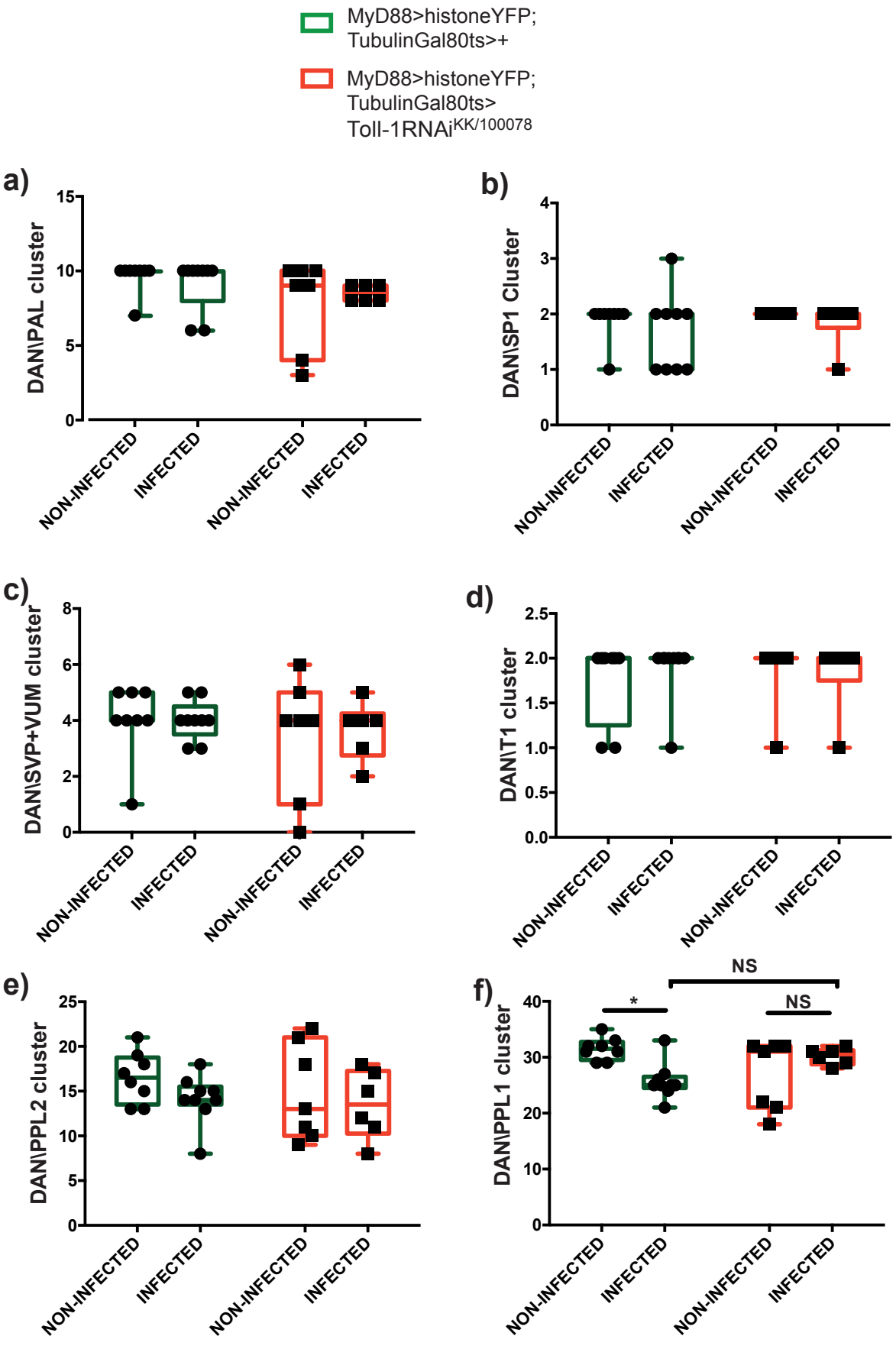


Figure 5.8 Adult *Toll-1*RNAi$^{KK/100078}$ knockdown rescued the loss of dopaminergic neurons in different cluster caused by *B. bassiana* infection

a) Box plot representing number of dopaminergic neurons in PAL cluster in control flies and in Toll-1 knockdown flies upon 7 days exposure to *B. bassiana*. PAL cluster of non-infected and infected controls are represented by green box plot. The number of neurons in PAL cluster of non-infected and infected Toll-1 knockdown flies are represented by red box plot.
b) Box plot representing number of dopaminergic neurons in SP1 cluster in control flies and in *Toll-1*RNAi$^{KK/100078}$ flies
c) Box plot representing number of dopaminergic neurons in SVP+VUM cluster in control flies and in *Toll-1*RNAi$^{KK/100078}$ flies
d) Box plot representing number of dopaminergic neurons in T1 cluster in control flies and in *Toll-1*RNAi$^{KK/100078}$ flies
e) Box plot representing number of dopaminergic neurons in PPL2 cluster in control flies and in *Toll-1*RNAi$^{KK/100078}$ flies
f) Box plot representing number of dopaminergic neurons in PPL1 cluster in control flies and in *Toll-1*RNAi$^{KK/100078}$ flies.

Two-way ANOVA followed by Turkey's multiple comparison test: **p value<0.05, **p value < 0.01, ***p value <0.001, ****p value < 0.0001 (Appendix 13, 14). N = 8 (Noninfected control), 9 (Infected control), 7 (*Toll-1*RNAi$^{KK/100078}$ Noninfected), 6 (*Toll-1*RNAi$^{KK/100078}$ Infected). Scale bar = 80um

Control:

Non-infected MyD88>HistoneYFP/+;TubulinGal80^{ts} > +
Infected MyD88>HistoneYFP/+;TubulinGal80^{ts} > +

Test:

Non-infected MyD88>HistoneYFP/> Toll1RNAi$^{KK/100078}$;TubulinGal80^{ts} > +
Infected MyD88>HistoneYFP/> Toll-1RNAi$^{KK/100078}$;TubulinGal80^{ts} > +

After validating that *Toll-1* is expressed in dopaminergic neurons. It was investigated if *B. bassiana* could induce dopaminergic neurons degeneration in the absence of Toll-1. To test this, Toll-1 was downregulated in MyD88 cells using UASToll-1RNAi$^{KK/100078}$ as described in (Fig 5.1a) and illustrated in (Fig 5.7 a). To visualize dopaminergic neurons in the brain, I used anti-TH. The dopaminergic neurons were counted in different clusters. Similar to my results of chapter 4, after exposing the control flies for 7 days with *B. bassiana* the number of neurons in PPM3 and PPL1 cluster decreased in the brain in infected control flies compared to non-infected control flies (Fig 5.7 d & Fig 5.8 f).

The adult specific *Toll-1* knock down in MyD88 cells in the adult flies rescued the loss of dopaminergic neurons in PPM3 and PPL1 clusters caused by *B. bassiana* infection (Fig 5.7c, d & Fig 5.8f). These data further validated MyD88>hisYFP+ cell count data and Repo+ glial cell count data upon *Toll-1* knock down. To summarise, these data showed that *B. bassiana* induced dopaminergic neurons loss requires Toll-1.

5.3 DISCUSSION

Table 5.1: Summary of the findings

Genotype	Reporter /staining	Data	Result
MyD88>HisYFP/>*Toll-1*RNAi^{KK100078};Tubulingal80	Histone YFP	MyD88>his YFP+ cell count	Toll-1RNAi^{kk100078} rescued the *B. bassiana* induced Myd88+ cell loss
MyD88>HistoneYFP/+;tubulingal80 />*Toll-1*RNAi^{JF10491}	Histone YFP	MyD88>his YFP+ cell count	Toll1RNAi^{JF10491} rescued the *B. bassiana* induced Myd88+ cell loss

MyD88>HistoneYFP/+;tubulingal80/>*Toll-1*^{10b}	Histone YFP	MyD88>hisYFP+ cell count	Overexpression of activated Toll-1^{10b} did not decrease MyD88+ cells upon *B. bassiana* infection
MyD88>HistoneYFP/+;tubulingal80/>*Toll-1*^{10b}	Histone YFP	Brain size	*B. bassiana* increased brain size in overexpressed activated Toll-1^{10b} flies
MyD88>HisYFP/>*Toll-1RNAi*^{KK100078};Tubulingal80	Anti-Repo Glial cells	Repo+ cell count	Toll-1RNAi^{kk100078} rescued the *B. bassiana* induced Repo+ glial cell loss
MyD88>HisYFP/>*Toll-1RNAi*^{KK100078};Tubulingal80	Anti-TH DAN neurons	PPM3, PPL1, PPL2	Toll-1RNAi^{kk100078} rescued the *B. bassiana* induced DAN neurons loss in PPM3, PPL1 cluster

The data of this chapter suggested that knocking down *Toll-1* with two RNAi lines, *Toll-1*RNAi^{KK100078} and *Toll-1*RNAi^{JF10491}, in MyD88 cells only in the adult flies rescued the MyD88>hisYFP+ cell loss induced by *B. bassiana* infection. However, overexpressing activated *Toll-1*^{10} in adult files did not decrease the MyD88>hisYFP+ cell number in both non-infected and infected flies. Additionally, knocking down *Toll-1* with *Toll-1*RNAi^{KK100078} in the adult brain rescued the loss in the Repo+ glial cells in the adult brain. The anti-TH+ dopaminergic neurons colocalised with Toll-1>hisYFP cells, suggesting that Toll-1 is expressed in the dopaminergic neurons. Knocking down *Toll-1* with *Toll-1*RNAi^{KK100078} in MyD88 cells only in the adult flies rescued the loss of neurons in PPM3 and PPL1 clusters induced by the *B. bassiana* infection in the adult brain. In summary, *B. bassiana* could not induce MyD88>hisYFP+ cell loss, Repo+ glial loss and loss in the dopaminergic neurons in PPM3 and PPL1 clusters in the absence of Toll-1. Together these results suggest that *B. bassiana* causes neuronal and glial loss by Toll-1 signalling.

To investigate if *B. bassiana* is causing cell loss I have performed the rescue experiment with two different RNAi lines. However, Drosophila RNAi's are susceptible to produce false positive results due to off-target effects (Kulkarni et al., 2006, Ma et al., 2006a, Heigwer et al., 2018). To overcome this, I have used a previously published RNAi line *Toll-1*RNAi^{JF10491} (li et al 2020) and to further validate it I have used a different RNAi line *Toll-1*RNAi^{KK100078}. qRT-PCR is another way of validating the qRT-PCR but since I have reproduced same result with two RNAi lines, I did not pursue it. An alternative to RNAi is to infect Toll-1 null mutants with *B. bassiana*, however, Toll-1 null mutation would be lethal as Toll-1 is involved in the development of the flies. Therefore, I have knocked down Toll-1 conditionally by using temperature sensitive Gal80^{ts} only in the adult nervous system for 48hrs. Downregulating Toll-1 in the adult brain rescued the *B. bassiana* induced MyD88>hisYFP+ cell loss in the central brain, suggesting that *B. bassiana* require Toll-1 to induce cell loss.

Moreover, Toll-1 knockdown in the adult brain resulted in an increased number of MyD88>hisYFP+ cells, indicating towards pro-apoptotic role of Toll-1. Previous work from our lab has also demonstrated that Toll-1 is proapoptotic in larvae (Foldi et al., 2017). A recent report has also suggested that Toll-9 interacts with Toll-1 which further upregulate apoptotic genes hid and reaper via MyD88 NF-kB pathway (Shields et al., 2022). Together these findings along with my data, indicate a pro-apoptotic role of Toll-1.

However, overexpressing activated *Toll-1^{10b}* also increased MyD88>hisYFP+ cells compared to non-infected controls, indicating that Toll-1 is not apoptotic. Due to this contradiction, brain size of the adult flies was analysed. The brain size of the flies

overexpressing activated *Toll-1*^{10b} decreased compared to non-infected controls. Surprisingly, *B. bassiana* infection rescued the decrease in brain size caused by activated Toll-1^{10b}. This can be explained in several ways. *B. bassiana* may affect the permeability of the blood brain barrier (see chapter 3), making it leaky, which could lead to influx of water into brain, thus increasing brain size upon infection. Alternatively, Toll-1 could cause apoptosis via Sarm, leading to a decreased brain size, but *B. bassiana* infection upregulates MyD88 pathway and increases survival, thus rescuing brain size and cell number. To investigate if brain size is increased due to proliferation of cells upon infection, an EdU experiment was designed. EdU (5-ethynyl-2'-deoxyuridine) is a nucleoside analog of Thymidine which bind to the DNA during replication. Anti-EdU fluorophore is used to detect the incorporated EdU in the DNA, thus providing evidence of cell proliferation (Chehrehasa et al., 2009). Flies were fed on EdU mixed food to induce EdU into the fly nervous system. However, the flyfood mixed with EdU were more prone to contamination by fungal spores. Thus, EdU experiment did not provide substantial data to validate cell proliferation in the brain upon infection. Therefore, my data cannot if Toll-1 is apoptotic and if *B. bassiana* cause cell loss through Toll-1.

To resolve the difference in the above data, antibody staining was used to investigate the effect of *B. bassiana* infection in the adult head in the absence of *Toll-1*. *Toll-1* RNAi knockdown rescued both anti-Repo labelled glial cells and anti-TH labelled dopaminergic neurons loss induced by *B. bassiana* infection, suggesting that *B. bassiana* could induce glial and neuron loss via Toll-1. Therefore, in this chapter, my data indicated, using different approaches, that *B. bassiana* requires Toll-1 to induce neuron and glial loss in the adult brain.

Chapter 6

Non-canonical Toll signalling in *B. bassiana* induced neurodegeneration

Abstract

Toll receptors regulate cell number via MyD88, Wek, and Sarm. Interestingly, RNA seq. data from a report by (C. Elya et al., 2018), showed an upregulation of Wek along with the innate immune response. Past studies from our lab revealed that downstream of Toll, Wek causes cell death by recruiting Sarm and inhibiting MyD88 (Foldi et al., 2017). Additionally, Wek could also promote cell proliferation potentially via Yorkie (Li et al., 2020). The role of Sarm in regulating cell death and causing axonal degeneration is well established (Coleman and Freeman, 2010). Thus, this chapter aims to investigate the role of non-canonical Toll signaling in B. bassiana-induced neuronal and cell loss.

6.1 Introduction

The result of the previous chapter demonstrated that RNAi knockdown of *Toll-1* rescued the loss of MyD88+ cells, glial cells and dopaminergic neurons in the adult *Drosophila* brain suggesting that *B. bassiana* induce neurodegeneration via Toll-1. Downstream of the Toll-1, Wek interacts with the Toll receptor and recruits MyD88 to the plasma membrane in close proximity to Toll-1 (Chen et al., 2006). Wek does not have an immune function as *wek* RNAi knockdown in S2 cells have no effect on *drosomycin* expression (Chen et al., 2006). Work from our lab has demonstrated that overexpression of *wek* increased DCP-1+ apoptotic cells in the pupae VNC (Foldi et al., 2017). Moreover, overexpressing *wek* in the *wek* mutant background rescued the loss of DCP1+ cells, indicating that Wek is pro apoptotic in the CNS (Foldi et al., 2017). Interestingly, RNAseq data suggest that *wek* was upregulated after *E. muscae*

infection in the adult *Drosophila* flies (Elya et al., 2018). Therefore, we hypothesised if *B. bassiana* could induce neurodegeneration through Wek.

Upon axon severance, the section of the axon located away from the injury site undergoes significant fragmentation, a phenomenon known as Wallerian degeneration (Coleman and Freeman, 2010, Conforti et al., 2014). Forward screening of mutants using mosaic analysis with a repressible cell marker (MARCM) clone, followed by next generation sequencing of mutant lines, has revealed that dSarm drive axonal destruction upon axotomy, as loss of dSarm inhibited Wallerian degeneration (Osterloh et al., 2012). Our lab showed that neuronal overexpression of dSarm in the MyD88 mutant background increased the DCP-1+ apoptotic cells in the pupae VNC, suggesting that dSarm is proapoptotic and inhibits MyD88 function (Foldi et al., 2017). Moreover, inhibiting the JNK pathway rescued apoptosis caused by dSarm overexpression, suggesting that Sarm causes apoptosis via the JNK pathway (Foldi et al., 2017). Since, dSarm causes apoptosis and axonal destruction we hypothesised if *B. bassiana* causes neurodegeneration via Sarm.

Therefore, the aim of this chapter is to investigate if *B. bassiana* causes neurodegeneration in the adult brain via Wek and Sarm downstream of Toll-1.

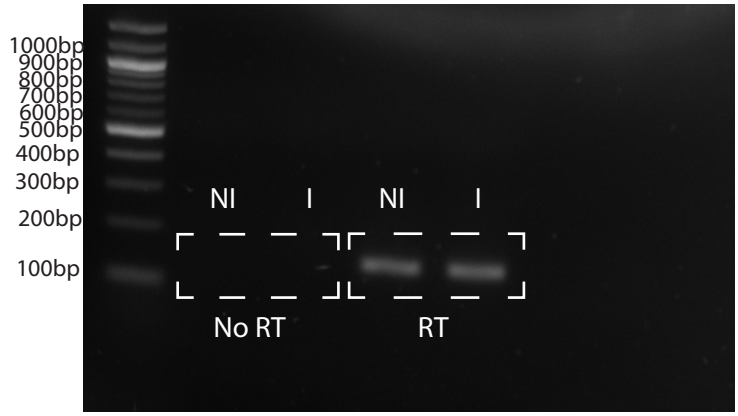
6.2 Results

6.2.1 *B. bassiana* infection upregulated the expression of *wek* in the dissected adult brain

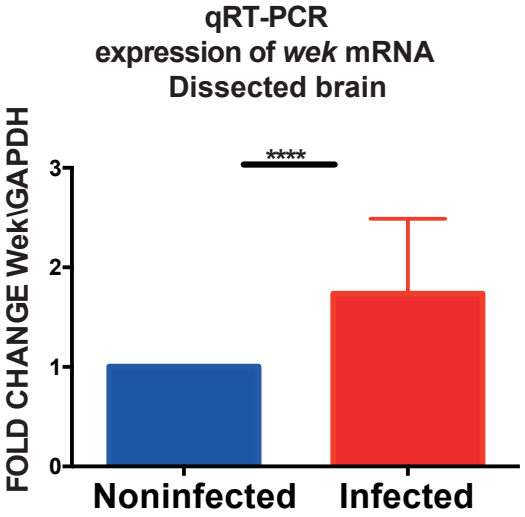
To investigate if *B. bassiana* exploits non-canonical Toll signalling in the brain, the expression of *wek* mRNA and *sarm* mRNA in dissected adult *Drosophila* brain was quantified via qRT-PCR 7 days post *B. bassiana* exposure. Wild type Oregon flies

Figure 6.1 *B. bassiana* infection increased the expression of *wek* mRNA and *sarm* mRNA in dissected adult brain

a)



b)



c)

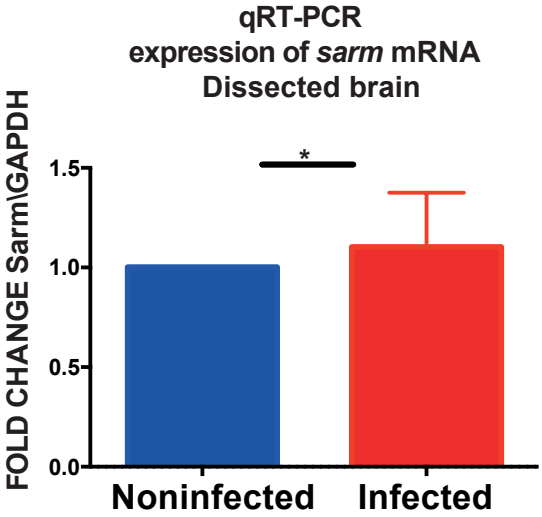


Figure 6.1 *B. bassiana* infection increased the expression of Wek mRNA and Sarm mRNA in dissected adult brain

a) Gel showing cDNA transcribed from RNA, catalysed by the reverse transcriptase.

b) Bar graph representing the fold change in the expression of *wek* mRNA in infected flies as compared to non-infected flies upon 7 days exposure to *B. bassiana.* The expression of *wek* mRNA was normalized by GAPDH as a housekeeping gene. The error bar shows standard deviation. Stats on deltaCT, unpaired student t-test, P value < 0.0001, N = 4 biological replicates.

c) Bar graph representing qRT-PCR the fold change in the expression of *sarm* mRNA in infected flies as compared to non-infected flies upon 7 days exposure to *B. bassiana.* The expression of *sarm* mRNA was normalized by GAPDH as a housekeeping gene. The error bar shows standard deviation. Stats on deltaCT, Unpaired student t-test, P value < 0.0221 (Appendix 6), N = 2 biological replicates.

Genotype: Control = Non-infected Oregon R
Experiment = Infected Oregon R

were raised at 25°C throughout development. Purified RNA was transcribed into cDNA by the reverse transcriptase. Transcribed cDNA showed the expected DNA band on the gel (Fig 6.1a). cDNA was then used as the template for the qPCR reaction. The expression of *sarm* and *wek* in infected and non-infected flies was first normalized to GAPDH, and then relative expression was calculated and indicated by the fold change. *Wek* expression in the dissected brain of infected flies increased compared to the non-infected flies (Fig 6.1b, c). Based on two biological replicates Sarm also showed an upregulation, but it is not conclusive. Therefore, the expression data suggest that 7 days exposure to *B. bassiana* also activated the *Wek* in the adult brain.

6.2.2 Adult Wek RNAi knockdown rescued MyD88+ cell loss induced by *B. bassiana*

Wek is downstream of the Toll receptor, and the qRT-PCR data suggested that *wek* was upregulated in the adult brain upon infection. Therefore, it was investigated if *B. bassiana* require Wek to induce MyD88 cell loss in the adult brain. To test this, *wek* was downregulated in MyD88 cells using UAS*wek*RNAi^{TRIPMHC046534}, followed by infecting the flies with *B. bassiana* for 7 days. Wek was knocked down in MyD88 cells in adult flies for 48 hrs using Tubulingal80ts, followed by 7 days exposure to *B. bassiana* (Fig 6.2a). To visualize MyD88 cells in the brain, a MyD88 driver, MyD88Gal4, was used to drive the expression of a nuclear reporter histoneYFP, and cells were counted automatically using *Deadeasy* software. MyD88 cells could be clearly seen in the images (Fig 6.2b, c). As seen in chapter 5, *B. bassiana* induced MyD88 cell loss in the central brain compared to the non-infected control (Fig 6.2b, d). When *wek* was knocked down in MyD88 cells, MyD88>hisYFP+ cell number in non-infected Wek knockdown flies and non-infected control flies remained same, indicated

Figure 6.2 Adult wekRNAi^{MHC046534} knockdown rescued the loss of MyD88+ cells caused by *B. bassiana* infection

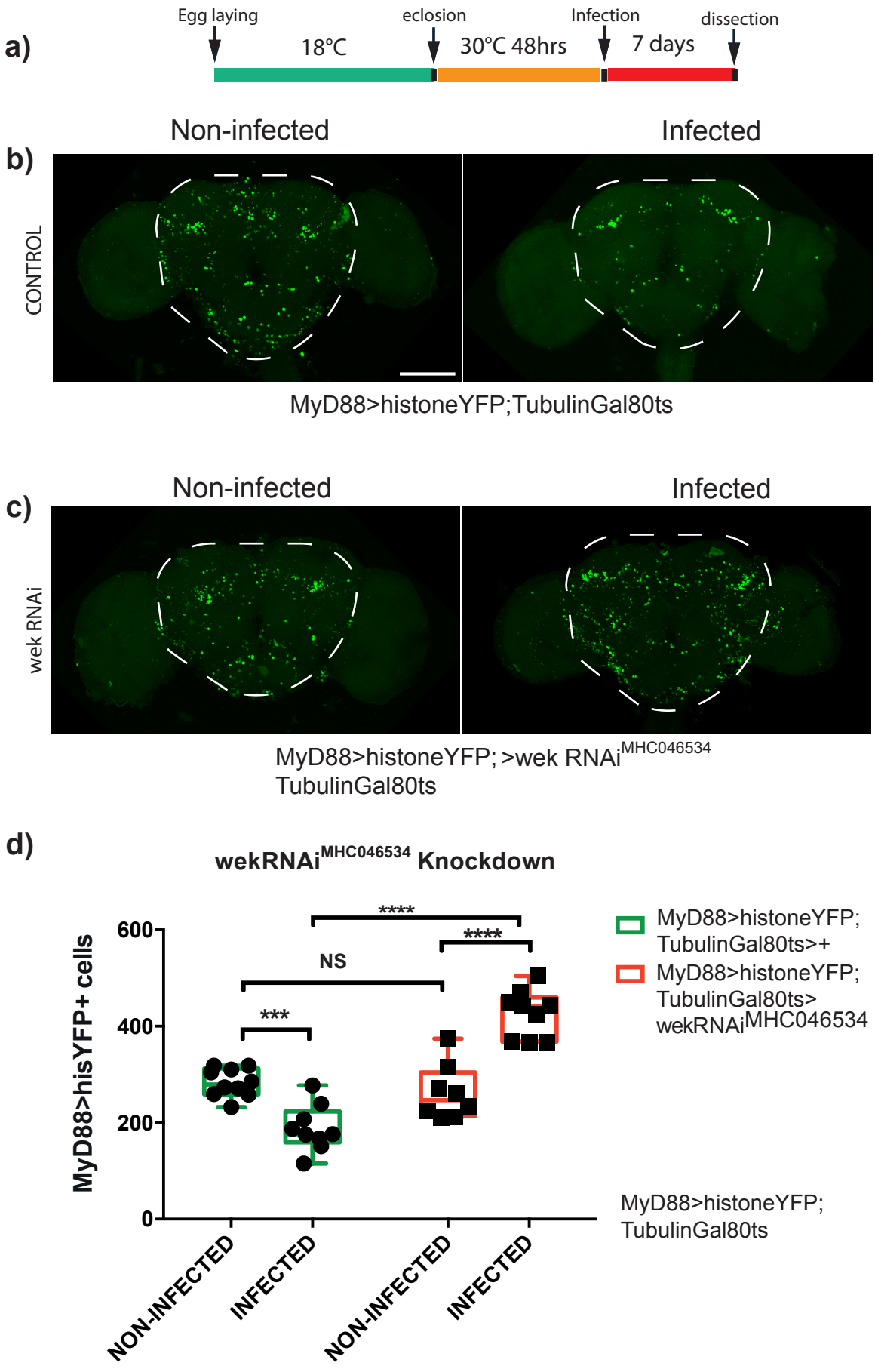


Figure 6.2 Adult *wek*RNAi^{TRIPMHC046534} knockdown rescued MyD88+ cell loss induced by *B. bassiana*

a) Diagram explaining the experimental regime.
b) Z-projection of the adult brain showing expression of MyD88+ cells in central brain of wild-type control non-infected and infected flies upon 7 days exposure to *B. bassiana*.
c) Z-projection of the adult brain showing expression of MyD88+ cells in central brain of *wek*RNAi^{TRIPMHC046534} non-infected and infected flies upon 7 days exposure to *B. bassiana*.
d) Box plot representing number of MyD88+ cells in central brain in control flies and in *wek* knockdown flies upon 7 days exposure to *B. bassiana*. The number of MyD88+ cells in central brain of non-infected and infected controls are represented by green box plot. The number of MyD88+ cells in central brain of non-infected and infected *wek*RNAi^{TRIPMHC046534} flies are represented by red box plot. Two-way ANOVA followed by Turkey's multiple comparison test (Appendix 15): **p value<0.05, **p value < 0.01, ***p value <0.001, ****p value < 0.0001. N = 10 (Noninfected control), 9 (Infected control), 8 (*wek*RNAi^{TRIPMHC046534} Non-infected), 9 (*wek*RNAi^{TRIPMHC046534} Infected)
Scale bar = 100 um

Genotype

Control:
Non-infected MyD88>HistoneYFP/+;TubulinGal80^{ts} /+
Infected MyD88>HistoneYFP/+;TubulinGal80^{ts} /+

Non-infected MyD88>HistoneYFP/+;TubulinGal80^{ts} > *wek*RNAi^{TRIPMHC046534}
Infected MyD88>HistoneYFP/+;TubulinGal80^{ts} > *wek*RNAi^{TRIPMHC046534}

at NS (Fig 6.2c, d). This indicated that without Wek, non-canonical immune signalling was inhibited and thus, did not induce apoptosis. Therefore, the number of MyD88 cells remain unchanged in the brain of Wek knock down flies compared to non-infected control (Fig 6.2c, d).

Interestingly, adult *wek*-RNAi knockdown in MyD88>hisYFP+ cells rescued the cell loss caused by *B. bassiana* infection (Fig 6.2c, d). Moreover, *wek* knocked down infected flies showed an increase in MyD88>hisYFP+ cells compared to non-infected *wek* knocked down flies. This suggests that without Wek, the MyD88 activated NF-kB pathway induced cell survival in the adult brain upon infection. This indicated that *B. bassiana* required Wek to induce MyD88>hisYFP+ cell loss in the adult brain.

6.2.3 Adult Wek-HA overexpression also rescued MyD88+ cell loss induced by *B. bassiana*

Next, to test whether Wek could induce cell loss in the absence of infection and if *B. bassiana* causes MyD88>hisYFP+ cell loss, *wek* was overexpressed in MyD88 cells using a *wek* overexpression line UAS*wek*HA. When *wek* was overexpressed the number of MyD88>hisYFP+ cells in the central brain noninfected flies increased as compared to the non-infected control flies (Fig 6.3c, d). This suggest that Wek is non-apoptotic and is required for MyD88>hisYFP+ cell proliferation in the adult brain.

When *wek* overexpression flies were exposed to *B. bassiana*, the number of MyD88 cells did not decrease in central brain of infected *wek* overexpression flies (Fig 6.3c, d). This result contradicted the hypothesis that *B. bassiana* may induce apoptosis via Wek.

Figure 6.3 Adult wekHA overexpression also rescued MyD88+ cell loss induced by *B. bassiana* in the central brain

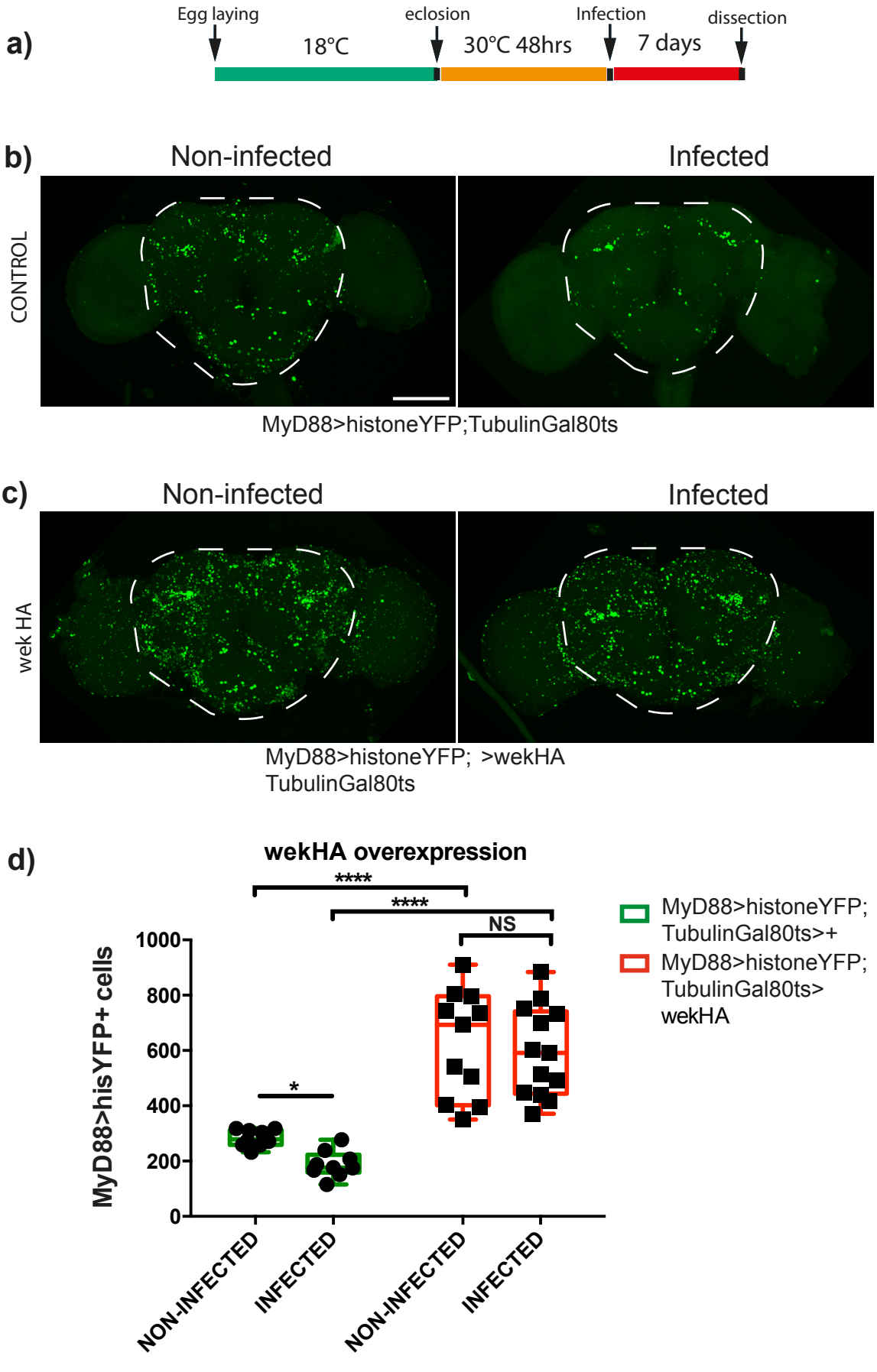


Figure 6.3 Adult *wek*-HA overexpression also rescued MyD88+ cell loss induced by *B. bassiana*

a) Diagram explaining the experimental regime.
b) Z-projection of the adult brain showing expression of MyD88+ cells in central brain of wild-type control non-infected and infected flies upon 7 days exposure to *B. bassiana*.
c) Z-projection of the adult brain showing expression of MyD88+ cells in central brain of Wek overexpression non-infected and infected flies upon 7 days exposure to *B. bassiana*.
d) Box plot representing number of MyD88+ cells in central brain in control flies and in *wek*-HA overexpression flies upon 7 days exposure to *B. bassiana*. The number of MyD88+ cells in central brain of non-infected and infected controls are represented by green box plot. The number of MyD88 cells in central brain of non-infected and infected *wek*-HA overexpression flies are represented by red box plot. Two-way ANOVA followed by Turkey's multiple comparison test (Appendix 16): **p value<0.05, **p value < 0.01, ***p value <0.001, ****p value < 0.0001. N = 10 (Noninfected control), 9 (Infected control), 11 (*wek*HA Noninfected), 13 (*wek*HA Infected), Scale bar = 100 um

Genotype

Control:
Non-infected MyD88>HistoneYFP/+;TubulinGal80^{ts} /+
Infected MyD88>HistoneYFP/+;TubulinGal80^{ts} /+

Experiment:
Non-infected MyD88>HistoneYFP/+ ;TubulinGal80^{ts}/> *wek*-HA
Infected MyD88>HistoneYFP/+;TubulinGal80^{ts} /> *wek*-HA

6.2.4 Adult Wek-RNAi knockdown rescued the loss of Repo+ glial cells caused by *B. bassiana* infection

Next, to resolve the contradictions in the MyD88>hisYFP+ cell count data, anti-REPO was used to label the glial cells and test if *B. bassiana* could induce glial loss without Wek. *wek* was downregulated using UASWekRNAi^{TRIPMHC046534} using the same experimental regime as described above (Fig 6.3a). Glial cells were labelled using anti-REPO and cell was counted with *Deadeasy*. Glial cells could be clearly seen in the images (Fig 6.4a, b). As observed in chapter 5, *B. bassiana* induced Repo+ glial cell loss in the adult brain compared to the non-infected control (Fig 6.4a, c). Glial cells did not decrease in the brain of infected *wek* knocked down flies upon 7 days exposure to *B. bassiana* compared to the non-infected *wek* knocked down flies (Fig 6.4b, c). This data suggests that without Wek, *B. bassiana* could not induce glial loss in the adult brain.

6.2.5 *wek* overexpression also rescued the loss of Repo+ glial cell number caused by *B. bassiana* infection

Next, to investigate if Wek overexpression is sufficient to decrease Repo+ glial cells without infection and whether *B. bassiana* induce more glial loss compared to the infected control. To test this, *wek* was upregulated in the adult flies using the same experimental regime as described above (Fig 6.3a). The number of glial cells remained unchanged in the brain of non-infected flies compared to the control flies (Fig 6.5 b, c), indicating that *wek* overexpression has no effect on the glial cells. Upon *B. bassiana* infection, Repo+ glial cells did not decrease in the brain of infected *wek* overexpression flies compared to non-infected *wek* overexpression flies (Fig 6.5b, c). Rather, Repo+

Figure 6.4 Adult wekRNAi^{MHC046534} knockdown rescued the loss of Repo+ cells caused by *B. bassiana* infection

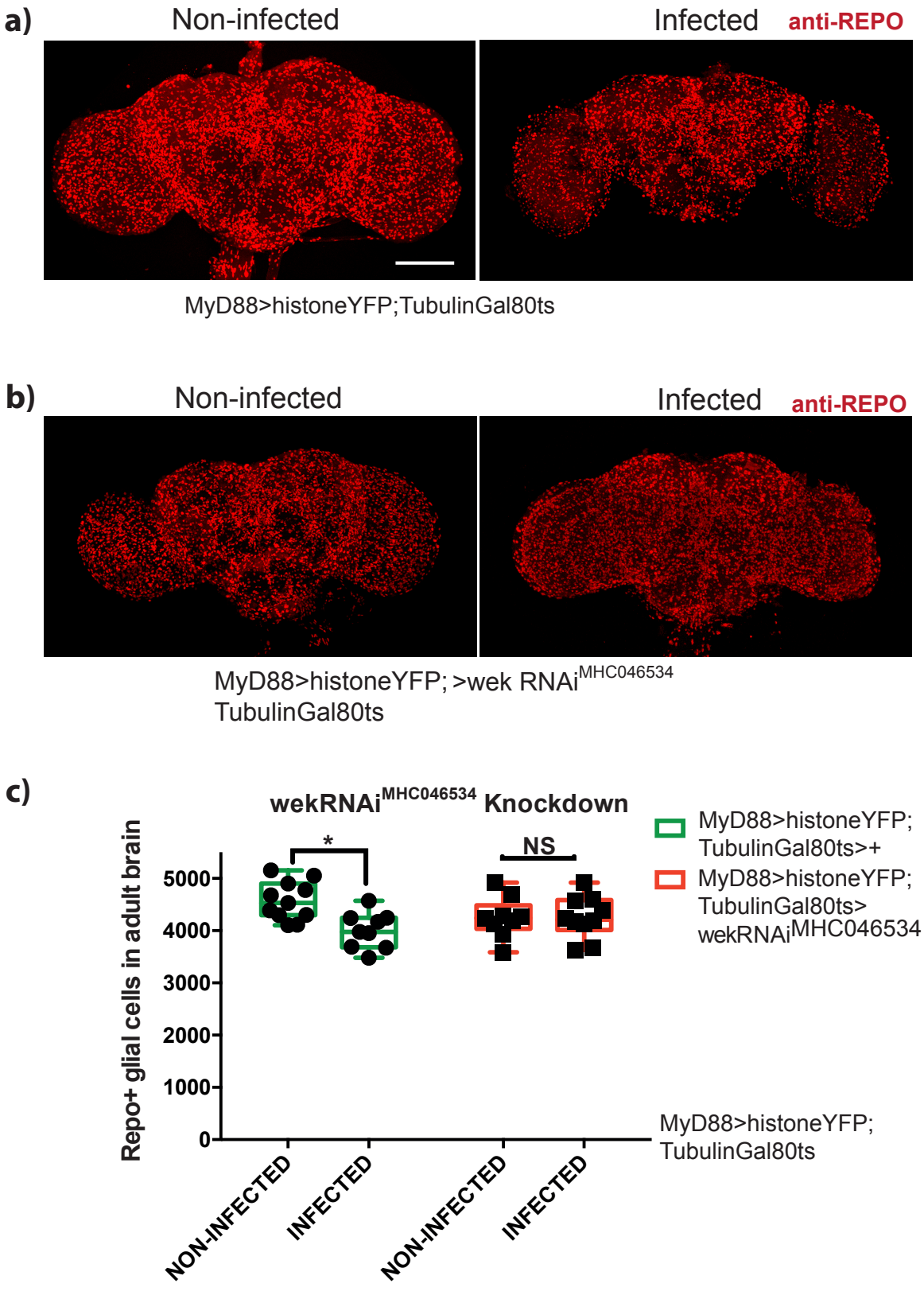


Figure 6.4 Adult *wek*RNAi^{TRIPMHC046534} knockdown rescued the loss of Repo+ glial caused by *B. bassiana* infection.

a) Z-projection of the adult brain showing brain glial cells labelled by anti-Repo in wild-type control non-infected and infected flies upon 7 days exposure to *B. bassiana*.
b) Z-projection of the adult brain showing brain glial cells labelled by anti-Repo in *wekRNAi^{TRIPMHC046534}* non-infected and infected flies upon 7 days exposure to *B. bassiana*.
c) Box plot representing brain glial cells in control flies and in *wekRNAi^{TRIPMHC046534}* flies upon 7 days exposure to *B. bassiana* counted by an automated cell counting program *Deadeasy*. The brain glial cells of non-infected and infected controls are represented by green box plot. The brain glial cells in central brain of non-infected and infected *wekRNAi^{TRIPMHC046534}* flies are represented by red box plot. Two-way ANOVA followed by Turkey's multiple comparison test (Appendix 17): **p value<0.05, **p value < 0.01, ***p value <0.001, ****p value < 0.0001. N = 11 (Noninfected control), 9 (Infected control), 9 (*wekRNAi^{TRIPMHC046534}* Noninfected), 11 (*wekRNAi^{TRIPMHC046534}* Infected) Scale bar = 100 um

Control:

Non-infected MyD88>HistoneYFP/+;TubulinGal80^{ts} /+
Infected MyD88>HistoneYFP/+;TubulinGal80^{ts} /+

Experiment:

Non-infected MyD88>HistoneYFP/+;TubulinGal80^{ts} > *wekRNAi^{TRIPMHC046534}*
Infected MyD88>HistoneYFP/+;TubulinGal80^{ts} > *wekRNAi^{TRIPMHC046534}*

Figure 6.5 Adult wekHA overexpression also rescued the loss of Repo+ glial cell number caused by *B.bassiana*

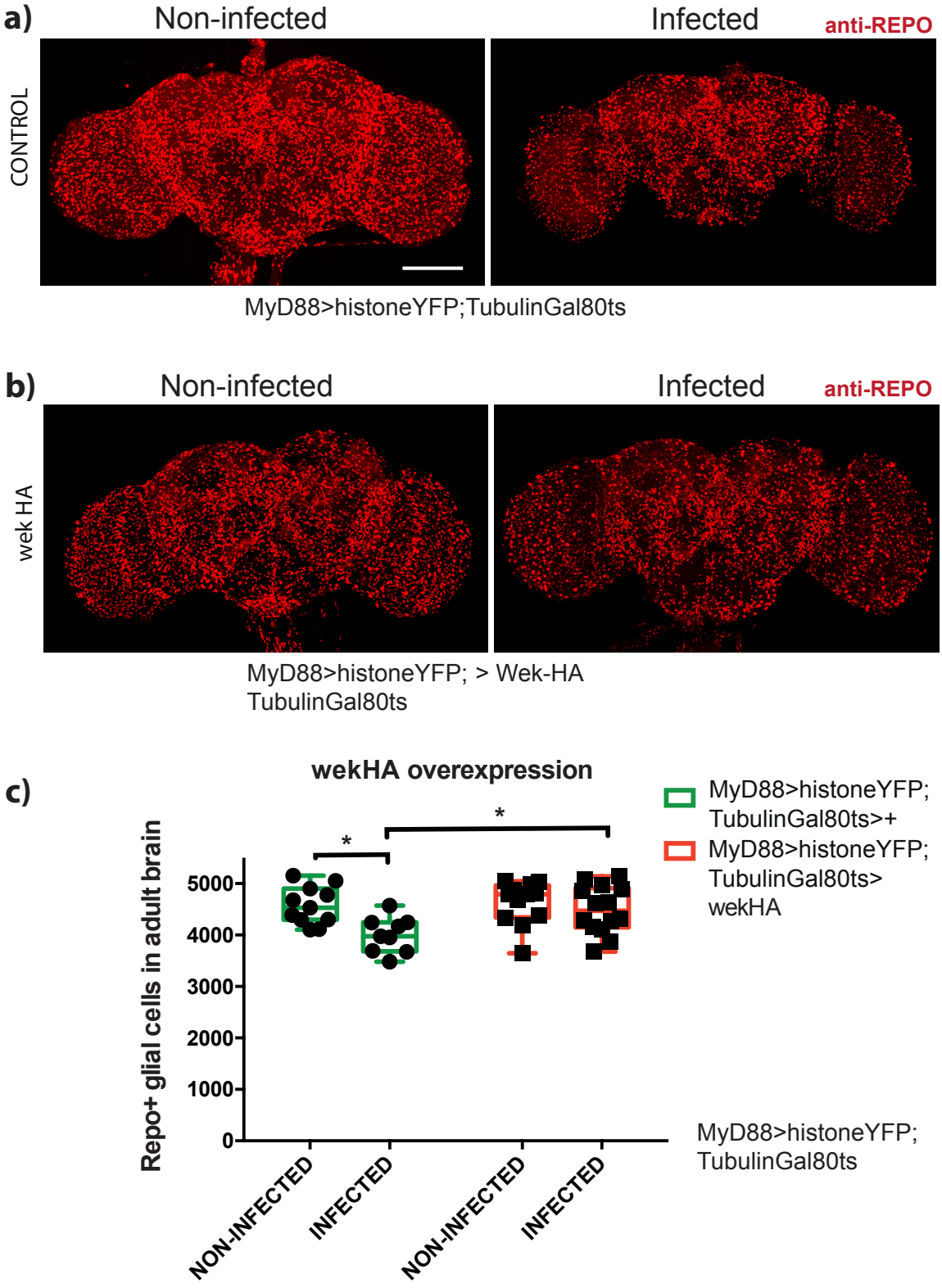


Figure 6.5 *wek* overexpression also rescued the loss of glial cell number caused by *B. bassiana* infection.

a) Z-projection of the adult brain showing brain glial cells labelled by anti-Repo in wild-type control non-infected and infected flies upon 7 days exposure to *B. bassiana*.
b) Z-projection of the adult brain showing brain glial cells labelled by anti-Repo in *wek*-HA overexpression non-infected and infected flies upon 7 days exposure to *B. bassiana*.
c) Box plot representing brain glial cells in control flies and in *wek*-HA overexpression flies upon 7 days exposure to *B. bassiana* counted by an automated cell counting program *Deadeasy*. The brain glial cells of non-infected and infected controls are represented by green box plot. The brain glial cells in central brain of non-infected and infected *wek*-HA overexpression flies are represented by red box plot. Two-way ANOVA followed by Turkey's multiple comparison test (Appendix 18): **p value<0.05, **p value < 0.01, ***p value <0.001, ****p value < 0.0001. N = 11 (Noninfected control), 8 (Infected control), 12 (*wek*HA Noninfected), 14 (*wek*HA Infected), Scale bar = 100 um

Control:

Non-infected MyD88>HistoneYFP/+;TubulinGal80^{ts} /+
Infected MyD88>HistoneYFP/+;TubulinGal80^{ts} /+

Test:

Non-infected MyD88>HistoneYFP/+ ;TubulinGal80^{ts}/>*wek*-HA
Infected MyD88>HistoneYFP/+;TubulinGal80^{ts} />*wek*-HA

glial cell showed a significant increase in the infected *wek* overexpression flies compared to infected control flies (Fig 6.5c). This indicate that *B. bassiana* is not causing neurodegeneration through Wek.

6.2.6 *wek*RNAi knockdown did not rescue the loss of dopaminergic neurons caused by *B. bassiana*

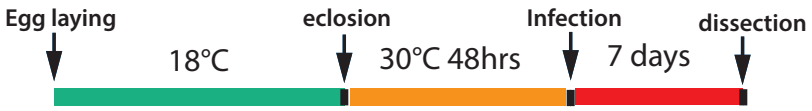
Next, the impact of altering Wek levels on DAN neurodegeneration induced by *B. bassiana* in the adult brain was investigated. To investigate this, *wek* was downregulated in MyD88 cells using UAS*wek*RNAi^{MHC046534} as described in (Fig 6.2a) and illustrated in (Fig 6.6a). To visualize dopaminergic neurons in the brain, anti-TH was used, and dopaminergic neurons in different clusters were counted. Dopaminergic neurons in PPM3 cluster could be clearly seen in the images (Fig 6.6b, c). Upon exposing the control flies for 7 days with *B. bassiana* the number of neurons in PPM3, PPL1 and PPL2 cluster decreased in the brain in infected control flies compared to non-infected control flies (Fig 6.6b, d, Fig 6.7a, b).

When *wek* was knocked down in MyD88 cells, the number of neurons in the PPM3, PPL1 & PPL2 cluster decreased in non-infected Wek RNAi flies compared to non-infected control flies (Fig 6.6c, d & Fig 6.7a, b). This indicated that Wek is required for the survival or differentiation of dopaminergic neurons, which is consistent with a previous report finding that Wek enables MyD88 signalling downstream of Tolls (Chen et al., 2006). The RNAi knockdown of *wek* did not rescue the loss of DAN neuron caused by the *B. bassiana* infection in PPM3, PPL1, and PPL2 clusters (Fig 6.6c, d & Fig 6.7a, b). This further suggests that *B. bassiana* does not require Wek to cause neurodegeneration in the adult brain.

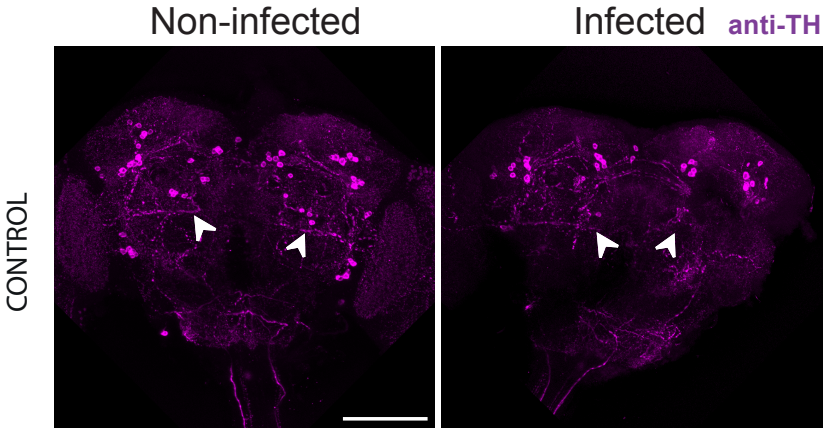
6.2.7 *B. bassiana* infection induced loss in the dopaminergic neurons in the adult flies overexpressing *wek*

Figure 6.6 *Wek*RNAi knockdown did not rescue the loss of dopaminergic neurons in PPM3 cluster caused by *B. bassiana*

a)

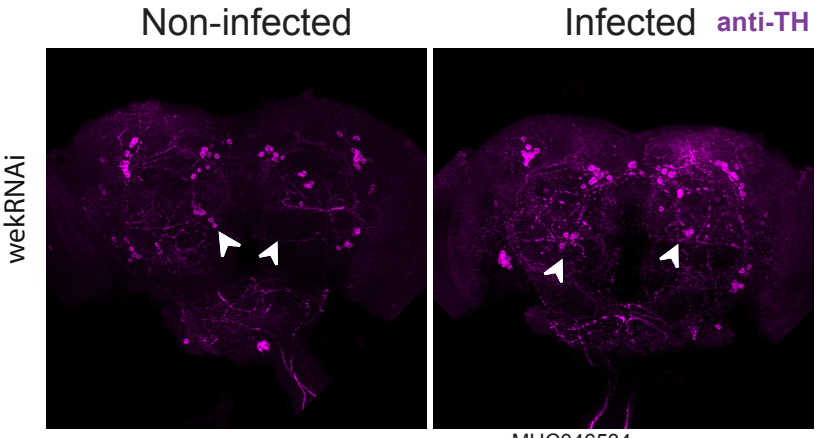


b)



MyD88>histoneYFP;TubulinGal80ts

c)



MyD88>histoneYFP;>wek RNAi^{MHC046534}
TubulinGal80ts

d)

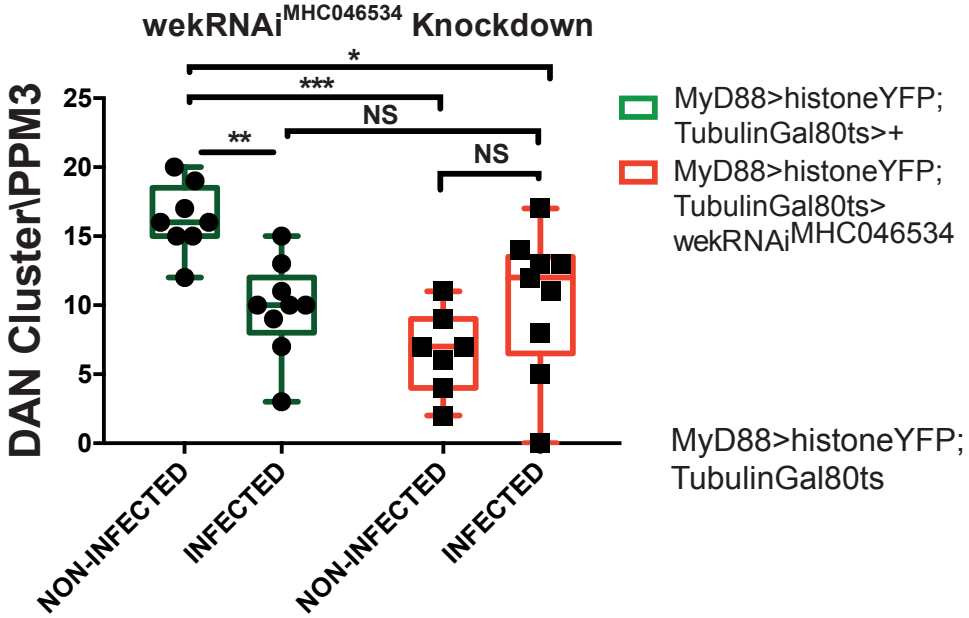


Figure 6.6 *Wek*RNAi knockdown did not rescue the loss of dopaminergic neurons in PPM3 cluster caused by *B. bassiana*

a) Diagram explaining the experimental regime.
b) Z-projection of the adult brain showing dopaminergic neurons of PPM3 cluster in central brain of wild-type control non-infected and infected flies upon 7 days exposure to *B. bassiana* labelled by anti-TH. White arrows indicate the dopaminergic neurons in PPM3 cluster.
c) Z-projection of the adult brain showing dopaminergic neurons of PPM3 cluster in central brain of *wekRNAi*^{TRIPMHC046534} non-infected and infected flies upon 7 days exposure to *B. bassiana* labelled by anti-TH. White arrows indicate the dopaminergic neurons in PPM3 cluster.
a. Box plot representing number of dopaminergic neurons in PPM3 cluster in control flies and in *wekRNAi*^{TRIPMHC046534} flies upon 7 days exposure to *B. bassiana*. The number of neurons in PPM3 cluster of non-infected and infected controls are represented by green box plot. The number of neurons in PPM3 cluster of non-infected and infected *wekRNAi*^{TRIPMHC046534} flies are represented by red box plot. Two-way ANOVA followed by Turkey's multiple comparison test (Appendix 19): **p value<0.05, **p value < 0.01, ***p value <0.001, ****p value < 0.0001. N = 8 (Noninfected control), 9 (Infected control), 7 (WekRNAi Noninfected), 9 (WekRNAi Infected) Scale bar = 80um

Genotype: Control:

Non-infected MyD88>HistoneYFP/+;TubulinGal80^{ts} /+
Infected MyD88>HistoneYFP/+;TubulinGal80^{ts} /+
Experiment:
Non-infected MyD88>HistoneYFP/+;TubulinGal80^{ts} > *wekRNAi*^{TRIPMHC046534}
Infected MyD88>HistoneYFP/+;TubulinGal80^{ts} > *wekRNAi*^{TRIPMHC046534}

Figure 6.7 ***WekRNAi knockdown did not rescue the loss of dopaminergic neurons in different clusters caused by B. bassiana***

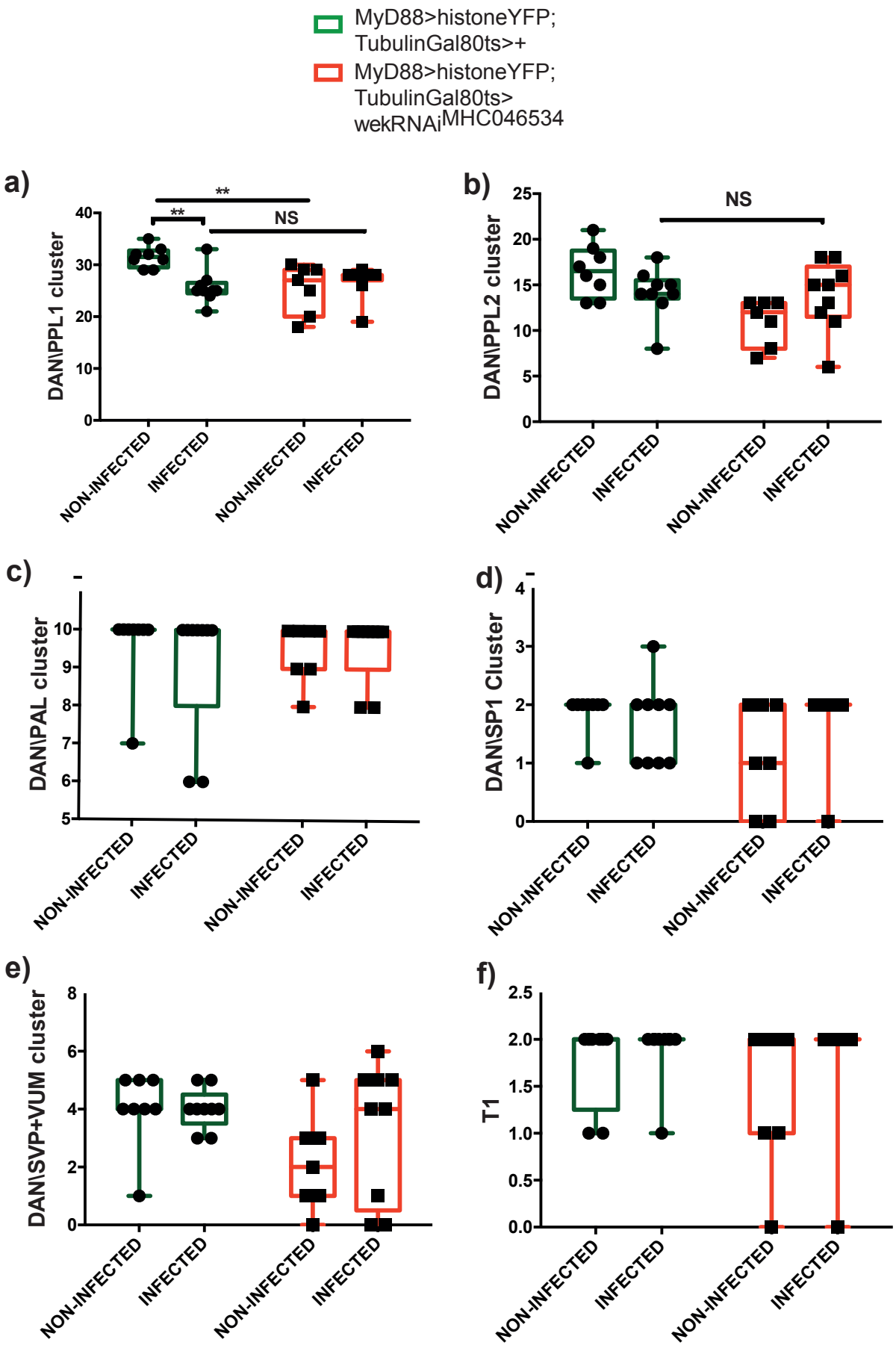


Figure 6.7 *Wek*RNAi knockdown did not rescue the loss of dopaminergic neurons in different clusters caused by *B. bassiana*

a) Box plot representing number of dopaminergic neurons in PPL1 cluster in control flies and in *wek* knockdown flies upon 7 days exposure to *B. bassiana*. The number of neurons in PPL1 cluster of non-infected and infected controls are represented by green box plot. The number of neurons in PPL1 cluster of non-infected and infected *wekRNAi*^{TRIPMHC046534} flies are represented by red box plot.
b) Box plot representing number of dopaminergic neurons in PPL2 cluster in control flies and in *wekRNAi*^{TRIPMHC046534} flies upon 7 days exposure to *B. bassiana*.
c) Box plot representing number of dopaminergic neurons in PAL cluster in control flies and in *wekRNAi*^{TRIPMHC046534} flies upon 7 days exposure to *B. bassiana*.
d) Box plot representing number of dopaminergic neurons in SP1 cluster in control flies and in *wekRNAi*^{TRIPMHC046534} flies upon 7 days exposure to *B. bassiana*.
e) Box plot representing number of dopaminergic neurons in SVP & VUM cluster in control flies and in *wekRNAi*^{TRIPMHC046534} flies upon 7 days exposure to *B. bassiana*
f) Box plot representing number of dopaminergic neurons in T1 cluster in control flies and in *wekRNAi*^{TRIPMHC046534} flies upon 7 days exposure to *B. bassiana*.

Two-way ANOVA followed by Turkey's multiple comparison test (Appendix 20, 21): **p value<0.05, **p value < 0.01, ***p value <0.001, ****p value < 0.0001. N = 8 (Noninfected control), 9 (Infected control), 7 (wekRNAi Noninfected), 6 (wekRNAi Infected).

Control:

Non-infected MyD88>HistoneYFP/+;TubulinGal80^{ts} > +
Infected MyD88>HistoneYFP/+;TubulinGal80^{ts} > +

Experiment:

Non-infected MyD88>HistoneYFP/+;TubulinGal80^{ts} > *wekRNAi*^{TRIPMHC046534}
Infected MyD88>HistoneYFP/+;TubulinGal80^{ts} > *wekRNAi*^{TRIPMHC046534}

Next, it was investigated if *B. bassiana* could further decrease the number of DAN neurons compared to the infected control in the presence of Wek. To test this, *wek* was overexpressed in the adult flies using the same experimental regime described in (Fig 6.3a). When Wek was overexpressed in MyD88 cells using UASWek-HA in the adult flies, the number of neurons in PPM3, PPL1 & PPL2 cluster did not change compared to non-infected control flies (Fig 6.8b, c & Fig 6.9d, e, f). This suggests that overexpression of *wek* has no effect on the dopaminergic neurons. Moreover, the number of neurons in PPM3, PPL1 & PPL2 cluster in infected *wek*-HA flies remained non-significant compared to infected controls upon 7 days exposure to *B. bassiana* (Fig 6.8 & Fig 6.9), indicating that *B. bassiana* infection does not require Wek to induce loss of dopaminergic neurons.

Surprisingly, in *wek* upregulated flies, *B. bassiana* reduced the neurons in PAL dopaminergic cluster as compared to non-infected *wek* upregulated flies (Fig 6.9e). In the controls for this experiment, *B. bassiana* did not decrease the number of neurons in the PAL cluster (Fig 6.9e). However, upregulation of *wek* was enough to induce neuronal degeneration in the PAL cluster which is usually protected by *B. bassiana* infection (Fig 6.9e). This suggests that *B. bassiana* induces loss of dopaminergic neurons in PAL cluster through Wek. Since *B. bassiana* did not cause loss in neurons without Wek but had an effect on dopaminergic neurons when overexpressed, indicates that *B. bassiana* may requires Wek to induce DAN neuron loss in the adult brain.

6.2.8 Overexpression of *wek* in DAN neurons in PAM cluster mimics the cell loss caused by *B. bassiana* infection

Since, overexpression of *wek* was enough to induce loss in the DAN PAL cluster upon *B. bassiana* infection (Fig 6.9e), indicate that further investigation is required to determine if *B. bassiana* induce loss of DAN neurons through Wek. Therefore, UAS*wek*HA was overexpressed in the dopaminergic PAM cluster using PAM specific driver, TH;R58E02GAL4.

Figure 6.8 *B. bassiana* induced loss of dopaminergic neurons in PPM3 cluster upon adult wek-HA overexpression

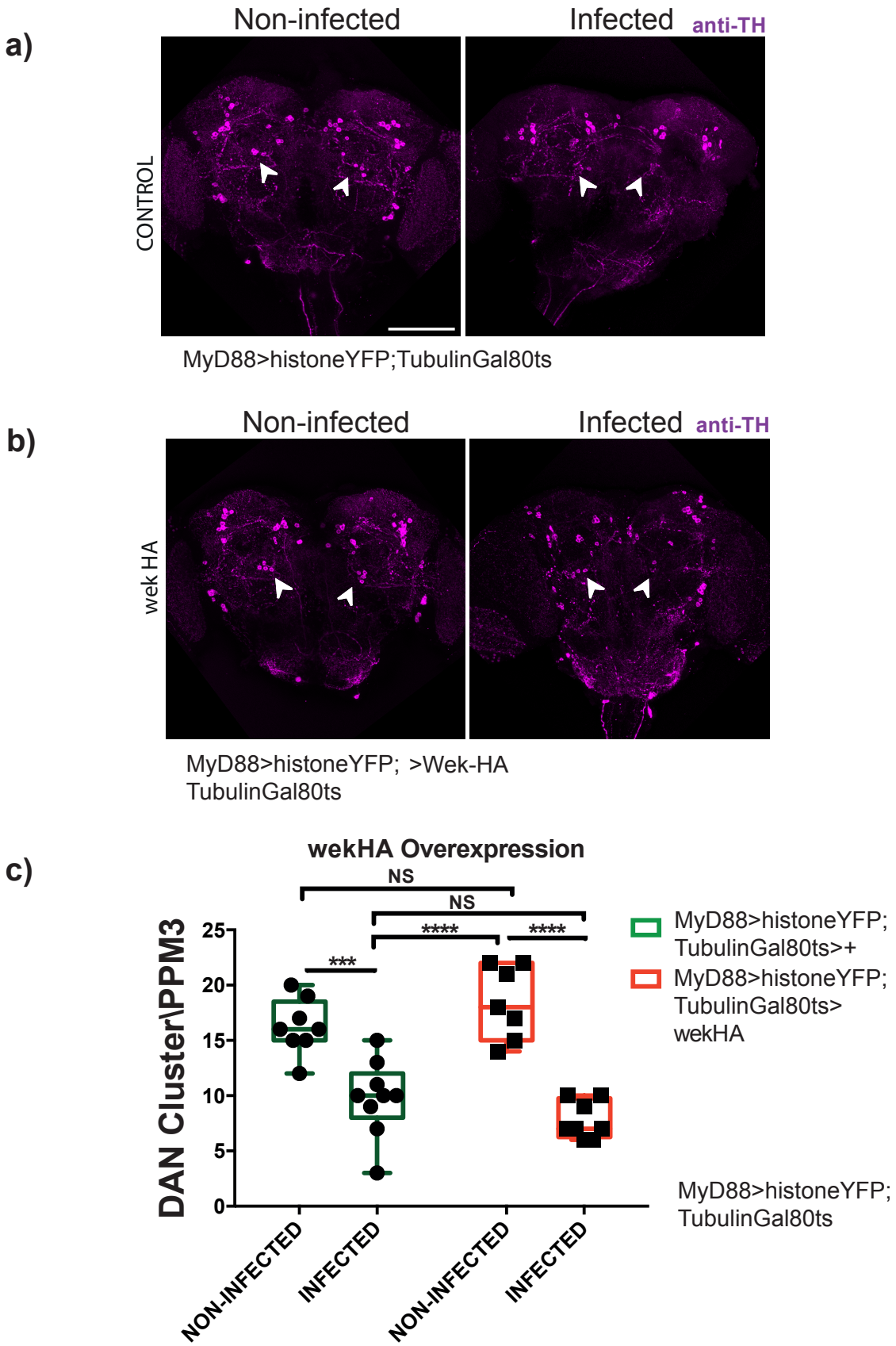


Figure 6.8 *B. bassiana* infection induced loss of dopaminergic neurons in PPM3 cluster in the adult flies overexpressing *wek*-HA

a) Z-projection of the adult brain showing dopaminergic neurons of PPM3 cluster in central brain of wild-type control non-infected and infected flies upon 7 days exposure to *B. bassiana* labelled by anti-TH. White arrows indicate the dopaminergic neurons in PPM3 cluster. Scale bar = 80um
b) Z-projection of the adult brain showing dopaminergic neurons of PPM3 cluster in central brain of *wek*-HA overexpression non-infected and infected flies upon 7 days exposure to *B. bassiana* labelled by anti-TH. White arrows indicate the dopaminergic neurons in PPM3 cluster.
c) Box plot representing number of dopaminergic neurons in PPM3 cluster in control flies and in *wek*-HA overexpression flies upon 7 days exposure to *B. bassiana*. The number of neurons in PPM3 cluster of non-infected and infected controls are represented by green box plot. The number of neurons in PPM3 cluster of non-infected and infected *wek* overexpression flies are represented by red box plot. Two-way ANOVA followed by Turkey's multiple comparison test (Appendix 22): **p value<0.05, **p value < 0.01, ***p value <0.001, ****p value < 0.0001. N = 8 (Noninfected control), 9 (Infected control), 7 (*wek*HA Noninfected), 8 (*wek*HA Infected) Scale bar = 80um

Genotype

Control:
Non-infected MyD88GALUASHistoneYFP;TubulinGal80^{ts} > Oregon
Infected MyD88GALUASHistoneYFP;TubulinGal80^{ts} > Oregon
Experiment:
Non-infected MyD88>HistoneYFP;TubulinGal80^{ts} /> WekHA
Infected MyD88>HistoneYFP;TubulinGal80^{ts} /> WekHA

Figure 6.9 *B. bassiana* induced loss of dopaminergic neurons in PAL, PPL1, and PPL2 cluster upon adult wek-HA overexpression

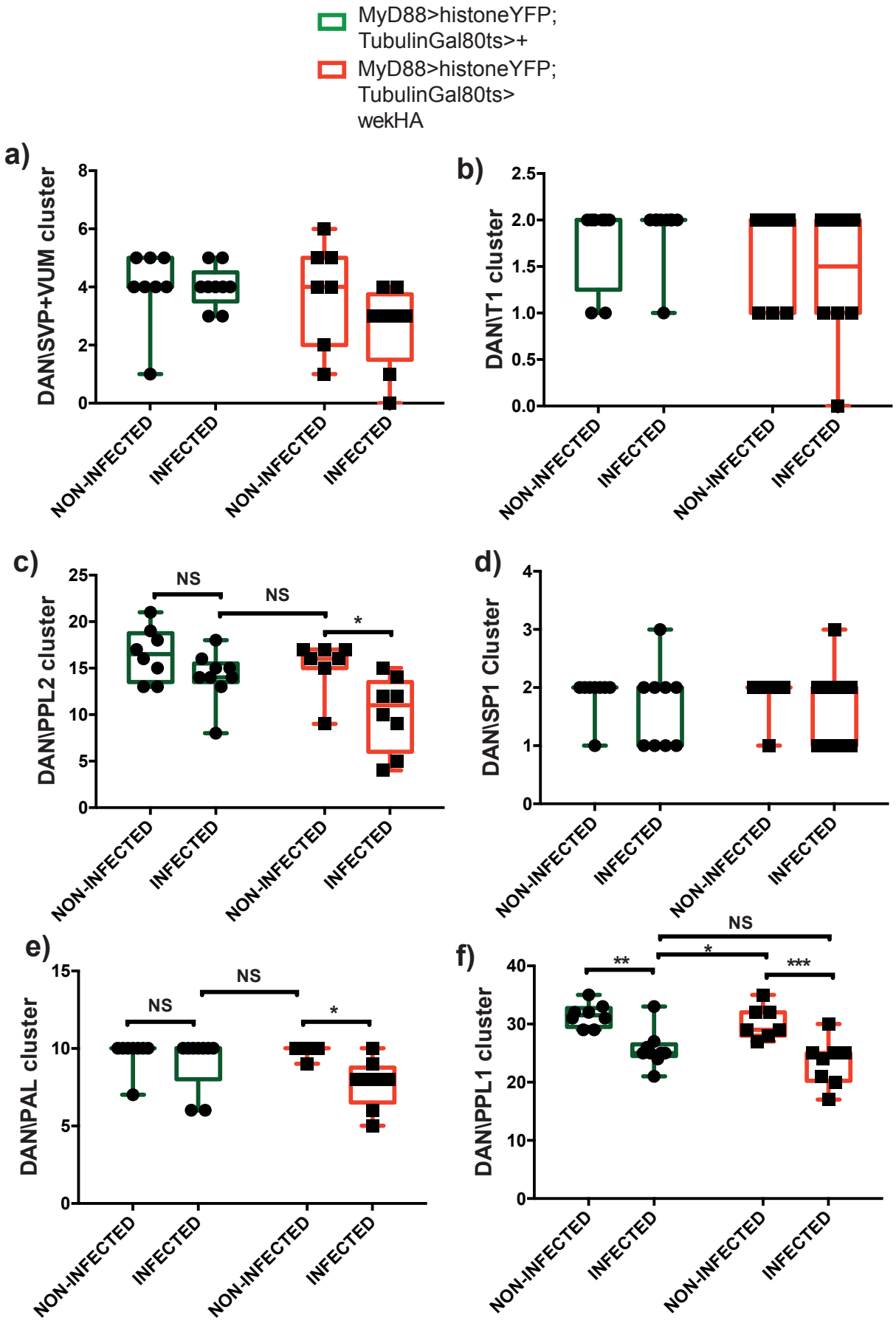


Figure 6.9 *B. bassiana* infection induced loss of dopaminergic neurons in PAL, PPL1 and PPL2 clusters upon adult *wek*-HA overexpression

a) Box plot representing number of dopaminergic neurons in SVP+VUM cluster in control flies and in *wek*-HA overexpression flies upon 7 days exposure to *B. bassiana*. The number of neurons in SVP+VUM cluster of non-infected and infected controls are represented by green box plot. The number of neurons in SVP+VUM cluster of non-infected and infected *wek* overexpression flies are represented by red box plot.
b) Box plot representing number of dopaminergic neurons in T1 cluster in control flies and in *wek*-HA overexpression flies upon 7 days exposure to *B. bassiana*.
c) Box plot representing number of dopaminergic neurons in PPL2 cluster in control flies and in *wek*-HA overexpression flies upon 7 days exposure to *B. bassiana*.
d) Box plot representing number of dopaminergic neurons in SP1 cluster in control flies and in *wek*-HA overexpression flies upon 7 days exposure to *B. bassiana*.
e) Box plot representing number of dopaminergic neurons in PAL cluster in control flies and in *wek*-HA overexpression flies upon 7 days exposure to *B. bassiana*.
f) Box plot representing number of dopaminergic neurons in PPL1 cluster in control flies and in *wek*-HA overexpression flies upon 7 days exposure to *B. bassiana*.

Two-way ANOVA followed by Turkey's multiple comparison test (Appendix 23, 24, 25): **p value<0.05, **p value < 0.01, ***p value <0.001, ****p value < 0.0001. N = 8 (Noninfected control), 9 (Infected control), 7 (wekHA Noninfected), 6 (wekHA Infected).

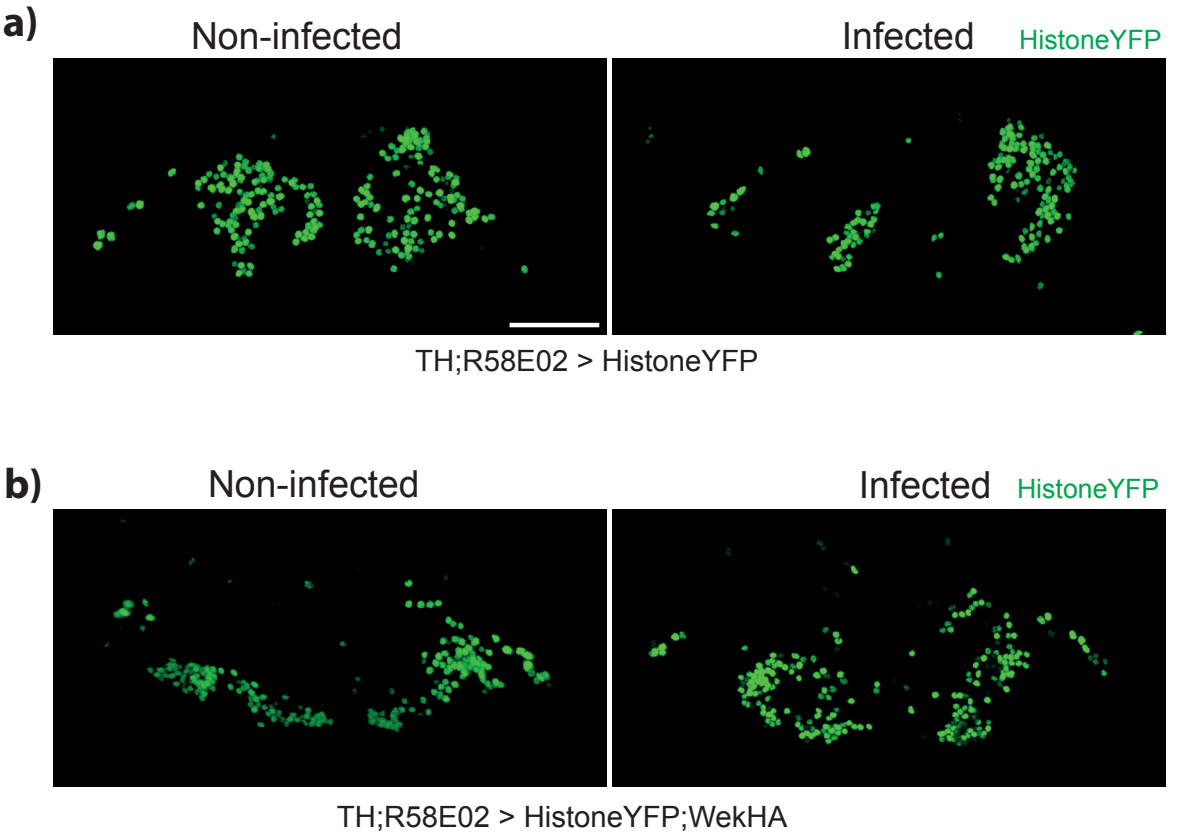
Control:

Non-infected MyD88>HistoneYFP/+;TubulinGal80^{ts} > +
Infected MyD88>HistoneYFP/+;TubulinGal80^{ts} > +

Experiment:

Non-infected MyD88>HistoneYFP;TubulinGal80^{ts} /> *wek*-HA
Infected MyD88>HistoneYFP;TubulinGal80^{ts} /> *wek*-HA

Figure 6.10 Overexpression of wek in dopaminergic neurons of PAM cluster mimics the cell loss caused by *B. bassiana* infection



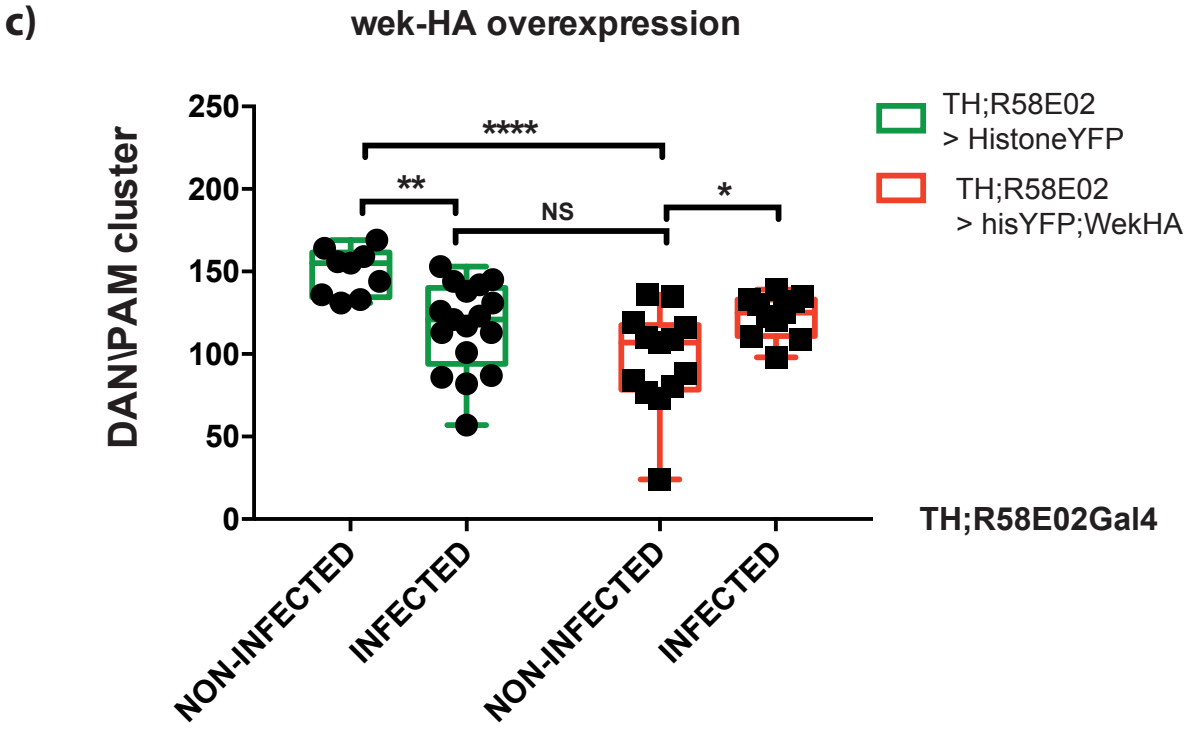


Figure 6.10 Overexpression of *wek in* dopaminergic neurons of PAM cluster mimics the cell loss caused by *B. bassiana* infection

a) Z-projection of the dopaminergic neurons showing expression of HistoneYFP in PAM cluster in central brain of wild-type control non-infected and infected flies upon 7 days exposure to *B. bassiana*.
b) Z-projection of the dopaminergic neurons showing expression of HistoneYFP in PAM cluster upon *wek*-HA overexpression in central brain of non-infected and infected flies upon 7 days exposure to *B. bassiana*.
c) Box plot representing number dopaminergic neurons in PAM cluster in control flies and in *wek* overexpression flies upon 7 days exposure to *B. bassiana*. The number of dopaminergic neurons in PAM cluster of non-infected and infected controls are represented by green box plot. The number of dopaminergic neurons in PAM cluster of non-infected and infected *wek* overexpression flies are represented by red box plot. Two-way ANOVA followed by Turkey's multiple comparison test (Appendix 26): **p value<0.05, **p value < 0.01, ***p value <0.001, ****p value < 0.0001. N = 8 (Noninfected control), 16 (Infected control), 13 (wekHA noninfected), 13 (WekHA Infected) Scale bar = 40 um

Genotype

Control:
Non-infected R58E02>HistoneYFP
Infected R58E02>HistoneYFP

Experiment:
Non-infected R58E02>HistoneYFP;wekHA
Infected R58E02>HistoneYFP;wekHA

HistoneYFP was used to visualize the neurons in the PAM cluster. Then an automated cell counting software *Deadeasy* was used to count the cells in PAM cluster. The number or TH>HisYP+ PAM neurons decreased compared to the non-infected controls in Wek overexpressing flies (Fig 6.10b, c). This suggest that Wek causes apoptosis in the PAM cluster. However, the number of TH>hisYFP+ cell increased in the infected *wek* overexpressing flies (Fig 6.10b, c), indicating that *B. bassiana* could not induce apoptosis via Wek.

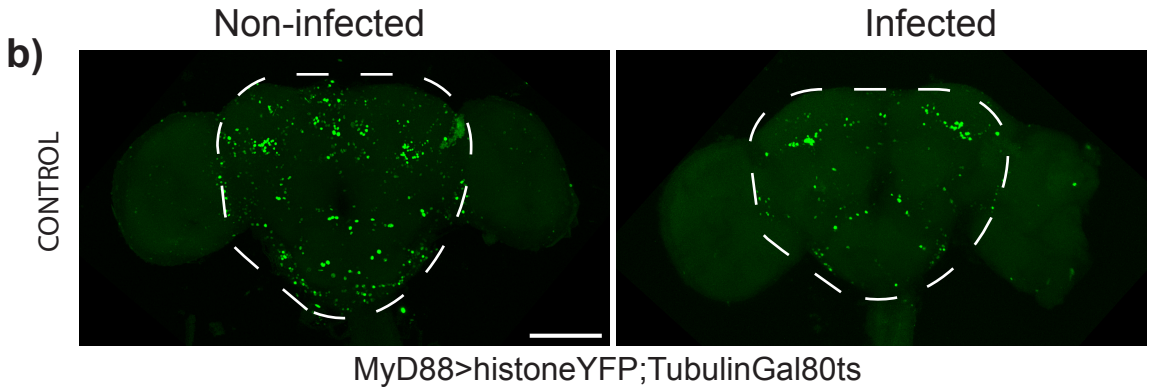
6.2.9 Adult sarmRNAi knockdown rescued MyD88+ cell loss induced by *B. bassiana*

The qRT-PCR data suggested that *sarm* was upregulated in the adult brain upon infection. Therefore, I asked if *B. bassiana* requires Sarm to induce MyD88 cell loss in the adult brain. To test this, *sarm* was downregulated in MyD88 cells using UASSarmRNAi^{TRIPJF01681} followed by infecting the flies with *B. bassiana* for 7 days. *sarm* was knocked down in MyD88 cells in adult flies for 48 hrs using Tubulingal80ts followed by 7 days exposure to *B. bassiana* (Fig 6.11a).

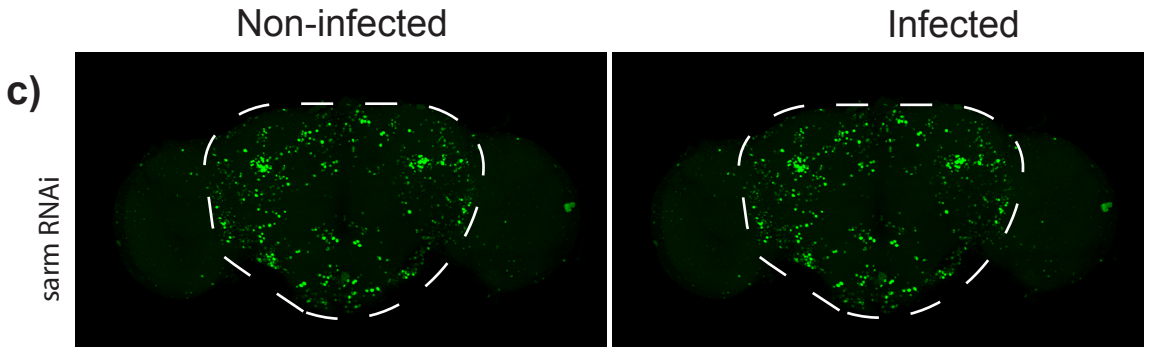
When *sarm* was knocked down in MyD88 cells, the number of MyD88>hisYFP+ cells did not change in the central brain compared to non-infected control flies (Fig 6.11c, d). This indicated that without Sarm, Wek did not induce apoptosis and therefore, the number of MyD88 cells remained unchanged in the brain of *sarm* knock down flies compared to non-infected control flies (Fig 6.11c, d). Interestingly, MyD88>hisYFP+ cells did not decrease in the central brain of infected *sarm* knocked down flies after 7 days exposure to *B. bassiana* compared to non-infected *sarm* knocked down flies (Fig 6.11c, d). This suggests that without Sarm, MyD88 activated NF-kB pathway to induce cell survival in adult brain upon infection. Since, *sarm* knock down rescued the MyD88

Figure 6.11 Adult SarmRNAi^{JF0181} knockdown rescued the loss of MyD88+ cells caused by *B. bassiana* infection





MyD88>histoneYFP;TubulinGal80ts



MyD88>histoneYFP; >sarm RNAi^{JF01681} TubulinGal80ts

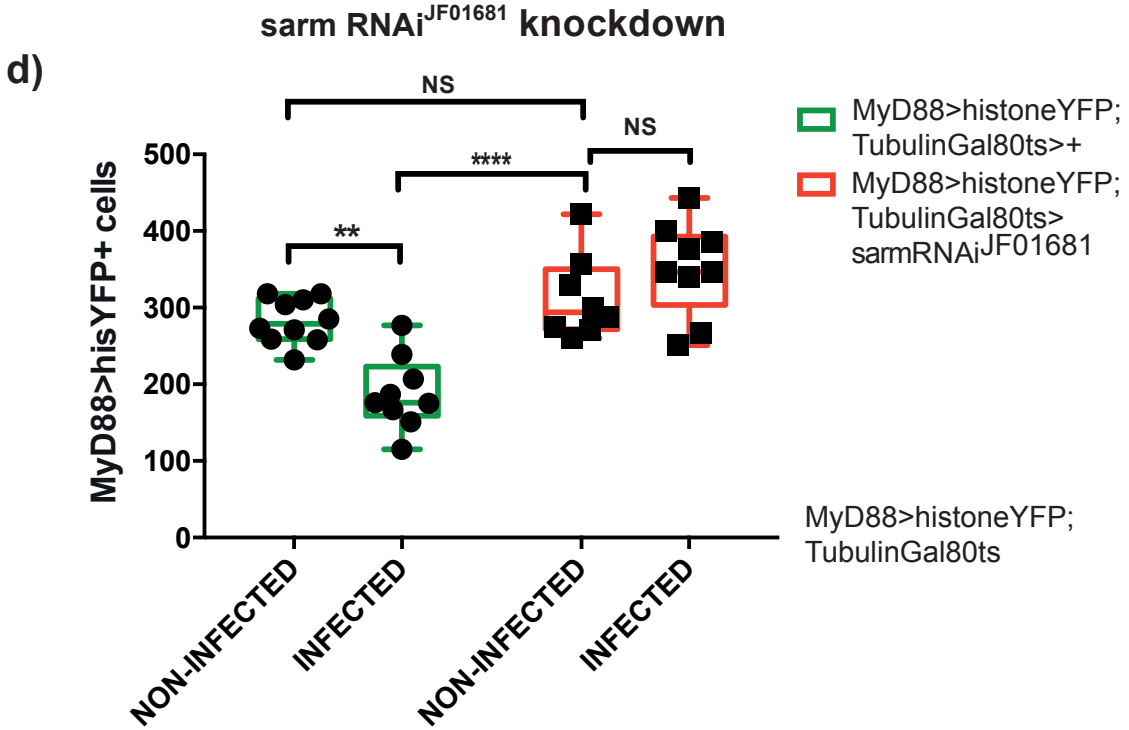


Figure 6.12 Adult *sarm*RNAi^{JF01681} knockdown rescued loss of Repo+ glial cells caused by *B. bassiana* infection

a) Z-projection of the adult brain showing brain glial cells labelled by anti-Repo in wild-type control non-infected and infected flies upon 7 days exposure to *B. bassiana*.
b) Z-projection of the adult brain showing brain glial cells labelled by anti-Repo in *sarm*RNAi^{JF01681} non-infected and infected flies upon 7 days exposure to *B. bassiana*.
c) Box plot representing brain glial cells in control flies and in *sarm*RNAi^{JF01681} flies upon 7 days exposure to *B. bassiana* counted by an automated cell counting program *Deadeasy*. The brain glial cells of non-infected and infected controls are represented by green box plot. The brain glial cells in central brain of non-infected and infected *sarm*RNAi^{JF01681} flies are represented by red box plot. Two-way ANOVA followed by Two-way ANOVA followed by Turkey's multiple comparison test (Appendix 28): **p value<0.05, **p value < 0.01, ***p value <0.001, ****p value < 0.0001. N = 11 (Noninfected control), 9 (Infected control), 8 (sarmRNAi Noninfected), 11 (sarmRNAi Infected) Scale bar = 100 um

Genotype: Control:

Non-infected MyD88>HistoneYFP/+;TubulinGal80^{ts} /+
Infected MyD88>HistoneYFP/+;TubulinGal80^{ts} /+
Experiment:
Non-infected MyD88>HistoneYFP/+;TubulinGal80^{ts} /> *sarm*RNAi^{JF01681}
Infected MyD88>HistoneYFP/+;TubulinGal80^{ts} /> *sarm*RNAi^{JF01681}

cell loss caused by *B. bassiana* infection indicated that *B. bassiana* require Sarm to induce MyD88 cell loss in adult brain.

6.2.10 Adult sarmRNAi knockdown rescued Repo+ glial loss induced by *B. bassiana*

Next, it was tested if *B. bassiana* could induce glial loss without Sarm. Sarm was knocked down using UASSarmRNAi$^{TRIP\ JF01681}$ under the same experimental conditions as described above (Fig 6.11a). When *sarm* was downregulated in MyD88 cells, the number of glial cells did not change in the brain of non-infected flies compared to the control flies (Fig 6.12b, c). This indicated that Sarm does not affect glial cell number in the adult brain. Interestingly, glial cells did not decrease in the brain of infected *sarm* knocked down flies upon 7 days exposure to *B. bassiana* compared to the non-infected *sarm* knocked down flies (Fig 6.12 b, c). This data suggests that without Sarm, *B. bassiana* could not induce glial loss in the adult brain.

6.2.11 Adult Sarm RNAi knockdown rescued loss of dopaminergic neurons in PPM3 cluster induced by *B. bassiana*

Next, it was tested if *B. bassiana* infection induces loss in dopaminergic neurons in the brain via Sarm. To investigate this, *sarm* was downregulated UASSarmRNAi$^{TRIP\ JF01681}$ under the same experimental conditions as described in (Fig 6.13a). When *sarm* was knocked down in MyD88 cells, the number of neurons in PPM3 cluster did not change compared to non-infected control flies (Fig 6.13c, d). The number of neurons in PPM3 cluster did not decrease in *sarm* knocked down infected flies upon 7 days exposure to *B. bassiana* compared to the non-infected *sarm* knocked down flies (Fig 6.13c, d).

Figure 6.12 Adult SarmRNAi^{JF0181} knockdown rescued the loss of Repo+ glial cells caused by *B. bassiana* infection

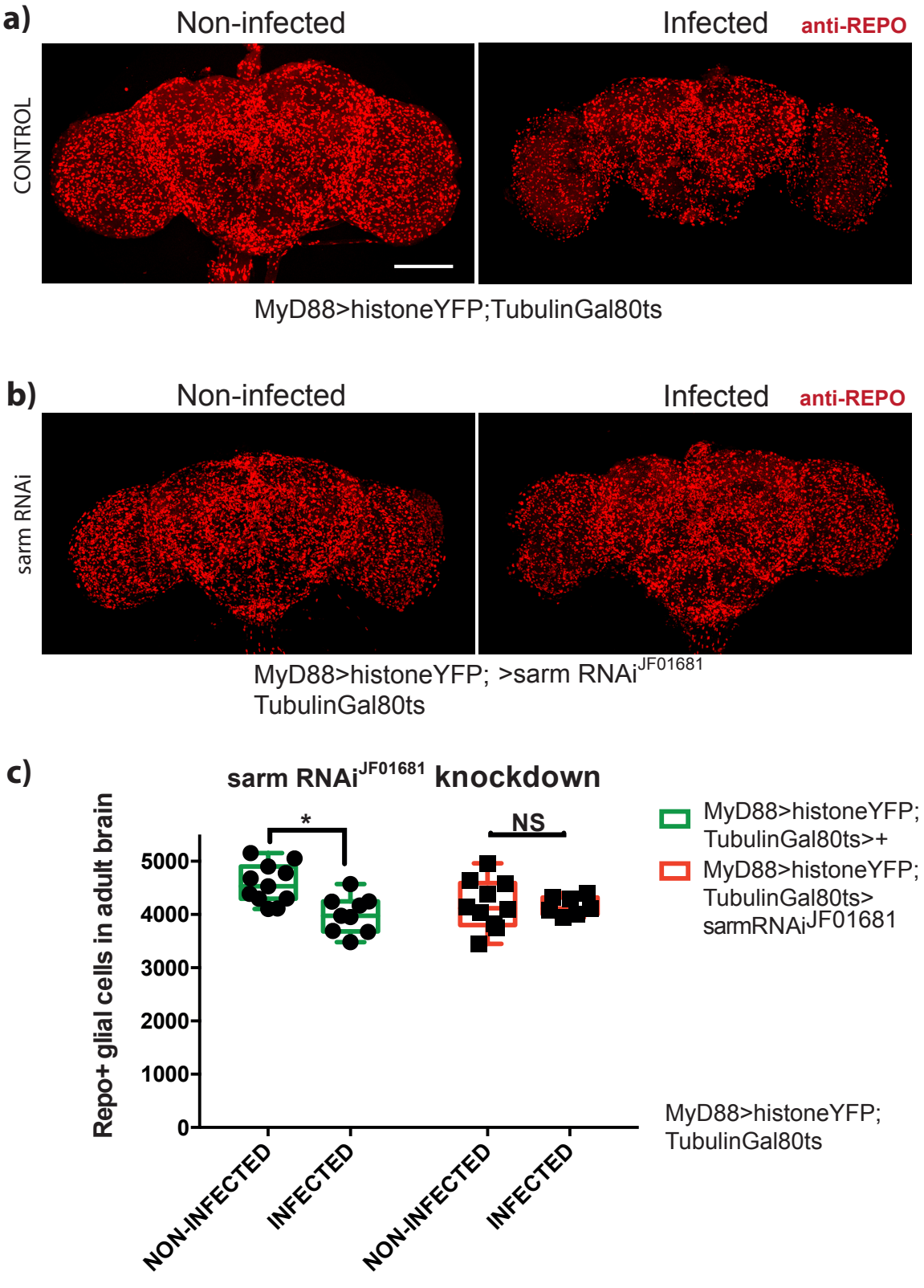


Figure 6.11 Adult *sarm*RNAi^{JF01681} knockdown rescued loss of MyD88+ cells caused by *B. bassiana* infection

a) Diagram explaining the experimental regime.

b) Z-projection of the adult brain showing expression of MyD88+ cells in central brain of wild-type control non-infected and infected flies upon 7 days exposure to *B. bassiana*.

c) Z-projection of the adult brain showing expression of MyD88+ cells in central brain of *sarm*RNAi^{JF01681}non-infected and infected flies upon 7 days exposure to *B. bassiana*.

d) Box plot representing number of MyD88+ cells in central brain in control flies and in *sarm*RNAi^{JF01681} flies upon 7 days exposure to *B. bassiana*. The number of MyD88+ cells in central brain of non-infected and infected controls are represented by green box plot. The number of MyD88+ cells in central brain of non-infected and infected *sarm*RNAi^{JF01681} flies are represented by red box plot. Two-way ANOVA followed by Two-way ANOVA followed by Turkey's multiple comparison test (Appendix 27): **p value<0.05, **p value < 0.01, ***p value <0.001, ****p value < 0.0001. N = 10 (Noninfected control), 9 (Infected control), 8 (SarmRNAi Noninfected), 9 (SarmRNAi Infected)

Scale bar = 100 um

Genotype

Control:

Non-infected MyD88>HistoneYFP/> +;TubulinGal80^{ts}/> +

Infected MyD88>HistoneYFP/> +;TubulinGal80^{ts}/ > +

Experiment:

Non-infected MyD88>HistoneYFP/+;TubulinGal80^{ts} /> *sarm*RNAi^{JF01681}

Infected MyD88>HistoneYFP/+;TubulinGal80^{ts}/> *sarm*RNAi^{JF01681}

Figure 6.13 Adult SarmRNAi^{JF0181} knockdown rescued the loss dopaminergic neurons in PPM3 cluster caused by *B. bassiana* infection

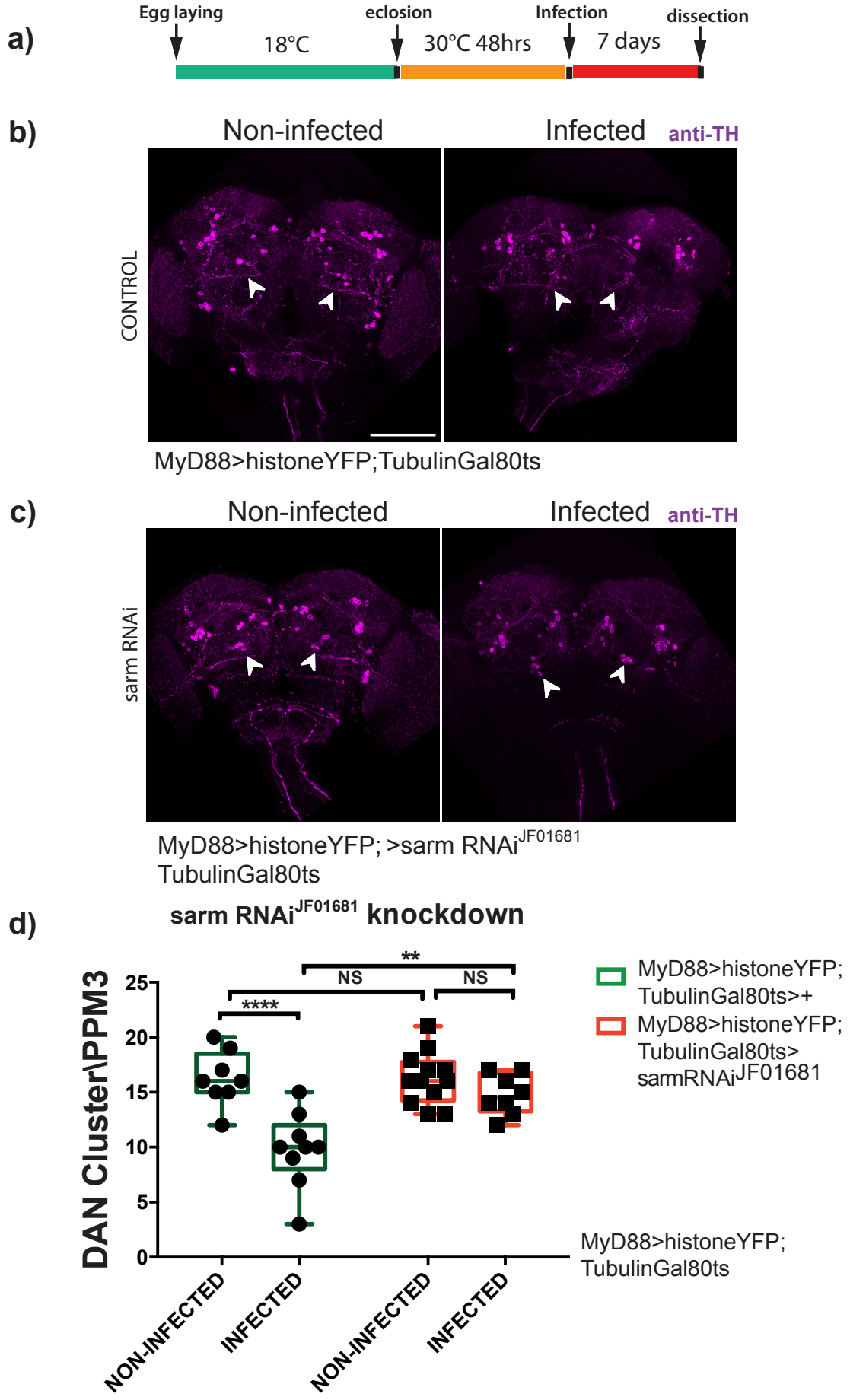


Figure 6.13 Adult *sarm*RNAi^{JF01681} knockdown rescued loss of dopaminergic neurons in PPM3 cluster caused by *B. bassiana* infection

a) Diagram explaining the experimental regime.

b) Z-projection of the adult brain showing dopaminergic neurons of PPM3 cluster in central brain of wild-type control non-infected and infected flies upon 7 days exposure to *B. bassiana* labelled by anti-TH. White arrows indicate the dopaminergic neurons in PPM3 cluster. Scale bar = 80 um

c) Z-projection of the adult brain showing dopaminergic neurons of PPM3 cluster in central brain of *sarm*RNAi^{JF01681} non-infected and infected flies upon 7 days exposure to *B. bassiana* labelled by anti-TH. White arrows indicate the dopaminergic neurons in PPM3 cluster. Scale bar = 80 um

b. Box plot representing number of dopaminergic neurons in PPM3 cluster in control flies and in *sarm*RNAi^{JF01681} flies upon 7 days exposure to *B. bassiana*. The number of neurons in PPM3 cluster of non-infected and infected controls are represented by green box plot. The number of neurons in PPM3 cluster of non-infected and infected *sarm*RNAi^{JF01681} flies are represented by red box plot. Two-way ANOVA followed by Two-way ANOVA followed by Turkey's multiple comparison test (Appendix 29): **p value<0.05, **p value < 0.01, ***p value <0.001, ****p value < 0.0001. N = 8 (Noninfected control), 9 (Infected control), 12 (SarmRNAi Noninfected), 8 (SarmRNAi Infected).

Genotype **Control:**

Non-infected MyD88>HistoneYFP/+;TubulinGal80^{ts} /+
Infected MyD88>HistoneYFP/+;TubulinGal80^{ts} /+

Experiment:

Non-infected MyD88>HistoneYFP/+;TubulinGal80^{ts} /> *sarm*RNAi^{JF01681}
Infected MyD88>HistoneYFP/+;TubulinGal80^{ts} /> *sarm*RNAi^{JF01681}

SarmRNAi rescued the loss of dopaminergic neurons caused by the *B. bassiana* infection confirmed that *B. bassiana* could not induce neuronal loss without Sarm.

6.3 Discussion

Table 6.1: Summary of Wek Data

Genotype	Reporter/ staining	Data	Result
MyD88>HisYFP/+;Tubulingal80> *wek*-RNAi^{MHC046534}	Histone YFP	MyD88>his YFP+ cell count	*wek*-RNAi^{MHC046534} rescued the *B. bassiana* induced Myd88+ cell loss
MyD88>HistoneYFP/+;tubulingal80/>*wek*-HA	Histone YFP	MyD88>his YFP+ cell count	*Wek*-HA rescued the *B. bassiana* induced Myd88+ cell loss
MyD88>HisYFP/+;Tubulingal80> *wek*-RNAi^{MHC046534}	Anti-Repo Glial cells	Repo+ cell count	*wek*-RNAi^{MHC046534} rescued the *B. bassiana* induced Repo+ glial cell loss
MyD88>HistoneYFP/+;tubulingal80/>*wek*-HA	Anti-Repo Glial cells	Repo+ cell count	*Wek*-HA also rescued the *B. bassiana* induced Repo+ glial loss
MyD88>HisYFP/+;Tubulingal80> *wek*-RNAi^{MHC046534}	Anti-TH DAN neurons	PPM3, PPL1,	*wek*-RNAi^{MHC046534} knockdown did not rescue loss of DAN neurons
MyD88>HistoneYFP/+;tubulingal80/>*wek*-HA	Anti-TH DAN neurons	PPM3, PPL1, PPL2 PAL	*B. bassiana* induced DAN neurons loss even in the PAL cluster usually protected by the infection.
TH;R58E02>hisYFP;*wek*-HA	Histone YFP	HistoneYFP + PAM cells	Overexpression of *wek* mimicked the cell loss caused by *B. bassiana*, but infection increased YFP+ cells in the brain.

Table 6.2: Summary of Sarm Data

Genotype	Reporter/ staining	Data	Result
MyD88>HisYFP/+;Tubulingal80> *sarm*-RNAi^{TRIPJF01681}	Histone YFP	MyD88>his YFP+ cell count	*sarm*-RNAi^{TRIPJF01681} rescued the *B. bassiana* induced Myd88+ cell loss
MyD88>HisYFP/+;Tubulingal80> *sarm*-RNAi^{TRIPJF01681}	Anti-Repo Glial cells	Repo+ cell count	*sarm*-RNAi^{TRIPJF01681} rescued the *B. bassiana* induced Repo+ glial cell loss
MyD88>HisYFP/+;Tubulingal80> *sarm*-RNAi^{TRIPJF01681}	Anti-TH DAN neurons	PPM3	*sarm*-RNAi^{TRIPJF01681} rescued the *B. bassiana* induced DAN neuron loss

The qRT-PCR analysis showed upregulation of *wek* mRNA in the dissected adult brain after 7 days of *B. bassiana* exposure, indicating that *B. bassiana* might also activate non-canonical Toll immune signalling in the brain. Downregulating *wek* in the adult flies rescued the loss of MyD88+ cells and Repo+ glial cells in the adult brain. However, overexpression of *wek* also rescued the MyD88+ and Repo+ cells induced by *B. bassiana* infection, suggesting that *B. bassiana* causes cell loss independently of Wek. Furthermore, *wek* knock-down in the adult brain did not rescue the loss of dopaminergic neurons in PPM3, PPL1 and PPL2 cluster induced by *B. bassiana.* This suggests that *B. bassiana* does not kill via Wek. Interestingly, overexpression of *wek* induced loss of DAN neurons in PAL cluster which is usually protected from *B. bassiana* infection. This indicated that Wek is necessary for *B. bassiana* to kill neurons in PAL cluster. To further test this hypothesis, *wek* was overexpressed in the DAN neurons of PAM cluster, which decreased the TH>HisYFP+ cells in PAM indicating

that Wek is pro-apoptotic in PAM cluster, but *B. bassiana* infection rather increased the TH>HisYFP+ cells in PAM. This indicated that *B. bassiana* is not causing neurodegeneration through *wek*.

Next, *sarm* knockdown in the adult brain rescued the number of MyD88+ cells, Repo+ cells and DAN neurons in PPM3 cluster induced by the *B. bassiana* infection. This indicates that *B. bassiana* is causing neurodegeneration in the brain through Sarm. To summarise, *B. bassiana* induces neurodegeneration through Sarm, while the role of Wek in this process remains unclear due to contradictory results.

In this chapter, various approaches were utilized to investigate whether *B. bassiana* exploits the non-canonical Toll signalling. This was achieved by manipulating the expression of *wek* and *sarm* in the adult brain using previously published RNAi knockdown and overexpression lines (Foldi et al., 2017, Li et al., 2020). This is followed by analysing the effect of *B. bassiana* infection on MyD88+ cells, glial cells and dopaminergic neurons. The qRT-PCR data showed upregulation of *wek* in the dissected adult brain after 7 days exposure to *B. bassiana* infection. This is consistent with a previous report that demonstrated upregulation of *wek* upon *E. muscae* infection in adult *Drosophila* (Elya et al., 2018). These results provide evidence that *B. bassiana* infection activates the non-canonical Toll signalling in the adult brain.

Wek is pro-apoptotic in the pupae CNS, but in adult brain it is non-apoptotic (Foldi et al., 2017, Li et al., 2020). Overexpression of *wek* or RNAi knockdown of *MyD88* resulted in an increase in MyD88>hisYFP+ cell number in the central brain of the 2 days old adult flies, and the effect was even more pronounced when both were

manipulated together (Li et al., 2020). This suggests that Wek is non-apoptotic. My data also indicates that RNAi knockdown of *wek* did not change the number of MyD88+ cells and Repo+ glial cells in the adult brain indicating that Wek is not pro-apoptotic. Furthermore, *wek*-RNAi rescued the number of MyD88+ and Repo+ cell loss caused by *B. bassiana*. This can be explained by the fact that Wek recruits Sarm which inhibit MyD88 to induce apoptosis (Foldi et al., 2017). In the absence of Wek, Sarm cannot inhibit MyD88 signalling which leads to the cell survival via NF-kB signalling. *B. bassiana* infection activate MyD88-NF-kB signalling in the wekRNAi knockdown, resulting in an increase in the number of MyD88+ cells in the brain. This suggest that *B. bassiana* requires Wek to cause MyD88 cell loss.

Overexpression of *wek* led to an increase in the number of MyD88+ cells in the central brain compared to non-infected controls. This suggest that *wek* causes proliferation which is consistent with the previous finding from our lab that Wek might induces cell proliferation through Yorkie in the adult brain (Li et al., 2020). However, *wek* overexpression also rescued the loss of MyD88+ and Repo+ cells caused by *B. bassiana* infection. This is contradictory to our hypothesis that *B. bassiana* induces glial and neuronal loss through Wek. One possibility is that since *wek* is already overexpressed and is causing proliferation, *B. bassiana* cannot activate it further to manipulate it for inducing cell death. To gain further insights, infecting adult flies with *B. bassiana* upon knocking down *yorkie* and overexpressing *wek* could provide more information on whether *B. bassiana* causes neurodegeneration through Wek.

The RNAi knockdown of *wek* did not rescue *B. bassiana* induced DAN neurons loss but interestingly, *wek* overexpression was sufficient to induce neurodegeneration in

the PAL cluster, which is typically unaffected by *B. bassiana* infection. Additionally, overexpression of *wek* in the PAM cluster decreased the number of TH>hisYFP+ cells, indicating that Wek is pro-apoptotic. However, *B. bassiana* infection failed to induce TH>hisYFP+ cell loss in the PAM cluster upon PAM specific *wek* overexpression, contradicting our hypothesis. Therefore, the role of Wek in *B. bassiana* infection remains unclear. Conversely, the RNAi knockdown of *sarm* rescued the loss of MyD88+, Repo+ and DAN neurons caused by *B. bassiana* infection suggesting that *B. bassiana* induced glial and neuronal loss might be mediated by Sarm.

Chapter 7

DISCUSSION

7.1 Summary of findings

The aim of this project was to investigate whether fungus *Beauveria bassiana* could cause neurodegeneration in the adult *Drosophila* brain via Toll signalling.

An infection chamber was designed to infect adult flies with *B. bassiana*, and a longevity assay confirmed the efficiency of the set-up by showing that exposure to *B. bassiana* reduced flies lifespan. Moreover, the climbing assay demonstrated that *B. bassiana* affects locomotion of adult flies. Next, Toll-1 Gal4 and Sarm Gal4 driven expression of GFP based reporter UASFlybow1.1 revealed the expression pattern of Toll-1 and Sarm in the sub-oesophageal ganglion (SOG) and in the proboscis. Additionally, the PER assay showed that Sarm neurons participate in proboscis extension.

The feeding assay showed that adult flies ingested *B. bassiana* spores, suggesting that spores could reach the brain via feeding through the proboscis. Exposure to *B. bassiana* resulted in damaged blood-brain barrier in adult flies. FM4-64 and calcofluor white staining were inconclusive, however, *bassiana* transgenic-GFP spores were observed in infected adult brains. In addition, qRT-PCR analysis demonstrated that *B. bassiana* spores activated Toll signalling in the brain, as *drosomycin* mRNA was upregulated in the adult brains after 7 days exposure to *B. bassiana*. Together, these findings suggest that adult flies could ingest spores through their proboscis while feeding. Additionally, the result indicated towards the possibility of *B. bassiana* invasion of the adult brain, leading to the activation of Toll signalling in the brain.

Exposure to *B. bassiana* causes MyD88+ cells, glial and dopaminergic neurons loss in the adult brain, as demonstrated by a decrease in the brain size, loss of Repo+ glial cells and Sarm>hisYFP+ cells, downregulation of *TH* mRNA, and loss of dopaminergic neurons in the adult brain. *B. bassiana* caused MyD88+ cells, glial and dopaminergic neurons loss via Toll-1 as *Toll-1*RNAi knockdown rescued the loss in MyD88+ cells, Repo+ glial cells and TH+ dopaminergic neurons caused by the *B. bassiana* infection in the adult brain.

B. bassiana could possibly activate non-canonical Toll signalling in the adult brain as qRT-PCR data showed that *wek* mRNA were upregulated in dissected adult brain upon 7 days exposure to *B. bassiana. wek*RNAi knockdown in adult flies rescued the loss of MyD88+ cells and Repo+ glial cells caused by *B. bassiana* infection in the brain. *wek*-HA overexpression in the adult brain reproduced the same results as *wek*RNAi, and rescued the loss of MyD88+ cells and Repo+ glial cells caused by *B. bassiana*

infection. However, TH+ dopaminergic neurons in the PPL1 and PPM3 decreased in the infected *wek*-HA overexpression adult brain. Moreover, *wek*-HA overexpression caused decrease in the DAN neurons in the PAM cluster but infection increased the number of DAN neurons in the PAM cluster. Therefore, it is unclear if *B. bassiana* induce neurodegeneration via Wek. RNAi knockdown of *sarm* rescued the loss in MyD88+ cells, Repo+ glial cells and TH+ dopaminergic neurons caused by *B. bassiana* demonstrating that *B. bassiana* causes neurodegeneration through Sarm. Sarm cannot bind Tolls directly. Instead, Wek binds both Tolls and Sarm, enabling Toll signalling through Sarm. Therefore, it is unclear how Sarm could cause cell loss downstream of Tolls without Wek during infection.

To conclude, the data of my thesis provided evidence that, *B. bassiana* affects the locomotion of adult flies. *Toll-1* and *sarm* are two candidate genes that can be exploited by the entomopathogenic fungi to control proboscis extension. *B. bassiana* spores could invade the adult brain through proboscis while feeding and activates both immune Toll signalling pathway and *Wek*. *B. bassiana* caused MyD88+ cells, glial and dopaminergic neuronal loss in the adult brain through Toll-1 and Sarm.

7.2 *B. bassiana* spores enters the adult *Drosophila* brain

The novel infection setup is a highly efficient and effective method for infecting flies with fungus. By constantly exposing the flies to the fungus at 25°C while also providing them with a source of food, this method provides a more natural and controlled approach to studying host-pathogen interactions. Unlike other methods that involves infecting flies with spores through injection (Gottar et al., 2006, Hanson et al., 2021, Lemaitre et al., 1997, Lemaitre et al., 1996, Weber et al., 2003), this setup eliminates

the potential for injury induced during injection, which could induce variability in results. Additionally, by avoiding the need to raise the flies at 29°C, as is often done to expedite germination of the fungal spores on the fly cuticle, this method eliminates any potential effects on gene expression that could arise from exposure to higher temperatures. However, despite these considerations, the infection setup is cumbersome and occupies a significant amount of space in the incubator due to its reliance on glass bottles. Additionally, it is crucial to avoid overcrowding the bottles with flies, as this can result in a decrease in the infection rate among the flies. As a result, it is recommended to limit the number of flies per bottle to N=20. This restriction can present a challenge when conducting experiments that necessitate large sample sizes, such as mass spectrometry analysis, HPLC, and mutant screens. This can be overcome by few modifications like using a vial instead of glass bottle, with fungal culture at the bottom and food on the side. Alternatively, flies can be infected by isolating fungal spores, followed by transferring to the Eppendorf. The flies then can be transferred in the Eppendorf and vortexed for few seconds. This method would be optimum to induce infection in the flies, however vortexing flies could result into head injury in the flies and would not be optimum for investigating the effect of infection in the brain. Overall, this new infection setup represents a significant improvement in the ability to infect flies with fungus in a controlled and efficient manner, making it a valuable tool for future studies of host-pathogen interactions. In this thesis, the infection set-up is used to study the effect of *B. bassiana* on adult *Drosophila* behaviour and brain.

While *E. muscae* and *O. unilateralis* induce abnormal climbing and walking behaviour in their host (Elya et al., 2018, de Bekker and Das, 2022), *B. bassiana* decreases the climbing ability of the adult flies. However, the climbing assay data does not provide

clarity on whether *B. bassiana* affects nervous system to decrease the climbing ability of infected flies. It is possible that the spores covering the flies might have affected their climbing ability. It remains unclear whether *B. bassiana* affects proboscis extension in adult flies. However, previous research from our lab has demonstrated that Toll-1 and Sarm are expressed in the SOG of the adult brain (Li et al., 2020). My findings have also shown that Toll-1 and Sarm are expressed in proboscis. Moreover, activating Sarm mediates proboscis extension. These findings suggest that *Toll-1* and *Sarm* could be the potential genes that can be manipulated by entomopathogenic fungi to control proboscis extension. Interestingly, adult flies ingested *B. bassiana* spores rather than avoiding them. This suggests that *B. bassiana* might secretes certain compounds or metabolites that are attractive to flies, and this could be investigated further using Liquid chromatography-mass Spectrometry (LC-MS).

B. bassiana is an opportunistic pathogen and can invade the insect system in different possible ways. Previous research suggested that *B. bassiana* spores adhere on fly cuticle and germinate to form hyphae which degrade fly cuticle by producing several proteases and chinases. The hyphae then invade fly abdomen and infect the gut the adult flies as hyphal filaments were found in the abdomen of the insects (Lewis et al., 2009). The spores can also adhere of fly legs, thorax and possible directly through eyes. The Drosophila eye comprises 800 ommatidia, with each ommatidium consisting of eight photoreceptors whose axons project as a unified bundle towards the optic lobes of the brain (Newsome et al., 2000). Since photoreceptors innervate the adult Drosophila brain, it could be one of the possible pathways via which *B. bassiana* spores reach the brain. In line with this possibility, I have observed fungal outgrowth on the eyes of flies that were exposed for 7 days while conducting adult brain

dissections. Additionally, structures resembling spores were detected in the optic lobes of the adult flies, as revealed by staining with FM4-64 and Calcofluor white. GFP-labelled spores were also detected in the optic lobes. The feeding assay suggested that spores could reach the brain through the proboscis during feeding, thereby indicating towards the possibility of another underlying route through which the spores invade the brain. Moreover, the integrity of the BBB was compromised in the adult flies after exposure to *B. bassiana*. A recent report has also showed that *E. muscae* infection permeabilized the BBB at the onset of summiting in adult *Drosophila* (Elya et al., 2022). However, further investigation is necessary to determine if it is a parasite strategy to invade the brain of their host or if the increased permeability of the BBB is a host response that facilitates macrophages clearance of the infection from the brain (Winkler et al., 2021).

A previous study demonstrated the presence of *E. muscae* spores in the adult *Drosophila* brain with two methods: staining the spores with safranin-o-fast green and In-situ tagging of spores with a fluorescent probe (Elya et al., 2018). Another study reported the use of FM4-64 dye to stain *B. bassiana* spores in-vivo in the haemolymph of tobacco budworm (Lewis et al., 2009). In this thesis, *B. bassiana* spores were stained in the adult brain using different tools, specifically, FM4-64, calcofluor white, and a transgenic *B. bassiana*-GFP strain. By using these different methods, the effectiveness of various techniques for detecting fungal spores in-vivo was demonstrated. Various staining conditions were attempted to label the spores in the brain using FM4-64 dye and Calcofluor white stain. However, both staining methods yielded high background signals and non-specific bindings. These outcomes strongly indicated that FM4-64 and Calcofluor white were not suitable dyes for effectively

staining the fungal spores in the brain. Compared to these staining methods GFP-tagged *B. bassiana* spores is an effective transgenic strain that can be used to visualise the fungal spores in the brain. GFP-tagged fungal transformants are valuable tools for studying host-pathogen interactions. However, they also have certain drawbacks and limitations. In my thesis, for example, I observed that the GFP-tagged *B. bassiana* strain exhibited higher virulence compared to the wild-type strain I utilized. This discrepancy could be attributed to the potential impact of the GFP gene and its expression on the physiology and behaviour of the fungus. Consequently, employing GFP-tagged *B. bassiana* spores might not be the most suitable approach for validating the presence of spores in the brain. Together these findings highlight different tools that can be used to detect the fungal spores in-vivo and demonstrated that entomopathogenic fungi might invade the brain of their host.

My findings have shown that invasion of *B. bassiana* spores upregulates *drosomycin* expression in the adult brain, confirming that *B. bassiana* activates the immune signalling in the adult brain. Previous studies have shown that activated immune signalling can lead to neurodegeneration in the brain (Cao et al., 2013, Kounatidis et al., 2017). Moreover, overexpression of *drosomycin* using a glial diver, Repo-Gal4 and pan-neuronal driver, ELAV-Gal4 increased the neurodegenerative index in the adult brain, suggesting that Drosomycin can cause neurodegeneration in the brain. Interestingly, Drosomycin is ineffective against *B. bassiana,* as flies expressing *drosomycin* could not survive natural *B. bassiana* infection (Tzou et al., 2002). Since, Drosomycin is ineffective against *B. bassiana* but causes neurodegeneration upon overexpression in the brain indicates that *B. bassiana* can induce neurodegeneration in the brain by inducing upregulation of *Drosomycin*. Infecting adult flies with *B.*

bassiana in the absence of Drosomycin would provide some interesting insights to explore whether *B. bassiana* can cause neurodegeneration through *Drosomycin*.

7.3 *B. bassiana* cause neurons and glial loss in the adult *Drosophila* brain

Fungal spores are predominant in poor (moldy and dampened) indoor air, that can cause flu like symptoms referred to as sick building disorder (Shi et al., 2014, Provost et al., 2013, Fischer et al., 2008, Claeson et al., 2002, Matysik et al., 2008). Some studies aimed to investigate the effect of fungi spores on human health using *Drosophila* as a model organism (Inamdar et al., 2013, Inamdar et al., 2010). Their findings suggest that fungal volatiles can cause neurodegeneration in the adult *Drosophila* brain (Inamdar et al., 2013, Inamdar et al., 2010). However, they have only measured TH expression and dopaminergic neuron counts in a few dopaminergic clusters to indicate neurodegeneration in the brain (Inamdar et al., 2013, Inamdar et al., 2010). Other studies have used a neurodegenerative index, which measures the size of vacuolar lesions in the brain neuropil, to quantify neurodegeneration in the adult brain (Cao et al., 2013, Kounatidis et al., 2017).

In this thesis, adult flies were exposed to the *B. bassiana* in the infection chamber for 7 days and various approaches, including antibody staining, the UAS-GAL4 system, and qRT-PCR, were employed to investigate the neurodegeneration caused by *B. bassiana* in the brain. Glial cells were labelled with anti-REPO, and a histoneYFP reporter was used to visualize Sarm cells. Cell numbers were quantified using an automated cell counting software called Deadeasy, which eliminated the error induced by manual counting (Forero et al., 2010). Exposure to *B. bassiana* resulted in a decrease in both glial cells and Sarm cells. Moreover 7 days post exposure the

expression of TH mRNA decreased in the adult brain. Tyrosine hydroxylase is an enzyme that convert tyrosine to L-DOPA, a precursor for the dopamine, indicate that *B. bassiana* might affect dopamine production. Furthermore, labelling dopaminergic neurons with anti-TH also revealed a reduction in the number of TH+ dopaminergic neurons in the adult brain. Dopamine and serotonin are neurotransmitters that are involved in various physiological and behavioural process such as locomotion, learning, memory, sleep, reward and motivation (Kasture et al., 2018, Dvořáček and Kodrík, 2021). Manipulating the levels of these neurotransmitters in the host brain could be a key strategy employed by behaviour-manipulating fungal pathogens to influence the behaviour of their hosts. Based on my data, there appears to be a downregulation of TH mRNA after infection. However, the effect of *B. bassiana* infection on serotonin levels in the brain remains unknown. Therefore, it would be intriguing to examine the impact of B. bassiana infection on serotonin levels to investigate whether this fungal infection affects neurotransmitters in the adult *Drosophila* brain.

The data from my thesis indicate a decrease in glia and neurons in the adult brain following infection. However, despite employing various techniques and strategies, my thesis could not provide evidence for cell death in the adult brain after *B. bassiana* infection. Detecting cell death in the adult brain is challenging as they are swiftly removed from the system via phagocytosis. In accordance with my experimental protocol, I transferred newly eclosed flies to the infection chamber. Previous research has shown that the adult brain of the newly eclosed flies is plastic evidenced by an increase in MyD88>His+ cells, mediated by the Toll-2 receptor (Li, 2020). Hence, it is plausible *B. bassiana* infection might impairs plasticity of the adult brain during the

critical period. To investigate this an EdU experiment was designed but no proliferative cells was detected in the adult brain. This could be due to the constant contamination of EdU mixed food from the fungal spores. Counting P35 positive cells after 7 days exposure to *B. bassiana* could be an interesting test that could provide evidence for *B. bassiana* induced neurodegeneration in the adult brain. Overall, the results suggest that exposure to *B. bassiana* showed sign of potential neurodegeneration as marked by the decrease in glial cells, neurons and TH mRNA expression in the brain. Altogether, these experiments covered different aspects of the adult brain to examine the effect of *B. bassiana* on the adult brain.

7.4 *B. bassiana* causes neurodegeneration via Toll-1 in the adult *Drosophila* brain

There are reports indicating an ongoing evolutionary arms race between TLR's and *C. albicans.* TLR-4 activates the immune response against *C. albicans* whereas *C. albicans* activates TLR-2, which leads to production of anti-inflammatory chemokines that help *C. albicans* to evade the host immune system (Netea et al., 2004, Netea et al., 2002, Netea et al., 2007). Similarly, *B. bassiana* and *Drosophila* are engaged in an evolutionary arms race. The Toll signalling pathway is known to protect flies from pathogens by activating immunity (Lemaitre et al., 1996, Lemaitre et al., 1997). However, Toll signalling also functions in development and CNS (Foldi et al., 2017, Anderson and Nüsslein-Volhard, 1986). Of the nine Toll receptors in *Drosophila,* only Toll-1 has a clear function in the immunity (Tauszig et al., 2000). Previous reports have shown that innate immunity mediated by IMD-NF-kB pathway can cause neurodegeneration in the brain (Cao et al., 2013, Kounatidis et al., 2017). Toll-1 is expressed in the adult brain and has been shown to induce apoptosis in larvae VNC

(Foldi et al., 2017, Li et al., 2020). Thus, in the context of an evolutionary arm race, adult flies use immune Toll signalling to protect themselves from *B. bassiana*, while the fungus exploits the non-immune Toll signalling pathway to cause neurodegeneration and kill the flies.

In this thesis, I investigated the expression of Toll-1 in the adult brain using a histone-YFP reporter. The result suggest that Toll-1 is widely distributed throughout the adult brain. This finding aligns with our lab previous research, which also reported the expression of Toll-1 in the adult brain (Li et al., 2020). Furthermore, qRT-PCR data suggested that Drosomycin, is upregulated after a 7-day exposure to *B. bassiana*. This implies that infection may trigger the upregulation of Drosomycin in a Toll-dependent manner. However, previous study has shown that overexpression of the IMD pathway using UAS-IMD in larval tracheal cells increased the expression of Drs-GFP in only a few tracheal cells (Akhouayri, 2011). Considering that the adult brain contains wide network of trachea, it indicates that the upregulation of *Drosomycin* in the adult brain may not be solely dependent on the Toll pathway. It would be interesting to quantify the expression of Drosomycin via qRT-PCR in Toll mutant flies upon 7 days exposure to *B. bassiana*. Such an experiment would provide insight if B. bassiana is inducing upregulation of Drosomycin in Toll dependent manner.

Interestingly, my expression data showed a colocalization of TH+ neurons with Toll-1>hisYFP cells in the brain, indicating that TH+ neurons do express Toll-1, additionally, when Toll-1 was knocked down, it rescued the loss of TH+ cells induced by *B. bassiana.* This indicate that *B. bassiana* induced TH+ neuronal loss could be cell

autonomous, however further investigation is required. Data from my thesis indicates towards the pro-apoptotic role of Toll-1 in the adult brain, as demonstrated by an increase in MyD88+ cell count in the central brain following RNAi knockdown of Toll-1 and the reduction in brain size upon Toll-1^{10b} overexpression. However, overexpression of Toll-1^{10b} also increased the MyD88+ cells in the brain, which may be due to the constitutive expression of the UAShistoneYFP protein driven by the MyD88Gal4 promoter, regardless of the Toll-1 RNAi/overexpression. Despite this, there was no significant difference in the number of Repo+ glial cells and TH+ dopaminergic neurons in RNAi knockdown of *Toll-1* and wildtype noninfected controls, further supporting the pro-apoptotic role of Toll-1.

Furthermore, *B. bassiana* infection failed to induce loss in MyD88+ cells, Repo+ glial cells, and TH+ dopaminergic neurons in the brain of *Toll-1* RNAi knockdown flies, indicating that Toll-1 plays a critical role in *B. bassiana* induced cell and neuronal loss. In contrast, *B. bassiana* infection increased the adult brain size in Toll-1^{10b} overexpressing flies, indicating two possibilities: *B. bassiana* could alter the permeability of the BBB via Toll-1 or Toll-1 could increase the permeability of BBB to facilitate the entry of macrophages in the adult brain (Winkler et al., 2021). Therefore, in this thesis different approaches were used to investigate the role of Toll-1 in glia, neurons and MyD88 cells upon *B. bassiana* infection.

However, it still remains unclear how Toll pathway is activated upon sensing *B. bassiana* spores by the adult flies. Previous research has demonstrated that the Toll pathway displayed distinct activation patterns in response to natural entomopathogenic infection compared to the injection of *B. bassiana* spores.

(Lemaitre, 1996; Gottar, 2006). GNBP3 encodes a hemolymphatic protein that detect fungal 1-3 glucan component of fungal cell wall that activates Toll signalling and upregulates Drosomycin upon injecting *B. bassiana* spores in the fat body (Ligoxygakis et al., 2002). However, Drosomycin was found to be regulated in the GNBP3 null mutant flies upon natural infection by *B. bassiana* (Gottar, 2006).

Furthermore, *B. bassiana* releases PR1 which is a fungal virulence factor in the hemolymph, which gets proteolytically cleaved by presophene and activates toll-signalling. In addition to PR1, *B. bassiana* secretes various secondary metabolites during different stages of its life cycle that could act as virulence factors (Pedrini, 2022). For example, the BbopS1 gene encodes for oosporein polyketide synthase, which is involved in host immune evasion and promotes fungal growth within the host system (Eley et al., 2007). Other secondary metabolites, such as beauverolides and destruxins, have also been identified to increase fungal virulence and promote fungal growth within the host system (Molnár et al., 2010). Since flies can efficiently detect fungal cell walls, one can argue that fungi have evolved these secondary metabolites to increase their chances of infecting and killing their hosts. Thus, these different virulence factors can be attributed to the ongoing evolutionary arms race between the fungus and its host.

Together these data support the evolutionary arm race theory, where *Drosophila* activates innate immunity via Toll-1 to protect itself from *B. bassiana* infection, while *B. bassiana,* in turn, causes neurodegeneration via Toll-1.

7.5 Non-canonical Toll signalling in *B. bassiana* induced neurodegeneration

Figure 7.1 *B. bassiana* cannot induce neurodegeneration without Wek

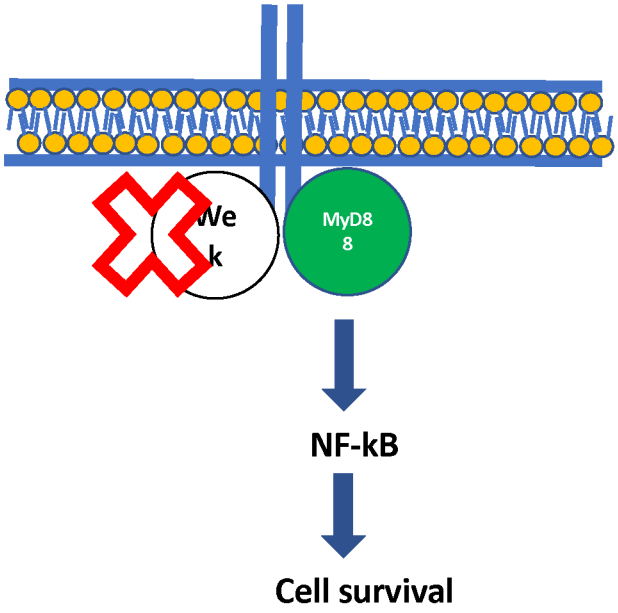


Figure 7.1 *B. bassiana* cannot induce neurodegeneration without Wek
The figure illustrates the when wek is knocked down by RNAi, Sarm is unable to inhibit MyD88 signalling. Due to unavailability of Wek, *B. bassiana* is unable to cause neurodegeneration.

A previous study had reported the upregulation of *wek* and Toll signalling upon *E. muscae* infection in the adult Drosophila flies (Elya et al., 2018). Evidence showed that Wek is downstream of Toll receptor and is pro-apoptotic in pupa CNS and non-apoptotic in the adult *Drosophila* brain (Foldi et al., 2017, Li et al., 2020). However, it's unclear if entomopathogenic fungi upregulate *wek* to induce cell death or if it is a host response to compensate for the cell death caused by fungi.

In this thesis, we found that *wek* mRNA gets upregulated in the dissected adult brain after 7 days exposure to *B. bassiana.* RNAi knockdown of *wek* did not decrease MyD88+ and Repo+ glial cell count in the adult brain, but caused a decrease in the TH+ dopaminergic neurons. Furthermore, overexpression of *wek*-HA increased the MyD88+ and TH+ dopaminergic neurons in the adult brain. These findings suggest that Wek is not pro-apoptotic in the adult brain. However, *wek* overexpression in the PAM dopaminergic neuron cluster decreased the hisYFP+ TH neurons in the PAM cluster, indicating that Wek is pro-apoptotic in this cluster. Therefore, these results support the previous findings that Wek has both apoptotic and non-apoptotic function.

Our investigation of the effects of *B. bassiana* infection on the adult brain in *wek*-RNAi knockdown showed that the MyD88+ cell count was increased, while the Repo+ glial cell count and TH+ neurons was unaffected. Without Wek, Sarm cannot inhibit MyD88 signalling which promotes cell survival and due to this *B. bassiana* cannot cause neurodegeneration (Fig 7.1). On the contrary, when *wek* was overexpressed, *B. bassiana* also increased MyD88+ cells. Moreover, upon PAM specific overexpression of *wek, B. bassiana* infection increased the hisYFP+ dopaminergic neurons in the PAM cluster. Since, Wek induces both proliferation and cell death, therefore, instead of

Figure 7.2 Wek causes both cell proliferation and cell death

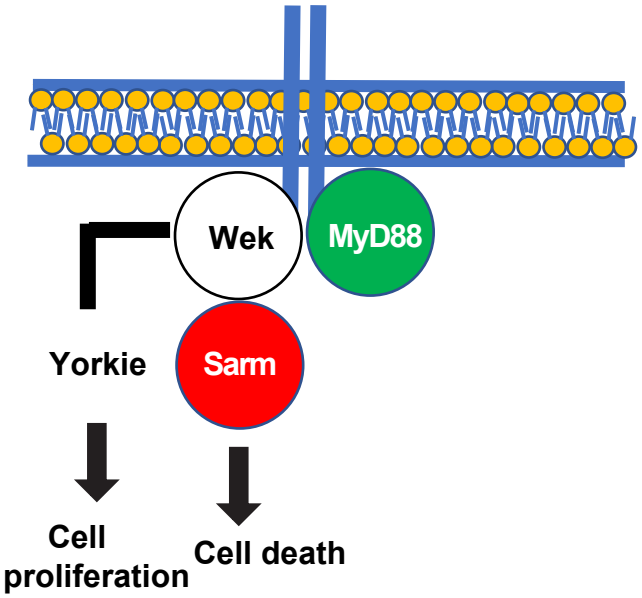


Figure 7.2 Wek causes both cell proliferation and cell death
The figure illustrates that Wek causes both cell proliferation and cell death. Therefore, it is possible that entomopathogenic fungi could regulate the cell number by modulating the expression of Wek.

Figure 7.3 *B. bassiana* induce neurodegeneration through Sarm

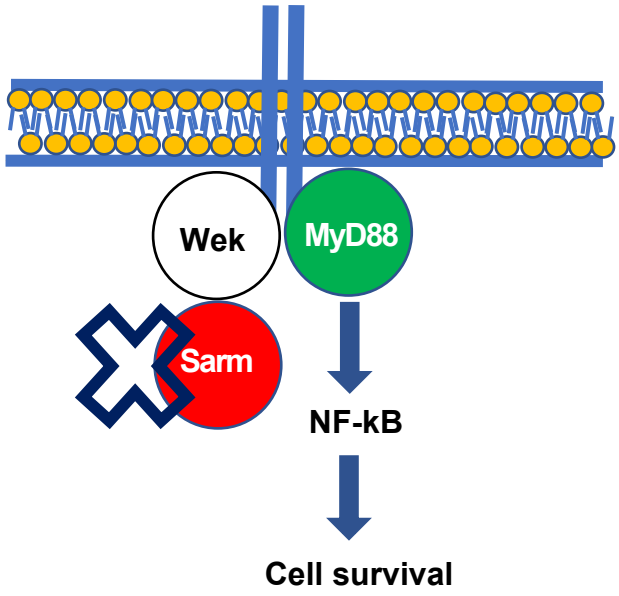


Figure 7.3 *B. bassiana* induce neurodegeneration through Sarm
The figure illustrate that when Sarm was knocked down using sarmRNAi, Sarm was unable to inhibit MyD88 signalling. Due to unavailability of Sarm, *B. bassiana* was unable to cause neurodegeneration.

causing apoptosis, Wek is activating proliferation upon infection or perhaps Wek is activating proliferation to compensate for *B. bassiana* induced cell loss caused by Wek and Sarm (Fig 7.2).

It is interesting to note that neurons in the PAL cluster, which remained unaffected by *B. bassiana* infection in the controls, underwent neuronal loss upon wek-HA overexpression. This finding suggests that *B. bassiana* causes neurodegeneration through Wek. Taken together, our Wek data indicate that *B. bassiana* may regulate cell number in the adult brain through Wek. *E. muscae* and *O. unilateralis* do not kill their host instantly. Instead, they manipulate their host and kill them once the conditions are favourable. Based on our data, *wek* could be the key gene exploited by *E. muscae* to regulate the cell number in their host, keeping them alive for a certain time, and then killing their host.

Sarm is recognised for its role in axon destruction as loss of dSarm completely prevented Wallerian degeneration (Osterloh et al., 2012). This function is also conserved in mammals, as demonstrated in mouse Sarm1$^{-/-}$ knockout mutants blocked Wallerian degeneration (Gerdts et al., 2013, Osterloh et al., 2012). Sarm triggers a localised destructive process that causes rapid degradation of nicotinamide adenine dinucleotide (NAD+) which is essential for maintaining axons (Wang et al., 2005b, Gerdts et al., 2015). dSarm induce apoptosis in the pupae VNC (Foldi et al., 2017). When Sarm binds to Wek it inhibits MyD88 signalling to cause apoptosis via JNK pathway (Foldi et al., 2017). Data from the thesis also showed that Sarm induced apoptosis, as demonstrated by an increase in MyD88+ cells in the central brain upon RNAi knockdown of *sarm*. Furthermore, both Repo+ glial cells and TH+ dopaminergic

Figure 7.4 Evolutionary arm race between *Drosophila* and *B. bassiana* for Toll signalling

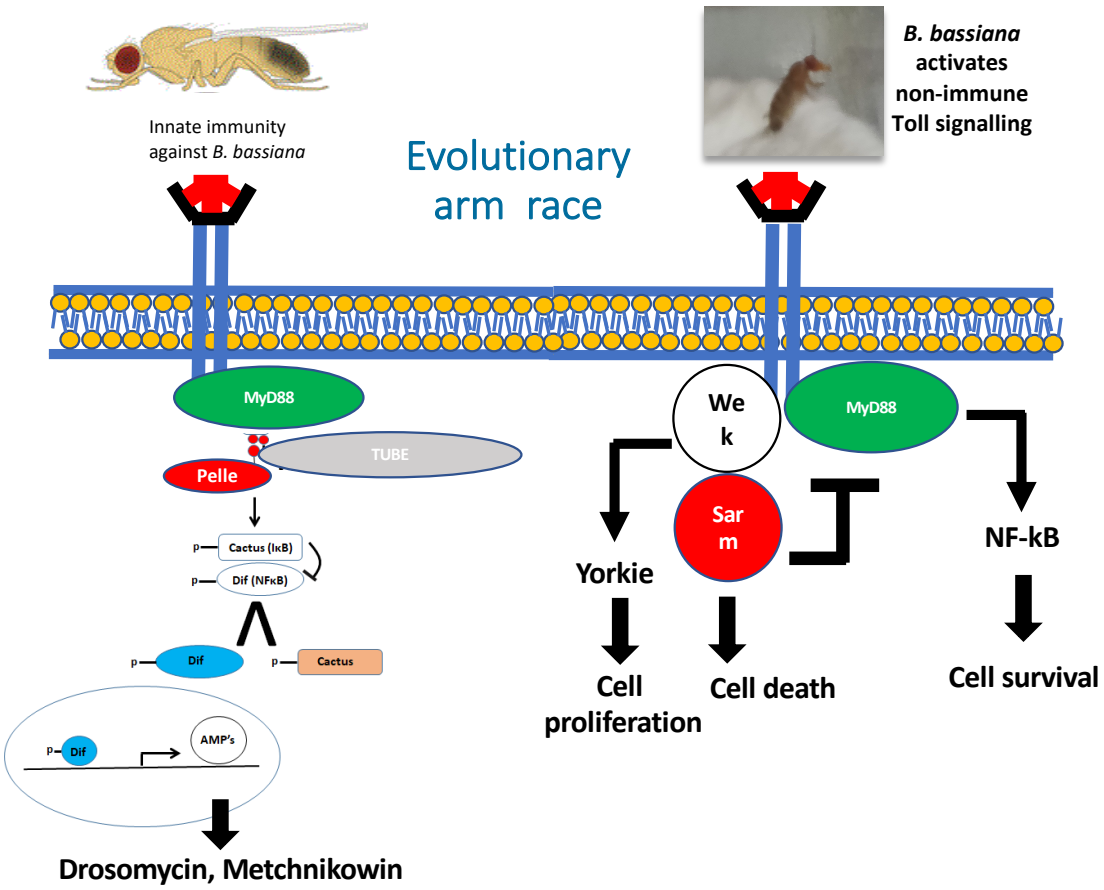


Figure 7.4 Evolutionary arm race between Drosophila and B. bassiana for Toll signalling

The figure illustrate that Drosophila activate the immune Toll pathway to protect itself from the *B. bassiana* infection, whereas the *B. bassiana* activates the non-canonical Toll signalling to cause neurodegeneration in the brain of the flies.

neurons did not exhibit significant differences compared to non-infected controls. Together these findings showed that Sarm is apoptotic.

When *sarm*-RNAi knockdown flies were infected with *B. bassiana*, the number of MyD88+ cells and TH+ neurons increased compared to infected controls. Moreover, the Repo+ glial cells did not show a significant decrease upon *B. bassiana* infection in *sarm*-RNAi knockdown flies. Together these results showed that Sarm is required for *B. bassiana* induced cell death in the adult brain.

7.6 Conclusion and implication

To conclude, this thesis investigated the effect of direct exposure to *B. bassiana* spores on the Drosophila brain and provided evidence that exposure to *B. bassiana* causes neurodegeneration in the adult brain. *B. bassiana* induces neurodegeneration through Toll signalling thus suggesting towards the existence of an evolutionary arm race between *Drosophila* and *B. bassiana* for Toll signalling. In this arm race, *Drosophila* activates the immune Toll signalling against *B. bassiana* infection to protect itself, whereas *B. bassiana* exploits the non-immune Toll signalling to induce neurodegeneration in *Drosophila* brain. In a broad perspective this thesis provides potential insights into the effect of direct exposure to fungal spore on the human health.

Appendix

Appendix 1: Statistics for survival assay

Comparison of Survival Curves		
Log-rank (Mantel-Cox) test		
Chi square	162.3	
df	1	
P value	< 0.0001	
P value summary	****	
Are the survival curves sig different?	Yes	
Gehan-Breslow-Wilcoxon test		
Chi square	122.4	
df	1	
P value	< 0.0001	
P value summary	****	
Are the survival curves sig different?	Yes	
Median survival		
OregonxContonS NON-INFECTED	44	
OregonxContonS INFECTED	8	
Ratio (and its reciprocal)	5.5	0.1818
95% CI of ratio	3.799 to 7.963	0.1256 to 0.2632
Hazard Ratio (Mantel-Haenszel)	A/B	B/A
Ratio (and its reciprocal)	0.0487	20.53
95% CI of ratio	0.03059 to 0.07754	12.90 to 32.69
Hazard Ratio (logrank)	A/B	B/A
Ratio (and its reciprocal)	0.1948	5.132
95% CI of ratio	0.03423 to 0.06930	14.43 to 29.22

Appendix 2: Statistics for climbing assay

Two-way ANOVA	Ordinary				
Alpha	0.05				
Source of Variation	**% of total variation**	**P value**	**P value summary**	**Significant?**	
Interaction	13.57	0.0048	**	Yes	
Row Factor	10.25	0.0122	*	Yes	
Column Factor	49.22	< 0.0001	****	Yes	
ANOVA table	**SS**	**DF**	**MS**	**F (DFn, DFd)**	**P value**
Interaction	0.1176	1	0.1176	F (1, 20) = 10.06	P = 0.0048
Row Factor	0.08882	1	0.08882	F (1, 20) = 7.601	P = 0.0122
Column Factor	0.4267	1	0.4267	F (1, 20) = 36.51	P < 0.0001
Residual	0.2337	20	0.01169		
Number of families	1				
Number of comparisons per family	6				
Alpha	0.05				
Tukey's multiple comparisons test	**Mean Diff.**	**95% CI of diff.**	**Significant?**	**Summary**	
3 DAYS OLD:NON-INFECTED vs. 3 DAYS OLD:INFECTED	0.1267	-0.04801 to 0.3013	No	ns	
3 DAYS OLD:NON-INFECTED vs. 7 DAYS OLD:NON-INFECTED	-0.01833	-0.1930 to 0.1563	No	ns	
3 DAYS OLD:NON-INFECTED vs. 7 DAYS OLD:INFECTED	0.3883	0.2137 to 0.5630	Yes	****	
3 DAYS OLD:INFECTED vs. 7 DAYS OLD:NON-INFECTED	-0.145	-0.3197 to 0.02968	No	ns	
3 DAYS OLD:INFECTED vs. 7 DAYS OLD:INFECTED	0.2617	0.08699 to 0.4363	Yes	**	
7 DAYS OLD:NON-INFECTED vs. 7 DAYS OLD:INFECTED	0.4067	0.2320 to 0.5813	Yes	****	

Appendix 3 Statistics for proboscis extension response assay

Chi-square			
Chi-square, df	109.9, 1		
z	10.48		
P value	< 0.0001		
P value summary	****		
One- or two-tailed	Two-tailed		
Statistically significant? (alpha<0.05)	Yes		
Data analyzed	**PER**	**No PER**	**Total**
Oregon>TrpA1	16	84	100
SarmNP0257>TrpA1	90	10	100
Total	106	94	200
Chi-square			
Chi-square, df	61.89, 1		
z	7.867		
P value	< 0.0001		
P value summary	****		
One- or two-tailed	Two-tailed		
Statistically significant? (alpha<0.05)	Yes		
Data analyzed	**PER**	**No PER**	**Total**
SarmNP7460>Trp	70	30	100
Oregon>TrpA1	15	85	100
Total	85	115	200

Appendix 4 Statistics for feeding assay

Table Analyzed	Feeding assay				
ANOVA summary					
F	47.38				
P value	< 0.0001				
P value summary	****				
Are differences among means statistically significant? (P < 0.05)	Yes				
R square	0.7636				
Brown-Forsythe test					
F (DFn, DFd)	9.900 (3, 44)				
P value	< 0.0001				
P value summary	****				
Significantly different standard deviations? (P < 0.05)	Yes				
Bartlett's test					
Bartlett's statistic (corrected)	31.67				
P value	< 0.0001				
P value summary	****				
Significantly different standard deviations? (P < 0.05)	Yes				
ANOVA table	**SS**	**DF**	**MS**	**F (DFn, DFd)**	**P value**
Treatment (between columns)	0.401	3	0.1337	F (3, 44) = 47.38	P < 0.0001
Residual (within columns)	0.1241	44	0.002821		
Total	0.5251	47			
Data summary					
Number of treatments (columns)	4				
Number of values (total)	48				
Number of families	1				
Number of comparisons per family	6				
Alpha	0.05				
Tukey's multiple comparisons test	**Mean Diff.**	**95% CI of diff.**	**Significant?**	**Summary**	
Water vs. Water+Dye	-0.09467	-0.1526 to -0.03677	Yes	***	
Water vs. Sucrose+Dye	-0.2513	-0.3092 to -0.1934	Yes	****	
Water vs. Spores+Dye	-0.1552	-0.2131 to -0.09727	Yes	****	
Water+Dye vs. Sucrose+Dye	-0.1567	-0.2146 to -0.09877	Yes	****	
Water+Dye vs. Spores+Dye	-0.0605	-0.1184 to -0.002603	Yes	*	
Sucrose+Dye vs. Spores+Dye	0.09617	0.03827 to 0.1541	Yes	***	

Appendix 5 Statistics for qRT-PCR analysis of anti-fungal peptides, *drosomycin* and *metchnikowin*

Table Analyzed	DeltaCt_Drosomycin
Column B	INFECTED
vs.	vs.
Column A	NON-INFECTED
Unpaired t test	
P value	0.0022
P value summary	**
Significantly different? (P < 0.05)	Yes
One- or two-tailed P value?	Two-tailed
t, df	t=4.097 df=10
How big is the difference?	
Mean ± SEM of column A	7.840 ± 0.3362, n=6
Mean ± SEM of column B	4.198 ± 0.8228, n=6
Difference between means	-3.642 ± 0.8888
95% confidence interval	-5.622 to -1.661
R squared	0.6267
F test to compare variances	
F,DFn, Dfd	5.990, 5, 5
P value	0.0716
P value summary	ns
Significantly different? (P < 0.05)	No
Table Analyzed	DeltaCt_Metchnikowin
Column B	INFECTED
vs.	vs.
Column A	NON-INFECTED
Unpaired t test	
P value	0.0634
P value summary	ns
Significantly different? (P < 0.05)	No
One- or two-tailed P value?	Two-tailed
t, df	t=1.994 df=16
How big is the difference?	
Mean ± SEM of column A	6.569 ± 0.5797, n=9
Mean ± SEM of column B	4.518 ± 0.8495, n=9
Difference between means	-2.051 ± 1.028
95% confidence interval	-4.231 to 0.1292
R squared	0.1991
F test to compare variances	
F,DFn, Dfd	2.148, 8, 8
P value	0.3003
P value summary	ns
Significantly different? (P < 0.05)	No

Appendix 6 Statistics for qRT-PCR analysis of non-canonical Toll signalling: *wek* and *sarm*

Table Analyzed	DeltaCT_Wek
Column B	INFECTED
vs.	vs.
Column A	NON-INFECTED
Unpaired t test	
P value	< 0.0001
P value summary	****
Significantly different? (P < 0.05)	Yes
One- or two-tailed P value?	Two-tailed
t, df	t=4.742 df=22
How big is the difference?	
Mean ± SEM of column A	6.761 ± 0.1029, n=12
Mean ± SEM of column B	6.082 ± 0.09976, n=12
Difference between means	-0.6797 ± 0.1434
95% confidence interval	-0.9770 to -0.3824
R squared	0.5054
F test to compare variances	
F,DFn, Dfd	1.065, 11, 11
P value	0.9187
P value summary	ns
Significantly different? (P < 0.05)	No
Table Analyzed	DeltaCT_Sarm
Column B	INFECTED
vs.	vs.
Column A	NON-INFECTED
Unpaired t test	
P value	0.0221
P value summary	*
Significantly different? (P < 0.05)	Yes
One- or two-tailed P value?	Two-tailed
t, df	t=2.707 df=10
How big is the difference?	
Mean ± SEM of column A	2.042 ± 0.1007, n=6
Mean ± SEM of column B	1.708 ± 0.07092, n=6
Difference between means	-0.3333 ± 0.1231
95% confidence interval	-0.6077 to -0.05894
R squared	0.4229
F test to compare variances	
F,DFn, Dfd	2.015, 5, 5
P value	0.4602
P value summary	ns
Significantly different? (P < 0.05)	No

Appendix 7 Statistics for the MyD88>HisYFP+ cell count data with UASToll-1RNAi$^{kk/100078}$ knockdown in adult brain.

Two-way ANOVA	Ordinary	Toll-1KK/100078			
Alpha	0.05				
Source of Variation	% of total variation	P value	P value summary	Significant?	
Interaction	9.522	< 0.0001	****	Yes	
Row Factor	0.02569	0.7557	ns	No	
Column Factor	81.01	< 0.0001	****	Yes	
ANOVA table	SS	DF	MS	F (DFn, DFd)	P value
Interaction	182516	1	182516	F (1, 41) = 36.36	P < 0.0001
Row Factor	492.4	1	492.4	F (1, 41) = 0.09808	P = 0.7557
Column Factor	1553000	1	1553000	F (1, 41) = 309.3	P < 0.0001
Residual	205821	41	5020		
Compare cell means regardless of rows and columns					
Number of families	1				
Number of comparisons per family	6				
Alpha	0.05				
Tukey's multiple comparisons test	Mean Diff.	95% CI of diff.	Significant?	Summary	
NON-INFECTED:Oregon vs. NON-INFECTED:Toll-1RNAi	-256.4	-337.4 to -175.3	Yes	****	
NON-INFECTED:Oregon vs. INFECTED:Oregon	126.8	56.30 to 197.3	Yes	***	
NON-INFECTED:Oregon vs. INFECTED:Toll-1RNAi	-397.1	-484.9 to -309.3	Yes	****	
NON-INFECTED:Toll-1RNAi vs. INFECTED:Oregon	383.2	303.2 to 463.2	Yes	****	
NON-INFECTED:Toll-1RNAi vs. INFECTED:Toll-1RNAi	-140.7	-236.3 to -45.09	Yes	**	
INFECTED:Oregon vs. INFECTED:Toll-1RNAi	-523.9	-610.7 to -437.0	Yes	****	

Appendix 8 Statistics for the MyD88>HisYFP+ cell count data with UASToll-1RNAiJF10491 knockdown in adult brain

Table Analyzed	MyD88His_Oregon_Toll1RNAi	Toll-1JF			
Two-way ANOVA	Ordinary				
Alpha	**0.05**				
Source of Variation	**% of total variation**	**P value**	**P value summary**	**Significant?**	
Interaction	3.464	0.0392	*	Yes	
Row Factor	18.94	< 0.0001	****	Yes	
Column Factor	45.23	< 0.0001	****	Yes	
ANOVA table	SS	DF	MS	F (DFn, DFd)	P value
Interaction	29570	1	29570	F (1, 38) = 4.564	P = 0.0392
Row Factor	161654	1	161654	F (1, 38) = 24.95	P < 0.0001
Column Factor	386132	1	386132	F (1, 38) =	P < 0.0001
Residual	246195	38	6479		
Number of families	1				
Number of comparisons per family	6				
Alpha	0.05				
Tukey's multiple comparisons test	**Mean Diff.**	**95% CI of diff.**	**Significant?**	**Summary**	**Adjusted P Value**
Non-infected:MyD88His_Oregon vs. Non-infected:MyD88His_Toll1RNAi	-140.4	-230.6 to -50.10	Yes	***	0.0009
Non-infected:MyD88His_Oregon vs. Infected:MyD88His_Oregon	179.3	89.01 to 269.5	Yes	****	< 0.0001
Non-infected:MyD88His_Oregon vs. Infected:MyD88His_Toll1RNAi	-68.5	-167.2 to 30.20	No	ns	0.2602
Non-infected:MyD88His_Toll1RNAi vs. Infected:MyD88His_Oregon	319.6	227.4 to 411.8	Yes	****	< 0.0001
Non-infected:MyD88His_Toll1RNAi vs. Infected:MyD88His_Toll1RNAi	71.86	-28.61 to 172.3	No	ns	0.2363
Infected:MyD88His_Oregon vs. Infected:MyD88His_Toll1RNAi	-247.8	-348.2 to -147.3	Yes	****	< 0.0001

Appendix 9 Statistics for MyD88>hisYFP+ cell count data in activated *Toll-1^{10b}* overexpression in adult brain.

Table Analyzed	MyD88His_Oregon_Toll1(10b)				
Two-way ANOVA	Ordinary				
Alpha	0.05				
Source of Variation	% of total variation	P value	P value summary	Significant?	
Interaction	5.518	0.0002	***	Yes	
Row Factor	1.594	0.0334	*	Yes	
Column Factor	80.74	< 0.0001	****	Yes	
ANOVA table	SS	DF	MS	F (DFn, DFd)	P value
Interaction	156080	1	156080	F (1, 42) = 16.76	P = 0.0002
Row Factor	45071	1	45071	F (1, 42) = 4.840	P = 0.0334
Column Factor	2283000	1	2283000	F (1, 42) = 245.2	P < 0.0001
Residual	391082	42	9311		
Number of families	1				
Number of comparisons per family	6				
Alpha	0.05				
Tukey's multiple comparisons test	Mean Diff.	95% CI of diff.	Significant?	Summary	
Non-infected:MyD88His_Oregon vs. Non-infected:MyD88His_Toll-1(10b)	-329.4	-434.8 to -224.0	Yes	****	
Non-infected:MyD88His_Oregon vs. Infected:MyD88His_Oregon	179.3	71.53 to 287.0	Yes	***	
Non-infected:MyD88His_Oregon vs. Infected:MyD88His_Toll-1(10b)	-383.4	-491.1 to -275.6	Yes	****	
Non-infected:MyD88His_Toll-1(10b) vs. Infected:MyD88His_Oregon	508.7	400.9 to 616.4	Yes	****	
Non-infected:MyD88His_Toll-1(10b) vs. Infected:MyD88His_Toll-1(10b)	-53.95	-161.7 to 53.80	No	ns	
Infected:MyD88His_Oregon vs. Infected:MyD88His_Toll-1(10b)	-562.6	-672.7 to -452.6	Yes	****	

Appendix 10 Statistics for adult brain size data in activated *Toll-1^{10b}* overexpression in adult brain

Table Analyzed	Overexpression of Toll1 (brain size)				
Two-way ANOVA	Ordinary				
Alpha	0.05				
Source of Variation	**% of total variation**	**P value**	**P value summary**	**Significant?**	
Interaction	27.26	< 0.0001	****	Yes	
Row Factor	6.75	0.0272	*	Yes	
Column Factor	1.239	0.3339	ns	No	
ANOVA table	SS	DF	MS	F (DFn, DFd)	P value
Interaction	1.627E+11	1	1.627E+11	F (1, 48) = 20.96	P < 0.0001
Row Factor	40300000000	1	4.03E+10	F (1, 48) = 5.191	P = 0.0272
Column Factor	7396000000	1	7.396E+09	F (1, 48) = 0.9527	P = 0.3339
Residual	3.726E+11	48	7.763E+09		
Compare cell means regardless of rows and columns					
Number of families	1				
Number of comparisons per family	6				
Alpha	0.05				
Tukey's multiple comparisons test	**Mean Diff.**	**95% CI of diff.**	**Significant?**	**Summary**	
NON-INFECTED:MyD88His_Oregon vs. NON-INFECTED:MyD88His_Toll-1(10b)	140901	56499 to 225302	Yes	***	
NON-INFECTED:MyD88His_Oregon vs. INFECTED:MyD88His_Oregon	58344	-36542 to 153231	No	ns	
NON-INFECTED:MyD88His_Oregon vs. INFECTED:MyD88His_Toll-1(10b)	-33034	-121875 to 55806	No	ns	
NON-INFECTED:MyD88His_Toll-1(10b) vs. INFECTED:MyD88His_Oregon	-82556	-184238 to 19125	No	ns	
NON-INFECTED:MyD88His_Toll-1(10b) vs. INFECTED:MyD88His_Toll-1(10b)	-173935	-269999 to -77871	Yes	****	
INFECTED:MyD88His_Oregon vs. INFECTED:MyD88His_Toll-1(10b)	-91379	-196774 to 14017	No	ns	

Appendix 11 Statistics for Repo+ cell count data in Toll-1RNAi$^{kk/100078}$ knockdown in adult brain

Table Analyzed	REPO_Tubulingal80ts:MyD88HisYFP_Toll1RNAi				
Two-way ANOVA	Ordinary				
Alpha	0.05				
Source of Variation	**% of total variation**	**P value**	**P value summary**	**Significant?**	
Interaction	9.444	0.0666	ns	No	
Row Factor	7.488	0.1003	ns	No	
Column Factor	6.362	0.1285	ns	No	
ANOVA table	**SS**	**DF**	**MS**	**F (DFn, DFd)**	**P value**
Interaction	685203	1	685203	F (1, 28) = 3.643	P = 0.0666
Row Factor	543333	1	543333	F (1, 28) = 2.888	P = 0.1003
Column Factor	461610	1	461610	F (1, 28) = 2.454	P = 0.1285
Residual	5267000	28	188112		
Number of families	1				
Number of comparisons per family	6				
Alpha	0.05				
Tukey's multiple comparisons test	**Mean Diff.**	**95% CI of diff.**	**Significant?**	**Summary**	
NON-INFECTED:Oregon vs. NON-INFECTED:Toll-1RNAi	54.27	-546.7 to 655.3	No	ns	
NON-INFECTED:Oregon vs. INFECTED:Oregon	572.5	40.24 to 1105	Yes	*	
NON-INFECTED:Oregon vs. INFECTED:Toll-1RNAi	21.11	-579.9 to 622.1	No	ns	
NON-INFECTED:Toll-1RNAi vs. INFECTED:Oregon	518.2	-105.9 to 1142	No	ns	
NON-INFECTED:Toll-1RNAi vs. INFECTED:Toll-1RNAi	-33.17	-716.9 to 650.5	No	ns	
INFECTED:Oregon vs. INFECTED:Toll-1RNAi	-551.4	-1176 to 72.73	No	ns	

Appendix 12 Statistics for TH+ dopaminergic neurons count data in PPM3 cluster upon Toll-1RNAi$^{kk/100078}$ knockdown in adult brain

Table Analyzed	PPM				
Two-way ANOVA	Ordinary				
Alpha	0.05				
Source of Variation	**% of total variation**	**P value**	**P value summary**	**Significant?**	
Interaction	4.933	0.176	ns	No	
Row Factor	25.17	0.0042	**	Yes	
Column Factor	0.08709	0.8548	ns	No	
ANOVA table	SS	DF	MS	F (DFn, DFd)	P value
Interaction	28.92	1	28.92	F (1, 26) = 1.935	P = 0.1760
Row Factor	147.5	1	147.5	F (1, 26) = 9.872	P = 0.0042
Column Factor	0.5105	1	0.5105	F (1, 26) = 0.03416	P = 0.8548
Residual	388.6	26	14.94		
Number of families	1				
Number of comparisons per family	6				
Alpha	0.05				
Tukey's multiple comparisons test	**Mean Diff.**	**95% CI of diff.**	**Significant?**	**Summary**	
NON-INFECTED:Oregon vs. NON-INFECTED:Toll-1RNAi	2.25	-3.239 to 7.739	No	ns	
NON-INFECTED:Oregon vs. INFECTED:Oregon	6.472	1.319 to 11.63	Yes	**	
NON-INFECTED:Oregon vs. INFECTED:Toll-1RNAi	4.75	-0.9774 to 10.48	No	ns	
NON-INFECTED:Toll-1RNAi vs. INFECTED:Oregon	4.222	-1.122 to 9.567	No	ns	
NON-INFECTED:Toll-1RNAi vs. INFECTED:Toll-1RNAi	2.5	-3.400 to 8.400	No	ns	
INFECTED:Oregon vs. INFECTED:Toll-1RNAi	-1.722	-7.312 to 3.867	No	ns	

Appendix 13 Statistics for TH+ dopaminergic neurons count data in PPL1 cluster upon Toll-1RNAi$^{kk/100078}$ knockdown in adult brain

Table Analyzed	PPL1				
Two-way ANOVA	Ordinary				
Alpha	0.05				
Source of Variation	**% of total variation**	**P value**	**P value summary**	**Significant?**	
Interaction	28.73	0.0024	**	Yes	
Row Factor	2.189	0.3628	ns	No	
Column Factor	0.007015	0.9586	ns	No	
ANOVA table	SS	DF	MS	F (DFn, DFd)	P value
Interaction	153.2	1	153.2	F (1, 26) = 11.26	P = 0.0024
Row Factor	11.67	1	11.67	F (1, 26) = 0.8581	P = 0.3628
Column Factor	0.0374	1	0.0374	F (1, 26) = 0.002749	P = 0.9586
Residual	353.7	26	13.6		
Number of families	1				
Number of comparisons per family	6				
Alpha	0.05				
Tukey's multiple comparisons test	**Mean Diff.**	**95% CI of diff.**	**Significant?**	**Summary**	
NON-INFECTED:Oregon vs. NON-INFECTED:Toll-1RNAi	4.643	-0.5938 to 9.880	No	ns	
NON-INFECTED:Oregon vs. INFECTED:Oregon	5.833	0.9168 to 10.75	Yes	*	
NON-INFECTED:Oregon vs. INFECTED:Toll-1RNAi	1.333	-4.131 to 6.798	No	ns	
NON-INFECTED:Toll-1RNAi vs. INFECTED:Oregon	1.19	-3.909 to 6.290	No	ns	
NON-INFECTED:Toll-1RNAi vs. INFECTED:Toll-1RNAi	-3.31	-8.939 to 2.320	No	ns	
INFECTED:Oregon vs. INFECTED:Toll-1RNAi	-4.5	-9.833 to 0.8327	No	ns	

Appendix 14 Statistics for TH+ dopaminergic neurons count data in PPL2 cluster upon Toll-1RNAi$^{kk/100078}$ knockdown in adult brain

Table Analyzed	PPL2				
Two-way ANOVA	Ordinary				
Alpha	0.05				
Source of Variation	**% of total variation**	**P value**	**P value summary**	**Significant?**	
Interaction	0.4868	0.7117	ns	No	
Row Factor	6.417	0.1865	ns	No	
Column Factor	2.323	0.4217	ns	No	
ANOVA table	SS	DF	MS	F (DFn, DFd)	P value
Interaction	1.951	1	1.951	F (1, 26) = 0.1396	P = 0.7117
Row Factor	25.72	1	25.72	F (1, 26) = 1.841	P = 0.1865
Column Factor	9.311	1	9.311	F (1, 26) = 0.6664	P = 0.4217
Residual	363.2	26	13.97		
Compare cell means regardless of rows and columns					
Number of families	1				
Number of comparisons per family	6				
Alpha	0.05				
Tukey's multiple comparisons test	**Mean Diff.**	**95% CI of diff.**	**Significant?**	**Summary**	
NON-INFECTED:Oregon vs. NON-INFECTED:Toll-1RNAi	1.643	-3.664 to 6.950	No	ns	
NON-INFECTED:Oregon vs. INFECTED:Oregon	2.389	-2.594 to 7.371	No	ns	
NON-INFECTED:Oregon vs. INFECTED:Toll-1RNAi	3	-2.538 to 8.538	No	ns	
NON-INFECTED:Toll-1RNAi vs. INFECTED:Oregon	0.746	-4.421 to 5.914	No	ns	
NON-INFECTED:Toll-1RNAi vs. INFECTED:Toll-1RNAi	1.357	-4.348 to 7.062	No	ns	
INFECTED:Oregon vs. INFECTED:Toll-1RNAi	0.6111	-4.793 to 6.015	No	ns	

Appendix 15 Statistics for the MyD88>HisYFP+ cell count data upon wekRNAi^{TRIPMHC046534} knockdown in adult brain

Two-way ANOVA	Ordinary				
Alpha	0.05				
Source of Variation	% of total variation	P value	P value summary	Significant?	
Interaction	45.24	< 0.0001	****	Yes	
Row Factor	0.7349	0.2327	ns	No	
Column Factor	29.14	< 0.0001	****	Yes	
ANOVA table	SS	DF	MS	F (DFn, DFd)	P value
Interaction	225754	1	225754	F (1, 42) = 90.29	P < 0.0001
Row Factor	3667	1	3667	F (1, 42) = 1.467	P = 0.2327
Column Factor	145401	1	145401	F (1, 42) = 58.16	P < 0.0001
Residual	105009	42	2500		
Number of families	1				
Number of comparisons per family	6				
Alpha	0.05				
Tukey's multiple comparisons test	Mean Diff.	95% CI of diff.	Significant?	Summary	
NON-INFECTED:Oregon vs. NON-INFECTED:WekRNAi	28.7	-30.58 to 87.98	No	ns	
NON-INFECTED:Oregon vs. INFECTED:Oregon	126.8	77.10 to 176.5	Yes	****	
NON-INFECTED:Oregon vs. INFECTED:WekRNAi	-135.2	-192.3 to -78.00	Yes	****	
NON-INFECTED:WekRNAi vs. INFECTED:Oregon	98.11	39.55 to 156.7	Yes	***	
NON-INFECTED:WekRNAi vs. INFECTED:WekRNAi	-163.8	-228.8 to -98.85	Yes	****	
INFECTED:Oregon vs. INFECTED:WekRNAi	-262	-318.4 to -205.6	Yes	****	

Appendix 16 Statistics for the MyD88>HisYFP+ cell count data upon wek-HA overexpression in adult brain

Two-way ANOVA	Ordinary				
Alpha	0.05				
Source of Variation	**% of total variation**	**P value**	**P value summary**	**Significant?**	
Interaction	0.8377	0.2629	ns	No	
Row Factor	4.112	0.0151	*	Yes	
Column Factor	57.07	< 0.0001	****	Yes	
ANOVA table	SS	DF	MS	F (DFn, DFd)	P value
Interaction	23730	1	23730	F (1, 58) = 1.278	P = 0.2629
Row Factor	116469	1	116469	F (1, 58) = 6.274	P = 0.0151
Column Factor	1617000	1	1617000	F (1, 58) = 87.09	P < 0.0001
Residual	1077000	58	18563		
Number of families	1				
Number of comparisons per family	6				
Alpha	0.05				
Tukey's multiple comparisons test	**Mean Diff.**	**95% CI of diff.**	**Significant?**	**Summary**	
NON-INFECTED:Oregon vs. NON-INFECTED:WekHA	-286.1	-422.3 to -149.9	Yes	****	
NON-INFECTED:Oregon vs. INFECTED:Oregon	126.8	-7.119 to 260.7	No	ns	
NON-INFECTED:Oregon vs. INFECTED:WekHA	-238.1	-365.1 to -111.2	Yes	****	
NON-INFECTED:WekHA vs. INFECTED:Oregon	412.9	279.0 to 546.8	Yes	****	
NON-INFECTED:WekHA vs. INFECTED:WekHA	47.93	-79.00 to 174.9	No	ns	
INFECTED:Oregon vs. INFECTED:WekHA	-364.9	-489.4 to -240.5	Yes	****	

Appendix 17 Statistics for the Repo+ cell count data upon wekRNAi^{TRIPMHC046534} knockdown in adult brain

Two-way ANOVA	Ordinary				
Alpha	0.05				
Source of Variation	% of total variation	P value	P value summary	Significant?	
Interaction	12.07	0.0231	*	Yes	
Row Factor	11.98	0.0236	*	Yes	
Column Factor	0.1734	0.7775	ns	No	
ANOVA table	SS	DF	MS	F (DFn, DFd)	P value
Interaction	796353	1	796353	F (1, 35) = 5.647	P = 0.0231
Row Factor	790317	1	790317	F (1, 35) = 5.605	P = 0.0236
Column Factor	11437	1	11437	F (1, 35) = 0.08111	P = 0.7775
Residual	4936000	35	141014		
Number of families	1				
Number of comparisons per family	6				
Alpha	0.05				
Tukey's multiple comparisons test	Mean Diff.	95% CI of diff.	Significant?	Summary	
NON-INFECTED:Oregon vs. NON-INFECTED:WekRNAi	321.2	-134.0 to 776.4	No	ns	
NON-INFECTED:Oregon vs. INFECTED:Oregon	572.5	117.3 to 1028	Yes	**	
NON-INFECTED:Oregon vs. INFECTED:WekRNAi	320.1	-122.4 to 762.6	No	ns	
NON-INFECTED:WekRNAi vs. INFECTED:Oregon	251.3	-226.1 to 728.7	No	ns	
NON-INFECTED:WekRNAi vs. INFECTED:WekRNAi	-1.089	-466.4 to 464.2	No	ns	
INFECTED:Oregon vs. INFECTED:WekRNAi	-252.4	-717.7 to 212.9	No	ns	

Appendix 18 Statistics for the Repo+ cell count data upon wek-HA overexpression in adult brain

Two-way ANOVA	Ordinary				
Alpha	0.05				
Source of Variation	**% of total variation**	**P value**	**P value summary**	**Significant?**	
Interaction	5.686	0.0802	ns	No	
Row Factor	15.06	0.0056	**	Yes	
Column Factor	9.12	0.0284	*	Yes	
ANOVA table	SS	DF	MS	F (DFn, DFd)	P value
Interaction	532155	1	532155	F (1, 42) = 3.214	P = 0.0802
Row Factor	1410000	1	1410000	F (1, 42) = 8.516	P = 0.0056
Column Factor	853583	1	853583	F (1, 42) = 5.155	P = 0.0284
Residual	6954000	42	165569		
Number of families	1				
Number of comparisons per family	6				
Alpha	0.05				
Tukey's multiple comparisons test	**Mean Diff.**	**95% CI of diff.**	**Significant?**	**Summary**	
NON-INFECTED:Oregon vs. NON-INFECTED:WekHA	-58.06	-512.4 to 396.3	No	ns	
NON-INFECTED:Oregon vs. INFECTED:Oregon	572.5	83.28 to 1062	Yes	*	
NON-INFECTED:Oregon vs. INFECTED:WekHA	78.7	-359.8 to 517.2	No	ns	
NON-INFECTED:WekHA vs. INFECTED:Oregon	630.6	150.6 to 1111	Yes	**	
NON-INFECTED:WekHA vs. INFECTED:WekHA	136.8	-291.4 to 565.0	No	ns	
INFECTED:Oregon vs. INFECTED:WekHA	-493.8	-958.8 to -28.76	Yes	*	

Appendix 19 Statistics for TH+ dopaminergic neurons count data in PPM3 cluster upon wekRNAi^{TRIPMHC046534} knockdown in adult brain

Two-way ANOVA	Ordinary				
Alpha	0.05				
Source of Variation	**% of total variation**	**P value**	**P value summary**	**Significant?**	
Interaction	27.37	0.0005	***	Yes	
Row Factor	1.919	0.3098	ns	No	
Column Factor	21.75	0.0016	**	Yes	
ANOVA table	SS	DF	MS	F (DFn, DFd)	P value
Interaction	213.7	1	213.7	F (1, 29) = 15.24	P = 0.0005
Row Factor	14.99	1	14.99	F (1, 29) = 1.069	P = 0.3098
Column Factor	169.8	1	169.8	F (1, 29) = 12.11	P = 0.0016
Residual	406.8	29	14.03		
Compare cell means regardless of rows and columns					
Number of families	1				
Number of comparisons per family	6				
Alpha	0.05				
Tukey's multiple comparisons test	**Mean Diff.**	**95% CI of diff.**	**Significant?**	**Summary**	
NON-INFECTED:Oregon vs. NON-INFECTED:WEKRNAi	9.679	4.398 to 14.96	Yes	***	
NON-INFECTED:Oregon vs. INFECTED:Oregon	6.472	1.514 to 11.43	Yes	**	
NON-INFECTED:Oregon vs. INFECTED:WEKRNAi	5.917	0.9585 to 10.87	Yes	*	
NON-INFECTED:WEKRNAi vs. INFECTED:Oregon	-3.206	-8.349 to 1.936	No	ns	
NON-INFECTED:WEKRNAi vs. INFECTED:WEKRNAi	-3.762	-8.904 to 1.380	No	ns	
INFECTED:Oregon vs. INFECTED:WEKRNAi	-0.5556	-5.366 to 4.255	No	ns	

Appendix 20 Statistics for TH+ dopaminergic neurons count data in PPL1 cluster upon wekRNAi^{TRIPMHC046534} knockdown in adult brain

Two-way ANOVA	Ordinary				
Alpha	0.05				
Source of Variation	% of total variation	P value	P value summary	Significant?	
Interaction	21.3	0.0038	**	Yes	
Row Factor	7.657	0.0695	ns	No	
Column Factor	9.415	0.0455	*	Yes	
ANOVA table	SS	DF	MS	F (DFn, DFd)	P value
Interaction	108.5	1	108.5	F (1, 29) = 9.880	P = 0.0038
Row Factor	39.02	1	39.02	F (1, 29) = 3.552	P = 0.0695
Column Factor	47.98	1	47.98	F (1, 29) = 4.367	P = 0.0455
Residual	318.6	29	10.99		
Number of families	1				
Number of comparisons per family	6				
Alpha	0.05				
Tukey's multiple comparisons test	Mean Diff.	95% CI of diff.	Significant?	Summary	
NON-INFECTED:Oregon vs. NON-INFECTED:WEKRNAi	6.071	1.398 to 10.75	Yes	**	
NON-INFECTED:Oregon vs. INFECTED:Oregon	5.833	1.445 to 10.22	Yes	**	
NON-INFECTED:Oregon vs. INFECTED:WEKRNAi	4.611	0.2231 to 8.999	Yes	*	
NON-INFECTED:WEKRNAi vs. INFECTED:Oregon	-0.2381	-4.789 to 4.313	No	ns	
NON-INFECTED:WEKRNAi vs. INFECTED:WEKRNAi	-1.46	-6.011 to 3.091	No	ns	
INFECTED:Oregon vs. INFECTED:WEKRNAi	-1.222	-5.479 to 3.035	No	ns	

Appendix 21 Statistics for TH+ dopaminergic neurons count data in PPL2 cluster upon wekRNAi^{TRIPMHC046534} knockdown in adult brain

Two-way ANOVA	Ordinary				
Alpha	0.05				
Source of Variation	% of total variation	P value	P value summary	Significant?	
Interaction	14.26	0.0217	*	Yes	
Row Factor	0.08081	0.8564	ns	No	
Column Factor	18.18	0.0104	*	Yes	
ANOVA table	SS	DF	MS	F (DFn, DFd)	P value
Interaction	54.47	1	54.47	F (1, 29) = 5.884	P = 0.0217
Row Factor	0.3086	1	0.3086	F (1, 29) = 0.03334	P = 0.8564
Column Factor	69.43	1	69.43	F (1, 29) = 7.501	P = 0.0104
Residual	268.4	29	9.257		
Number of families	1				
Number of comparisons per family	6				
Alpha	0.05				
Tukey's multiple comparisons test	Mean Diff.	95% CI of diff.	Significant?	Summary	
NON-INFECTED:Oregon vs. NON-INFECTED:WEKRNAi	5.5	1.210 to 9.790	Yes	**	
NON-INFECTED:Oregon vs. INFECTED:Oregon	2.389	-1.639 to 6.417	No	ns	
NON-INFECTED:Oregon vs. INFECTED:WEKRNAi	2.722	-1.306 to 6.750	No	ns	
NON-INFECTED:WEKRNAi vs. INFECTED:Oregon	-3.111	-7.289 to 1.066	No	ns	
NON-INFECTED:WEKRNAi vs. INFECTED:WEKRNAi	-2.778	-6.955 to 1.400	No	ns	
INFECTED:Oregon vs. INFECTED:WEKRNAi	0.3333	-3.574 to 4.241	No	ns	

Appendix 22 Statistics for TH+ dopaminergic neurons count data in PPM3 cluster upon wek-HA overexpression in adult brain

Two-way ANOVA	Ordinary				
Alpha	0.05				
Source of Variation	**% of total variation**	**P value**	**P value summary**	**Significant?**	
Interaction	4.253	0.0446	*	Yes	
Row Factor	70.71	< 0.0001	****	Yes	
Column Factor	0.005466	0.9404	ns	No	
ANOVA table	SS	DF	MS	F (DFn, DFd)	P value
Interaction	35.11	1	35.11	F (1, 28) = 4.423	P = 0.0446
Row Factor	583.7	1	583.7	F (1, 28) = 73.53	P < 0.0001
Column Factor	0.04512	1	0.04512	F (1, 28) = 0.005684	P = 0.9404
Residual	222.3	28	7.938		
Number of families	1				
Number of comparisons per family	6				
Alpha	0.05				
Tukey's multiple comparisons test	**Mean Diff.**	**95% CI of diff.**	**Significant?**	**Summary**	
NON-INFECTED:Oregon vs. NON-INFECTED:Wek-HA	-2.179	-6.160 to 1.803	No	ns	
NON-INFECTED:Oregon vs. INFECTED:Oregon	6.472	2.734 to 10.21	Yes	***	
NON-INFECTED:Oregon vs. INFECTED:Wek-HA	8.5	4.654 to 12.35	Yes	****	
NON-INFECTED:Wek-HA vs. INFECTED:Oregon	8.651	4.774 to 12.53	Yes	****	
NON-INFECTED:Wek-HA vs. INFECTED:Wek-HA	10.68	6.697 to 14.66	Yes	****	
INFECTED:Oregon vs. INFECTED:Wek-HA	2.028	-1.710 to 5.766	No	ns	

Appendix 23 Statistics for TH+ dopaminergic neurons count data in PPL1 cluster upon wek-HA overexpression in adult brain

Two-way ANOVA	Ordinary				
Alpha	0.05				
Source of Variation	% of total variation	P value	P value summary	Significant?	
Interaction	0.374	0.6271	ns	No	
Row Factor	52.33	< 0.0001	****	Yes	
Column Factor	3.96	0.1212	ns	No	
ANOVA table	SS	DF	MS	F (DFn, DFd)	P value
Interaction	2.303	1	2.303	F (1, 28) = 0.2413	P = 0.6271
Row Factor	322.3	1	322.3	F (1, 28) = 33.76	P < 0.0001
Column Factor	24.39	1	24.39	F (1, 28) = 2.555	P = 0.1212
Residual	267.3	28	9.547		
Number of families	1				
Number of comparisons per family	6				
Alpha	0.05				
Tukey's multiple comparisons test	Mean Diff.	95% CI of diff.	Significant?	Summary	
NON-INFECTED:Oregon vs. NON-INFECTED:Wek-HA	1.214	-3.152 to 5.580	No	ns	
NON-INFECTED:Oregon vs. INFECTED:Oregon	5.833	1.734 to 9.932	Yes	**	
NON-INFECTED:Oregon vs. INFECTED:Wek-HA	8.125	3.907 to 12.34	Yes	****	
NON-INFECTED:Wek-HA vs. INFECTED:Oregon	4.619	0.3677 to 8.870	Yes	*	
NON-INFECTED:Wek-HA vs. INFECTED:Wek-HA	6.911	2.545 to 11.28	Yes	***	
INFECTED:Oregon vs. INFECTED:Wek-HA	2.292	-1.807 to 6.391	No	ns	

Appendix 24 Statistics for TH+ dopaminergic neurons count data in PPL2 cluster upon wek-HA overexpression in adult brain

Two-way ANOVA	Ordinary				
Alpha	0.05				
Source of Variation	**% of total variation**	**P value**	**P value summary**	**Significant?**	
Interaction	3.336	0.2233	ns	No	
Row Factor	24.75	0.0021	**	Yes	
Column Factor	11.74	0.0268	*	Yes	
ANOVA table	SS	DF	MS	F (DFn, DFd)	P value
Interaction	15.25	1	15.25	F (1, 28) = 1.551	P = 0.2233
Row Factor	113.1	1	113.1	F (1, 28) = 11.51	P = 0.0021
Column Factor	53.66	1	53.66	F (1, 28) = 5.460	P = 0.0268
Residual	275.2	28	9.828		
Number of families	1				
Number of comparisons per family	6				
Alpha	0.05				
Tukey's multiple comparisons test	**Mean Diff.**	**95% CI of diff.**	**Significant?**	**Summary**	
NON-INFECTED:Oregon vs. NON-INFECTED:Wek-HA	1.214	-3.216 to 5.644	No	ns	
NON-INFECTED:Oregon vs. INFECTED:Oregon	2.389	-1.770 to 6.548	No	ns	
NON-INFECTED:Oregon vs. INFECTED:Wek-HA	6.375	2.095 to 10.65	Yes	**	
NON-INFECTED:Wek-HA vs. INFECTED:Oregon	1.175	-3.139 to 5.488	No	ns	
NON-INFECTED:Wek-HA vs. INFECTED:Wek-HA	5.161	0.7307 to 9.591	Yes	*	
INFECTED:Oregon vs. INFECTED:Wek-HA	3.986	-0.1731 to 8.145	No	ns	

Appendix 25 Statistics for TH+ dopaminergic neurons count data in PAL cluster upon wek-HA overexpression in adult brain

Table Analyzed	PAL				
Two-way ANOVA	Ordinary				
Alpha	0.05				
Source of Variation	% of total variation	P value	P value summary	Significant?	
Interaction	7.008	0.1079	ns	No	
Row Factor	18.97	0.0108	*	Yes	
Column Factor	3.519	0.2491	ns	No	
ANOVA table	SS	DF	MS	F (DFn, DFd)	P value
Interaction	5.037	1	5.037	F (1, 28) = 2.759	P = 0.1079
Row Factor	13.63	1	13.63	F (1, 28) = 7.466	P = 0.0108
Column Factor	2.529	1	2.529	F (1, 28) = 1.385	P = 0.2491
Residual	51.12	28	1.826		
Number of families	1				
Number of comparisons per family	6				
Alpha	0.05				
Tukey's multiple comparisons test	Mean Diff.	95% CI of diff.	Significant?	Summary	
NON-INFECTED:Oregon vs. NON-INFECTED:WEK-HA	-0.2321	-2.141 to 1.677	No	ns	
NON-INFECTED:Oregon vs. INFECTED:Oregon	0.5139	-1.279 to 2.307	No	ns	
NON-INFECTED:Oregon vs. INFECTED:WEK-HA	1.875	0.03040 to 3.720	Yes	*	
NON-INFECTED:WEK-HA vs. INFECTED:Oregon	0.746	-1.113 to 2.605	No	ns	
NON-INFECTED:WEK-HA vs. INFECTED:WEK-HA	2.107	0.1978 to 4.016	Yes	*	
INFECTED:Oregon vs. INFECTED:WEK-HA	1.361	-0.4315 to 3.154	No	ns	

Appendix 26 Statistics for TH>HisYFP+ dopaminergic neurons count in PAM cluster upon wek-HA overexpression

Two-way ANOVA	Ordinary				
Alpha	0.05				
Source of Variation	**% of total variation**	**P value**	**P value summary**	**Significant?**	
Interaction	25.95	< 0.0001	****	Yes	
Row Factor	0.3412	0.6189	ns	No	
Column Factor	15.51	0.0015	**	Yes	
ANOVA table	**SS**	**DF**	**MS**	**F (DFn, DFd)**	**P value**
Interaction	10540	1	10540	F (1, 46) = 19.07	P < 0.0001
Row Factor	138.6	1	138.6	F (1, 46) = 0.2508	P = 0.6189
Column Factor	6299	1	6299	F (1, 46) = 11.40	P = 0.0015
Residual	25426	46	552.7		
Number of families	1				
Number of comparisons per family	6				
Alpha	0.05				
Tukey's multiple comparisons test	**Mean Diff.**	**95% CI of diff.**	**Significant?**	**Summary**	
NON-INFECTED:TH;R58EO2>HisYFP vs. NON-INFECTED:HisYFP;WekHA	52.9	25.72 to 80.07	Yes	****	
NON-INFECTED:TH;R58EO2>HisYFP vs. INFECTED:TH;R58EO2>HisYFP	33.25	7.422 to 59.09	Yes	**	
NON-INFECTED:TH;R58EO2>HisYFP vs. INFECTED:HisYFP;WekHA	26.48	-1.682 to 54.65	No	ns	
NON-INFECTED:HisYFP;WekHA vs. INFECTED:TH;R58EO2>HisYFP	-19.64	-42.73 to 3.446	No	ns	
NON-INFECTED:HisYFP;WekHA vs. INFECTED:HisYFP;WekHA	-26.41	-52.09 to -0.7396	Yes	*	
INFECTED:TH;R58EO2>HisYFP vs. INFECTED:HisYFP;WekHA	-6.77	-31.02 to 17.48	No	ns	

Appendix 27 Statistics for the MyD88>HisYFP+ cell count data upon sarmRNAi^{TRIPJF01681} knockdown in adult brain

Two-way ANOVA	Ordinary				
Alpha	0.05				
Source of Variation	% of total variation	P value	P value summary	Significant?	
Interaction	20.16	< 0.0001	****	Yes	
Row Factor	5.892	0.0077	**	Yes	
Column Factor	32.17	< 0.0001	****	Yes	
ANOVA table	SS	DF	MS	F (DFn, DFd)	P value
Interaction	72411	1	72411	F (1, 42) = 26.82	P < 0.0001
Row Factor	21167	1	21167	F (1, 42) = 7.839	P = 0.0077
Column Factor	115579	1	115579	F (1, 42) = 42.81	P < 0.0001
Residual	113404	42	2700		
Number of families	1				
Number of comparisons per family	6				
Alpha	0.05				
Tukey's multiple comparisons test	Mean Diff.	95% CI of diff.	Significant?	Summary	
NON-INFECTED:Oregon vs. NON-INFECTED:SarmRNAi	-21.68	-83.28 to 39.93	No	ns	
NON-INFECTED:Oregon vs. INFECTED:Oregon	126.8	75.15 to 178.5	Yes	****	
NON-INFECTED:Oregon vs. INFECTED:SarmRNAi	-59.48	-118.9 to -0.09811	Yes	*	
NON-INFECTED:SarmRNAi vs. INFECTED:Oregon	148.5	87.63 to 209.3	Yes	****	
NON-INFECTED:SarmRNAi vs. INFECTED:SarmRNAi	-37.81	-105.3 to 29.73	No	ns	
INFECTED:Oregon vs. INFECTED:SarmRNAi	-186.3	-244.9 to -127.7	Yes	****	

Appendix 28 Statistics for the Repo+ cell count data upon sarmRNAi^{TRIPJF01681} knockdown in adult brain

Two-way ANOVA	Ordinary				
Alpha	0.05				
Source of Variation	% of total variation	P value	P value summary	Significant?	
Interaction	11.12	0.0295	*	Yes	
Row Factor	12.73	0.0205	*	Yes	
Column Factor	1.813	0.3649	ns	No	
ANOVA table	SS	DF	MS	F (DFn, DFd)	P value
Interaction	687921	1	687921	F (1, 33) = 5.179	P = 0.0295
Row Factor	787193	1	787193	F (1, 33) = 5.927	P = 0.0205
Column Factor	112119	1	112119	F (1, 33) = 0.8441	P = 0.3649
Residual	4383000	33	132825		
Number of families	1				
Number of comparisons per family	6				
Alpha	0.05				
Tukey's multiple comparisons test	Mean Diff.	95% CI of diff.	Significant?	Summary	
NON-INFECTED:Oregon vs. NON-INFECTED:SarmRNAi	388.3	-42.46 to 819.0	No	ns	
NON-INFECTED:Oregon vs. INFECTED:Oregon	572.5	129.4 to 1016	Yes	**	
NON-INFECTED:Oregon vs. INFECTED:SarmRNAi	407.6	-69.08 to 884.2	No	ns	
NON-INFECTED:SarmRNAi vs. INFECTED:Oregon	184.2	-268.7 to 637.2	No	ns	
NON-INFECTED:SarmRNAi vs. INFECTED:SarmRNAi	19.29	-466.5 to 505.1	No	ns	
INFECTED:Oregon vs. INFECTED:SarmRNAi	-164.9	-661.7 to 331.9	No	ns	

Appendix 29 Statistics for TH+ dopaminergic neurons count data in PPM3 cluster upon sarmRNAi^{TRIPJF01681} knockdown in the adult brain

Two-way ANOVA	Ordinary				
Alpha	0.05				
Source of Variation	% of total variation	P value	P value summary	Significant?	
Interaction	11.48	0.0071	**	Yes	
Row Factor	29.52	< 0.0001	****	Yes	
Column Factor	11.48	0.0071	**	Yes	
ANOVA table	SS	DF	MS	F (DFn, DFd)	P value
Interaction	55.63	1	55.63	F (1, 33) = 8.239	P = 0.0071
Row Factor	143	1	143	F (1, 33) = 21.18	P < 0.0001
Column Factor	55.63	1	55.63	F (1, 33) = 8.239	P = 0.0071
Residual	222.8	33	6.752		
Number of families	1				
Number of comparisons per family	6				
Alpha	0.05				
Tukey's multiple comparisons test	Mean Diff.	95% CI of diff.	Significant?	Summary	
NON-INFECTED:Oregon vs. NON-INFECTED:SarmRNAi	0	-3.208 to 3.208	No	ns	
NON-INFECTED:Oregon vs. INFECTED:Oregon	6.472	3.057 to 9.887	Yes	****	
NON-INFECTED:Oregon vs. INFECTED:SarmRNAi	1.5	-2.014 to 5.014	No	ns	
NON-INFECTED:SarmRNAi vs. INFECTED:Oregon	6.472	3.373 to 9.572	Yes	****	
NON-INFECTED:SarmRNAi vs. INFECTED:SarmRNAi	1.5	-1.708 to 4.708	No	ns	
INFECTED:Oregon vs. INFECTED:SarmRNAi	-4.972	-8.387 to -1.557	Yes	**	

Appendix 30 Statistics for exposure to *B. bassiana* causes reduction in the TH neurons in different dopaminergic cluster

Two-way RM ANOVA	Matching: Stacked				
Alpha	0.05				
Source of Variation	% of total variation	P value	P value summary	Significant ?	
Interaction	1.223	< 0.0001	****	Yes	
Time	1.295	< 0.0001	****	Yes	
Column Factor	90.78	< 0.0001	****	Yes	
Subjects (matching)	3.823	0.0935	ns	No	
ANOVA table	SS	DF	MS	F (DFn, DFd)	P value
Interaction	99.23	7	14.18	F (7, 88) = 5.337	P < 0.0001
Time	105	1	105	F (1, 88) = 39.54	P < 0.0001
Column Factor	7364	7	1052	F (7, 88) = 298.5	P < 0.0001
Subjects (matching)	310.1	88	3.524	F (88, 88) = 1.327	P = 0.0935
Residual	233.8	88	2.656		
Number of families	1				
Number of comparisons per family	8				
Alpha	0.05				
Sidak's multiple comparisons test	Mean Diff.	95% CI of diff.	Significant ?	Summary	Adjusted P Value
NON-INFECTED - INFECTED					
PAL	1.167	-0.6923 to 3.026	No	ns	0.5001
PPL1	3.75	1.891 to 5.609	Yes	****	< 0.0001
PPM1/2	3.083	1.224 to 4.942	Yes	****	< 0.0001
SP1	-0.08333	-1.942 to 1.776	No	ns	> 0.9999
T1	-0.08333	-1.942 to 1.776	No	ns	> 0.9999
PPL2	2.083	0.2244 to 3.942	Yes	*	0.0188
PPM3	2.167	0.3077 to 4.026	Yes	*	0.0128
SVP+VUM	-0.25	-2.109 to 1.609	No	ns	> 0.9999

References

1. ADHIKARI, A., XU, M. & CHEN, Z. 2007. Ubiquitin-mediated activation of TAK1 and IKK. *Oncogene,* 26**,** 3214-3226.
2. AKIRA, S. & TAKEDA, K. 2004. Toll-like receptor signalling. *Nature reviews immunology,* 4**,** 499-511.
3. AKIRA, S., UEMATSU, S. & TAKEUCHI, O. 2006. Pathogen recognition and innate immunity. *Cell,* 124**,** 783-801.
4. ALEKSEYENKO, O. V., CHAN, Y.-B., LI, R. & KRAVITZ, E. A. 2013. Single dopaminergic neurons that modulate aggression in Drosophila. *Proceedings of the National Academy of Sciences,* 110**,** 6151-6156.
5. ANDERSEN, S. B., GERRITSMA, S., YUSAH, K. M., MAYNTZ, D., HYWEL-JONES, N. L., BILLEN, J., BOOMSMA, J. J. & HUGHES, D. P. Natural History Note.
6. ANDERSON, K. V. & NÜSSLEIN-VOLHARD, C. 1986. Dorsal-group genes of Drosophila. *Gametogenesis and the early embryo,* 43**,** 177-194.
7. APITZ, H. & SALECKER, I. 2015. A region-specific neurogenesis mode requires migratory progenitors in the Drosophila visual system. *Nature neuroscience,* 18**,** 46.
8. ASHBURNER, M., MISRA, S., ROOTE, J., LEWIS, S., BLAZEJ, R., DAVIS, T., DOYLE, C., GALLE, R., GEORGE, R. & HARRIS, N. 1999. An exploration of the sequence of a 2.9-Mb region of the genome of Drosophila melanogaster: the Adh region. *Genetics,* 153**,** 179-219.
9. ÅSLING, B., DUSHAY, M. S. & HULTMARK, D. 1995. Identification of early genes in the Drosophila immune response by PCR-based differential display: the Attacin A gene and the evolution of attacin-like proteins. *Insect biochemistry and molecular biology,* 25**,** 511-518.
10. ASO, Y., HERB, A., OGUETA, M., SIWANOWICZ, I., TEMPLIER, T., FRIEDRICH, A. B., ITO, K., SCHOLZ, H. & TANIMOTO, H. 2012. Three dopamine pathways induce aversive odor memories with different stability. *PLoS genetics,* 8**,** e1002768.
11. BAI, Y., GAO, X., WANG, H., YE, L., ZHANG, X., HUANG, W., LONG, X., YANG, K., LI, G. & LUO, J. 2022. Comparative mitogenome analysis reveals mitochondrial genome characteristics in eight strains of Beauveria. *PeerJ,* 10**,** e14067.
12. BARELLI, L., MORERIA, C. C., SEMENTCHOUKOVA, I., BEHIE, S. W., BIDOCHKA, M. J. & ZELISKO, P. M. 2017. Carbon translocation from a plant to an insect-pathogenic endophytic fungus.
13. BEHIE, S., ZELISKO, P. & BIDOCHKA, M. 2012. Endophytic insect-parasitic fungi translocate nitrogen directly from insects to plants. *Science,* 336**,** 1576-1577.
14. BEHIE, S. W., JONES, S. J. & BIDOCHKA, M. J. 2015. Plant tissue localization of the endophytic insect pathogenic fungi Metarhizium and Beauveria. *Fungal Ecology,* 13**,** 112-119.
15. BELLEN, H. J., LEVIS, R. W., LIAO, G., HE, Y., CARLSON, J. W., TSANG, G., EVANS-HOLM, M., HIESINGER, P. R., SCHULZE, K. L. & RUBIN, G. M. 2004. The BDGP gene disruption project: single transposon insertions associated with 40% of Drosophila genes. *Genetics,* 167**,** 761-781.
16. BELLEN, H. J., TONG, C. & TSUDA, H. 2010. 100 years of Drosophila research and its impact on vertebrate neuroscience: a history lesson for the future. *Nature Reviews Neuroscience,* 11**,** 514-522.
17. BELLOCCHIO, S., MONTAGNOLI, C., BOZZA, S., GAZIANO, R., ROSSI, G., MAMBULA, S. S., VECCHI, A., MANTOVANI, A., LEVITZ, S. M. & ROMANI, L. 2004. The contribution of the Toll-like/IL-1 receptor superfamily to innate and adaptive immunity to fungal pathogens in vivo. *The Journal of Immunology,* 172**,** 3059-3069.
18. BELVIN, M. & ANDERSON, K. 1996a. A conserved signalling Spn27A, and Df (2L) 6374 [6, 16]. pathway: the Toll-dorsal pathway. *Annu. Rev. Cell Dev. Biol,* 12**,** 393-416.

19. BELVIN, M. P. & ANDERSON, K. V. 1996b. A conserved signaling pathway: the Drosophila toll-dorsal pathway. *Annual review of cell and developmental biology,* 12**,** 393-416.
20. BERDOY, M., WEBSTER, J. P. & MACDONALD, D. W. 2000. Fatal attraction in rats infected with Toxoplasma gondii. *Proceedings of the Royal Society of London. Series B: Biological Sciences,* 267**,** 1591-1594.
21. BIER, E. 2005. Drosophila, the golden bug, emerges as a tool for human genetics. *Nature Reviews Genetics,* 6**,** 9-23.
22. BILAK, H., TAUSZIG-DELAMASURE, S. & IMLER, J.-L. 2003. Toll and Toll-like receptors in Drosophila. *Biochemical Society Transactions,* 31**,** 648-651.
23. BISCHOFF, V., VIGNAL, C., BONECA, I. G., MICHEL, T., HOFFMANN, J. A. & ROYET, J. 2004. Function of the drosophila pattern-recognition receptor PGRP-SD in the detection of Gram-positive bacteria. *Nature immunology,* 5**,** 1175-1180.
24. BLUM, I. D., KELEŞ, M. F., BAZ, E.-S., HAN, E., PARK, K., LUU, S., ISSA, H., BROWN, M., HO, M. C. & TABUCHI, M. 2021. Astroglial calcium signaling encodes sleep need in Drosophila. *Current Biology,* 31**,** 150-162. e7.
25. BOOMSMA, J. J., JENSEN, A. B., MEYLING, N. V. & EILENBERG, J. 2014. Evolutionary interaction networks of insect pathogenic fungi. *Annual Review of Entomology,* 59**,** 467-485.
26. BOOTHROYD, C. E., WIJNEN, H., NAEF, F., SAEZ, L. & YOUNG, M. W. 2007. Integration of light and temperature in the regulation of circadian gene expression in Drosophila. *PLoS genetics,* 3**,** e54.
27. BOUCIAS, D., PENDLAND, J. & LATGE, J. 1988. Nonspecific factors involved in attachment of entomopathogenic deuteromycetes to host insect cuticle. *Appl. Environ. Microbiol.,* 54**,** 1795-1805.
28. BRAND, A. H. & PERRIMON, N. 1993. Targeted gene expression as a means of altering cell fates and generating dominant phenotypes. *development,* 118**,** 401-415.
29. BRANINE, M., BAZZICALUPO, A. & BRANCO, S. 2019. Biology and applications of endophytic insect-pathogenic fungi. *PLoS Pathogens,* 15**,** e1007831.
30. BRENNAN, C. A. & ANDERSON, K. V. 2004. Drosophila: the genetics of innate immune recognition and response. *Annu. Rev. Immunol.,* 22**,** 457-483.
31. BROGDEN, K. A. 2005. Antimicrobial peptides: pore formers or metabolic inhibitors in bacteria? *Nature reviews microbiology,* 3**,** 238-250.
32. BULET, P., URGE, L., OHRESSER, S., HETRU, C. & OTVOS JR, L. 1996. Enlarged scale chemical synthesis and range of activity of drosocin, an O-glycosylated antibacterial peptide of Drosophila. *European journal of biochemistry,* 238**,** 64-69.
33. BUTT, T., BECKETT, A. & WILDING, N. 1981. Protoplasts in the in vivo life cycle of Erynia neoaphidis. *Microbiology,* 127**,** 417-421.
34. BUTT, T. M., HAJEK, A. E. & HUMBER, R. A. 1996. Gypsy moth immune defenses in response to hyphal bodies and natural protoplasts of entomophthoralean fungi. *Journal of invertebrate pathology,* 68**,** 278-285.
35. BUWITT-BECKMANN, U., HEINE, H., WIESMÜLLER, K.-H., JUNG, G. N., BROCK, R., AKIRA, S. & ULMER, A. J. 2006. TLR1-and TLR6-independent recognition of bacterial lipopeptides. *Journal of Biological Chemistry,* 281**,** 9049-9057.
36. CAO, Y., CHTARBANOVA, S., PETERSEN, A. J. & GANETZKY, B. 2013. Dnr1 mutations cause neurodegeneration in Drosophila by activating the innate immune response in the brain. *Proceedings of the National Academy of Sciences,* 110**,** E1752-E1760.
37. CARPENTIER, P. A., D'ANNE, S. D. & MILLER, S. D. 2008. Glial toll-like receptor signaling in central nervous system infection and autoimmunity. *Brain, behavior, and immunity,* 22**,** 140-147.

38. CHAMBERS, M. C., JACOBSON, E., KHALIL, S. & LAZZARO, B. P. 2014. Thorax injury lowers resistance to infection in Drosophila melanogaster. *Infection and immunity,* 82**,** 4380-4389.
39. CHASAN, R., JIN, Y. & ANDERSON, K. 1992. Activation of the easter zymogen is regulated by five other genes to define dorsal-ventral polarity in the Drosophila embryo. *Development,* 115**,** 607-616.
40. CHEHREHASA, F., MEEDENIYA, A. C., DWYER, P., ABRAHAMSEN, G. & MACKAY-SIM, A. 2009. EdU, a new thymidine analogue for labelling proliferating cells in the nervous system. *Journal of neuroscience methods,* 177**,** 122-130.
41. CHEN, L.-Y., WANG, J.-C., HYVERT, Y., LIN, H.-P., PERRIMON, N., IMLER, J.-L. & HSU, J.-C. 2006. Weckle is a zinc finger adaptor of the toll pathway in dorsoventral patterning of the Drosophila embryo. *Current biology,* 16**,** 1183-1193.
42. CLAESON, A.-S., LEVIN, J.-O., BLOMQUIST, G. & SUNESSON, A.-L. 2002. Volatile metabolites from microorganisms grown on humid building materials and synthetic media. *Journal of Environmental Monitoring,* 4**,** 667-672.
43. CLARIDGE-CHANG, A., ROORDA, R. D., VRONTOU, E., SJULSON, L., LI, H., HIRSH, J. & MIESENBÖCK, G. 2009. Writing memories with light-addressable reinforcement circuitry. *Cell,* 139**,** 405-415.
44. CLARKSON, J. M. & CHARNLEY, A. K. 1996. New insights into the mechanisms of fungal pathogenesis in insects. *Trends in microbiology,* 4**,** 197-203.
45. CLEMMONS, A. W., LINDSAY, S. A. & WASSERMAN, S. A. 2015. An effector peptide family required for Drosophila Toll-mediated immunity. *PLoS Pathogens,* 11**,** e1004876.
46. COCIANCICH, S., GHAZI, A., HETRU, C., HOFFMANN, J. & LETELLIER, L. 1993. Insect defensin, an inducible antibacterial peptide, forms voltage-dependent channels in Micrococcus luteus. *Journal of Biological Chemistry,* 268**,** 19239-19245.
47. COLEMAN, M. P. & FREEMAN, M. R. 2010. Wallerian degeneration, wlds, and nmnat. *Annual review of neuroscience,* 33**,** 245.
48. CONFORTI, L., GILLEY, J. & COLEMAN, M. P. 2014. Wallerian degeneration: an emerging axon death pathway linking injury and disease. *Nature Reviews Neuroscience,* 15**,** 394-409.
49. CUDIC, M., BULET, P., HOFFMANN, R., CRAIK, D. J. & OTVOS JR, L. 1999. Chemical synthesis, antibacterial activity and conformation of diptericin, an 82-mer peptide originally isolated from insects. *European journal of biochemistry,* 266**,** 549-558.
50. DAUBNER, S. C., LE, T. & WANG, S. 2011. Tyrosine hydroxylase and regulation of dopamine synthesis. *Archives of biochemistry and biophysics,* 508**,** 1-12.
51. DAWKINS, R. 1982. *The extended phenotype*, Oxford University Press Oxford.
52. DE BEKKER, C. 2019. Ophiocordyceps–ant interactions as an integrative model to understand the molecular basis of parasitic behavioral manipulation. *Current opinion in insect science,* 33**,** 19-24.
53. DE BEKKER, C. & DAS, B. 2022. Hijacking time: How Ophiocordyceps fungi could be using ant host clocks to manipulate behavior. *Parasite Immunology,* 44**,** e12909.
54. DE BEKKER, C., OHM, R. A., LORETO, R. G., SEBASTIAN, A., ALBERT, I., MERROW, M., BRACHMANN, A. & HUGHES, D. P. 2015. Gene expression during zombie ant biting behavior reflects the complexity underlying fungal parasitic behavioral manipulation. *BMC genomics,* 16**,** 1-23.
55. DELOTTO, Y. & DELOTTO, R. 1998. Proteolytic processing of the Drosophila Spätzle protein by easter generates a dimeric NGF-like molecule with ventralising activity. *Mechanisms of development,* 72**,** 141-148.

56. DESALVO, M. K., MAYER, N., MAYER, F. & BAINTON, R. J. 2011. Physiologic and anatomic characterization of the brain surface glia barrier of Drosophila. *Glia,* 59**,** 1322-1340.
57. DVOŘÁČEK, J. & KODRÍK, D. 2021. Drosophila reward system-A summary of current knowledge. *Neuroscience & Biobehavioral Reviews,* 123**,** 301-319.
58. EKENGREN, S. & HULTMARK, D. 1999. Drosophila cecropin as an antifungal agent. *Insect biochemistry and molecular biology,* 29**,** 965-972.
59. ELEY, K. L., HALO, L. M., SONG, Z., POWLES, H., COX, R. J., BAILEY, A. M., LAZARUS, C. M. & SIMPSON, T. J. 2007. Biosynthesis of the 2-pyridone tenellin in the insect pathogenic fungus Beauveria bassiana. *ChemBioChem,* 8**,** 289-297.
60. ELYA, C., LAVRENTOVICH, D., LEE, E., PASADYN, C., DUVAL, J., BASAK, M., SAYKINA, V. & DE BIVORT, B. 2022. Neural mechanisms of parasite-induced summiting behavior in “zombie” Drosophila. *bioRxiv***,** 2022.12.01.518723.
61. ELYA, C., LOK, T. C., SPENCER, Q. E., MCCAUSLAND, H., MARTINEZ, C. C. & EISEN, M. 2018. Robust manipulation of the behavior of Drosophila melanogaster by a fungal pathogen in the laboratory. *Elife,* 7**,** e34414.
62. ETGES, W. J., DE OLIVEIRA, C. C., RAJPUROHIT, S. & GIBBS, A. G. 2017. Effects of temperature on transcriptome and cuticular hydrocarbon expression in ecologically differentiated populations of desert Drosophila. *Ecology and evolution,* 7**,** 619-637.
63. EVANS, H. 1982. Entomogenous fungi in tropical forest ecosystems: an appraisal. *Ecological Entomology,* 7**,** 47-60.
64. EVANS, H. 1988. Coevolution of entomogenous fungi and their insect hosts. *Coevolution of fungi with plants and animals/edited by KA Pirozynski and DL Hawksworth*.
65. FAN, Y., FANG, W., GUO, S., PEI, X., ZHANG, Y., XIAO, Y., LI, D., JIN, K., BIDOCHKA, M. J. & PEI, Y. 2007. Increased insect virulence in Beauveria bassiana strains overexpressing an engineered chitinase. *Appl. Environ. Microbiol.,* 73**,** 295-302.
66. FANG, W., FENG, J., FAN, Y., ZHANG, Y., BIDOCHKA, M. J., LEGER, R. J. S. & PEI, Y. 2009. Expressing a fusion protein with protease and chitinase activities increases the virulence of the insect pathogen Beauveria bassiana. *Journal of invertebrate pathology,* 102**,** 155-159.
67. FEANY, M. B. & BENDER, W. W. 2000. A Drosophila model of Parkinson's disease. *Nature,* 404**,** 394-398.
68. FEHLBAUM, P., BULET, P., MICHAUT, L., LAGUEUX, M., BROEKAERT, W. F., HETRU, C. & HOFFMANN, J. A. 1994. Insect immunity. Septic injury of Drosophila induces the synthesis of a potent antifungal peptide with sequence homology to plant antifungal peptides. *Journal of Biological Chemistry,* 269**,** 33159-33163.
69. FERRANDON, D., IMLER, J.-L., HETRU, C. & HOFFMANN, J. A. 2007. The Drosophila systemic immune response: sensing and signalling during bacterial and fungal infections. *Nature reviews immunology,* 7**,** 862-874.
70. FERRANDON, D., JUNG, A., CRIQUI, M.-C., LEMAITRE, B., UTTENWEILER-JOSEPH, S., MICHAUT, L., REICHHART, J.-M. & HOFFMANN, J. 1998. A drosomycin–GFP reporter transgene reveals a local immune response in Drosophila that is not dependent on the Toll pathway. *The EMBO journal,* 17**,** 1217-1227.
71. FERRON, P. 1978. Biological control of insect pests by entomogenous fungi. *Annual review of entomology,* 23**,** 409-442.
72. FISCHER, G., ALBRECHT, A., JÄCKEL, U. & KÄMPFER, P. 2008. Analysis of airborne microorganisms, MVOC and odour in the surrounding of composting facilities and implications for future investigations. *International journal of hygiene and environmental health,* 211**,** 132-142.

73. FOLDI, I., ANTHONEY, N., HARRISON, N., GANGLOFF, M., VERSTAK, B., NALLASIVAN, M. P., ALAHMED, S., ZHU, B., PHIZACKLEA, M. & LOSADA-PEREZ, M. 2017. Three-tier regulation of cell number plasticity by neurotrophins and Tolls in Drosophila. *Journal of Cell Biology,* 216**,** 1421-1438.
74. FONTAINE, T., SIMENEL, C., DUBREUCQ, G., ADAM, O., DELEPIERRE, M., LEMOINE, J., VORGIAS, C. E., DIAQUIN, M. & LATGÉ, J.-P. 2000. Molecular organization of the alkali-insoluble fraction ofAspergillus fumigatus cell wall. *Journal of Biological Chemistry,* 275**,** 27594-27607.
75. FORERO, M. G., LEARTE, A. R., CARTWRIGHT, S. & HIDALGO, A. 2010. Deadeasy Mito-Glia: Automatic counting of mitotic cells and glial cells in Drosophila. *PloS one,* 5**,** e10557.
76. FORERO, M. G., PENNACK, J. A., LEARTE, A. R. & HIDALGO, A. 2009. DeadEasy caspase: automatic counting of apoptotic cells in Drosophila. *PLoS One,* 4**,** e5441.
77. FRIEDMAN, R. & HUGHES, A. L. 2002. Molecular evolution of the NF-κB signaling system. *Immunogenetics,* 53**,** 964-974.
78. GANETZKY, B. & FLANAGAN, J. R. 1978. On the relationship between senescence and age-related changes in two wild-type strains of Drosophila melanogaster. *Experimental gerontology,* 13**,** 189-196.
79. GAY, N. J. & GANGLOFF, M. 2007. Structure and function of Toll receptors and their ligands. *Annu. Rev. Biochem.,* 76**,** 141-165.
80. GEORGEL, P., NAITZA, S., KAPPLER, C., FERRANDON, D., ZACHARY, D., SWIMMER, C., KOPCZYNSKI, C., DUYK, G., REICHHART, J.-M. & HOFFMANN, J. A. 2001. Drosophila immune deficiency (IMD) is a death domain protein that activates antibacterial defense and can promote apoptosis. *Developmental cell,* 1**,** 503-514.
81. GERDTS, J., BRACE, E., SASAKI, Y., DIANTONIO, A. & MILBRANDT, J. 2015. SARM1 activation triggers axon degeneration locally via NAD+ destruction. *Science,* 348**,** 453-457.
82. GERDTS, J., SUMMERS, D. W., SASAKI, Y., DIANTONIO, A. & MILBRANDT, J. 2013. Sarm1-mediated axon degeneration requires both SAM and TIR interactions. *Journal of Neuroscience,* 33**,** 13569-13580.
83. GOTTAR, M., GOBERT, V., MATSKEVICH, A. A., REICHHART, J.-M., WANG, C., BUTT, T. M., BELVIN, M., HOFFMANN, J. A. & FERRANDON, D. 2006. Dual detection of fungal infections in Drosophila via recognition of glucans and sensing of virulence factors. *Cell,* 127**,** 1425-1437.
84. GROSS, O., POECK, H., BSCHEIDER, M., DOSTERT, C., HANNESSCHLÄGER, N., ENDRES, S., HARTMANN, G., TARDIVEL, A., SCHWEIGHOFFER, E. & TYBULEWICZ, V. 2009. Syk kinase signalling couples to the Nlrp3 inflammasome for anti-fungal host defence. *Nature,* 459**,** 433-436.
85. HADJIECONOMOU, D., ROTKOPF, S., ALEXANDRE, C., BELL, D. M., DICKSON, B. J. & SALECKER, I. 2011. Flybow: genetic multicolor cell labeling for neural circuit analysis in Drosophila melanogaster. *Nature methods,* 8**,** 260-266.
86. HALFON, M. S., HASHIMOTO, C. & KESHISHIAN, H. 1995. The Drosophila toll gene functions zygotically and is necessary for proper motoneuron and muscle development. *Developmental biology,* 169**,** 151-167.
87. HANSON, M. A., COHEN, L. B., MARRA, A., IATSENKO, I., WASSERMAN, S. A. & LEMAITRE, B. 2021. The Drosophila Baramicin polypeptide gene protects against fungal infection. *PLoS pathogens,* 17**,** e1009846.
88. HARTENSTEIN, V., OMOTO, J. J., NGO, K. T., WONG, D., KUERT, P. A., REICHERT, H., LOVICK, J. K. & YOUNOSSI-HARTENSTEIN, A. 2018. Structure and development of the subesophageal zone of the Drosophila brain. I. Segmental architecture, compartmentalization, and lineage anatomy. *Journal of Comparative Neurology,* 526**,** 6-32.

89. HECHT, P. M. & ANDERSON, K. V. 1993. Genetic characterization of tube and pelle, genes required for signaling between Toll and dorsal in the specification of the dorsal-ventral pattern of the Drosophila embryo. *Genetics,* 135**,** 405-417.
90. HEDENGREN, M., BORGE, K. & HULTMARK, D. 2000. Expression and evolution of the Drosophila attacin/diptericin gene family. *Biochemical and biophysical research communications,* 279**,** 574-581.
91. HEIGWER, F., PORT, F. & BOUTROS, M. 2018. RNA interference (RNAi) screening in Drosophila. *Genetics,* 208**,** 853-874.
92. HEISENBERG, M. 1998. What do the mushroom bodies do for the insect brain? An introduction. *Learning & Memory,* 5**,** 1-10.
93. HEMMI, H., KAISHO, T., TAKEUCHI, O., SATO, S., SANJO, H., HOSHINO, K., HORIUCHI, T., TOMIZAWA, H., TAKEDA, K. & AKIRA, S. 2002. Small anti-viral compounds activate immune cells via the TLR7 MyD88–dependent signaling pathway. *Nature immunology,* 3**,** 196-200.
94. HEMMI, H., TAKEUCHI, O., KAWAI, T., KAISHO, T., SATO, S., SANJO, H., MATSUMOTO, M., HOSHINO, K., WAGNER, H. & TAKEDA, K. 2000. A Toll-like receptor recognizes bacterial DNA. *Nature,* 408**,** 740-745.
95. HINDSBO, O. 1972. Effects of Polymorphus (Acanthocephala) on colour and behaviour of Gammarus lacustris. *Nature,* 238**,** 333-333.
96. HISE, A. G., TOMALKA, J., GANESAN, S., PATEL, K., HALL, B. A., BROWN, G. D. & FITZGERALD, K. A. 2009. An essential role for the NLRP3 inflammasome in host defense against the human fungal pathogen Candida albicans. *Cell host & microbe,* 5**,** 487-497.
97. HOCH, H., GALVANI, C., SZAROWSKI, D. & TURNER, J. 2005. Two new fluorescent dyes applicable for visualization of fungal cell walls. *Mycologia,* 97**,** 580-588.
98. HOLDER, D. J. & KEYHANI, N. O. 2005. Adhesion of the entomopathogenic fungus Beauveria (Cordyceps) bassiana to substrata. *Appl. Environ. Microbiol.,* 71**,** 5260-5266.
99. HOLDER, D. J., KIRKLAND, B. H., LEWIS, M. W. & KEYHANI, N. O. 2007. Surface characteristics of the entomopathogenic fungus Beauveria (Cordyceps) bassiana. *Microbiology,* 153**,** 3448-3457.
100. HOLMES, J. C. 1972. Modification of intermediate host behaviour by parasites. *Behavioural aspects of parasite transmission*.
101. HU, X., YAGI, Y., TANJI, T., ZHOU, S. & IP, Y. T. 2004. Multimerization and interaction of Toll and Spätzle in Drosophila. *Proceedings of the National Academy of Sciences,* 101**,** 9369-9374.
102. HUGHES, D. P., ANDERSEN, S. B., HYWEL-JONES, N. L., HIMAMAN, W., BILLEN, J. & BOOMSMA, J. J. 2011. Behavioral mechanisms and morphological symptoms of zombie ants dying from fungal infection. *BMC ecology,* 11**,** 1-10.
103. HULTMARK, D. 2003. Drosophila immunity: paths and patterns. *Current opinion in immunology,* 15**,** 12-19.
104. HULTMARK, D., STEINER, H., RASMUSON, T. & BOMAN, H. G. 1980. Insect immunity. Purification and properties of three inducible bactericidal proteins from hemolymph of immunized pupae of Hyalophora cecropia. *European Journal of Biochemistry,* 106**,** 7-16.
105. IMLER, J.-L. & HOFFMANN, J. A. 2001. Toll receptors in innate immunity. *Trends in cell biology,* 11**,** 304-311.
106. IMLER, J.-L. & HOFFMANN, J. A. 2003. Toll signaling: the TIReless quest for specificity. *Nature immunology,* 4**,** 105-106.
107. IMLER, J. L. & ZHENG, L. 2004. Biology of Toll receptors: lessons from insects and mammals. *Journal of leukocyte biology,* 75**,** 18-26.
108. INAMDAR, A. A., HOSSAIN, M. M., BERNSTEIN, A. I., MILLER, G. W., RICHARDSON, J. R. & BENNETT, J. W. 2013. Fungal-derived semiochemical 1-octen-3-ol disrupts dopamine packaging

and causes neurodegeneration. *Proceedings of the National Academy of Sciences,* 110**,** 19561-19566.
109. INAMDAR, A. A., MASUREKAR, P. & BENNETT, J. W. 2010. Neurotoxicity of fungal volatile organic compounds in Drosophila melanogaster. *Toxicological Sciences,* 117**,** 418-426.
110. INGLIS, G. D., GOETTEL, M. S., BUTT, T. M. & STRASSER, H. 2001. Use of hyphomycetous fungi for managing insect pests. *Fungi as biocontrol agents***,** 23-69.
111. IP, Y. T., REACH, M., ENGSTROM, Y., KADALAYIL, L., CAI, H., GONZÁLEZ-CRESPO, S., TATEI, K. & LEVINE, M. 1993. Dif, a dorsal-related gene that mediates an immune response in Drosophila. *Cell,* 75**,** 753-763.
112. ITO, K., SHINOMIYA, K., ITO, M., ARMSTRONG, J. D., BOYAN, G., HARTENSTEIN, V., HARZSCH, S., HEISENBERG, M., HOMBERG, U. & JENETT, A. 2014. A systematic nomenclature for the insect brain. *Neuron,* 81**,** 755-765.
113. JANG, I.-H., CHOSA, N., KIM, S.-H., NAM, H.-J., LEMAITRE, B., OCHIAI, M., KAMBRIS, Z., BRUN, S., HASHIMOTO, C. & ASHIDA, M. 2006. A Spätzle-processing enzyme required for toll signaling activation in Drosophila innate immunity. *Developmental cell,* 10**,** 45-55.
114. JIN, L. H., SHIM, J., YOON, J. S., KIM, B., KIM, J., KIM-HA, J. & KIM, Y.-J. 2008. Identification and functional analysis of antifungal immune response genes in Drosophila. *PLoS pathogens,* 4**,** e1000168.
115. JOLY, S., MA, N., SADLER, J. J., SOLL, D. R., CASSEL, S. L. & SUTTERWALA, F. S. 2009. Cutting edge: Candida albicans hyphae formation triggers activation of the Nlrp3 inflammasome. *The Journal of Immunology,* 183**,** 3578-3581.
116. JOO, H.-S., FU, C.-I. & OTTO, M. 2016. Bacterial strategies of resistance to antimicrobial peptides. *Philosophical Transactions of the Royal Society B: Biological Sciences,* 371**,** 20150292.
117. KARTHIK, L., KUMAR, G., KESWANI, T., BHATTACHARYYA, A., CHANDAR, S. S. & BHASKARA RAO, K. 2014. Protease inhibitors from marine actinobacteria as a potential source for antimalarial compound. *PloS one,* 9**,** e90972.
118. KASTURE, A. S., HUMMEL, T., SUCIC, S. & FREISSMUTH, M. 2018. Big lessons from tiny flies: Drosophila melanogaster as a model to explore dysfunction of dopaminergic and serotonergic neurotransmitter systems. *International Journal of Molecular Sciences,* 19**,** 1788.
119. KAVALIERS, M., COLWELL, D. & CHOLERIS, E. 1999. Parasites and behavior: an ethopharmacological analysis and biomedical implications. *Neuroscience & Biobehavioral Reviews,* 23**,** 1037-1045.
120. KAWAGOE, T., SATO, S., MATSUSHITA, K., KATO, H., MATSUI, K., KUMAGAI, Y., SAITOH, T., KAWAI, T., TAKEUCHI, O. & AKIRA, S. 2008. Sequential control of Toll-like receptor–dependent responses by IRAK1 and IRAK2. *Nature immunology,* 9**,** 684.
121. KEITH, F. J. & GAY, N. J. 1990. The Drosophila membrane receptor Toll can function to promote cellular adhesion. *The EMBO Journal,* 9**,** 4299-4306.
122. KELLER, S. 1987. Arthropod-pathogenic Enthomophthorales of Switzerland. I. Conidiobolus, Entomophaga and Entomophthora. *Sydowia,* 40**,** 122-167.
123. KLEVE, C. D., SILER, D. A., SYED, S. K. & ELDON, E. D. 2006. Expression of 18-wheeler in the follicle cell epithelium affects cell migration and egg morphology in Drosophila. *Developmental dynamics: an official publication of the American Association of Anatomists,* 235**,** 1953-1961.
124. KOUNATIDIS, I., CHTARBANOVA, S., CAO, Y., HAYNE, M., JAYANTH, D., GANETZKY, B. & LIGOXYGAKIS, P. 2017. NF-κB immunity in the brain determines fly lifespan in healthy aging and age-related neurodegeneration. *Cell reports,* 19**,** 836-848.

125. KRAGOL, G., LOVAS, S., VARADI, G., CONDIE, B. A., HOFFMANN, R. & OTVOS, L. 2001. The antibacterial peptide pyrrhocoricin inhibits the ATPase actions of DnaK and prevents chaperone-assisted protein folding. *Biochemistry,* 40**,** 3016-3026.
126. KULKARNI, M. M., BOOKER, M., SILVER, S. J., FRIEDMAN, A., HONG, P., PERRIMON, N. & MATHEY-PREVOT, B. 2006. Evidence of off-target effects associated with long dsRNAs in Drosophila melanogaster cell-based assays. *Nature methods,* 3**,** 833-838.
127. KUMAGAI, Y. & AKIRA, S. 2010. Identification and functions of pattern-recognition receptors. *Journal of Allergy and Clinical Immunology,* 125**,** 985-992.
128. KUMAR, H., KAWAI, T. & AKIRA, S. 2009. Pathogen recognition in the innate immune response. *Biochemical Journal,* 420**,** 1-16.
129. KURUP, S., RUNIONS, J., KÖHLER, U., LAPLAZE, L., HODGE, S. & HASELOFF, J. 2005. Marking cell lineages in living tissues. *The Plant Journal,* 42**,** 444-453.
130. LAI, Y. & GALLO, R. L. 2009. AMPed up immunity: how antimicrobial peptides have multiple roles in immune defense. *Trends in immunology,* 30**,** 131-141.
131. LAUGHON, A., DRISCOLL, R., WILLS, N. & GESTELAND, R. F. 1984. Identification of two proteins encoded by the Saccharomyces cerevisiae GAL4 gene. *Molecular and cellular biology*.
132. LAUGHON, A. & GESTELAND, R. F. 1984. Primary structure of the Saccharomyces cerevisiae GAL4 gene. *Molecular and cellular biology*.
133. LE BOURG, E. & LINTS, F. A. 1992. Hypergravity and aging in Drosophila melanogaster. 4. Climbing activity. *Gerontology,* 38**,** 59-64.
134. LEFEVRE, T., ADAMO, S. A., BIRON, D. G., MISSÉ, D., HUGHES, D. & THOMAS, F. 2009. Invasion of the body snatchers: the diversity and evolution of manipulative strategies in host–parasite interactions. *Advances in parasitology,* 68**,** 45-83.
135. LEMAITRE, B., KROMER-METZGER, E., MICHAUT, L., NICOLAS, E., MEISTER, M., GEORGEL, P., REICHHART, J.-M. & HOFFMANN, J. A. 1995. A recessive mutation, immune deficiency (imd), defines two distinct control pathways in the Drosophila host defense. *Proceedings of the National Academy of Sciences,* 92**,** 9465-9469.
136. LEMAITRE, B., NICOLAS, E., MICHAUT, L., REICHHART, J.-M. & HOFFMANN, J. A. 1996. The dorsoventral regulatory gene cassette spätzle/Toll/cactus controls the potent antifungal response in Drosophila adults. *Cell,* 86**,** 973-983.
137. LEMAITRE, B., REICHHART, J.-M. & HOFFMANN, J. A. 1997. Drosophila host defense: differential induction of antimicrobial peptide genes after infection by various classes of microorganisms. *Proceedings of the National Academy of Sciences,* 94**,** 14614-14619.
138. LETSOU, A., ALEXANDER, S., ORTH, K. & WASSERMAN, S. A. 1991. Genetic and molecular characterization of tube, a Drosophila gene maternally required for embryonic dorsoventral polarity. *Proceedings of the National Academy of Sciences,* 88**,** 810-814.
139. LEULIER, F. & LEMAITRE, B. 2008. Toll-like receptors—taking an evolutionary approach. *Nature Reviews Genetics,* 9**,** 165-178.
140. LEULIER, F., VIDAL, S., SAIGO, K., UEDA, R. & LEMAITRE, B. 2002. Inducible expression of double-stranded RNA reveals a role for dFADD in the regulation of the antibacterial response in Drosophila adults. *Current biology,* 12**,** 996-1000.
141. LEVASHINA, E. A., OHRESSER, S., BULET, P., REICHHART, J. M., HETRU, C. & HOFFMANN, J. A. 1995. Metchnikowin, a novel immune-inducible proline-rich peptide from Drosophila with antibacterial and antifungal properties. *European Journal of Biochemistry,* 233**,** 694-700.
142. LEWIS, M., ARNOT, C. J., BEESTON, H., MCCOY, A., ASHCROFT, A. E., GAY, N. J. & GANGLOFF, M. 2013. Cytokine Spätzle binds to the Drosophila immunoreceptor Toll with a neurotrophin-like

specificity and couples receptor activation. *Proceedings of the National Academy of Sciences,* 110**,** 20461-20466.
143. LEWIS, M. W., ROBALINO, I. V. & KEYHANI, N. O. 2009. Uptake of the fluorescent probe FM4-64 by hyphae and haemolymph-derived in vivo hyphal bodies of the entomopathogenic fungus Beauveria bassiana. *Microbiology,* 155**,** 3110-3120.
144. LI, F., SHI, H.-Q., YING, S.-H. & FENG, M.-G. 2015. Distinct contributions of one Fe-and two Cu/Zn-cofactored superoxide dismutases to antioxidation, UV tolerance and virulence of Beauveria bassiana. *Fungal Genetics and Biology,* 81**,** 160-171.
145. LI, G., FORERO, M. G., WENTZELL, J. S., DURMUS, I., WOLF, R., ANTHONEY, N. C., PARKER, M., JIANG, R., HASENAUER, J. & STRAUSFELD, N. J. 2020. A Toll-receptor map underlies structural brain plasticity. *Elife,* 9**,** e52743.
146. LIGOXYGAKIS, P., PELTE, N., HOFFMANN, J. A. & REICHHART, J.-M. 2002. Activation of Drosophila Toll during fungal infection by a blood serine protease. *Science,* 297**,** 114-116.
147. LIU, C., PLAÇAIS, P.-Y., YAMAGATA, N., PFEIFFER, B. D., ASO, Y., FRIEDRICH, A. B., SIWANOWICZ, I., RUBIN, G. M., PREAT, T. & TANIMOTO, H. 2012. A subset of dopamine neurons signals reward for odour memory in Drosophila. *Nature,* 488**,** 512-516.
148. LLOYD, T. E. & TAYLOR, J. P. 2010. Flightless flies: Drosophila models of neuromuscular disease. *Annals of the New York Academy of Sciences,* 1184**,** e1.
149. LOSADA-PEREZ, M. 2018. Glia: from 'just glue'to essential players in complex nervous systems: a comparative view from flies to mammals. *Journal of Neurogenetics,* 32**,** 78-91.
150. LUO, C. & ZHENG, L. 2000a. Independent evolution of Toll and related genes in insects and mammals. *Immunogenetics,* 51**,** 92-98.
151. LUO, C. & ZHENG, L. 2000b. Independent evolution of Toll and related genes in insects and mammals. *Immunogenetics,* 51**,** 92-98.
152. LUSCHNIG, S., MOUSSIAN, B., KRAUSS, J., DESJEUX, I., PERKOVIC, J. & NÜSSLEIN-VOLHARD, C. 2004. An F1 genetic screen for maternal-effect mutations affecting embryonic pattern formation in Drosophila melanogaster. *Genetics,* 167**,** 325-342.
153. LYCKE, E. & ROOS, B.-E. 1974. Influence of changes in brain monoamine metabolism on behaviour of herpes simplex-infected mice. *Journal of the neurological sciences,* 22**,** 277-289.
154. MA, Y., CREANGA, A., LUM, L. & BEACHY, P. A. 2006a. Prevalence of off-target effects in Drosophila RNA interference screens. *Nature,* 443**,** 359-363.
155. MA, Y., LI, J., CHIU, I., WANG, Y., SLOANE, J. A., LÜ, J., KOSARAS, B., SIDMAN, R. L., VOLPE, J. J. & VARTANIAN, T. 2006b. Toll-like receptor 8 functions as a negative regulator of neurite outgrowth and inducer of neuronal apoptosis. *The Journal of cell biology,* 175**,** 209-215.
156. MADAR, R., ROTTER, A., BEN-ASHER, H. W., MUGHAL, M. R., ARUMUGAM, T. V., WOOD 3RD, W., BECKER, K., MATTSON, M. P. & OKUN, E. 2015. Postnatal TLR2 activation impairs learning and memory in adulthood. *Brain, behavior, and immunity,* 48**,** 301-312.
157. MAO, Z. & DAVIS, R. L. 2009. Eight different types of dopaminergic neurons innervate the Drosophila mushroom body neuropil: anatomical and physiological heterogeneity. *Frontiers in neural circuits***,** 5.
158. MARELLA, S., MANN, K. & SCOTT, K. 2012. Dopaminergic modulation of sucrose acceptance behavior in Drosophila. *Neuron,* 73**,** 941-950.
159. MATSKEVICH, A. A., QUINTIN, J. & FERRANDON, D. 2010. The Drosophila PRR GNBP3 assembles effector complexes involved in antifungal defenses independently of its Toll-pathway activation function. *European journal of immunology,* 40**,** 1244-1254.

160. MATYSIK, S., HERBARTH, O. & MUELLER, A. 2008. Determination of volatile metabolites originating from mould growth on wall paper and synthetic media. *Journal of microbiological methods,* 75**,** 182-187.
161. MAURER, P., REJASSE, A., CAPY, P., LANGIN, T. & RIBA, G. 1997. Isolation of the transposable element hupfer from the entomopathogenic fungus Beauveria bassiana by insertion mutagenesis of the nitrate reductase structural gene. *Molecular and General Genetics MGG,* 256**,** 195-202.
162. MAYER, F., MAYER, N., CHINN, L., PINSONNEAULT, R. L., KROETZ, D. & BAINTON, R. J. 2009. Evolutionary conservation of vertebrate blood–brain barrier chemoprotective mechanisms in Drosophila. *Journal of Neuroscience,* 29**,** 3538-3550.
163. MCCLURE, C. D., HASSAN, A., AUGHEY, G. N., BUTT, K., ESTACIO-GÓMEZ, A., DUGGAL, A., SIA, C. Y., BARBER, A. F. & SOUTHALL, T. D. 2022. An auxin-inducible, GAL4-compatible, gene expression system for Drosophila. *Elife,* 11**,** e67598.
164. MCCOY, C. 1990. Entomogenous fungi as microbial pesticides. *Entomogenous fungi as microbial pesticides.,* 112**,** 139-159.
165. MCILROY, G., FOLDI, I., AURIKKO, J., WENTZELL, J. S., LIM, M. A., FENTON, J. C., GAY, N. J. & HIDALGO, A. 2013. Toll-6 and Toll-7 function as neurotrophin receptors in the Drosophila melanogaster CNS. *Nature neuroscience,* 16**,** 1248.
166. MCKELLAR, C. E., SIWANOWICZ, I., DICKSON, B. J. & SIMPSON, J. H. 2020. Controlling motor neurons of every muscle for fly proboscis reaching. *Elife,* 9**,** e54978.
167. MEANS, T. K., GOLENBOCK, D. T. & FENTON, M. J. 2000. The biology of Toll-like receptors. *Cytokine & growth factor reviews,* 11**,** 219-232.
168. MEDZHITOV, R., PRESTON-HURLBURT, P., KOPP, E., STADLEN, A., CHEN, C., GHOSH, S. & JANEWAY, C. A. 1998. MyD88 is an adaptor protein in the hToll/IL-1 receptor family signaling pathways. *Molecular cell,* 2**,** 253-258.
169. MEUNIER, N., BELGACEM, Y. H. & MARTIN, J.-R. 2007. Regulation of feeding behaviour and locomotor activity by takeout in Drosophila. *Journal of Experimental Biology,* 210**,** 1424-1434.
170. MEYLAN, E., BURNS, K., HOFMANN, K., BLANCHETEAU, V., MARTINON, F., KELLIHER, M. & TSCHOPP, J. 2004. RIP1 is an essential mediator of Toll-like receptor 3–induced NF-κB activation. *Nature immunology,* 5**,** 503-507.
171. MICHEL, T., REICHHART, J.-M., HOFFMANN, J. A. & ROYET, J. 2001. Drosophila Toll is activated by Gram-positive bacteria through a circulating peptidoglycan recognition protein. *Nature,* 414**,** 756-759.
172. MILLER, D. J., HEMMRICH, G., BALL, E. E., HAYWARD, D. C., KHALTURIN, K., FUNAYAMA, N., AGATA, K. & BOSCH, T. C. 2007. The innate immune repertoire in Cnidaria-ancestral complexity and stochastic gene loss. *Genome biology,* 8**,** R59.
173. MIZUGUCHI, K., PARKER, J. S., BLUNDELL, T. L. & GAY, N. J. 1998. Getting knotted: a model for the structure and activation of Spätzle. *Trends in biochemical sciences,* 23**,** 239-242.
174. MOLNÁR, I., GIBSON, D. M. & KRASNOFF, S. B. 2010. Secondary metabolites from entomopathogenic Hypocrealean fungi. *Natural product reports,* 27**,** 1241-1275.
175. MOORE, J. 2002. *Parasites and the behavior of animals*, Oxford University Press on Demand.
176. MOORE, J. & GOTELLI, N. 1990. A phylogenetic perspective on the evolution of altered host behaviours: A critical look at the manipulation hypothesis. *Parasitism and host behaviour***,** 193-233.
177. MORISALO, D. & ANDERSON, K. V. 1995. Signaling pathways that establish the dorsal-ventral pattern of the Drosophila embryo. *Annual review of genetics,* 29**,** 371-399.

178. MORISATO, D. & ANDERSON, K. V. 1994. The spätzle gene encodes a component of the extracellular signaling pathway establishing the dorsal-ventral pattern of the Drosophila embryo. *Cell,* 76**,** 677-688.
179. MOUSSIAN, B. & ROTH, S. 2005. Dorsoventral axis formation in the Drosophila embryo—shaping and transducing a morphogen gradient. *Current biology,* 15**,** R887-R899.
180. NARBONNE-REVEAU, K., CHARROUX, B. & ROYET, J. 2011. Lack of an antibacterial response defect in Drosophila Toll-9 mutant. *PloS one,* 6**,** e17470.
181. NÉRIEC, N. & DESPLAN, C. 2016. From the eye to the brain: development of the Drosophila visual system. *Current topics in developmental biology.* Elsevier.
182. NETEA, M. G., SUTMULLER, R., HERMANN, C., VAN DER GRAAF, C. A., VAN DER MEER, J. W., VAN KRIEKEN, J. H., HARTUNG, T., ADEMA, G. & KULLBERG, B. J. 2004. Toll-like receptor 2 suppresses immunity against Candida albicans through induction of IL-10 and regulatory T cells. *The Journal of Immunology,* 172**,** 3712-3718.
183. NETEA, M. G., VAN DER GRAAF, C. A., VONK, A. G., VERSCHUEREN, I., VAN DER MEER, J. W. & KULLBERG, B. J. 2002. The role of toll-like receptor (TLR) 2 and TLR4 in the host defense against disseminated candidiasis. *Journal of Infectious Diseases,* 185**,** 1483-1489.
184. NETEA, M. G., VAN DER MEER, J. W. & KULLBERG, B. J. 2007. Recognition of fungal pathogens by Toll-like receptors. *Immunology of Fungal Infections***,** 259-272.
185. NEWSOME, T. P., ÅSLING, B. & DICKSON, B. J. 2000. Analysis of Drosophila photoreceptor axon guidance in eye-specific mosaics. *Development,* 127**,** 851-860.
186. OCHIAI, M. & ASHIDA, M. 2000. A pattern-recognition protein for β-1, 3-glucan: the binding domain and the cDNA cloning of β-1, 3-glucan recognition protein from the silkworm, Bombyx mori. *Journal of Biological Chemistry,* 275**,** 4995-5002.
187. OKUN, E., BARAK, B., SAADA-MADAR, R., ROTHMAN, S. M., GRIFFIOEN, K. J., ROBERTS, N., CASTRO, K., MUGHAL, M. R., PITA, M. A. & STRANAHAN, A. M. 2012. Evidence for a developmental role for TLR4 in learning and memory.
188. OKUN, E., GRIFFIOEN, K., BARAK, B., ROBERTS, N. J., CASTRO, K., PITA, M. A., CHENG, A., MUGHAL, M. R., WAN, R. & ASHERY, U. 2010. Toll-like receptor 3 inhibits memory retention and constrains adult hippocampal neurogenesis. *Proceedings of the National Academy of Sciences,* 107**,** 15625-15630.
189. OKUN, E., GRIFFIOEN, K. J. & MATTSON, M. P. 2011. Toll-like receptor signaling in neural plasticity and disease. *Trends in neurosciences,* 34**,** 269-281.
190. OLSON, J. K. & MILLER, S. D. 2004. Microglia initiate central nervous system innate and adaptive immune responses through multiple TLRs. *The Journal of Immunology,* 173**,** 3916-3924.
191. OOI, J. Y., YAGI, Y., HU, X. & IP, Y. T. 2002. The Drosophila Toll-9 activates a constitutive antimicrobial defense. *EMBO reports,* 3**,** 82-87.
192. ORTIZ-URQUIZA, A. & KEYHANI, N. 2016a. Molecular genetics of Beauveria bassiana infection of insects. *Advances in genetics.* Elsevier.
193. ORTIZ-URQUIZA, A. & KEYHANI, N. 2016b. Molecular genetics of Beauveria bassiana infection of insects. *Advances in Genetics,* 94**,** 165-249.
194. OSTERLOH, J. M., YANG, J., ROONEY, T. M., FOX, A. N., ADALBERT, R., POWELL, E. H., SHEEHAN, A. E., AVERY, M. A., HACKETT, R. & LOGAN, M. A. 2012. dSarm/Sarm1 is required for activation of an injury-induced axon death pathway. *Science,* 337**,** 481-484.
195. OZINSKY, A., UNDERHILL, D. M., FONTENOT, J. D., HAJJAR, A. M., SMITH, K. D., WILSON, C. B., SCHROEDER, L. & ADEREM, A. 2000. The repertoire for pattern recognition of pathogens by the innate immune system is defined by cooperation between toll-like receptors. *Proceedings of the National Academy of Sciences,* 97**,** 13766-13771.

196. PAN, Y., ZHOU, Y., GUO, C., GONG, H., GONG, Z. & LIU, L. 2009. Differential roles of the fan-shaped body and the ellipsoid body in Drosophila visual pattern memory. *Learning & Memory,* 16**,** 289-295.
197. PARÉ, A. C., VICHAS, A., FINCHER, C. T., MIRMAN, Z., FARRELL, D. L., MAINIERI, A. & ZALLEN, J. A. 2014. A positional Toll receptor code directs convergent extension in Drosophila. *Nature,* 515**,** 523-527.
198. PASARE, C. & MEDZHITOV, R. 2005. Toll-like receptors: linking innate and adaptive immunity. *Mechanisms of Lymphocyte Activation and Immune Regulation X.* Springer.
199. PEDRINI, N. 2022. The entomopathogenic fungus Beauveria bassiana shows its toxic side within insects: expression of genes encoding secondary metabolites during pathogenesis. *Journal of Fungi,* 8**,** 488.
200. PEDRINI, N., ZHANG, S., JUÁREZ, M. P. & KEYHANI, N. O. 2010. Molecular characterization and expression analysis of a suite of cytochrome P450 enzymes implicated in insect hydrocarbon degradation in the entomopathogenic fungus Beauveria bassiana. *Microbiology,* 156.
201. PFEIFFER, B. D., NGO, T.-T. B., HIBBARD, K. L., MURPHY, C., JENETT, A., TRUMAN, J. W. & RUBIN, G. M. 2010. Refinement of tools for targeted gene expression in Drosophila. *Genetics,* 186**,** 735-755.
202. PICCININI, A. & MIDWOOD, K. 2010. DAMPening inflammation by modulating TLR signalling. *Mediators of inflammation,* 2010.
203. PIPER, M. D. & PARTRIDGE, L. 2016. Protocols to study aging in Drosophila. *Drosophila: Methods and Protocols***,** 291-302.
204. POINAR, G. & YANOVIAK, S. P. 2008. Myrmeconema neotropicum ng, n. sp., a new tetradonematid nematode parasitising South American populations of Cephalotes atratus (Hymenoptera: Formicidae), with the discovery of an apparent parasite-induced host morph. *Systematic parasitology,* 69**,** 145-153.
205. POLTORAK, A., HE, X., SMIRNOVA, I., LIU, M.-Y., HUFFEL, C. V., DU, X., BIRDWELL, D., ALEJOS, E., SILVA, M. & GALANOS, C. 1998. Defective LPS signaling in C3H/HeJ and C57BL/10ScCr mice: mutations in Tlr4 gene. *Science,* 282**,** 2085-2088.
206. POULIN, R. 1995. "Adaptive" changes in the behaviour of parasitized animals: a critical review. *International journal for parasitology,* 25**,** 1371-1383.
207. POULIN, R. 2010. Parasite manipulation of host behavior: an update and frequently asked questions. *Advances in the Study of Behavior.* Elsevier.
208. POULIN, R. & THOMAS, F. 1999. Phenotypic Variability Induced by Parasites:: Extent and Evolutionary Implications. *Parasitology Today,* 15**,** 28-32.
209. PROVOST, N. B., SHI, C., SHE, Y.-M., CYR, T. D. & MILLER, J. D. 2013. Characterization of an antigenic chitosanase from the cellulolytic fungus Chaetomium globosum. *Sabouraudia,* 51**,** 290-299.
210. PUTNUM, N., SRIVASTAVA, M., HELLSTEN, U., DIRKS, B., CHAPMAN, J., SALAMOV, A., TERRY, A., SHAPIRO, H., LINDQUIST, E. & KAPITONOV, V. Sequencing Team JGI, Steele R, Finnerty JR, Technau U, Martindale MQ, Rokhsar D (2007) Sea anemone genome reveals the gene repertoire and genomic organization of the eumetazoan ancestor. *Science,* 317**,** 86-94.
211. RAJASHEKHAR, K. & SINGH, R. N. 1994. Neuroarchitecture of the tritocerebrum of Drosophila melanogaster. *Journal of Comparative Neurology,* 349**,** 633-645.
212. RAO, X., HUANG, X., ZHOU, Z. & LIN, X. 2013. An improvement of the 2ˆ (–delta delta CT) method for quantitative real-time polymerase chain reaction data analysis. *Biostatistics, bioinformatics and biomathematics,* 3**,** 71.

213. RIEMENSPERGER, T., ISSA, A.-R., PECH, U., COULOM, H., NGUYỄN, M.-V., CASSAR, M., JACQUET, M., FIALA, A. & BIRMAN, S. 2013. A single dopamine pathway underlies progressive locomotor deficits in a Drosophila model of Parkinson disease. *Cell reports,* 5**,** 952-960.
214. ROEDER, A. D. & SHAW, J. M. 1996. Vacuole partitioning during meiotic division in yeast. *Genetics,* 144**,** 445-458.
215. ROLLS, A., SHECHTER, R., LONDON, A., ZIV, Y., RONEN, A., LEVY, R. & SCHWARTZ, M. 2007. Toll-like receptors modulate adult hippocampal neurogenesis. *Nature cell biology,* 9**,** 1081-1088.
216. ROSE, D., ZHU, X., KOSE, H., HOANG, B., CHO, J. & CHIBA, A. 1997. Toll, a muscle cell surface molecule, locally inhibits synaptic initiation of the RP3 motoneuron growth cone in Drosophila. *Development,* 124**,** 1561-1571.
217. ROSE, T., LEMOSY, E. K., CANTWELL, A. M., BANERJEE-ROY, D., SKEATH, J. B. & DI CERA, E. 2003. Three-dimensional models of proteases involved in patterning of the Drosophila embryo: Crucial role of predicted cation binding sites. *Journal of Biological Chemistry,* 278**,** 11320-11330.
218. RUIZ-LOSADA, M., GONZÁLEZ, R., PEROPADRE, A., GIL-GÁLVEZ, A., TENA, J. J., BAONZA, A. & ESTELLA, C. 2022. Coordination between cell proliferation and apoptosis after DNA damage in Drosophila. *Cell Death & Differentiation,* 29**,** 832-845.
219. SAKAI, T., KASUYA, J., KITAMOTO, T. & AIGAKI, T. 2009. The Drosophila TRPA channel, Painless, regulates sexual receptivity in virgin females. *Genes, Brain and Behavior,* 8**,** 546-557.
220. SAMSON, R. A., EVANS, H. C. & LATGÉ, J.-P. 1988. Taxonomy of entomopathogenic fungi. *Atlas of entomopathogenic fungi.* Springer.
221. SAMSON, R. A., EVANS, H. C. & LATGÉ, J.-P. 2013. *Atlas of entomopathogenic fungi*, Springer Science & Business Media.
222. SAROV-BLAT, L., SO, W. V., LIU, L. & ROSBASH, M. 2000. The Drosophila takeout gene is a novel molecular link between circadian rhythms and feeding behavior. *Cell,* 101**,** 647-656.
223. SATO, S., SUGIYAMA, M., YAMAMOTO, M., WATANABE, Y., KAWAI, T., TAKEDA, K. & AKIRA, S. 2003. Toll/IL-1 receptor domain-containing adaptor inducing IFN-β (TRIF) associates with TNF receptor-associated factor 6 and TANK-binding kinase 1, and activates two distinct transcription factors, NF-κB and IFN-regulatory factor-3, in the Toll-like receptor signaling. *The Journal of Immunology,* 171**,** 4304-4310.
224. SCHNEIDER, D. S., HUDSON, K. L., LIN, T.-Y. & ANDERSON, K. V. 1991. Dominant and recessive mutations define functional domains of Toll, a transmembrane protein required for dorsal-ventral polarity in the Drosophila embryo. *Genes & development,* 5**,** 797-807.
225. SHAW, M. H., REIMER, T., KIM, Y.-G. & NUÑEZ, G. 2008. NOD-like receptors (NLRs): bona fide intracellular microbial sensors. *Current opinion in immunology,* 20**,** 377-382.
226. SHAW, M. H., REIMER, T., SÁNCHEZ-VALDEPEÑAS, C., WARNER, N., KIM, Y.-G., FRESNO, M. & NUÑEZ, G. 2009. T cell–intrinsic role of Nod2 in promoting type 1 immunity to Toxoplasma gondii. *Nature immunology,* 10**,** 1267-1274.
227. SHI, C., PROVOST, N. B., DESROCHES, T. & MILLER, J. D. 2014. Quantification of Chaetomium globosum spores in house dust samples. *Annals of Agricultural and Environmental Medicine,* 21.
228. SHIELDS, A., AMCHESLAVSKY, A., BROWN, E., LEE, T. V., NIE, Y., TANJI, T., IP, Y. T. & BERGMANN, A. 2022. Toll-9 interacts with Toll-1 to mediate a feedback loop during apoptosis-induced proliferation in Drosophila. *Cell Reports,* 39**,** 110817.
229. SILBERING, A. F., OKADA, R., ITO, K. & GALIZIA, C. G. 2008. Olfactory information processing in the Drosophila antennal lobe: anything goes? *Journal of Neuroscience,* 28**,** 13075-13087.

230. SILVERMAN, N., ZHOU, R., STÖVEN, S., PANDEY, N., HULTMARK, D. & MANIATIS, T. 2000. A Drosophila IκB kinase complex required for Relish cleavage and antibacterial immunity. *Genes & development,* 14**,** 2461-2471.
231. STATHOPOULOS, A. & LEVINE, M. 2002. Dorsal gradient networks in the Drosophila embryo. *Developmental biology,* 246**,** 57-67.
232. STORK, T., ENGELEN, D., KRUDEWIG, A., SILIES, M., BAINTON, R. J. & KLÄMBT, C. 2008. Organization and function of the blood–brain barrier in Drosophila. *Journal of Neuroscience,* 28**,** 587-597.
233. STÖVEN, S., ANDO, I., KADALAYIL, L., ENGSTRÖM, Y. & HULTMARK, D. 2000. Activation of the Drosophila NF-κB factor Relish by rapid endoproteolytic cleavage. *EMBO reports,* 1**,** 347-352.
234. SULLIVAN, J. C., KALAITZIDIS, D., GILMORE, T. D. & FINNERTY, J. R. 2007. Rel homology domain-containing transcription factors in the cnidarian Nematostella vectensis. *Development genes and evolution,* 217**,** 63-72.
235. SUN, J., XU, A. Q., GIRAUD, J., POPPINGA, H., RIEMENSPERGER, T., FIALA, A. & BIRMAN, S. 2018. Neural control of startle-induced locomotion by the mushroom bodies and associated neurons in Drosophila. *Frontiers in systems neuroscience,* 12**,** 6.
236. SUTCLIFFE, B., FORERO, M. G., ZHU, B., ROBINSON, I. M. & HIDALGO, A. 2013. Neuron-type specific functions of DNT1, DNT2 and Spz at the Drosophila neuromuscular junction. *PloS one,* 8.
237. TAKEUCHI, O., HOSHINO, K., KAWAI, T., SANJO, H., TAKADA, H., OGAWA, T., TAKEDA, K. & AKIRA, S. 1999. Differential roles of TLR2 and TLR4 in recognition of gram-negative and gram-positive bacterial cell wall components. *Immunity,* 11**,** 443-451.
238. TAUSZIG, S., JOUANGUY, E., HOFFMANN, J. A. & IMLER, J.-L. 2000. Toll-related receptors and the control of antimicrobial peptide expression in Drosophila. *Proceedings of the National Academy of Sciences,* 97**,** 10520-10525.
239. THOMAS, F., ADAMO, S. & MOORE, J. 2005. Parasitic manipulation: where are we and where should we go? *Behavioural processes,* 68**,** 185-199.
240. TZOU, P., OHRESSER, S., FERRANDON, D., CAPOVILLA, M., REICHHART, J.-M., LEMAITRE, B., HOFFMANN, J. A. & IMLER, J.-L. 2000. Tissue-specific inducible expression of antimicrobial peptide genes in Drosophila surface epithelia. *Immunity,* 13**,** 737-748.
241. TZOU, P., REICHHART, J.-M. & LEMAITRE, B. 2002. Constitutive expression of a single antimicrobial peptide can restore wild-type resistance to infection in immunodeficient Drosophila mutants. *Proceedings of the National Academy of Sciences,* 99**,** 2152-2157.
242. ULIAN-BENITEZ, S., BISHOP, S., FOLDI, I., WENTZELL, J., OKENWA, C., FORERO, M. G., ZHU, B., MOREIRA, M., PHIZACKLEA, M. & MCILROY, G. 2017. Kek-6: A truncated-Trk-like receptor for Drosophila neurotrophin 2 regulates structural synaptic plasticity. *PLoS genetics,* 13**,** e1006968.
243. UNDERHILL, D. M., OZINSKY, A., HAJJAR, A. M., STEVENS, A., WILSON, C. B., BASSETTI, M. & ADEREM, A. 1999. The Toll-like receptor 2 is recruited to macrophage phagosomes and discriminates between pathogens. *Nature,* 401**,** 811-815.
244. VERBLE, R. M., MEYER, A. D., KLEVE, M. G. & YANOVIAK, S. P. 2012. Exoskeletal thinning in Cephalotes atratus ants (Hymenoptera: Formicidae) parasitized by Myrmeconema neotropicum (Nematoda: Tetradonematidae). *Journal of Parasitology,* 98**,** 226-228.
245. VIAUD, M., COUTEAUDIER, Y., LEVIS, C. & RIBA, G. 1996. Genome Organization inBeauveria bassiana: Electrophoretic Karyotype, Gene Mapping, and Telomeric Fingerprint. *Fungal Genetics and Biology,* 20**,** 175-183.

246. VIDAL, S., KHUSH, R. S., LEULIER, F., TZOU, P., NAKAMURA, M. & LEMAITRE, B. 2001. Mutations in the Drosophila dTAK1 gene reveal a conserved function for MAPKKKs in the control of rel/NF-κB-dependent innate immune responses. *Genes & development,* 15**,** 1900-1912.
247. VYAS, A. & SAPOLSKY, R. 2010. Manipulation of host behaviour by Toxoplasma gondii: what is the minimum a proposed proximate mechanism should explain? *Folia parasitologica,* 57**,** 88.
248. WANG, H., PENG, H., LI, W., CHENG, P. & GONG, M. 2021. The toxins of Beauveria bassiana and the strategies to improve their virulence to insects. *Frontiers in Microbiology***,** 2375.
249. WANG, J., TAO, Y., REIM, I., GAJEWSKI, K., FRASCH, M. & SCHULZ, R. A. 2005a. Expression, regulation, and requirement of the toll transmembrane protein during dorsal vessel formation in Drosophila melanogaster. *Molecular and cellular biology,* 25**,** 4200-4210.
250. WANG, J., ZHAI, Q., CHEN, Y., LIN, E., GU, W., MCBURNEY, M. W. & HE, Z. 2005b. A local mechanism mediates NAD-dependent protection of axon degeneration. *The Journal of cell biology,* 170**,** 349-355.
251. WARD, A., HONG, W., FAVALORO, V. & LUO, L. 2015. Toll receptors instruct axon and dendrite targeting and participate in synaptic partner matching in a Drosophila olfactory circuit. *Neuron,* 85**,** 1013-1028.
252. WEBER, A. N., GANGLOFF, M., MONCRIEFFE, M. C., HYVERT, Y., IMLER, J.-L. & GAY, N. J. 2007. Role of the Spätzle pro-domain in the generation of an active Toll receptor ligand. *Journal of Biological Chemistry,* 282**,** 13522-13531.
253. WEBER, A. N., TAUSZIG-DELAMASURE, S., HOFFMANN, J. A., LELIÈVRE, E., GASCAN, H., RAY, K. P., MORSE, M. A., IMLER, J.-L. & GAY, N. J. 2003. Binding of the Drosophila cytokine Spätzle to Toll is direct and establishes signaling. *Nature immunology,* 4**,** 794-800.
254. WILL, I., DAS, B., TRINH, T., BRACHMANN, A., OHM, R. A. & DE BEKKER, C. 2020. Genetic underpinnings of host manipulation by Ophiocordyceps as revealed by comparative transcriptomics. *G3: Genes, Genomes, Genetics,* 10**,** 2275-2296.
255. WINKLER, B., FUNKE, D., BENMIMOUN, B., SPÉDER, P., REY, S., LOGAN, M. A. & KLÄMBT, C. 2021. Brain inflammation triggers macrophage invasion across the blood-brain barrier in Drosophila during pupal stages. *Science Advances,* 7**,** eabh0050.
256. WU, C., CHEN, Y., WANG, F., CHEN, C., ZHANG, S., LI, C., LI, W., WU, S. & XUE, L. 2015. Pelle modulates dFoxO-mediated cell death in Drosophila. *PLoS genetics,* 11**,** e1005589.
257. XIAO, G., YING, S.-H., ZHENG, P., WANG, Z.-L., ZHANG, S., XIE, X.-Q., SHANG, Y., LEGER, R. J. S., ZHAO, G.-P. & WANG, C. 2012. Genomic perspectives on the evolution of fungal entomopathogenicity in Beauveria bassiana. *Scientific reports,* 2**,** 483.
258. XIE, X., TABUCHI, M., BROWN, M. P., MITCHELL, S. P., WU, M. N. & KOLODKIN, A. L. 2017. The laminar organization of the Drosophila ellipsoid body is semaphorin-dependent and prevents the formation of ectopic synaptic connections. *Elife,* 6**,** e25328.
259. XIE, X.-Q., LI, F., YING, S.-H. & FENG, M.-G. 2012. Additive contributions of two manganese-cored superoxide dismutases (MnSODs) to antioxidation, UV tolerance and virulence of Beauveria bassiana. *PLoS One,* 7**,** e30298.
260. XIE, X.-Q., WANG, J., HUANG, B.-F., YING, S.-H. & FENG, M.-G. 2010. A new manganese superoxide dismutase identified from Beauveria bassiana enhances virulence and stress tolerance when overexpressed in the fungal pathogen. *Applied microbiology and biotechnology,* 86**,** 1543-1553.
261. YAGI, Y., NISHIDA, Y. & IP, Y. T. 2010. Functional analysis of Toll-related genes in Drosophila. *Development, growth & differentiation,* 52**,** 771-783.
262. YAMAGATA, N., ICHINOSE, T., ASO, Y., PLAÇAIS, P.-Y., FRIEDRICH, A. B., SIMA, R. J., PREAT, T., RUBIN, G. M. & TANIMOTO, H. 2015. Distinct dopamine neurons mediate reward signals for

short-and long-term memories. *Proceedings of the National Academy of Sciences,* 112**,** 578-583.
263. YANAGAWA, A., CHABAUD, M.-A., IMAI, T. & MARION-POLL, F. 2018. Olfactory cues play a significant role in removing fungus from the body surface of Drosophila melanogaster. *Journal of invertebrate pathology,* 151**,** 144-150.
264. YANOVIAK, S. P., KASPARI, M. E., DUDLEY, R. K. & POINAR JR, G. 2008. Parasite induced fruit mimicry in a tropical canopy ant. *American Naturalist*.
265. ZHANG, S., WIDEMANN, E., BERNARD, G., LESOT, A., PINOT, F., PEDRINI, N. & KEYHANI, N. O. 2012. CYP52X1, representing new cytochrome P450 subfamily, displays fatty acid hydroxylase activity and contributes to virulence and growth on insect cuticular substrates in entomopathogenic fungus Beauveria bassiana. *Journal of Biological Chemistry,* 287**,** 13477-13486.
266. ZHANG, S. X., ROGULJA, D. & CRICKMORE, M. A. 2016. Dopaminergic circuitry underlying mating drive. *Neuron,* 91**,** 168-181.
267. ZHANG, Y.-J., FENG, M.-G., FAN, Y.-H., LUO, Z.-B., YANG, X.-Y., WU, D. & PEI, Y. 2008. A cuticle-degrading protease (CDEP-1) of Beauveria bassiana enhances virulence. *Biocontrol Science and Technology,* 18**,** 543-555.
268. ZHU, B., PENNACK, J. A., MCQUILTON, P., FORERO, M. G., MIZUGUCHI, K., SUTCLIFFE, B., GU, C.-J., FENTON, J. C. & HIDALGO, A. 2008. Drosophila neurotrophins reveal a common mechanism for nervous system formation. *PLoS biology,* 6.
269. ZHU, Y. 2013. The Drosophila visual system: From neural circuits to behavior. *Cell adhesion & migration,* 7**,** 333-344.